UNIVERSITY of STIRLING

Improving the Scalability of 6TiSCH Wireless Industrial Networks using Scalable Scheduling Reservation Protocol

Kaushal Kumar

Department of Computing Science and Mathematics

University of Stirling

Thesis submitted for the degree of Doctor of Philosophy

November 2024

Declaration

I, Kaushal kumar, hereby declare that the work in this thesis is original and produced by myself, except where reference is made to other works, and has not been submitted for examination for any other degree at this university or any other institution.

Stirling, November 2024

Kaushal Kumar

Kaushal Kumar

Abstract

The Internet of Things is currently evolving. The demand for scalable and high throughput low-power wireless sensor networks is transforming the concept of automation of industrial processes. IPv6 is considered a potential solution allowing a large number of sensor devices connected to multi-hop low power wireless sensor networks to exchange information over a range of 1-2 km and without being dependent on infrastructure. TSCH over IEEE 802.15.4 standard is a proposal at the MAC layer in the low power IPv6 protocol suite called 6TiSCH. However, the implementation of TSCH has been subject to poor scalability in the 6TiSCH networks beyond 50 nodes where nodes frequently appear and disappear. The main cause is poor scheduling of link-layer resources.

In 6TiSCH networks, the reservation of TSCH cells without a context leads to under-or-over estimation of actual bandwidth requirements, while monitoring the buffer condition for traffic adaption leads to a high level of additional overheads. Existing proposals employ an ‘On the fly’ reservation approach using a fixed threshold to tune up cell consumption and incur performance trade-offs.

More generally, cell selection in TSCH-led scheduling has been a key challenge, as allocating a Tx cell closer to each other in TSCH slotframe reduces delay; however, this causes collisions during transmission to increase. Furthermore, delay is also increased by not allocating a sufficient volume of cells to a node probing the shortest path to the root. Existing approaches adapt cell selection based on the requirements of the application.

Apart from poor traffic adaption, and inefficient cell selection, a fixed distribution of traffic in the network undermines the ability of nodes to adapt their behavior according to demand as some nodes may be able to transmit higher payload than the others depending on their distance to the root and volume of overprovisioned cells. This inability negatively affects propagation. Existing algorithms have not addressed this issue.

This thesis introduces the Scalable Scheduling Reservation Protocol (SSR) to tackle these issues. SSR uses an analytical technique called cake-slicing for traffic adaptation, prioritizing higher resource allocation to nodes closer to the network root. It employs schedule compactness via cell selection and collision-free scheduling for faster, more reliable delivery, and integrates dynamic queue optimization to minimize congestion. While SSR delivers a strong proposal for

medium-sized networks using lower consumption of TSCH resources, its performance in terms of reliability, a ratio between the number of data packets successfully received over the volume sent by a transmitter, declines in larger networks due to limited proliferation of information, causing fewer routes in the network.

SSR is then implemented under hybrid scheduling design, aiming to further improve reliability. The results showed improved performance in terms of reliability within the network size of 100, compared to the minimal scheduling function, for all tested conditions. However, with more challenging traffic conditions, the performance still deteriorates. The main reason is the poor proliferation of information.

To further improve the scalability, an increased penetration to shared resources (cells) is necessary. That is, any node under the common ancestry (in the topology) can negotiate for available cells. This functionality of distributed scheduling is incorporated in the proposed Decentralized and Broadcast-based Scalable Scheduling Reservation protocol (DeSSR), which exhibits high reliability under heavy traffic conditions, incurs low latency, and low consumption of TSCH cells compared to other solutions under this category.

Acknowledgement

I thank the **Goddess of wisdom - Mother Gayatri** for grace and wisdom, bestowed on me. I also thank my **principal supervisor- Dr. Mario Kolberg** for leading my way patiently throughout this journey.

List of Publications

During the journey of this research, the following journal articles were produced, with one currently under peer review in the IEEE Sensors Journal.

K. Kumar and M. Kolberg, "DeSSR: A Decentralized, Broadcast-Based Scalable Scheduling Reservation Protocol for 6TiSCH Networks," in *IEEE Internet of Things Journal*, vol. 11, no. 7, pp. 12728-12744, 1 April1, 2024, doi: 10.1109/JIOT.2023.3338289(Material from this paper has been used in Section 4, 5, and 6).

K. Kumar and M. Kolberg, “Hybrid Scalable Scheduling Reservation Protocol for Industrial IoT Networks”, in IEEE Sensor journal, Under review, 2024 (Material from this paper has been used in Section 3, and 4).

Table of Contents

List of Figures

List of Tables

List of Acronyms

3GPP - 3rd Generation Partnership Project

4G/5G - Fourth Generation/Fifth Generation

5G - Fifth Generation

6G - Sixth Generation

6LoWPAN - IPv6 over Low-Power Wireless Personal Area Networks

6LBR - IPv6 6LoWPAN Border Router

6LR - IPv6 6LoWPAN Local Router

6TiSCH - IPv6 over the TSCH mode of IEEE 802.15.4e

6Top - 6TiSCH Operation Sublayer

AI - Artificial Intelligence

AID - Hierarchical Association Identifier

ALOHA – Word that have many translations over different languages

AM - Amplitude Modulation

AMQP - Advanced Message Queuing Protocol

AODV- Ad hoc On-Demand Distance Vector

AoA - Angle of Arrival

ALICE - Autonomous Link-based Cell Scheduling

ALICE-FP - Autonomous Link-based Cell Scheduling- Frame pending

AMSF – Adaptive Minimal Scheduling Function

AP - Access Point

API - Application Programming Interface

ADP - Approximate Dynamic Programming

ASN – Absolute Serial Number

BLAST - Bursty, Asynchronous, Stealth, Transitive

BER – Bit Error rate

BLE - Bluetooth Low Energy

BPSK: Binary Phase Shift Keying

BPS – Bit Encoded per Second

BS - Base Station

BSC - Base Station Controller

CI – Confidence Interval

CDF – Cumulative Distribution Function

CIoT - Cellular-based Internet of Things

CAT- M1 - Category M1

CoAP - Constrained Application Protocol

CSMA/CA - Carrier Sense Multiple Access with Collision Avoidance

CSS - Cell Selection Strategy

CSS - Chirp Spread Spectrum

CPS – Cyber-Physical System

CRC – Cyclic Redundancy Check

D7A - DASH7 Alliance Protocol

D7AActP - DASH7 Application Protocol Action Protocol

D7AAdvP - DASH7 Application Protocol Advertisement Protocol

D7AP - DASH7 Application Protocol

DALI - Digital Addressable Lighting Interface

DAO - Destination Oriented Dynamic Acyclic Graph Advertisement Object

DAO- ACK - Destination Oriented Dynamic Acyclic Graph Advertisement Object Acknowledgement

DIO - Destination Oriented Dynamic Acyclic Graph Information Object

DIS - Destination Oriented Dynamic Acyclic Graph Information Solicitation

DISCA - Distributed Scheduling Converge cast in multichannel Wireless Sensor Networks

dBm: Decibels relative to one milliwatt

DBPSK: Differential Binary Phase Shift Keying

DDS - Data Distribution Service

DeAMON - Decentralized Adaptive Multi-Hop Scheduling Protocol for 6TiSCH Wireless Networks

DeSSR - Decentralized Scalable Scheduling Reservation Protocol

DeBRaS - Decentralized, Broadcast-based Scheduler

DeTAS - Decentralized Traffic Aware Scheduling Algorithm

DHCPv6 - Dynamic Host Configuration Protocol for IPv6

DoD - Department of Defence

DL – DL

DSSS - Direct Sequence Spread Spectrum

DSR – Dynamic Source Routing

DTS - Dynamic Traffic Strategy

EC-GSM - Extended Coverage Global System for Mobile Communications

EDSF – Enhanced Distributed Scheduling Function

eDRX - Extended Discontinuous Reception

EB – Enhanced Beacon

ELF - Extremely Low Frequency

EI - External Interference
EOTF - Extension of OTF
ESF0 - Enhanced Scheduling Function Zero
EMSF - Enhanced Minimal Scheduling Function
ETX - Expected Transmission Count
ETSI - European Telecommunications Standards Institute
FDD - Frequency Division Duplex
FDMA: Frequency Division Multiple Access
FEC - Forward Error Correction
FHSS - Frequency-Hopping Spread Spectrum
FIFO – First In First Out
FM - Frequency Modulation
FSPL - Free Space Path Loss
GFSK- Gaussian Frequency Shift Keying
GMSK - Gaussian Minimal Shift Keying
GHz – Gigahertz
GMSC - Gateway MSC
GMPLS - Generalized Multiprotocol Label Switching
GPS - Global Positioning System
GSM - Global System for Mobile Communications
GUI - Graphical User Interface
HARQ – Hybrid Automatic Repeat Request
HART - Highway Addressable Remote Transducer
HVAC – Heating ventilation and Air Conditioning
HF - High Frequency
HF- OTF – Hysteresis Free OTF
HTTP - Hypertext Transfer Protocol
HLR - Home Location Register
IEEE - Institute of Electrical and Electronics Engineers
IETF - Internet Engineering Task Force
IEC - International Electrotechnical Commission
IoT - Internet of Things
IIoT – Industrial Internet of Things
IMSF - Improved Minimal Scheduling Function
IP - Internet Protocol
IPv6 - Internet Protocol Version 6

IHC - IPv6 Header Compression

IR - Impulse Radio

ISA- Instrument Society of America

ISI – Inter Symbol Interference

ISM - Industrial, Scientific, and Medical

IT - Information Technology

JP - Join Proxy

KA – Keep Alive

KPI – Key Performance Indicator

LBT- Listen Before Talk

LF - Low Frequency

LLNs - Low-Power and Lossy Networks

LLSF- Low latency Scheduling Function

LoRa - Long Range

LPWA: Low-Power Wide Area

LPWAN - Low Power Wide Area Network

LPWANs - Low Power Wide Area Networks

LSP - Label Switched Path

LTE - Long-Term Evolution

LTE-M - Long Term Evolution-M

LV - Local Voting

M2M - Machine to Machine

MAC - Media Access Control

mAh: Milliampere-hours

MCU – Microcontroller Unit

MP2P - Multipoint-to-Point

MPLS- Multiprotocol Label Switching

MPL - Multicast Protocol for Low-power and Lossy Networks

MQTT - Message Queuing Telemetry Transport

MSC - Mobile Switching Centre

MSF - Minimal Scheduling Function

MTU - Maximum Transmission Unit

MVHR – Mechanical ventilation and Heat Recovery

MRHOF - Minimum Rank with Hysteresis Objective Function

NB-IoT - Narrowband Internet of Things

NDS – Network Depth Strategy

NFC - Near Field Communication

NS - Network Server

OF0 – Objective Function Zero

OFDMA - Orthogonal Frequency Division Multiple Access

O-QPSK - Offset Quadrature Phase Shift Keying

OSCORE - Object Security for Constrained RESTful Environments

OT - Operational Technology

OTF - On-The-Fly Bandwidth Allocation

PCE - Path-based Computation Engine

P2MP - Point-to-Multipoint

P2P - Point-to-Point

PAN ID - Personal Area Network Identifier

PAS - Packet Aggregation Strategy

PDR - Packet Delivery Ratio

PER - Packet Error Rate

PN - Pseudorandom Noise

PP - Preferred Parent

PRB - Physical Resource Block

PRBS - Pseudo-Random Binary Sequence

PSTN - Public Switched Telephone Network

PSK – Pre-Shared Key

QAM - Quadrature Amplitude Modulation

QOS - Queue Optimization Strategy

QoS - Quality of Service

QPSK - Quadrature Phase Shift Keying

QSS - Quick Setup Scheduling

RFC – Request For Comment

RA – Route Advertisement

RF - Radio Frequency

RFID - Radio Frequency Identification

RF-LoRaWAN - Radio Frequency Long Range Wide Area Network

RFTDMA - Random Frequency Time Division Multiple Access

RL - Reinforced Learning

Rel – Release

ReSF - Recurrent Scheduling Function

RPL - Routing Protocol for Low-power and Lossy Networks

RPMA - Random Phase Multiple Access

RSVP-TE - Resource Reservation Protocol-Traffic Engineering

Rx – Receive

RAW - Restricted Access Window

SDO – Standard Development Organization

SDN - Software-Defined Networking

SF - Scheduling Function

SF – Spread Factor

SF0 - Scheduling Function Zero

SGSN - Serving GPRS Support Node

SLAAC - Stateless Address Auto Configuration

SLF - Super Low Frequency

SNR - Signal-to-Noise Ratio

SNIR- Signal-to- Noise-plus- Interference Ratio

SoC - System on Chips

SPS - Smart Parking Systems

SSR - Scalable Scheduling Reservation Protocol

SUN – Smart Utility Network

TASA - Traffic-Aware Scheduling Algorithm

TTF - Tag-Talk-First

TCP - Transmission Control Protocol

TDMA - Time Division Multiple Access

TDoA - Time Difference of Arrival

Thread - A low-power wireless mesh networking protocol

THz – Terahertz

TESLA - Traffic Aware Elastic Slotframe Adjustment

TIM - Traffic Indication Map

TLS - Transport Layer Security

ToF - Time of Flight

TPMS - Tire Pressure Monitoring Systems

TSCH - Time-Slotted Channel Hopping

TSMP - Time Synchronized Mesh Protocol

TWR - Two-Way Ranging

Tx – Transmit

UDP - User Datagram Protocol

UHF - Ultra High Frequency

UL – UL

UNB - Ultra Narrow Band

VHF - Very High Frequency

VoIP - Voice Over Internet Protocol

VRB – Virtual Assembly Buffer

Weightless -P (Refers to a series of LPWA standards, no specific expansion given)

Wi-Fi - Wireless Fidelity

Wi-Fi SUN - Wireless Fidelity Smart Utility Network

WirelessHART - Wireless Highway Addressable Remote Transducer

WPAN - Wireless Personal Area Network

WSN - Wireless Sensor Networks

YSF- (no full form provided)

ZigBee - (No specific expansion given, it is a proprietary term)

Z-Wave - (no full form provided but it is a wireless communication protocol)

1. INTRODUCTION

1.1. Background and motivation

The Internet of Things (IoT) is a new paradigm, allowing data gathering using sensors and actuators on a real-time basis. From smart kitchens to smart homes, and to smart cars, the applications of IoT are increasingly becoming popular, with or without internet support [1], with home application alone holding the largest share witnessing growth of 48% while connected car applications are growing at 30%. Ericsson's report predicts that by 2029 there will be 38.9 billion IoT connections globally. Of these, 32.3 billion will be dedicated to short-range IoT devices [2]. This significant growth is driven by the enhanced capabilities of wireless networks, enabling spectrum sharing, and cooperation with frequency division duplex (FDD) bands to facilitate the integration of operational technology (OT) with information technology (IT). Using these capabilities, IoT navigates key areas in fourth industrial revolution (Industry 4.0) where it contributes to improved production and reduced cost of operation via automation.

Currently, IEEE 802.15.4 is a popular low power radio standard due to its global penetration and is allowed to operate without any restriction worldwide [3]. The standard supports multiple frequency bands, with the 2.4 GHz band being the default setting. Apart from this, it also includes sub-GHz bands (868 MHz in Europe, 915 MHz in the Americas, and 780 MHz in China) to cater to specific regional requirements and applications needing longer range and improved propagation using lower band frequencies.

Traditional low-power short range wireless technologies such as ZigBee [4], BLE [5], WirelessHART [6], and ISA 100.11a [7] by default use IEEE 802.15.4 standard. However, managing communication is critical, especially handling frequent interaction among heterogenous devices assembled with varying amount of processing and memory capacity, payload incompatibility (a pronounced vulnerability as the heavy User Datagram Protocol (UDP) payload of 127 bytes is hardly transmitted by resource-constrained IoT devices), and poor reliability due to technological barriers such as Multipath-fading, External Interferences (EIs), and increased collision on carrier frequencies.

Many low-power variants of standard Wi-Fi have been seen evolving recently where Wi-Fi-802.11ah [8] is specifically designed to address payload interoperability: each sensor device is capable of transmitting a large amount of payload distances over hundreds of meters from the gateway router using an asynchronous connectivity model. The device can sleep for long duration; however, reliability cannot be guaranteed due to poor resistance to wireless interferences.

To overcome existing challenges and improve communication reliability, IPv6 Low Power Wireless Personal Area Network (6LoWPAN) [9] was proposed, which provided with adaption and compression capabilities. For adaption, it divides the total payload into manageable number of fragments so the payload is transmitted reliably and in a timely manner and compression of headers is carried out using Ipv6 Header Compression (IHC) technique [10].

In low-power short-range wireless sensor networks, due to EIs, particularly those caused by noise from metallic surfaces of sensor nodes, which tend to worsen as the number of nodes increases beyond 30-50 nodes, leading to more frequent collisions, and loss of data packets. With increased density of nodes beyond 30-50, the complexity of the multipath interactions increases, leading to deep fade where the received signal strength is insufficient for decoding a packet successfully. The EIs from the coexisting networks, operating in the same frequencies, can further deteriorate the signal quality.

Wireless sensor networks are evolving with spectrum-sharing and a densely populated network is prone to suffer from an increasingly congested medium without a rule-based order. This congestion can be worsened by noise from metallic surfaces, which adds to the overall interference and reduces the effective bandwidth available for communication.

As the number of nodes increases, the cumulative noise from all these sources can significantly reduce the signal to noise ratio. SNR determines the quality of the received signal. It is defined as the ratio of the power of the desired signal to the power of the background noise, usually expressed in decibels, making it harder for nodes to distinguish between valid signals and noise (thus difficult to decode). This leads to increased packet loss and retransmissions.

With more nodes, the likelihood of nodes being within each other's interference range increases. This is particularly problematic in multipath environments with signals reflecting off the metallic surfaces of the sensor devices. The interference range can be unpredictable due to reflections and scattering of signals. The overlapping interference ranges create zones where multiple nodes suffer from severe signal-fading.

In dense networks, nodes are often forced to reduce their transmission power to avoid excessive interference. However, low power transmissions are more susceptible to interference, especially from metallic surfaces, leading to fragile connectivity. The cumulative effect of interference from multiple nodes can lead to a saturation point where the network can no longer effectively manage the interference. This saturation is more likely to occur in the presence of metallic surfaces, which amplify and reflect signals, adding to the overall noise floor.

Overall, the presence of metallic surfaces introduces complex interference patterns and additional noise that compound the challenges already present in large-scale wireless sensor networks. As the number of nodes increases beyond 30-50, these factors interact in ways that significantly degrade network performance, leading to increased packet loss, reduced throughput, and lower overall reliability.

Vendors often recommend site testing to assess signal reception quality before actual deployment. This approach helps evaluate the impact of coexisting networks such as Wi-Fi, Bluetooth, and ZigBee, which operate on similar frequency bands. In a multipath environment, signals from these technologies can overlap; this results in amplification momentarily if these signals align constructively (trough to trough and crest to crest) or causes path-loss due to destructive interferences when multiple echoes are received within different phase with a smaller delay (nanoseconds). The path loss is more pronounced when a signal is hit by a metal or concreate compared to the wood or glass, and the more barriers the signal has to pass through, the greater the path loss; it can be triggered on a selective carrier frequency, called *selective frequency fading* or through the entire bandwidth, called *flat-fading*.

Typically, path-fading is divided into fast-fading and slow-fading. The fast-fading mainly occurs in the multipath propagation as the signal encounters the physical objects such as *wall, floors, or machinery*; the reflected signal creates multiple echoes, and get received via different alternative paths, causing constructive or destructive interferences. The destructive interference can cause *deep fade* (the areas where the signal strength is 0); the receiver is unable to decode such signals. Contrarily, the signal echoes arrived within the same phase and time add up to boost the signal strength. The slow-fading is caused by the shadowing where the signal is completely blocked by an obstacle such as tall building or hills. The signal loss follows a uniform distribution

The different causes of signal loss are as follows:

<u>Free Space based path Loss or FSPL</u>: According to FSPL, the signal strength is degraded due to free space which increases as square of distance.

<u>Shadowing:</u> When larger objects such as hills and large buildings are blocking the line of sight between sender and receiver, resulting in a steady degradation of signal strength over an increased distance. The signal loss follows a normal distribution.

<u>Reflection:</u> This occurs when signals encounter obstacles and are redirected, altering their propagation path. This phenomenon contributes to multipath propagation where multiple copies of a signal arrive at the receiver using different-different paths. Here, some signals may arrive within the time, and without shifting the angle too much and the others may arrive a slightly outside the time, with different phase. Those arrived in time and within the same angle add up and boost the strength of the signal while the destructive signals tend to reduce the signal strength, creating black spots (areas with no connectivity). This is because signals did not bend around obstacles to reach hidden regions. The constructive interference from reflected signals can amplify signal strength in certain areas, forming hot spots (areas with good reception) with unexpectedly high signal altitude.

<u>Diffraction:</u> This aspect leads to bending of a signal as it hits an obstacle and reaches edges and hidden regions using diffraction. The signal loss is more pronounced depending on the wavelength and the height of an objects.

<u>Scattering:</u> This refers to a scenario when signals hits small particles (dust, metal object, factory floor) or irregularities in the medium that it propagates through. The signal changes direction causing it to loose strength.

<u>Atmospheric Effects:</u> A signal gets weaker and may cause a propagation loss especially within selective frequencies (higher frequency range) caused by the atmosphere itself (rain, snow, time of the day, season etc.). The impact of ground noise can attenuate the signal as the signal propagates closer to the earth surface. This type of loss is measured using Signal to Noise Ratio (SNR).

<u>Doppler Shift</u>: It is caused by the relative movement between the two devices and leads to a change of frequency of received signal. It is normally exhibited within mobile telecommunication network.

Multipath-fading persists in nearly all wireless networks where the path-loss can vary depending on the shortest path and non-shortest path, with Line of Sight (LoS), the shortest path signal is the strongest; with Non-line of Sight (NLoS) a non-shortest path signal likely to be strongest due to reflection and diffraction; for example, in an outdoor environment, the LoS conditions can be inferred when the received signal strength along the shortest path remains more reliable. Signal degradation primarily occurs over longer paths (links). In an indoor environment, a signal can take multiple trajectories (short paths) where some are relatively shorter than the others. Here, the non-shortest path is a result of the signal bouncing off the physical objects where an exact pattern of its propagation is difficult to predict. As a result, the shortest path is the weakest path: the receiver often encounters black spots despite the minimal separating distance between a single transmitter and a single receiver [11]. The effect of multipath fading is such that the non-shortest link offers an average good reception.

To mitigate this effect of multipath fading, one must to relocate the device with extended inter-path distance, when using a single channel. The other solution is *channel-hopping*. Both techniques focus on transition from black spots to an area with good signal quality. Here relocating a device is less practical approach. In contrast, channel-hopping can combat multipath-fading effectively with rapid switching of channels between a transmitter and receiver. Using sufficient separating bandwidth, it can maintain sufficient transitioning distance from black spots, which move around as signals are successfully spread out widely using available channels; thus all areas get an averaged signal of hopefully acceptable strength. The rapid switching between the available channels randomly provides an additional security in terms of preventing jamming and eavesdropping while successfully combating the EIs and multipath fading [11].

In Low Power and Lossy Networks (LLNs), a receiver computes Packet Delivery Ratio (PDR) based on the estimated value of Received Signal Strength Indicator (RSSI). PDR is a key link metric representing the success rate of transmitted packets between two sensor devices. It is defined as the ratio of successfully received packets to the total number of packets sent over a given time. A high PDR (close to 1 or 100%) indicates a stable and reliable link, whereas a low PDR may suggest interference, signal degradation, or congestion. IEEE 802.15.4-enabled devices can monitor PDR along with other link metrics like RSSI to maintain accuracy of link quality.

RSSI is a measurement of the power level that a received radio signal has at a device, typically characterized in decibel-milliwatts(dBm). It is energy-efficient approach, commonly used in wireless communication to gauge signal quality and determine the physical distance between devices (proximity), and strength of a signal from a transmitter, to help assess connection quality and reliability.

The Internet Engineering Task Force (IETF) and Institute of Electrical and Electronics Engineers (IEEE) promoted new standards that mitigate these barriers and allow seamless connections. The IETF is known for developing and promoting Internet standards. It operates as an open standards organization, composed of various working groups (WGs) focusing on different aspects of Internet functionalities. The other key organization is the IEEE- a leading professional association focused on gearing technological innovation in the fields of electrical, electronics, computing, and related disciplines. IETF & IEEE, in 2013, jointly rolled out Time Slotted Channel Hopping (TSCH) over IEEE 802.15.4 as a MAC layer protocol [3]. That was 1 year after the introduction of routing protocol for low power and lossy operation (RPL) routing protocol [12].

TSCH is the combined strength of Time Division Multiple Access (TDMA) [13] with channel hopping capability. **Channel-hopping** mitigates the impact of obstacles on signal transmission, particularly in environments where **multipath propagation** affects reliability. **It** enhances robustness by dynamically switching frequencies. For example, the radio of IEEE 802.15.4 under ISM 2.4GHz can constantly ‘‘hop’’ approximately 1600 times in a second among different channels where the approximate slot time is 10ms and total channels being 16, each separated with 5MHz (sufficient to avoid black spots [11]).

TDMA is a MAC-layer protocol that allows spectrum by dividing the available bandwidth time into timeslots and channel-hopping translates the single channel into different-2 radio frequencies; however, the implementation of TSCH has ignored efficient utilization of these resources. The main reason is that the sensor nodes tend to reassess their routing position frequently seeking shortest path to root where the demand of bandwidth required per node is difficult to predict in advance using fixed patterns. This caused under or over evaluation of link-layer resources against actual traffic demand. To improve the communication performance, a cross layer called 6TiSCH Operation (*6Top) layer* [14] was introduced to synergize TSCH with the rest of the IPv6 LoWPAN stack. The resultant stack was called IPv6 over the TSCH mode of IEEE 802.15.4e (6TiSCH) [15], which is used in this thesis.

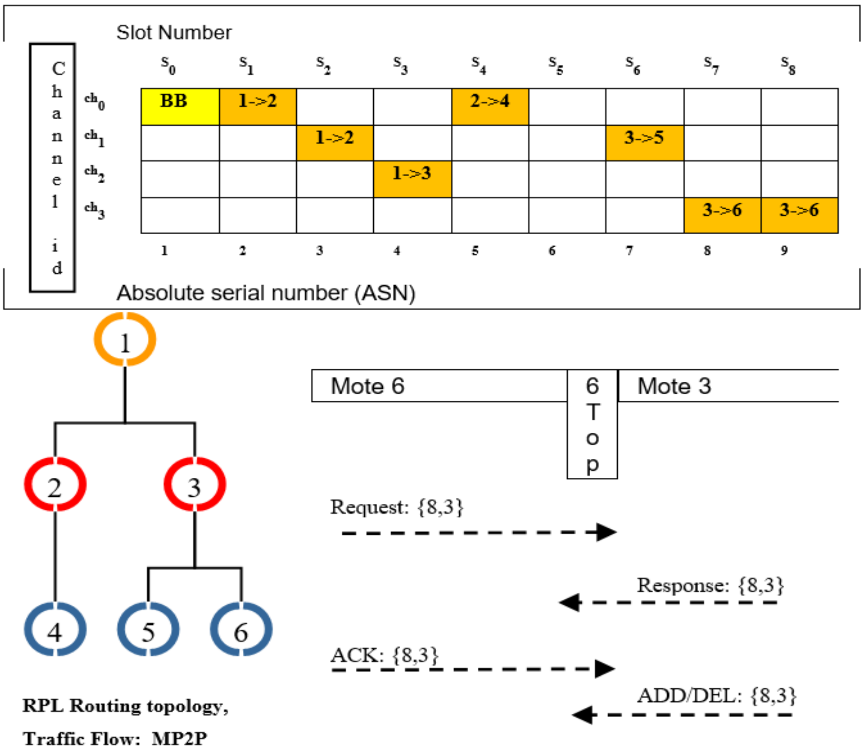

Figure 1: TSCH operation using RPL topology, slotframe and 6top operation.

Figure 1 incorporates 3 key diagrams within its structure. This includes a routing topology using 5 sensor nodes headed by a single representation of controller (root), TSCH slotframe comprising 9 timeslots and 4 channels is located at the top, and 6Top mediation as the way to acquire cells for transmission or reception using negotiations between sensor nodes (motes).

RPL is a routing protocol designed to be lightweight solution for a low-power, short-range wireless sensor network. It is a proactive protocol that maintains a routing table in advance at the root level. This is a crucial difference between a proactive and reactive routing protocol where reactive protocols do not maintain any routing entry in their buffer and the routes are formed concurrently using broadcasting and multicasting techniques; hence providing a more accurate and reliable routing information avoiding asymmetric bidirectional paths in the network. The key weakness of the reactive approaches is the high energy consumption. In contrast, the proactive approaches do not perform transmission of broadcast beacons frequently across the network. Here, each node must maintain a sufficient storage where a complete routing table is available for path searching (look up). This allows routing with the shorter number of hops (or one-hop) to the destination, causing reduced latency (by a significant margin) and improved throughput in comparison to reactive approaches. However, proactive approaches are less transparent with underlay topology management, causing longer source path or no source path to the destination, which eventually leads to packet loss. The standard wireless protocols like Ad hoc On-Demand Distance Vector (AODV) [16] and Dynamic Source Routing (DSR) [17] offer high reliability due to being reactive but are not as lightweight as RPL, making them poorly scalable for IIoT networks; hence RPL remains the standard routing protocol for LLNs.

A TSCH cell is a tuple comprising a timeslot (*Ts)* and a channel id (*Ch)*. In the given slotframe, the top-left cell is a *minimal cell* (single broadcast schedule used for propagation ensuring that nodes are tightly synchronized and network is operational), shared by all sensor nodes for *joining* the network topology, while the other *cells* are used for communication purposes in TSCH-led operation.

The implementation of slotframe can be customized to meet the varying demands of industrial IoT applications. For example, for a larger network comprising hundreds of nodes, a single broadcast cell is not enough, so it is possible to use more than 1 advertising medium (cell) at the risk of increased energy consumption. The rest of the slotframe is utilized for various communication activities in the wireless sensor network including managing network topology and sending data packets.

In the example shown in Figure 1, cells for reception and transmission are scheduled in a half-duplex manner. TSCH is inherently half-duplex. So that sender and receiver cannot use the same cell simultaneously. All connected nodes follow the pseudo-random sequence as provided in equation (1). While timeslots can be programmed using the scheduling function (SF), the channel-hopping proceeds according to the equation below:

$$\boldsymbol{Channel} = \boldsymbol{F}(\boldsymbol{channel\ offset} + \boldsymbol{ASN})\%\ \boldsymbol{channel\ density}\ldots\ldots\ldots\ldots\ldots(1)$$

The *channel offset* represents frequency, ranging from 0 to 15, provided by default. Absolute Slot Number (*ASN*) counts timeslots elapsed since network started. It is a five byte long counter, which can keep the network going for a long time without wrapping. Furthermore, *ASN* is used to track the global clock time across all devices in the network. Every time slot in the TSCH schedule has a unique ASN, and it is incremented by 1 at the beginning of each new time slot. By knowing the current ASN, nodes can stay synchronized and communicate during their assigned time slots. However, this design does not completely eliminate the possibility of collisions, which remains an open issue, especially in scalable, load-intensive 6TiSCH applications.

Channel density represents the number of available channels at given spectrum of 2.4GHz. Typically, the number of channels available at 2.4 GHz in IEEE 802.15.4 is 16, comprising a sequence of numbers 11,12,13,14,15,16,17,18,19,20,21,22,23,24,25,&26. The *base channel* is the starting frequency in the hopping sequence. *Function F* provides mapping between integers (0-15) into a actual physical channel [18]. It generates a sequence, which is predictable without applying randomness. Figure 1 showed a small slotframe comprising 9 slots (S_0 , S_1, S_2.... S_8) and 4 (ch_0, ch_1...ch_3) channel offsets, with ASN increasing after each slots to maximum of 9.

Prior applying randomness, the formula becomes F(x)= x here x = channel offset + ASN. This value is an index, used for mapping between actual channels; for example using 4 channels as per the example shown in Figure 1, the index value will fetch the appropriate channel from the list of available channels where the first 4 channels are 11, 12, 13, and 14. The equation performs 4 rounds of channel selection, assuming non-randomness using equation 1:

ASN= 1, and channel offset (*Ch)= 0, channel density = 4 channel = F(0+1) % 4 = 12 % 4 = 0*

ASN= 1, and channel offset (*Ch)= 1, channel density= 4 channel = F(1+1) % 4= 13 % 4 = 1*

ASN= 1, and channel offset (*Ch)= 2, channel density= 4 channel = F(2+1) % 4= 14 % 4 = 2*

ASN= 1, and channel offset (*Ch)= 3, channel density= 4 channel = F(3+1) % 4= 11 % 4 = 3*

ASN= 2, and channel offset (*Ch)= 0, channel density = 4 channel = F(0+2) % 4 = 13 % 4 = 1*

ASN= 2, and channel offset (*Ch)= 1, channel density= 4 channel = F(1+2) % 4= 14 % 4 = 2*

ASN= 2, and channel offset (*Ch)= 2, channel density= 4 channel = F(2+) % 4 = 11 % 4 = 3*

ASN= 2, and channel offset (*Ch)= 3, channel density= 4 channel = F(3+2) % 4= 12 % 4 = 0*

The output in sequence (0,1,2,3, 1,2,3,0.) seems predictable hence randomness is required. The channel hopping applied over TSCH mode of IEEE 802.15.4 use pseudo-random sequence to provide randomness . Using an example of F(x)= (x*3+1) where x = channel offset + ASN, the following channels are provided over the given parameters:

ASN= 1, and channel offset (*Ch)= 0, channel density = 4 channel = F(3(0+1) + 1)% 4 = 11%4= 3*

ASN= 1, and channel offset (*Ch)= 1, channel density= 4 channel = F(3(1+1)+1) % 4= 14 % 4 = 1*

ASN= 1, and channel offset (*Ch)= 2, channel density= 4 channel = F(3(2+1)+1) % 4= 13 % 4 = 1*

ASN= 1, and channel offset (*Ch)= 3, channel density= 4 channel = F (3(3+1)+1) % 4= 12 % 4 = 0*

ASN= 2, and channel offset (*Ch)= 1, channel density = 4 channel = F(3(1+2)+1)% 4 = 13%4 = 1*

ASN= 3, and channel offset (*Ch)= 1, channel density= 4 channel = F(3(1+3)+1) % 4= 12 % 4 = 0*

ASN= 4, and channel offset (*Ch)= 1, channel density= 4 channel = F(3(1+4)+1) % 4= 11 % 4 = 3*

ASN= 5, and channel offset (*Ch)= 0, channel density= 4 channel = F (3(1+5)+1) % 4= 14 % 4 = 1*

The output in sequence demonstrates random numbers (3, 1, 1, 0, 1, 0, 3, 1), just with 4 channels, and with more channels allowed, the sequence will be unpredictable, leading to channel-hopping. It allows nodes to select a times slot with a channel offset to perform transmission and reception.

The example in Figure 1 shows interaction between nodes in the slotframe using the routing topology (on bottom-left): node 2 is scheduled to hear from node 1, on channel $ch_{0,}$ indicated with forwarding arrow and that the node 2 can use the same cell to transmit data packet to node 1 provided the half-duplex nature of TSCH, and it has further scheduled next timeslot S_2, on ch_1. Similarly, at (S_3, ch_2), node 1 sends information to node 3. Node 2 is scheduled to turn on radio at (S_4, ch_0). Then there is a gap in which no node is either sending or receiving packets during $S_{5.}$ After this slot, node 3 has scheduled transmission to *node 5* at (S_6 , ch_1). As shown in the slotframe, this node has further scheduled two more slots ($S_{7\,,}$ S_8) consecutively on ch_3. This example is a reflection of channel use over varying slot number by different nodes. The sequence of channels in use by the nodes over time (ASN) followed a randomness (0,1,3,0, no activity, 1, 3, & 3). The downside of the channel-hopping is that it does not guarantee collision under frequent transmission. The channel id does not wrap, as it repeats over time.

The example in Figure 1 further illustrates a communication pattern allowing multiple nodes to send data packets assuming symmetrical bidirectional path to root, and once the packets have reached root, a compressed header translating path to the destination in the topology is attached to each packet. There are three communication patterns incorporating data collection in the wireless network: Multi Point to Point (MP2P), Point to Multi Point (P2MP), and Point to Point (P2P). These patterns are further illustrated in Figure 23. Currently, 6TiSCH is only optimized for MP2P and P2MP. This means, nodes are not provisioned to store the entire routing table and that the decision to compute the optimal path is taken by the root. The root node is a powered device that has sufficient resources required to carry out key operations in addition to network startup and managing various aspects of wireless activities.

Figure 1 also depicts a 2-way negotiation of cells mediated by 6Top. According to this, 'mote *6' or* node 6 sends a request for a cell (*8,3*) that is primarily held by 'mote *3'* in the slotframe. 'mote *3'* then sends a successful response while awaiting an acknowledgment from *'*mote *6'* so that it can get 6Top to *ADD* the cells to the schedule of 'mote *6'*.

In 6TiSCH, SF is responsible for providing key instructions related to scheduling. 6TiSCH scheduling is divided into three main categories, including *Centralized*, *Distributed*, and *Hybrid* scheduling. SFs implementing centralized scheduling use excess signaling to acquire collision-free cells directly due to one-hop access to the controller; though a majority of SFs under this category have suffered from scalability limitations due to high communication overheads. Distributed scheduling uses negotiations between sensor nodes to promote a bargain of bandwidth in the form of TSCH cells. Here, collision is likely when two or more nodes can end up adding to an already active schedule or a schedule that has resulted in other conflicts.

A cell can be described as a hard cell or a soft cell whereas the hard cell can only be configured once, and cannot added or removed after the bootstrapping period. Conversely, a soft cell can be added and deleted on the run time. Distributed SFs mainly use soft cells for meeting traffic demands in the network and this too is left unto the SF which then decides whether to declare the cell as shared or dedicated in addition to adding or removing it through the buffer of the node. A shared cell is accessed on contention-basis where the delay accessing it is attributed to resulting latency while upstreaming the traffic to the root. But the dedicated cell uses a unique schedule leading to a comparatively faster execution. However not only are these costly but they can also; can strike collision over excess use. Thus, collision in the slotframe can not be ruled out in distributed scheduling.

To reduce overheads, a negotiation-free distributed approach was introduced where each node has to have at least one active cell computed at the time network formation and to be shared with other nodes in a unicast manner. It is active at all times (autonomous) and nodes can use this schedule at anytime to exchange information with connected neighbors; utilizing *autonomous* cells. From the scalability point of view, nodes not only suffer from increased delay in transmission over accessing the autonomous cells but also drop packets due to a temporary peak of the traffic. This is because most nodes follow shortest-best path to root and it is likely for some nodes to experience heavier traffic conditions than the others in the network. Thus neither SFs are scalable for large-scale networks.

Hybrid scheduling harnesses the benefits of more than one scheduling approach by appropriately adjusting them into the TSCH frame. Recently, the Minimal Scheduling Function (MSF) has emerged as a full-featured SF using on the fly bandwidth allocation (OTF) for adaption of data traffic and autonomous scheduling for managing network dynamics. However, both MSF and OTF use a fixed threshold-based allocation per node, which under-or-over estimates the demand of cells by sensor nodes in a dynamic network. This triggers bandwidth wastage and *idle-listening* (current consumption under *Idle* listening is explained in Chapter 3).

Recent studies have shown that scalability is an open challenge, attributed to the poor performance of SFs. This includes lack of traffic awareness, poor control over demand and supply of cells, inefficient cell selection, and congestion in queue (node's transmission buffer).

In this thesis, a novel scheduling model is proposed, which is a combination of four strategies and an analytical approach called, '*cake-slicing*'. The proposed solution uses *cake-slicing* to adapt the TSCH slotframe across distribution patterns, which is dependent on fluctuating the routing topology depth. The proposed solution assumes that the nodes closer to the border router (root) must be given more cells to fast forward the traffic compared to the nodes further-away from the root. The *cell selection* ensures that under normal traffic conditions, SF must not scan the entire slotframe. This was necessary to prevent *idle-listening* and cut down waiting time. To reduce the collision in transmission schedule, the proposed scheme utilizes the *channel-change* approach, which was initially suggested by *Duy et al.,*

[19]. However, the channel-change has limited use in this thesis since it is applied to unicast-based distributed scheduling alone. For the remaining approaches, channel offset is selected randomly and is subject to implementation. As far as *queue* balancing is concerned, the proposed scheme implies keeping the network resilient using the slicing-based traffic calming measure called Packet Aggregation Strategy (PAS). The proposed work will use 6Top dynamics to locate a node's real-time routing position in the topology and it does not trigger additional overheads to establish distance from root to source node. This will provide a context for pre-assessing overprovisioning requirements in the network. The *cake-slicing* technique will provide SF with an opportunity to adapt traffic conditions in a context-aware manner and it will also be utilized for *cell selection* and *queue optimization* purposes.

The solution offers improved scalability, improved **throughput**, with improved Quality-of-Service (QoS), and enhanced coverage (1- 2 km) using densely populated multi-hop topology. That is, **50-70** IoT devices per subnet (depending on traffic conditions) by unicast-based distributed scheduler and **100 devices** per subnet with an extended coverage range of up to 2 km through hybrid scheduler and **up to 700 devices** per subnet under broadcast-based scheduling design.

1.2. Aims and Objectives

This research project aims to improve scalability by optimizing the communication performance of the 6TiSCH network for a dense, and large-scale operation using SSR. The proposal adheres to 6TiSCH QoS considerations unanimously (these are key performance measures such as latency, reliability, and energy-efficiency, used to fulfill the design objectives of 6TiSCH) and guarantees improved communication performance of 6TiSCH networks. Hence, building a proposal to improve scalability of single-sink headed IPv6 subnet using IoT devices under synchronous network model. The following are the key objectives of this research:

1. The thesis reviews popular IoT communication technologies and standards, followed by the evaluation of related technologies in the context of industrial automation.
2. The thesis briefly navigates through the core components of the 6TiSCH Architecture and reviews SFs where it assesses the suitability of MSF being a scalable solution based on the traffic conditions, energy saving, latency and reliability.
3. The thesis reviews existing 6TiSCH scheduling approaches and provides justification over the selection of evaluation methodology.
4. This thesis will design an analytical technique called *cake-slicing* to facilitate efficient scheduling operation in 6TiSCH network. This technique is further exploited to optimize synergies between key scheduling metrics (network depth, traffic adaptation, cell selection, and queue optimization).

5. This thesis will evaluate the performance of the proposed solution (SSR) using distributed scheduling, benchmark results against key related distributed SFs, and outlines the key limitations in terms of scalability.

6. To address scalability limitation posed by distributed scheduling using dedicated cells, the thesis proposes implementation of SSR in a hybrid scheduling model. This thesis evaluates the performance of the SSR and benchmarked results using MSF.

7. To further improve scalability, the thesis proposes an enhancement of SSR using additional sets of measures and implementing the final solution in a decentralized, broadcast-based scheduling operation. This thesis evaluates the performance of the DeSSR using steady traffic, bursty traffic experimentation where key algorithms (LV and OTF) were included for analysis

8. This thesis evaluates the performance of the DeSSR using steady traffic, bursty traffic experimentation where state-of-art algorithms (LV and OTF) were included for analysis.

9. The thesis now evaluates the scalability limit of DeSSR under exceptionally challenging traffic load in a dense, and large-scale deployment, and concludes the study undertaken.

1.3. Contribution

This section provides a list of contributions based on the content of each of the chapters within the thesis, is as follows:

1. **Review of IoT communication technologies:**

Chapter 2 carries out a comprehensive review IoT communication technologies. It was identified that Low Power Wide Area (LPWA) technologies offer sustainable, long range solution, while transmitting small amounts of payload more frequently. However, industrial networks require a reliable solution, which continues to uphold the same standard even under changing traffic conditions. Clearly, LPWANs are not meant for industrial-grade networks, which necessitates real-time flow of information. Cellular-based IoT (CIoT) can meet the industrial goals and they are largely scalable (can allow millions of devices configured with registered network). However, these standard technologies are mostly subscriber-based where the user does not have full control over the network, and adding more devices is expensive. In addition, both LPWA and CIoT are susceptible to signal loss over long distance. For industrial networks, short-range low power wireless personal area networks are more suitable. The evaluation carried out in Section 2.4 in Chapter 2 concluded that 6TiSCH is by far the most advanced solution considering low-power efficiency, latency, impact of wireless interference, and scalability among given Low Power-Wireless Personal Area Networks (LP-WPANs). However, there is more work needed to address the scheduling inconsistencies, which are identified as an area of interest for this thesis.

2. Review of 6TiSCH Building Blocks and Scheduling Functions

The work in the thesis, for the first time, comprehensively reviews the key components of 6TISCH in a layered architecture highlighting key strengths and weaknesses. This review of SFs, is aligned across various categories using a unique taxonomy, with the key focus on communication performance and scalability. This has highlighted potential gray areas where scheduling performance can be further optimized to permit more devices in the same subnet. Section 3.2 in Chapter 3 reviews SFs dedicated to deterministic 6TiSCH network in detail and evaluates the given solutions in line with scalability and communication performance.

3. Design of SSR

A proposal to draft *SSR* is designed in Chapter 4. It begins with the *cake-slicing* technique that is aimed to provide a distribution environment to key processes or strategies: *Network Depth Strategy* (*NDS)* collects nodes' dynamics and makes scheduling a topology-aware process. *Dynamic Traffic Strategy* (*DTS)* provides novel mechanisms to adapt traffic conditions in the dynamic network. *Cell Selection Strategy (CSS)* preserves resources and reduces collisions. Finally, *Queue Optimization Strategy (QOS)* is used to ease congestion using hysteresis-free *PAS*, to smoothen the incoming and outgoing traffic on the nodes. A detailed description of each is provided in Chapter 4.

4. Evaluation of SSR under unicast-based distributed scheduling

Chapter 4 deploys the designed solution in the 6TiSCH simulator, developed by a member of the IETF 6TiSCH working group. The performance of the proposed scheduling solution (SSR) was tested under varying network sizes and traffic conditions, with the results compared to key SFs. Many of these SFs were tested using the same evaluation tool. The results showed strong performance, including reduced energy consumption, lower latency, improved reliability, relatively high battery life, and fewer collisions at a traffic rate of 30 ppm. However, the proposal exhibits a steady decline in reliability beyond a network size of 70 nodes when the traffic rate was doubled from 30 ppm to 60 ppm. Additionally, the reliability performance of the current SFs dropped sharply beyond 50 nodes. Key insights from this evaluation that, unlike other SFs, SSR did not experience packet drops due to high collisions or cell outages. Instead, the main issue was the poor propagation of information within the network, which resulted in fewer routes for nodes. Other SFs suffered from poor spectral efficiency because dedicated cells could not be shared. Furthermore, the high volume of 6Top packets was concerning, as most traffic was relayed using dedicated cells, which are limited in the slotframe. Poor propagation and traditional packet forwarding rules, such as First In First Out (FIFO) (where nodes wait for the entire packet to be reassembled before relaying), further strained queue utilization, as all packets were sent along the single best path.

5. SSR using Hybrid Scheduling Design

SSR using unicast-based distributed scheduler suffered from poor reliability beyond 70 nodes following periodic steady traffic of 60ppm. To overcome this limitation, SSR is implemented through a hybrid scheduling model where dedicated unicast cells are used for traffic adaption on run time and *autonomous* cells (shared) are pre-computed for handling network dynamics. This proposal provides improved goodput (it refers to the actual amount of useful data successfully delivered to the application layer per unit of time, excluding protocol overhead, retransmissions, and control messages. Goodput provides a more accurate measure of network efficiency and application performance) compared to the distributed-led version of SSR.

Chapter 5 contains implementation-specific information. The evaluation is carried out using a generic solution (MSF). To analyze scalability, the evaluation was conducted using increased network densities up to 100 nodes, together with challenge traffic conditions (60ppm, 120ppm) and random placement of nodes. The results showed that SSR delivers roughly 20% more packets, leading to 99% or above end-to-end reliability, achieved roughly 1/3rd of latency experienced by MSF, and improved energy consumption following both traffic loads. The hybrid proposal was further tested using linear topology as so far, the experimentation had only used random topology. Finaly, over increasingly higher traffic rates, ranging from 30- 600 ppm, SSR delivers approximately 15% more payload than MSF and offers 96% reliability following 600ppm. The remaining cases with decreasing traffic patterns showed an improved reliability of 99% or above. The latency showed a linear increment as the traffic condition tightens up and battery life remains superior for less challenging traffic. However, hybrid scheduling design is complex, and a single broadcast cell is not sufficient for the entire network. This triggers frequent joining for the nodes at increased distance from the root.

6. Decentralized, and Broadcast-based Scalable Scheduling Reservation Protocol

DeSSR is an enhanced version of SSR, adopting a decentralized, broadcast-based scheduling approach. It primarily uses three randomly located broadcast cells for advertisements, enabling the operation of densely populated networks in a tightly synchronized manner. In contrast, the conventional DeBRaS solutions are known for high energy consumption, which is an inherent drawback of its approach. DeSSR, however, optimizes the number of cells used to improve spectral efficiency and bandwidth utilization so that more nodes can be added to the same network without compromising reception loss of signal. This also minimized unnecessary resource wastage in smaller networks. DeSSR combines features from adaptive NDS allowing increased participation of nodes, and DTS, which incorporates additional link scanning measures, such as PDR, to prevent poorly performing nodes from being assigned excess Tx cells, thereby reducing bandwidth wastage. These planned enhancements were necessary to further boost network scalability, addressing the needs of high-density industrial solutions.

7. Evaluation of DeSSR

The performance of DeSSR was evaluated under steady and bursty traffic conditions using the 6TiSCH simulator. The results demonstrated that DeSSR outperforms key SFs like OTF [20] and Local Voting [21]. This makes DeSSR a robust solution, well-suited for industrial applications requiring high throughput. Benchmarking DeSSR against current solutions, including E-OTF, showed that it provides enhanced reliability even under challenging traffic loads and with networks of several hundred nodes.

8. Conclusion

Our conclusions are based on adoption of the proposed solution and cake-slicing technique to benefit 6TiSCH, providing reliable, low-latency, and energy-efficient communication. The proposal leads to the steady improvement in overall communication performance using varying implementations of SSR, each with improved scalability for industrial applications. Among these, DeSSR is preferable for a highly dense network used in various purposes across IoT deployments. The following application scenarios are depicted corresponding to the proposal described in the thesis:

Using SSR under Unicast-based Distributed Scheduling for 50-70 nodes:

a. Home automation [22] [23].
b. Small factory automation [24].
c. Smart Parking Systems (SPS) [25].
d. Industrial plant automation in remote areas and providing sustainable independent coverage [26].
e. Monitoring soil texture and detecting heat signatures in critical locations [27].
f. IoT-based volcano Surveillance [28].
g. Food processing industry [29].
h. IoT prison break monitoring and altering systems for remotely located centers [30].
i. Monitoring and controlling heating, ventilation and air conditioning in homes [31].
j. IoT-based ward medical monitoring systems for remotely located care homes [32].

SSR using Hybrid Scheduler for up to 100 nodes per access point:

k. Heating Ventilation, and Air Conditioning (HVAC) systems for commercial properties and industrial units [31].
l. Hospitality operation with enabled door locks and sensors for enhanced security [33].
m. Real time asset tracking within manufacturing plants and warehouses [34].
n. Plant automation or factory automation [26].
o. Monitoring equipment failure [29].
p. Automating lighting systems in buildings with a view to providing better control [35].
q. Integrating various security devices for centralized monitoring and control [25].
r. Smart water for automating waterways [36].

DeSSR for up to 600 nodes per access point

s. Monitoring of Oil and Gas pipelines for leak detection [37].
t. Automating irrigation systems and moisture detection in real-time [27] [38].
u. Tracking livestock and monitoring pasture time [39].
v. Factory automation in large industrial plant [40].
w. Component assembly using a robotic arm considering critical material handling [41].
x. Logistics and transportation for efficient supply chain management [34].
y. Industry 4.0 [41].
z. Collecting data on air quality, noise levels, and other environmental factors to improve urban living conditions [41].
aa. Real-time data collection from patients for continuous and timely intervention [32].
bb. Hospitality and meat processing factories in urban areas [29].

It was found that SSR is an energy-efficient, reliable, and scalable solution particularly suited for rural or remote areas when configured appropriately. However, it is less effective for frequent data collection. A hybrid version of SSR could enhance scalability, allowing for more frequent data gathering, though it would not reduce energy consumption as effectively in smaller networks, something the distributed design of SSR handles well. DeSSR, on the other hand, provides high throughput and an extended range of up to 2 km within a single subnet. This makes it ideal for urban or easily accessible areas, where it can manage demanding and variable data traffic. The study concludes by identifying open issues, such as dependency on RPL routing, collision control, and 6LoWPAN fragment recovery. The limitations of the research include constraints in the cake-slicing algorithm, areas for further optimization in energy-saving within the DeBRaS model, and considerations in tested implementations. Future work could explore enhancements like extending the IEEE 802.15.4 radio module, implementing adaptive duty cycles, and adjusting 6TiSCH specifications to support diverse spectrums similar to those used in LPWANs.

1.4. Thesis Structure

The structure of the rest of the thesis is as follows:

Chapter 2 - Internet of Things: This chapter reviews IoT communication technologies, categorized into LPWA, CIoT, and LP-WPAN, with a focus on the RF spectrums outlined in Table 1. A comparative evaluation follows, using selected IoT communication technologies and emphasizing key parameters: low power consumption, latency, interference resistance, and scalability. This analysis supports the selection of the most suitable low-power wireless communication technology for industrial applications.

Chapter 3 - 6TiSCH: This chapter provides an in-depth review of the 6TiSCH architecture, covering essential components such as routing, payload adaptation and header compression through 6LoWPAN, the 6Top layer, the MSF, and key physical layer capabilities, including energy consumption model, end-to-end transmission and reception using a sender and a receiver, with both devices implemented TSCH mode on IEEE 802.15.4 over 2.4GHz. The literature review focused on 6TiSCH scheduling includes various surveys, analyzed in the context of scalability and communication performance in large networks. It represents the most up-to-date review of SFs compatible with deterministic 6TiSCH network, distinguishing itself by excluding contributions that are not suitable for the deterministic 6TiSCH networks. This is because TSCH is adopted as default mode of IEEE 802.15.4 standard technology. After the literature review, an evaluation is conducted, identifying key challenges impacting scheduling performance in large-scale 6TiSCH networks. Based on these findings, an evaluation methodology is selected, and the chapter then reproduces some results from the most cited paper (OTF) in the literature using the chosen evaluation tool (6TiSCH simulator).

Chapter 4 – Scalable Scheduling Reservation: This chapter presents the design the proposed solution, evaluated across several representative scenarios, including an analysis of each strategy's impact, comparisons with other SFs, and testing specific cases with medium and increasing node counts under challenging traffic conditions (60 ppm). Results indicate a significant performance drop when SSR's strategies are not applied. While SSR demonstrates competitive advantages over existing SFs, its reliability gradually decreases with network sizes beyond 70 nodes due to various factors. However, other SFs register a sharp drop in reliability under the same traffic conditions.

Chapter 5 – SSR Using Hybrid Scheduling Design: To address limitations in SSR's reliability for networks with over 70 nodes under 60 ppm traffic, Chapter 5 proposes a redesigned approach, implementing SSR within a hybrid scheduling model. This includes enhancements to DTS and NDS, while QoS and the cake-slicing technique remain unchanged. Performance evaluation was conducted under increasingly challenging periodic traffic (intervals between 1s and 0.5s) with 100 nodes, variable slotframe lengths, and different topologies (random and linear). Results indicate that Hybrid SSR is advantageous for larger networks, overcoming the limitations seen with the unicast distributed scheduler version of SSR.

Chapter 6- Decentralized, and Broadcast-based Scalable Scheduling Reservation Protocol: This chapter further enhances SSR by incorporating the DeBRaS scheduler, as hybrid-led SSR shows limitations in scalability beyond 100 nodes. The proposed extension effectively addresses reliability issues by isolating poorly performing nodes and improving network dynamics with an enhanced NDS. DeSSR is thoroughly evaluated under both steady and bursty traffic scenarios. Finally, a scalability test was conducted over time, concluding the work on DeSSR.

Chapter 7 - Conclusion: This section concludes the thesis by revisiting the aims and objectives as they were presented at the beginning of the thesis. After that, the conclusion finishes with a summary of the whole thesis listing the limitations of what we have found and possibilities for future work.

2. INTERNET OF THINGS

IoT is a new paradigm that uses sensors and actuators for real-time tracking, monitoring and controlling. It was first introduced to the modern world in the 1990s. Currently, the evolution of IoT has led to a steady transformation of the industries via automation, for example; Heating Ventilation and Air Conditioning (HVAC) systems for providing clean air in commercial buildings and industrial outlet by regulating the temperature, humidity, and the overall air quality [42]; Mechanical Ventilation and Heat Recovery (MVHR) for providing insulated spaces for smart homes and smart buildings [31], smart supply chain and logistics management, allowing efficient tracking of shipments and other goods [34], using sensors and actuators in smart power grid, and to maximize energy production [43], smart water grid technology [44], and many industrial and enterprise-based solutions [45]. This thesis is aimed to improve the scalability of low power wireless communication technology that is most suitable for industrial automation.

2.1. Overview

Over the decade, the IoT has outgrown the traditional Cyber-Physical Systems (that integrate physical components (mechanical, electrical, or biological processes) with cyber components (computation, communication, and control) to operate interactively in real-time) based on the low power wireless communication technologies, using spectrum sharing and Frequency Division Duplexing (FDD) [46]. Spectrum sharing allows multiple devices and networks to coexist within the same radio frequency bands, and share resources of the spectrum. Meanwhile, Frequency-division Duplexing enables two-way communication (Uplink (UL) and Downlink (DL)) by using separate frequencies for transmitting and receiving data at the same time, leading to an improved network performance [46].

The IoT technologies are advancing further, utilizing proprietary or non-proprietary-based IoT devices, manufactured globally, with diverse design goals. Over time, the hardware capability of IoT devices has expanded supporting increased storage, improved processing capacity, and enhanced battery life. To ensure reliable data transfer between the heterogenous devices, the emerging low-power wireless technologies follow IoT communication architecture model [47] suitable for most IoT domains. This thesis is aimed at studying the spectrum of popular IoT technologies and standards, and evaluates them in the context of industrial-grade networks.

2.2. IoT Architecture

IoT Architecture consists of sensors and actuators, network gateway to internet. It has evolved using Edge computing (these devices positioned within the close vicinity of IoT devices such as sensors and actuators), Fog computing (to allow storage and computation to reduce the need to send data to Cloud (so that only relevant data is sent), and the devices are often positioned close to the edge of the network), and Cloud computing for allowing access to abundant volume of resources for data processing at a massive scale to strengthen decision-making capabilities [48]. Typically an IoT device embeds RF modules, sensors and actuators used for data gathering in a IoT network [48]. These are battery powered End-Devices (EDs), constrained by memory and processing capability.

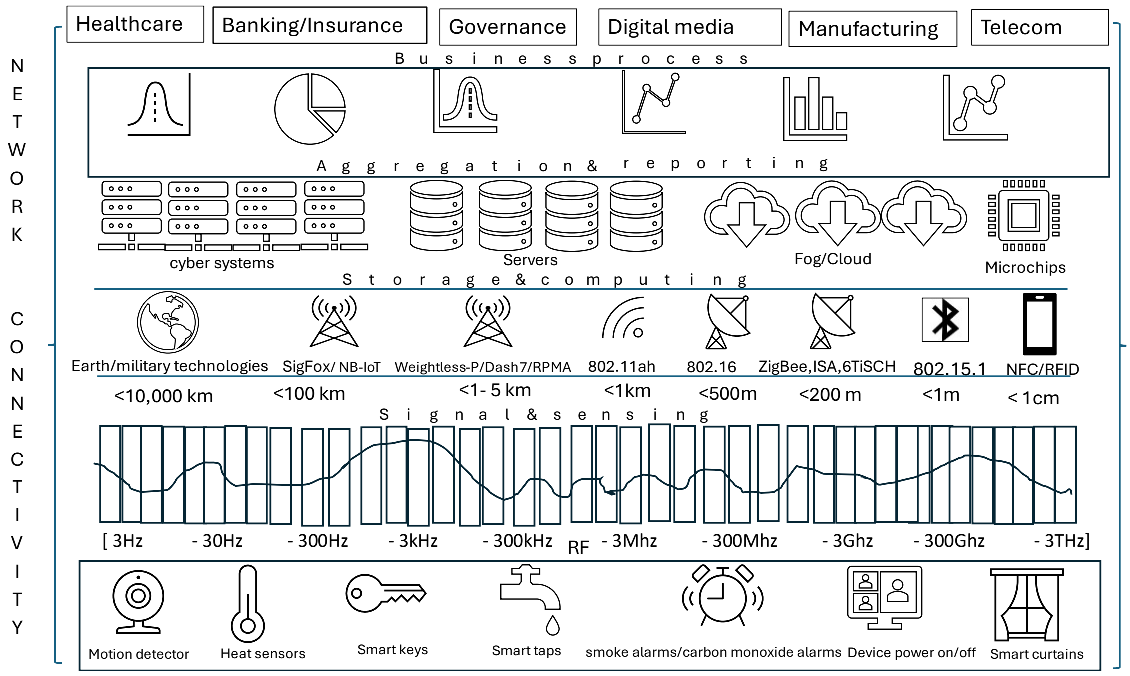

Figure 2. IoT Architecture

Figure 2 illustrates the IoT architecture reference model, organized into layers, each highlighting key characteristics based on core functionalities. At the bottom is the physical layer, which includes IoT devices such as motion and humidity sensors, heat sensors, smart keys, smart taps, smoke alarm, power-off sensors, and smart curtains. These devices are responsible for data collection through sensing, monitoring, and controlling. Above this layer lies the RF spectrum, utilized by communication technologies, showcasing a chronological increase in RF bands from left to right. Lower RF bands offer a higher transmission coverage, as illustrated across the *signal and sensing* layer. Here, the signal is depicted as fluctuations across the RF bands (detailed in Table 1), while sensing aligns with channel-access protocols, is a capability provided by the MAC layer within the most devices.

The collected data stream is transmitted via a suitable RF band, with operating technologies ensuring end-to-end transmission; typically, long-range technologies are more suitable for transmission across wider geographical zones (100 km - 10,000km), aligned based the underlying RF bands in the spectrum: those with wider area, long-range coverage are on the left (LTE-M, NB-IoT, EC-GSM, Sigfox, LoRa), while moderate (Weightless-P, Dash 7), short-range (IEEE 80.11ah, IEEE 802.16, IEEE 802.15.4, IEEE

802.15.1), and extremely limited-range (NFC, RFID) technologies are positioned progressively to the right. These are described in Section 2.3 in more detail.

The next layer is the **storage and computing layer**, responsible for **processing** and storing data for analysis [49]. Computational resources are positioned on the left, storage units are centered, and local chip-based processing is shown on the right of the diagram within the layer [50]. A downward arrow in the icon indicates cloud access for accessing resources. Local data processing is performed using embedded microprocessors, within edge devices, and using cyber systems [50], while global data processing requires gateway connectivity to the internet, facilitated by the **network connectivity layer**, positioned vertically on the left side of the diagram due to its universal role.

The **aggregation and reporting layer,** involves aggregating and analyzing data to transform it into actionable insights, necessary for effective monitoring and control. Finally, at the top, the **application layer** highlights IoT applications across various domains or industries, including healthcare, banking, governance, digital media, manufacturing, and telecom [51]. These industries benefit from IoT-driven advancements in processes such as reporting, analysis, and decision-making. To protect both back-end and base-line infrastructure, the **network security layer** is positioned vertically on the right side of the diagram safeguarding data transitioning between layers through a set of protocols and indigenous cybersecurity systems [52].

Over the decade, IoT architecture has evolved across various segments of the global market including enterprise, public sector, private sector, and service providers [53]. Ericssons, and Cisco have provided quantitative projections based on emerging trends on IoT connectivity [1] [2] suggesting that the eco-system of IoT is rapidly booming with various design goals projecting future demands [1]. The role of Standard Development Organizations (SDOs) has been to facilitate the Working Groups (WGs) [54], with development of standard protocols towards flexible integration to the internet and allowing inter-flow of services seamlessly. The standard IoT architecture is divided into several layers, as follows:

2.2.1. Physical Layer

The physical layer determines the selection of modulation techniques and other functionalities, such as the spread mechanism (by which the signal is spread over a wider wavelength to detect and eliminate interferences and to provide long distance transmission), and encoding schemes (for error detection and correction). These topics are discussed briefly in Section 2.4, followed by the evaluation of selected IoT communication technologies. With the rapid growth of the IoT ecosystem, several key companies worldwide are specializing in IoT component manufacturing and assembly, tailored to diverse technological specifications and communication portfolios: for example, ARM [55], Atmel [56], Silicon Labs [57], Texas Instruments [58], Intel [49], NVIDIA [59], Samsung [60], etc. ARM and Intel are popular ones, offering computation units such as *microprocessors*; while Atmel mainly offers *microchips*. Silicon Labs performs assembly of the components as per the system-on-chip (SoC) specification (that varies from one technology to another, though it must comply with relevant standards and RF modules).

In Figure 2, the signal and sensing layer is responsible for collecting data using IoT devices. The collected data is then scheduled on a specific carrier frequency using the MAC layer protocol. In the IoT architecture, these components are integral to the existing physical layer. An internet connection is thus necessary to allow IoT devices to transmit and receive communication from/to servers via gateway routers, though, not all collected data is useful.

2.2.2. Edge Layer

The edge layer is used to filter the collected data by using a separate edge computation unit within the EDs or relay devices. The edge layer minimizes the resource consumption in line with the requirement to transfer the collected data from EDs and only transmits the computed or relevant data [50]. That way, it reduces the operational cost and avoids frequent use of baseline infrastructure for processing locally. In Figure 2, the storage and computing layer shows a number of options allowing filtering and storing data. This includes edge devices which come with an embedded microchip allowing processing locally. It requires the specific alignment of edge devices within the close vicinity of the IoT devices. Contrarily, filtering or sorting data using fog/cloud requires an Internet connection, which can be provided within the network connectivity layer in Figure 2.

2.2.3. Processing layer

The role of the processing layer is to accumulate relevant data from the gateway network layer and provide storage in the form of customer cloud, chips, or servers, and abstraction based on computational abilities. Intel is a popular and trusted brand offering AI-based solutions [49]: A significant amount of database work is carried out at this layer in an attempt to find the best patterns for mapping data against various possible options. This is because processing at the physical layer carries a risk of failure, as devices are constrained by their hardware design. The data accumulation process is divided into three main stages, where data is accumulated regularly or based on specific times, events, or queries. Therefore, the processing layer acts as a programmable interface for data collection and accumulation. Further, data accumulation (abstraction) is complex, as data from different domains is mixed and analysed to identify new patterns (as is shown in aggregation and reporting layer in Figure 2).

2.2.4. Application Layer

The application layer enables a wide range of IoT systems, software, middleware, and APIs to integrate with the existing infrastructure (cloud), allowing the mapping of collected data to provide new insights that can address specific business problems. IoT applications utilize computing technologies like Edge/Fog, and Cloud to process and analyse data [53]. Currently, these technologies are becoming increasingly domain-centric, and there is no standard API that addresses all key requirements that can solve global challenges ubiquitously. In IoT, real-time data collection plays a significant role in decision-making, as this data is often highly private and sensitive [61]. IoT systems thus require transparency as to what is truly achievable with the existing systems; for instance, from an application point of view, it is vital to consider the accuracy of the data received. The generated data may be influenced by limits imposed by the regional regulations in terms of how allowably a device can receive updates from core network or application servers.

2.2.5. Business Layer

The IoT business layer provides methods to derive meaningful insights from the application layer after data processing. The business layer represents an abstraction of the top hierarchy, where decision-making and leadership take place (such as return on investment). It takes a broader perspective to solving problems by assimilating inputs from other systems or software solutions, ensuring that the insights are aligned with strategic objectives.

2.2.6. Security Layer

Security is paramount at every layer of the IoT architecture ensuring the successful adoption of IoT systems. In fact, both connectivity and security are pervasive across the entire IoT architecture. In Figure 2, each layer uses security protocols that are appropriate, based on the design goals of the IoT communication system, ensuring the protection of data flows both in and out, from the end device to backhaul connectivity.

This thesis focuses on base-line performance of industrial IoT networks, aiming to improve scalability by addressing key challenges at the MAC layer. This is an integral component of signal and sensing layer shown in the IoT architecture. The next section reviews IoT communication technologies and standards.

2.3. IoT Communication Standards and Technologies

Low-power wireless communication predates the IoT, as it was originally used before the 1990s to protect critical infrastructure. Today, it is commonly used for data collection and reporting purposes across public and private sectors organizations, leveraging diverse design objectives by numerous short-range and long-range technologies, deployed using various RF bands across the radio spectrum. The radio spectrum comprises a vast range of frequencies, each suited to different applications due to their propagation characteristics. This includes Extremely Low Frequencies (ELF), which are used for long-distance communication, allowing penetration deep into the Earth or water, while Higher Frequencies (HF) and Ultra High Frequencies (UHF) are used for high-bandwidth applications such as broadcasting, mobile communications, and advanced research. Table 1 illustrates a range of frequencies divided based on RF-bands. These frequencies enable a myriad of technologies and standards that form the backbone of modern communication systems, from everyday radio and television networks to advanced satellite networks. However, IoT communication faces various challenges, which have slowed its adoption compared to standard wireless communication networks. This includes poor security [62], privacy [63], mobility [64], interoperability between devices [65], lack of standardization [65], legal issues [65], and poor scalability [65].

This thesis focuses on key challenges related to communication inefficiencies within industrial IoT network. These include poor coverage, low data rate, connection losses, synchronization delay, unsatisfactory received signal quality or path loss due to multipath interferences and environmental obstructions, end-to-end packet delay, network longevity, and robustness. Most of these challenges are perceived as limitations of the physical layer in the IoT architecture reference model.

Spectrums	Frequency range	Wavelength	Applications
Super Low Frequency (SLF) and Extremely Low Frequency (ELF)	30- 300Hz, and 3- 30Hz	10,000- 100,00 km, and 1000- 10,000 km	Communication with submarines, space, geophysical monitoring, and in certain scientific applications.
Ultra Low Frequency (ULF)	300Hz- 3kHz	100- 1000 km	Used in mining and other earth communication, for example caves.
Very Low Frequency (VLF)	3kHz- 30kHz	10-100 km	Long-range communication, navigation, non-terrestrial applications [61].
Low Frequency (LF)	30kHz- 300kHz	1-10 km	Used for **AM** broadcasting, navigation signals and maritime communication.
Medium Frequency (MF)	300kHz- 3MHz	100m – 1 km	Used for AM radio broadcasting.
High frequencies (HF)	3MHz- 30Mhz	10 m – 100 m	Used for shortwave radio, amateur radio and long-distance communication [66].
Very high Frequency (VHF)	30-MHz- 300MHz	1 m – 10 m	FM radio broadcasting, mobile phones, GPS, Wi-Fi and 2-way radio communication.
Ultra High Frequency (UHF)	300MHz- 3GHz	10 cm – 1 m	Television broadcast, Mobile phones, GPS, Wi-Fi, Bluetooth and 2-way radios [66].
Super High Frequency (SHF)	3GHz- 30GHz	1 cm – 10 cm	Satellite communication [67], radar, microwaves links, and some Wi-Fi standards
Extremely High Frequency (EHF)	30GHz- 300GHz	1 mm – 1 cm	High frequency radio astronomy, remote sensing and advances communication technologies like 5G [68]
Tremendously High Frequency (THF)	300GHz- 3THz	Less than 1 mm or 100 µm- 1 mm	Submillimetre wave technology, terahertz imaging and certain scientific research applications (sspectroscopy, security scanning, advanced communication systems, research and development).

Table 1: Radio spectrums used by IoT communication technologies.

This thesis divides IoT networks into three main categories: LPWANs for long-range communication (up to 5- 50 km, depending on deployment conditions and infrastructure support), CIoT networks for long-range communication (up to 15-100 km) using licensed spectrum, and LP-WPANs for low power and short-range communication. Each category consists of serval technologies, with each operating on a specific RF band according to the specifications shown in Table 1.

This section provides a review of popular LPWA, CIoT, and LP-WPANs technologies.

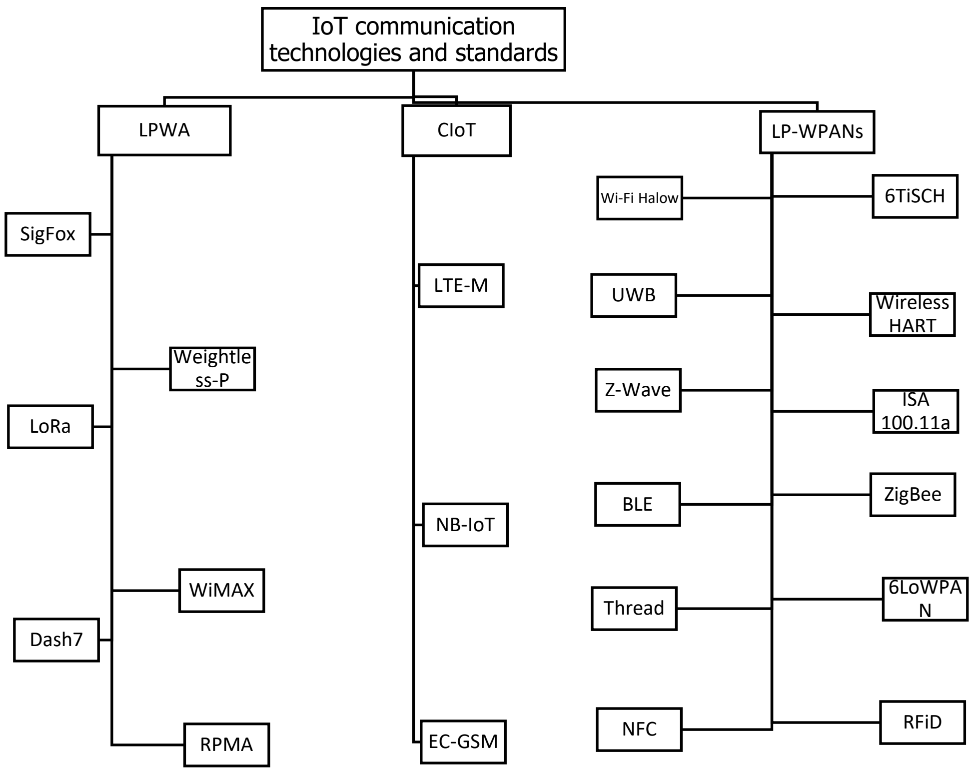

Figure 3. Classification IoT wireless communication technologies and standards.

Figure 3 categorized IoT technologies into three groups, with each one tailored to different propagation characteristics and connectivity needs; such as transmission range, data rate, power consumption, and hardware designs. These technologies collectively address the diverse requirements of IoT applications across various sectors.

2.3.1. LPWA

LPWA technologies are designed for less frequent, long-range transmission, with small amount of data, while operating under unlicensed spectrum bands. These frequencies impose regulatory constraints in terms of transmission power and radio sensitivity. The communication fails due to wireless interference and multipath signal loss. Typically, LPWANs are asynchronous networks using periodic beaconing to operate, allowing enhanced power-savings, subject to their physical layer modeling (specifications). Table 2 highlights applications of LPWA technologies along with their operational characteristics.

Technologies	Coverage	Frequency	Data rate	Latency	Battery life	Applications
LoRa [69]	10-15 km in rural areas, 2-5 km in urban areas [70],	30kHz, 433MHz, 868MHz, 915MHz, [71] 2.4GHz [72]	300 bits/s- 50 kbps, [73]	High [50]	10 year on 9V [50]	Smart metering [73], smart agriculture [73], smart city infrastructure monitoring [69]**.** smart cities [74], building automation [75].
Sigfox [76]	10 km (urban), 50km (rural) [77]	200Khz, 868MHz, 915MHz	100- 600 bits/s [73]	High [50]	4 years on 3.3 V and 10 years on Lithium AA-cell [50]	Asset tracking [73], remote monitoring [73], electric metering [77]. industry 4.0 [78], environmental sensing [38].
Dash7 [79]	1- 2 km (urban and rural) [80]	433MHz, 868MHz and 915MHz [80]	200-256 bytes/s [80]	8s [80]	10 years using Coin-cell [80] [81]	Tyre pressure monitoring systems [82] Logistics, supply chain management [83], Automative [83], and asset management.
RPMA [84] [85]	5-15 km where 5 km in urban and 15 in rural areas [86]	2.4 Ghz Bands [87] [85]	100-100Kbits/s [86]	High but also depends on conditions [50]	10 years (19 Ah D-cell Lithium) [87]	Monitor oil and gas pipeline [84], Smart grid [84], Underwater tracking [84], Navigation, Industrial automation [84].
Weightless-P [88]	2-5km (urban), 25km (rural)	163 MHz, 433 MHz, 470 MHz, 780 MHz [71], 868 MHz, 915 MHz [81].	100Kbits/s [71]	10-100ms depending on network traffic [71]	3-8 years using Coin-cell [81].	Environment monitoring, energy harvesting, industrial automation [88].
EC-GSM-IoT [89]	< 15 km (urban), 15 (rural) [89]	900MHz, 1800MHz (cellular band) [81].	100 Kbits/s	0.7s- 2s	10-14 year (5 W h battery) [87]	Smart metering [89], asset tracking, energy-efficient wearables [87], environment monitoring [87].

Table 2. Low Power Wide Area technologies.

This section reviews prominent LPWA technologies.

2.3.1.1. Long Range (LoRa)

LoRa is a popular technology, developed by Semtech Corporation, specifically designed for long-range, low-power, and low-data-rate applications. As a license-free technology, LoRa can operate across various grant-free RF bands also shared by other networks [90]. Typically, it uses LF to UHF bands, ranging from 30kHz- 915MHz, as shown in Table 2.

Being a proprietary technology, LoRa does not have a full communication stack and this is a key weakness, causing a rather slower adoption in long-range segment. At the physical layer, it uses Chirp Spread Spectrum (CSS) modulation. CSS is not a new modulation technique as it has been used earlier in the 1940s for military applications. This scheme (CSS) modulate or translates signals into frequencies that are increasing and decreasing over time, based on the spread factors; a spread factor inflates a signal into the wider wavelength to achieve improved coverage and resilient communication. However, the data rate varies depending on the connectivity and distance from the nearest base station (BS).

LoRaWAN is a standard designed to support MAC-layer communication. It is comprised of a set of channel-access protocols, providing an adaptive duty-cycle based on scheduling [91]. Typically, a LoRa network operates using star topology where the requirement to routing and scheduling is directly managed between the EDs and the corresponding BS. EDs implementing LoRaWAN can use different network settings based on the classification of LoRa devices to address specific traffic conditions:

Class A follows ALOHA based scheduling. For example, a LoRaWAN device can send a message via UL frequencies at any time, followed by two reception windows; for example if there is no response received from the core network then the device immediately schedules the next UL transmission, but if the device receives a reply from the first message then it keeps the next reception time window off and, if the message response arrives in the 2nd reception window then it keeps the radio on till that time period.

ALOHA is one of the earliest and simplest form of random-access protocols developed for wireless networks. Class A devices are prone to tensions between existing carrier frequencies. TDMA is more efficient in terms of avoiding collision. The protocol divides the bandwidth into timeslots and in that way, it provides a specific slot for each device to initiate transmission or reception but in a half-duplex manner using random channel-access if there are more than one channel available to use in; therefore a single channel is prone to multipath failures.

Class B extends Class A devices where each DL message follows a time reference provided by the network server after the clock synchronization. While Class A devices periodically open the time slots for reception, Class B devices use a pre-assessed model, where the network server oversees all DL messaging using Time Division Multiple Access (TDMA). It schedules multicast, unicast and broadcast slots towards DL communication, which is mainly used to provide firmware updates, and scheduling instructions. For locating a device, it uses Time Differential of Arrival (TDOA)- a commonly known technique to detect the transceiver's proximity.

Class C devices use Listen Before Talk (LBT) [92] which requires a device to listen first for channel to check for any ongoing communication before it begins its own transmission. This process involves the device to be continuously monitoring for all ongoing transmissions; during this period, the device checks for the presence of a carrier signal across the band. This process will continue until a free channel is found that means no other device is currently transmitting. If the channel is clear, the device proceeds with its transmission, ensuring that the communication is uninterrupted by ongoing transmissions, leading to more reliable data transfer. It only triggers a random backoff period if the chosen frequency is found to be engaged and make another attempt to listen again; thus, it minimizes the chances of collisions between data packets from different devices, enhancing overall network reliability.

The devices used by LoRa has to adjusts the duty-cycle to balance Tx and Rx activities dynamically, using physical layer capabilities. By increasing Tx power, these can extend their communication range and offer resilience against interference where higher spread factor is beneficial. However, transmitting a large payload using frequencies below 1GHz, would require more frequent transmissions, which may reduce power savings and network efficiency. Conversely, using ISM 2.4 GHz, the demand for frequent transmission is reduced but the communication is subject to heavy interference from co-existing networks such as Wi-Fi, and ZigBee. Thus, reliability cannot be guaranteed [72]. The author [72] concludes that LoRa is not scalable and that it drops packets under extended range.

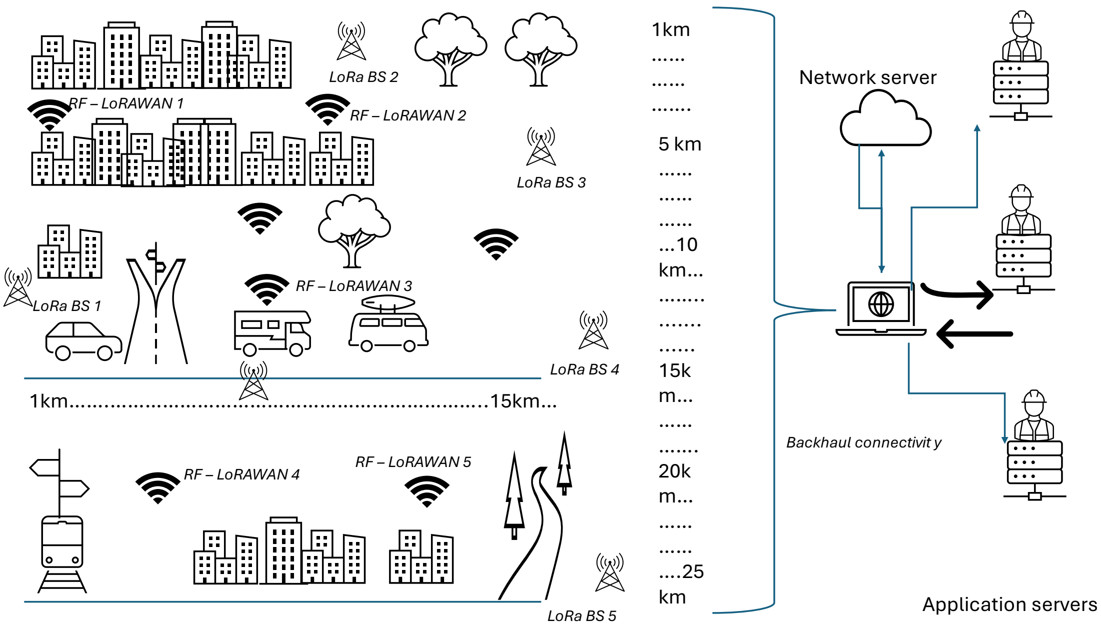

Figure 4. Network model of LoRa (using an example of a smart city).

The networking model of LoRa in Figure 4 illustrates a smart city setup, featuring 7 EDs, 5 BSs, a network gateway router, an application cloud for bidirectional communication, and remote users. In this example, each LoRa device (RF-LoRaWAN) connects to the nearest BS within coordinates that span horizontally from 1 to 15 km and vertically from 1 to 25 km. Typically, the devices can connect over hundreds of kilometers under clear LoS alignment and using an appropriate RF medium; however the range is constrained to 10-25 km in rural areas with the presence of vegetation, houses, buildings and transportation means such as bus and trains. Further, the coverage range of each BS depends on deployment conditions; for example a LoRa network can achieve a maximum range of up to 25 km in rural areas [70], while in urban settings, the signal strength degrades rapidly due to multipath propagation under LoS and NLoS placement, thus the defined range between EDs and the BS can be usually within 1-5 km, subject to the deployment conditions.

The communication between the sender and receiver follows a half-duplex pattern whereby a device cannot send and receive messages simultaneously. The backhaul connectivity is provided to and from each BS via the network gateways, linking them to the core LoRa network. The connection from the network gateway to the Network Server (NS) can utilize optional means such as 4G/5G, Wi-Fi, or the Ethernet. The Application Server of LoRa is part of the core network, making deployment more user-centric. (users can program new applications independently). Today, LoRa supports various domains of IoT applications [93] with enforced mobility. These applications are directly implemented at the application server, allowing exchange of information on demand.

As far as the limitations are concerned, the network architecture of LoRa largely is built on two key layers (Physical layer and LoRaWAN layer) and the rest of the stack is left undecided (to be used by application developers). This poses key concerns of lack of standardization, since developer-driven selection of protocols can make it complex and costly for larger installations [72]. LoRa does not provide real-time communication, which makes it unviable for industrial automation and other critical applications where reliability and latency are critical quality controls. Additionally, LoRa's stringent duty-cycle obligations (depending on where across the globe it is deployed) makes packet loss likely if a device takes longer than 1% of the assigned duration, and that is in addition to poor DL performance.

2.3.1.2. Sigfox

Sigfox [76] is a proprietary LPWA IoT technology launched in 2010 by a French start-up, designed for IoT and M2M communications. It operates within unlicensed ISM bands ranging from 30kHz- 300MHz (LF to VHF) and supports long-range, low-power, and low-data-rate applications like smart utility networks [94], environmental monitoring [95] and asset tracking and leak detection [96]. Table 2 illustrates further domains of applicability. The technology operates in Ultra-Narrow Band (UNB) frequencies [97], enabling extensive network coverage with fewer BSs compared to LoRa and other

LPWA technologies. UNB offers low data rates, high sensitivity to weak signals, and efficient long-range communication.

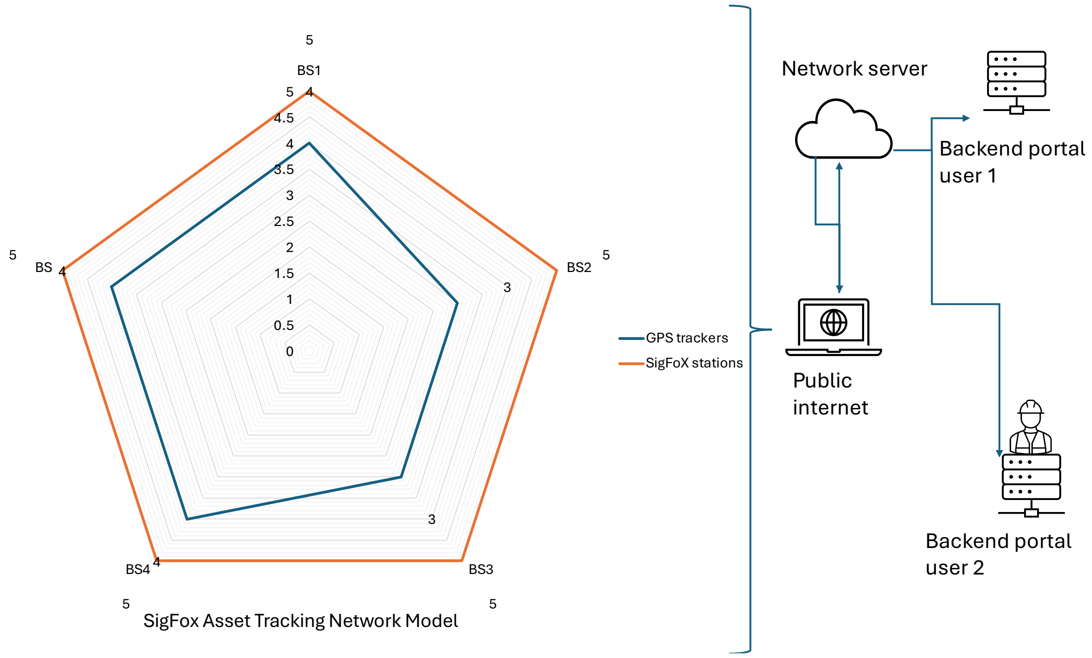

Figure 5. Sigfox architecture using asset tracking model.

Figure 5 illustrates the Sigfox-driven *Asset Tracking* scenario, comprising three primary components: EDs, BSs, and NS. The radar chart shown in the figure above visually represents two sets of data: GPS trackers (shown in blue) and Sigfox stations (shown in orange). The chart has five axes, each corresponding to a controller station (BS1, BS2, BS3, BS4, BS5). The values on the chart range from 0 to 5, indicating the coverage of each tracker or station in relation to the controller. The blue line shows the coverage range for GPS trackers, while the orange line represents the coverage range of the Sigfox stations. On the right side of the diagram, the NS is shown which is connected to the public internet; the Backend Portals (User 1 and User 2) connected to the NS, indicating that multiple users can access the data processed by the server. This architecture suggests that data from the GPS trackers is collected via Sigfox BS, processed, and made accessible to users through the NS. The arrows indicate the flow of data transfer between the NS and the backend users, highlighting the role of the public internet in facilitating communication between the network components and users.

Overall, the example illustrates a scenario where 5 BSs are deployed assuming a critical deployment condition, where GPS trackers are fitted within the ED. Each device can send data (12 bytes UL) and receive updates or queries (8-12 bytes DL) more efficiently than LoRa (see Tables 2 for data rate differences). In terms of the duty-cycle restriction, Sigfox devices are flexible compared to LoRa [50], allowing 0.1% - 10% of the total time taken to acquiring a channel for transmission of data packet, and it puts the base-station on hold until the next slot becomes available ensuring half-duplexity in channel access, which avoids collision on the operating frequencies.

Sigfox devices are equipped with modules used for transmitting small data packets over distinct channels which can cover up to 50 km in rural areas and up to 10 km in urban areas. This is provided by Frequency Hopping Spread Spectrum (FHSS) which separates channels and avoids overlapping between channels provided the carrier frequencies used by Sigfox are narrowband and nonorthogonal.

Currently, Sigfox is supported by many telecom operators worldwide, though most products are vendor-locked. Unlike open-access technologies, Sigfox offers specialized solutions for long-range, low-power communication. However, it is primarily suited for small, infrequent data transmissions due to its low data rate.

As far as the limitations are concerned, it is not equally efficient under downward communication where NS is supplying updates to each device, but it is comparatively less stringent than the LoRa. In addition, devices take tens of seconds to relay the information to the BS, and from BS to the ED, it can be even higher. This is due to the prolonged duty-cycle and the sudden requirement to synchronization for data transmission by devices. This makes Sigfox more suitable for environment monitoring and Smart Utility Network (SUN) but less suitable for industrial IoT or critical IoT applications [68] or those requiring immediate guaranteed feedback. Apart from that, network coverage of Sigfox in rural areas is lower compared to LoRa despite being part of public networks. This is due to a less evolved eco-system, which may leave the rural and remote areas with limited or no coverage; and because Sigfox devices are expensive, deploying extra BSs is costly and time-consuming [77]. Sigfox is further evaluated in Section 2.4.

2.3.1.3. Weightless-P

Weightless-P [88] is one three standards (Weightless-W, Weightless-N, and Weightless-P), designed to support high data rate based IoT applications using the multi-hop transmission model. The technology operates under the unlicensed RF spectrum with Weightless-P being tailored specifically for LPWA applications using sub-GHz band (LF- UHF).

The diagram in Figure 6 illustrates the Weightless-P communication model within a network, showcasing the interactions between cells, BSs, the network server (NS), and the cloud. The sensor devices in each cell use either Gaussian Minimum Shift Keying (GMSK) or Offset Quadrature Phase Shift Keying (O-QPSK) [71] as modulation schemes. GMSK is a type of continuous phase shift keying technique where the rapid and continuous signal phase shifting using the gaussian method leads to slight frequency shift depending on the input bits. GMSK symbol is either 0 or 1 and it can only offer 1 bit at a time. It using filters to smooth signal transition reliably over long distance. Unlike GMSK, O-QPSK is a variant of QPSK, where phase is shifted by half a symbol period compared to QPSK, keeping well away from the origin (in the constellation diagram). O-QPSK is widely used in the short-range and long range IoT technologies and it offers 2 bit per symbol (these schemes are further discussed in Section 2.4).

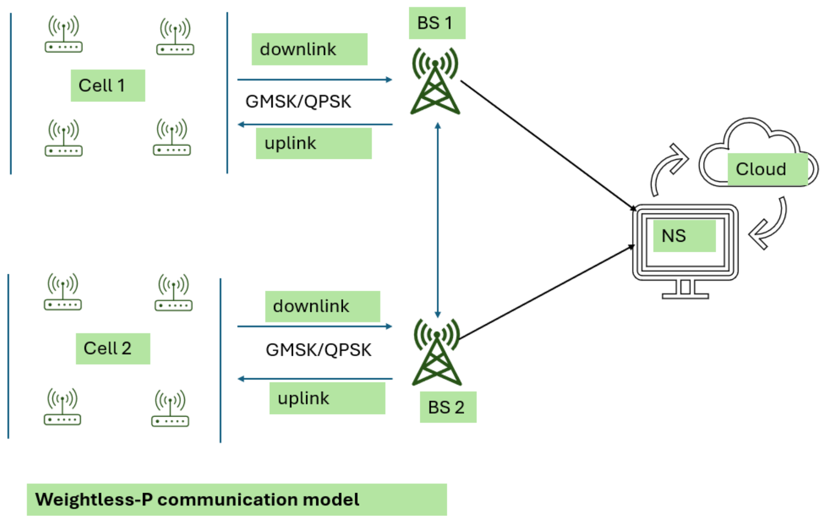

Figure 6. Weightless network architecture

The above diagram shows the network architecture of Weightless-P with base-line deployment. It is divided into cells where each cell includes a group of EDs that are used to perform UL and DL communication with their nearest BSs implementing FDD where UL channels and DL channels are separated. The diagram shows two BSs that act as intermediaries between the EDs and the core network (NS). Each BS is responsible for receiving data from end devices and transmitting data back to them in the half-duplex manner. The **NS** aggregates data received from multiple base stations, while coordinating communication across the network; it also manages data processing and ensures that messages from the cloud reach the appropriate base station for delivery to the end devices. The cloud enables bidirectional communication with the NS, allowing remote users to access and control the data collected by the IoT devices. The cloud can provide additional processing power, data storage, and analytics capabilities, enabling a wide range of applications in IoT environments.

Weightless-P is inspired by standards like 3GPP [50] and thus is supporting hundreds of thousands of devices to be connected to a single BS. It also offers flexibility over managing vendor- manufactured devices and allows interoperability on the air, though selection of security protocols and Tx power and link budget configuration depends on the deployment conditions. Unlike LoRa and Sigfox, it utilizes increased Tx power for high resistance against path loss and long range communication, piggybacked with higher frame size (260 – 514 bytes) depending on the modulation schemes in use. That means the data can be uploaded or downloaded with fewer attempts in an uninterrupted manner. This is achieved by the LBT channel-access mechanism, defined at the MAC-Layer [50] and it is one of the critical features in Weightless-P ensuring efficient and interference-free communication.

Today, many regulatory bodies propose the use of LBT in unlicensed frequency bands to prevent internal interference and ensure fair spectrum use [98]. This makes Weightless-P a clear champion offering high data rate, and long range solution, crucial for high throughput demanding IoT applications [86]. Conversely, it shows poor response to energy consumption [50].

In terms of other challenges, it registers **highest latency** among the group of LPWA technologies due to LBT-based channel access; thus, adoption of Weightless-P for IoT industrial networks is limited to fewer applications (as shown in Table 2). Weightless-P is further evaluated in Section 2.4.

2.3.1.4. Dash 7

Dash 7 is an open standard LPWA technology developed by the DASH7 Alliance Protocol (D7AP) [79] using Active Radio Frequency Identification (Active RFID) that was some time ago utilized by the US Department of Defense (DoD) [50]. Dash 7 devices can be configured with payload security where these devices are flexible to operate across various RF bands including VHF to UHF (433MHz, 868MHz, and 915MHz) forming an active air interface. In vendor-specific devices, the security can be disabled while using broadcasting as an attempt to connect devices.

For the active air interface, at 433MHz, it inherits the ISO 18000-7 open specification with compete set of layers and adequate parameters, enabling tag (RFID) to tag communication - a very different approach from the legacy RFID technology. Dash 7 offers on-the-fly code upgrades allowing successful paring between short range technologies such as Bluetooth, and ZigBee and the long range solutions such as LTE [99]. Over time, Dash7 has evolved and with D7 Alliance capable to connect to most devices used by IoT technologies based on the BLAST principles [99].

BLAST [50] stands for **Bursty** (sudden gust of data packets), '**Asynchronous**' (stateless, periodic handshaking with the devices), '**Stealth'** (jamming incoming communications without needing to initiate beaconing), and '**Transitive'** (degree of mobility across gateways'**)**. The tag devices form active mesh connections where devices can adjust their data rate in an on-the-fly manner based on the transmission range. Dash 7 devices can communicate over 1-2 km and each device can yield over 9-256 byes, subject to spectrum in use and deployment conditions (see Table 2).

The communication model of Dash7 (in Figure 7) showcases a structured IoT network, designed for low-power and long-range data transfer. It includes D7AP (DASH7 Alliance Protocol) nodes that act as EDs, collecting data for applications [99]. These D7AP nodes communicate with a central network gateway, which aggregates data from multiple nodes to streamline communication.

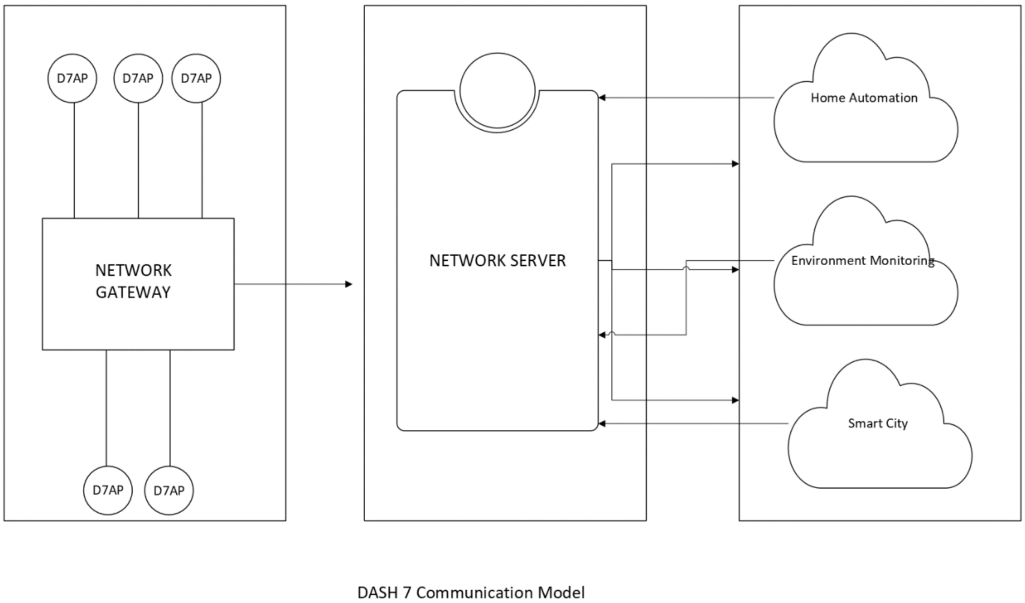

Figure 7. Dash 7 network architecture.

The connectivity between EDs and gateways is aided by the D7AP deciding the frequency of the D7AP Action Protocol (D7AActP) [99] and D7AP Advertisement Protocol (D7AAdvP) [50] [99]. These are unicast and broadcast protocols utilized for connectivity purposes; for example, if unicast takes longer to respond, it uses D7AP advertisement protocol seeking the next hop relay [99].

The collected data is upstreamed using the 'Tag-Talk-First (TTF)' approach [50], allowing tags devices to ping the gateway so that the data packet can be transmitted whenever there is information available to send. This reduces energy consumption by eliminating the listening period. In terms of downward communications, the ***tags*** must sync well for a prolonged period, with each waking up at a scheduled intervention (to receive the data). TTF seeks an acknowledgement from receiving devices to ensure reliability. Once received, the packet is then forwarded to the NS via the gateway, serving as the main hub for processing and distributing information providing remote access in the application cloud such as home automation, environmental monitoring (for real-time analysis of air quality, temperature, etc.), and smart city solutions (for intelligent infrastructure management). Other than the network domain, Dash7 is utilized for M2M communication; for example: Dash7-led Tyre-Pressure Monitoring Systems (TPMS) systems for reducing tyre wear and improving public safety [82].

As far as limitations are concerned, it poses significant challenges in terms of transmission range, data-rate (see Table 2), high latency (depending on the traffic rate and network conditions), and high overheads for DL messaging (due to the mesh network). In terms of scheduling and duty-cycle utilization, the EDs underestimate collisions while sending data as soon as being awake [86] and generate overheads, which could further limit the scalability [50]. Dash 7 is evaluated in Section 2.4 in more detail.

2.3.1.5. Random Phase Multiple Access (RPMA)

RPMA is a proprietary LPWA technology developed by Ingenu [85] for long-range communication using the UHF spectrum. It has gained global attention since most LPWA technologies are confined to (LF-UHF) bands or essentially below 1Ghz bands. RPMA has been around for over two decades, and its extensive coverage capabilities make it a preferred solution in industries like Oil and Gas, where it is used for automation and provide remote monitoring.

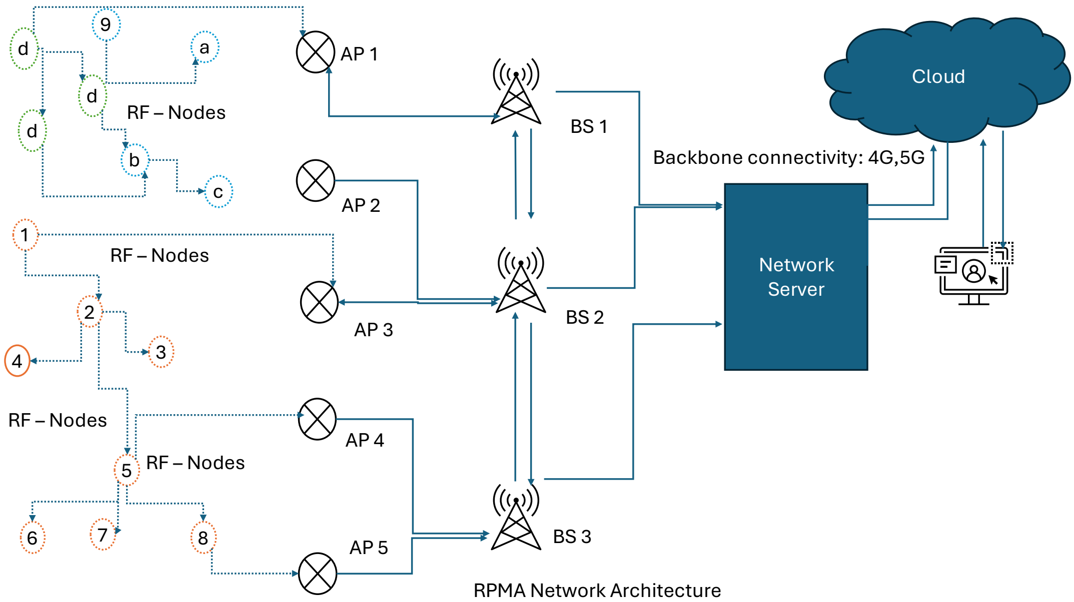

Figure 8. Network architecture of RPMA technology.

The diagram in Figure 8 illustrates the architecture of RPMA. Here each AP that collects data is composed of RF-Nodes which form a multi-hop network, these communicate with the BS. The APs act as intermediate nodes in the network responsible for collecting and forwarding data to and from the BS. The BSs are positioned several miles apart from the AP, as can be seen in diagram. Each BS (BS1, BS2, BS3) serve is a central point connecting NS using the backbone network connection. The NS is the core of the network architecture, where data is processed and managed. The server can connect to the cloud using the public internet or mobile networks such as 4G/5G. The external systems such as an application server can access the data using centralized API (cloud).

RPMA operates slightly differently compared to the other LPWA technologies while operating in ISM 2.4GHz. This is because unlike the rest of the LPWA technologies, the device can use higher bandwidth up to 2-5 MHz, making it possible to meet heavy traffic conditions. This can be done by adding more devices to the existing network, yielding extended coverage and more efficient propagation by the use of amplifiers placed en route to the nearest AP. Currently, it is scalable up to 50000 devices per BS, where the transmission range of each RPMA manufactured ED in urban areas is roughly 3 times lower than the coverage provided in rural areas; the downside is that compared to the UL data rate, the DL performance is four times lower. As LPWANs are designed for a small amount of data transfer, the channel-access mechanism can decide the ability to deal with congestion on carrier frequencies that are also shared with other networks too. In this regards, each device is designed to follow CSMA/CA, which, with more devices added to the network, leads to increased delay in accessing the medium (10 second or higher). This is in addition to the delay experienced by devices sending data in hop by hop manner, essentially because it forms a multi-hop network headed by controller (AP). RPMA triggers a high volume of overheads towards maintaining network functionalities and requires more transmission power; clearly it is not energy-efficient technology. The technology has been around for over two decades, where many of its performance aspects remain relatively unknown or underexplored compared to the more widely adopted alternatives [86].

RPMA faces criticism for yielding a lower SNR despite using higher negative RSSI value and superior Tx power. The reason is that ISM 2.4GHz is widely used by traditional short-range technologies, for example Wi-Fi, and Bluetooth. The frequency of data transmission by these networks, when in the range of a RPMA network, triggers packet loss due to multipath challenges. The signal coverage is therefore limited [50] to a clear LoS deployment where a shortest-best path provides strong signal strength. The other challenges include poor encryption of payload and authentication according to [100]. The author [100] stresses that RPMA relies on an outdated algorithm where data is prone to be tampered with or intercepted.

IoT technologies like LoRa, Sigfox, and Dash 7 are gaining widespread adoption due to strong industry support from major players like Samsung, Ericsson, and Huawei, as well as backing from standardization bodies such as European Telecommunications Standards Institute (ETSI). These technologies provide a broad range of services, contributing to their significant market penetration and rapidly growing ecosystems. In contrast, RPMA, while offering promising features for long-range, low-power communications, faces challenges in gaining similar traction.

2.3.2. Cellular IoT technologies

Cellular IoT (CIoT) operates under paid frequencies designated for cellular communications. These bands typically extends from LF to UHF (as shown in Table 1) frequencies; for example, 700 MHz, 800 MHz, 900 MHz as well as higher frequencies such as 1.8 GHz, 2.1 GHz, and up to 2.6 GHz. Since this is a licensed spectrum of frequencies, there is less risk of interference from coexisting networks such as Wi-Fi and Bluetooth unless using the same frequency bands. For that matter CIoT benefits from well-established cellular security protocols as well as infrastructure support. As far as the disadvantages are concerned, the use of the licensed frequencies often results in a licensing cost for network operators and requires advanced infrastructure to maintain coverage and connectivity. Table 3 illustrates basic features of Cellular IoT technologies and standards.

Technologies	**Coverage**	**Frequency**	**Data rate**	**Latency**	**Battery life**	**Applications**
LTE-M [101]	< 15 km (urban) 15 km (rural) [100]	Cellular wideband [87]	1-4 Mbits/s [50], and higher in Rel- 17 [102]	1- 1.6s [50]	10 years using (5 W h battery) [87]	Mobile IoT applications [73], wearables, healthcare monitoring, asset tracking [73], fleet and logistics management [73].
NB-IoT [103]	<100 km under urban, and 100 in rural [104]	Cellular narrowband [103]	64 - 350 Kbits/s in Rel-16 [104], 1Mbps in Rel-17 [102]	10s -15s [104]	10 years using (5 W h battery) [50]	Utility metering, smart farming, manufacturing automation, smart building, Asset tracking and logistics [73]
EC-GSM-IoT [89]	< 15 km (urban), 15 (rural) [89]	900MHz, 1800MHz (cellular band) [64]	100 Kbits/s	0.7s- 2s	10-14 year (5 W h battery) [87]	Smart metering, asset tracking, wearables, environment monitoring
WiMAX [105]	30 miles [106]	2GHz- 11GHz [106]	40 Mbps [106]	50ms [106]	Not designed for low power Communication [106]	Military applications, No longer being used as other technologies such as LTE, 4G, 5G are more suitable

Table 3. Comparison of prominent CIoT Technologies based on basic features.

This section reviews various CIoT technologies, known for providing extensive coverage allowing the user to host a private network in line with the advertised tariffs and services.

2.3.2.1. Long Term Evolution-M (LTE-M)

LTE-M (Long-Term Evolution for Machines) [101] is a standard supported by The Third Generation Partnership Project (3GPP) for Machine-Type Communication (MTC). Currently, there is more than one version available and each follows a new release (Rel-13) (CAT-M1). LTE-M is designed for low-power wide area communication by including sensors, actuators, and machines for the benefit of telecom operators worldwide. Today, with enhanced coverage, and improved throughput, LTE-M is used by hundreds of vendors globally.

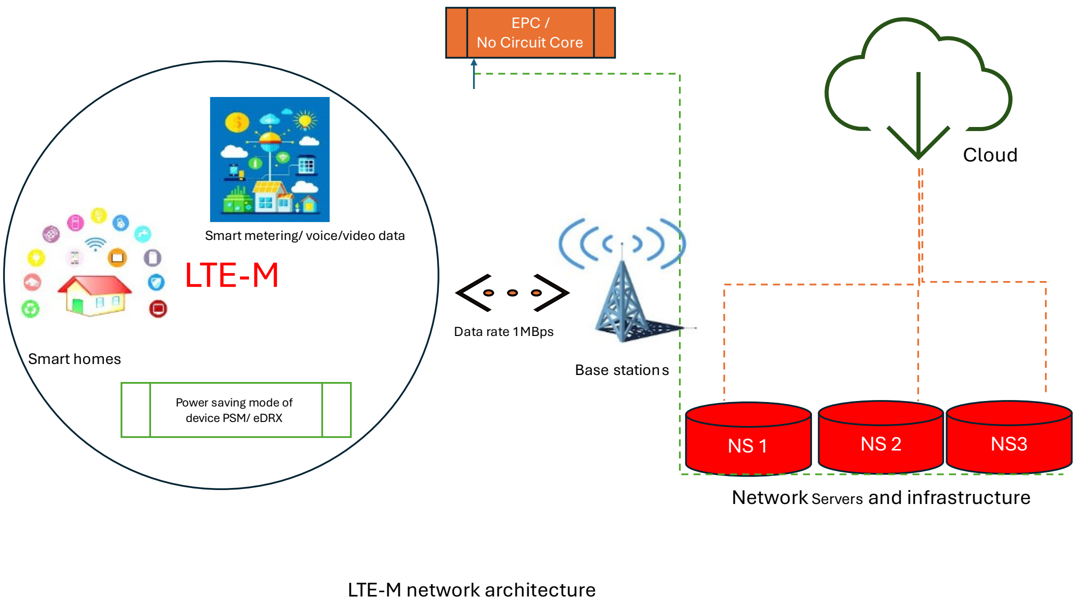

Figure 9. LTE-M network architecture.

LTE-M is wideband technology using wider bandwidth from 1.4MHz to 5 MHz which allows unique advantages such as fastest delivery, high throughput, mobility and responsiveness. The connected devices can offer exceptionally high data rates up to 1Mbps (as per Rel-16), and even higher with the latest release (Rel-17). Until Rel-16, LTE-M has remained the sole provider of the *Voice over the network, and Media streaming* and no other low power IoT technology could rival.

LTE-M has continued to evolve where its recent release (Rel-17) emphasizes the introduction of higher-order modulation, specifically the Quadrature Amplitude Modulation (16 QAM). The transition from QPSK to 16 QAM has enhanced DL throughput capacity; The number of Hybrid Automatic Repeat request (HARQ) also increased to 14 in line with data rate, optimizing UL and DL resource utilization, and improving reliability. HARQ integrates Forward Error Correction (FEC) with Automatic Repeat request (ARQ), allowing a receiver to request retransmission of erroneous subframes (segments of data) while FEC is determined to minimize retransmissions. With an increased HARQ capacity, LTE-M exhibits resilience to anomalies that cause data corruption or high bit errors, ensuring more reliable communication. See Table 3 for comparison with other Cellular IoT technologies in terms of data rate, range, spectrum, applications, etc.

The LTE-M network is comprised of a core network and base-line deployment (indicated in circle). The network architecture of LTE-M is shown in Figure 9. It depicts multiple scenarios including a smart utility monitoring and home automation applications where ported devices to LTE-M network, such as smart meters or home sensors, are managed by a central entity called the Evolved Packet Core (EPC) which ensures connectivity from base line to core network of LTE.

The core network is comprised of NSs and infrastructure. EPC handles mobility, session management, security aspects of the IoT devices and routes from the BS to the core network and back to the base-line network. Consequently, the data is transmitted within fraction of a second.

The base-line network is formed using star topology where each device is one hop away from the nearest BS ("*eNodeB*"). These are LTE cellular towers that provide the link between the IoT devices and the core LTE-M network via EPC. The BSs can add millions of devices and offer better performance across both UL and DL communications compared to remaining CIoT technologies.

LTE-M has an existing eco-systems where devices are benefited from reusability of GSM infrastructure and provide roaming in bandwidth constrained area (including areas currently served with 3G and 4G, GSM network), which is a new surplus.

In terms of power-saving, LTE-M features Power Saving Mode (PSM) and Extended Discontinuous Reception (eDRX) as is shown in Figure 9. **PSM** is a key feature of LTE-M (mobile devices such as smart phones), designed to extend the battery life by allowing EDs to enter into deep sleep period. During this period, the devices perform little or no network activity. This improves network longevity allowing tens of years of life span [107]. **eDRX** is another key feature that is designed to enhance power-savings without compromising the receipt of important incoming stream of messages. To do so, the device wakes up over regular interval of time to ensure incoming messages are received. The use of eDRX and PSM depends on deployment conditions and suitability of domain [107]. Currently, LTE-M is being tested for a wide range of applications including smart metering (Sony) [108], smart wearables [109], supply chain and logistics [34], freight management systems [110].

Existing LPWA and CIoT technologies are both infrastructure dependent where CIoT networks keep the devices synchronized, operate under less congested bands which are designated for cellular technologies, and use relatively higher bandwidth for transmission. The EDs can easily be configured to use a CIoT based network on a subscription basis and can easily perform handover. Setting up a private network is subject to subscription and limits applied as per the tariff by service provider. As far as the challenges are concerned, the LTE-M's transmission range is shorter than other CIoT technologies such as NB-IoT and it suffers from signal loss, high cost of back-end infrastructure, and poor resistance to path loss scenarios (Doppler shift) [111].

2.3.2.2. Narrowband - IoT

NB-IoT is a cellular IoT technology, developed by 3GPP as part of 4G project in release-13. Both LTE-M and NB-IoT provide wide area connectivity to IoT devices supporting machine to machine communication and can integrate well using mobile communication networks such as 5G, legacy GSM, and LTE. The main difference is that the latter operates within narrowband leading to concern over ultra-low power and narrow bandwidth (180kHz) in comparison to 1.3MHz to 5MHz by LTE-M (CAT-M1). It continued to evolve from Rel-13 to Rel-15, allowing improvement in latency, power consumption, and spectrum usage [102]. Under Rel-15, NB-IoT was adopted in 5G networks. Under Rel-16, new improvements were incorporated in terms of optimization of bandwidth, by allowing pre-configured UL communication with enhanced cooperation with 5G networks in 3GPP. The latest release 17 (Rel-17) is focused on improvement in power consumption (to do with duty-cycle following both UL and DL transmission). Currently, it operates within cellular bands to meet long distance communication demands, allowing enhanced coverage using ultra-low power IoT devices. The main applications include marine life tracking [112], animal tracking, and environment monitoring [95].

NB-IoT is the most advanced **3GPP standard**, widely adopted in both industry and research domains globally [113]. Since Rel-15, FDD has become a common framework providing an increased gap between each channel. In comparison to LTE-M, and popular LPWANs such as LoRa and Sigfox, NB-IoT offers increased penetration to coverage and offers good power dynamics (using link budget of over 160-170 dB), allowing tens of years of battery life. This is a maximum transmission power sought by a transceiver. From the deployment perspective, most service providers can allow on the fly deployment of NB-IoT, allowing it to choose a frequency band from both legacy mobile service providers and 5G-oriented networks. However, the choice of deployment can constrain the available bandwidth to the NB-IoT devices via the LTE-network (180kHz), where it is only allowed to use the single Physical Resource Block (PRB) [114]. PRB is referred to as the total available bandwidth where part of its share is dedicated to the LTE-based operation and the remaining share is used by the NB-IoT. It operates across three different modes (*standalone*, *In-band*, and *Guard band.*), with each utilizing PRB distinctly:

The **standalone mode** of NB-IoT is one of the deployment options using its own dedicated frequency spectrum. It is an expensive mode of deployment that requires installation of new hardware equipment. For example, GSM-based NB-IoT implementation in standalone mode not only allow reharnessing and reusability of existing infrastructure like GSM [115] but also requires updated hardware systems to be installed for new service to operate: these are expensive. The key benefit is the simple network architecture and reusability of broadly available spectrum to further improve the network coverage. The application under this mode requires accuracy and reliability; for example, satellite communication by refarming GSM over 100kHz- 200kHz, smart-metering, and asset monitoring [116]. The limitation of the dedicated mode is that it may affect network performance if more devices are added.

Using **In-band mode** of NB-IoT, the bandwidth is as shared LTE-based PRB, which is estimated to be between 180kHz and 200MHz. The benefit is that more devices can be added to perform wireless transmission and reception in a scalable manner using the existing infrastructure of LTE. In summary, the In-band mode of operation of NB-IoT is dedicated to improved coverage. Currently, NB-IoT is being employed with ‘In-band’ mode by *Huawei*, and *Ericsson* for supporting diverse M2M applications such as wearables, smart city applications [50].

The Guard band of NB-IoT mode essentially is an empty space between unused radio frequency bands (100kHz); that is the frequencies that are otherwise reserved to prevent interference with the adjacent LTE spectrum of frequencies being utilized [109]. The applications of such functionalities of NB-IoT include *environment monitoring*, *smart buildings*, and *smart utility*-based applications [86]. *Nokia*, *Ericsson*, and *Huawei* are some of the companies that are using the guard-band mode of NB-IoT.

In terms of internal interference prevention and reduction in the maximum coupling rate (arises due to multipath propagation which affects the signal quality), the narrowband modulation and OFDMA provide effective resistance on carrier frequencies. Notably, NB-IoT isn't the only technology that is using the narrowband; Sigfox also operates within the unpaid narrowband spectrum with a fairly small portion of bandwidth (100Hz) [104]. Sigfox channels are non-orthogonal; hence it necessitates frequency diversity, achieved by FHSS. However, the important distinction is that NB-IoT operates under the licensed spectrum is inherently less prone to EIs and signal degradation over long range. In addition, the NB-IoT-enabled devices are free to use a higher Tx power and can frequently transmit information (about 200 messages a day) compared to the Sigfox (6 attempts per day).

In terms of energy consumption, the devices can last over tens of years after deployment. With the continued focus on energy conservation, the EDs are programmed to only send the relevant data which results in a reduction in control traffic. Apart from that, some of the functionalities that could have been borrowed from LTE are no longer adopted by NB-IoT due to the trade-off with energy consumption. These include *mobility*, *dual-radio connectivity*, and *emergency calling* [50]. Apart from that, NB-IoT applications are mostly confined to ones witnessed in relation to M2M communication for handling a large amount of non-IP traffic via the cellular network. In a recent version of NB-IoT, the key focus is to introduce a location service using multicast capabilities and improve data rate through both UL and DL communication channels, thereby making it suitable for additional IoT applications.

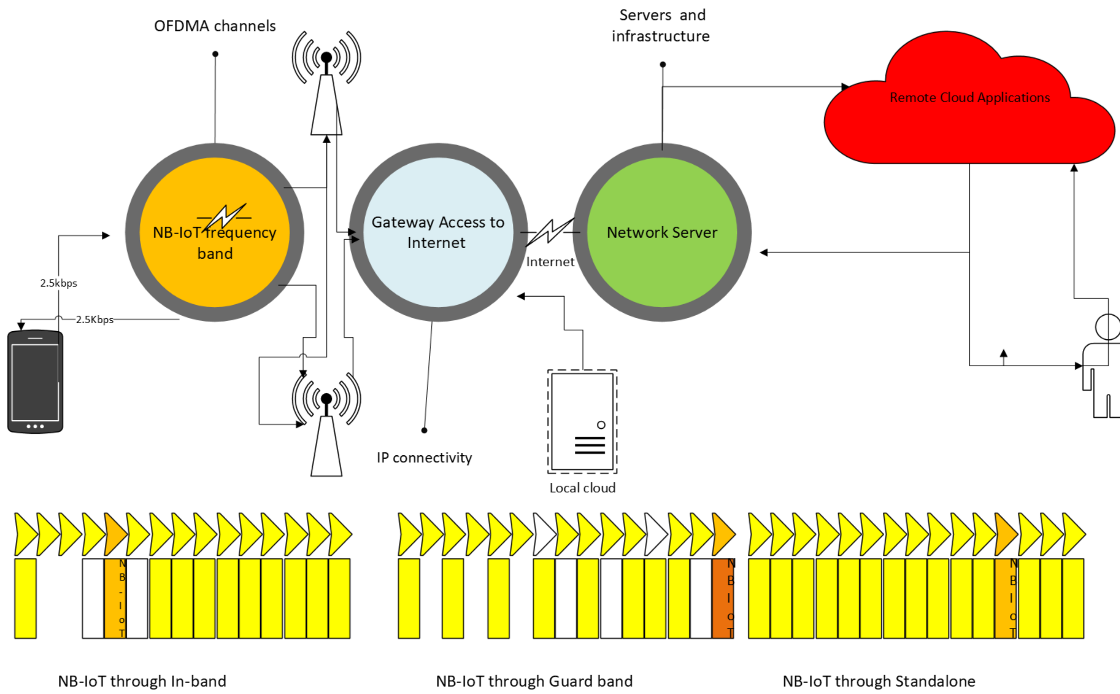

Figure 10. NB-IoT network architecture.

The network architecture of NB-IoT is shown in Figure 10. The EDs are smart mobile devices like smartphones, configured with the NB-IoT network. The attached sensors and actuators are used for data gathering. In terms of deployment, these devices form a centralized alignment with the nearest BS (eNodeB).The example in Figure 10 is showing 2 BSs positioned remotely several miles apart from one another. NB-IoT devices are secure and can communication over 50-100 km with clear LoS, using a small amount of data transmission. That means a single device is sufficient to cover the entire geographical zone, with fewer BSs. Notably, NB-IoT uses only a fraction of the bandwidth compared to the LTE carriers where each BS can configure thousands of devices. The example in Figure 10, demonstrates network operation where useful data is sent through OFDMA clearance to BS and then relayed to the NS via a gateway router, which is the primarily medium to connect the core system or the core network of NB-IoT, linking to the NS. The remote users can upload and download stored data archives, analyze them through cloud applications, and set new priorities for the data collection via the NS [45].

As far as the limitations are concerned, NB-IoT deployment is already complex, and managing NB-IoT for specific IoT applications adds to the complexity due to the cost-benefit trade-offs and competition from existing LPWA technologies, such as **LoRa** and **Sigfox**, as well as the growing adoption of **5G networks**. NB-IoT operates using the 4G spectrum for wider connectivity. Further NB-IoT devices (Digi NB-IoT, Fibocom, SIMCom, etc) are relatively expensive and come in a variety of shapes and sizes, driven by their growing market penetration [117]. Recently, coin battery-powered NB-IoT devices have been introduced, but these devices have limited power, resulting in lower SNR. This can lead to poor energy efficiency and influence packet loss [80]. Some of the NB-IoT's common weaknesses include poor resilience to interference in the guard band, higher latency compared to LTE-M (clearly latency is not prioritized for NB-IoT-based communication, though the delay is subject to the mode of operation), lower data rates in Rel-16 (making it less versatile than LTE such as LTE-M which can offer up to 1Mbps, while NB-IoT is limited to few hundreds of Kilobytes using the same carrier), Under Rel-17 [102], NB-IoT aimed to achieve a higher data rate by employing the higher-order modulation, such as 16-QAM, with support for 14 HARQ processes to enhance resilience against packet loss in both UL and DL communication. However, deployment and spectrum licensing costs vary based on global regulations, and the trade-offs between power consumption and coverage can be substantial [118]. Section 2.4 provides analysis, while further assessing NB-IoT based on KPIs.

2.3.2.3. Extended Coverage--GSM

EC-GSM [89] is another low power CIoT technology using existing traditional GSM networks thereby reaching areas that may have been difficult for other technologies due to their high setup cost. EC-GSM is one of the three releases (Rel-15, Rel-16, Rel-17) under CIoT [87], supported by 3GPP. Under Rel-16, 3GPP offered support for industrial IoT networks using ultra reliable low latency communication; it offers extended coverage and improved coexistence with GPRS capability under GSM architecture, which generally involves low data rates and sporadic transmissions. EC-GSM-IoT is a secure technology that can coexists with 2G, 3G, 4G, and 5G networks while operating under licensed bands. With supported mobile equipment and by reusing the same hardware (core infrastructure that existed with GSM networks), the deployment cost is very low compared to NB-IoT, and LTE-M. Therefore, EC-GSM is an optimized version of GSM that has a strong presence in countries, committed to continue use of 2G, 3G, and 4G networks for example, Africa, and Middle East.

The Architecture of EC-GSM- IoT is depicted in Figure 11. This includes key components of EC-GSM such as the BSs, Transceiver (optimized for extended coverage and low-power devices), Base Station Controllers (BSC) for managing radio resources and multiple BSs, The Mobile Switching Center (MSC) for call setup and mobility management along with the Home Location Register (HLR) databases storing subscriber information. The BS can be utilized for both uploading and downloading with the assistance of packet control unit (PCU) through the BSC.

Packet-switched data is a mechanism where a data packet is broken into smaller fragments before being sent over a network. Each packet is then transmitted independently and can take different paths to reach its destination, where the packets are reassembled into the original message. The role of the Serving GPRS Support Node (SGSN) is to manage adaptation of the packet-switched data within the GSM network and further support the network in terms of routing, mobility support, session management, and security services.

The gateway support is offered by the backbone routers available within the GPRS core network, allowing data delivery to a remotely connected mobile device or customer API.

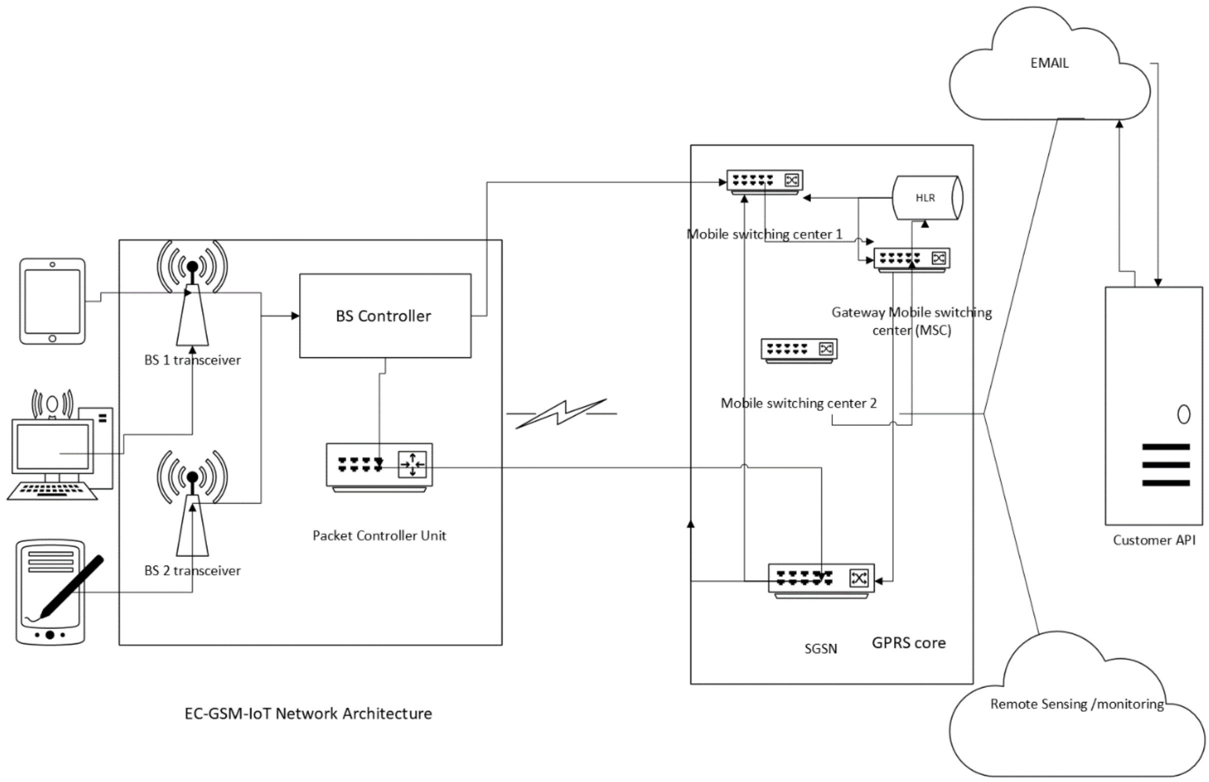

Figure 11. network architecture of EC-GSM.

The Mobile Switching Center (MSC) is a vital component that manages communications and connections between the end devices and the wider telecommunication network, ensuring that mobile subscribers can make and receive calls, send and receive text messages, and access other services as they move through the network. For example, when a call is placed, and routed through the Public Switched Telephone Network (PSTN), (PSTN is the traditional circuit-switched telephone network that has been universally applied for voice communication embraced with network of interconnected telephone lines and switches that provides the infrastructure for public telecommunication), to the Gateway MSC or GMSC (coordinated with other MSCs in terms of locating the mobile user), a dedicated connection path is established between the caller and the recipient for the duration of the call rendering a continuous and stable connection. Before the connection is established, it instructs HLR (Home Location register) to find the location of the mobile device before it is routed to the appropriate MSC, which then forwards its respective BSC and then to the BS transceiver to the mobile device. The HLR is a central repository that stores detailed information about each mobile subscriber that is part of the network.

As far as the limitations are concerned, upgrading the infrastructure for the sake of new IoT applications is infeasible for private investors and shareholders [50]. Thus, the influence of EC-GSM is highly likely in line with the fixed application requirements (long range, low power, scalable communication), with energy-saving and extended range being subject to traffic conditions and sensitivity of GSM towers and cannot be compared with LTE-M and NB-IoT, which use modern infrastructure [87]. Further EC-GSM suffers from the trade-off with energy consumption and data rate [87]. Currently, it does not have the capability to support the *voice over network*s feature in cellular mode, which previously existed with the GSM network [80].

The other vulnerabilities include *interferences* because it operates on the same traditional cellular bands (1800Mhz, 900MHz) as used in GSM. Despite these limitations, EC-GSM relatively offer high latency compared to LPWA and CIoT technologies. It uses the traditional GSM network, which may still have a larger marker share worldwide; however, a majority of developed countries are preferring to use networks like LTE-M, NB-IoT, and 5G for the same purpose. This leads to slower growth in ecosystem development for EC-GSM [50].

In terms of scalability, EC-GSM-IoT offers several benefits while leveraging existing GSM infrastructure. It supports a very high density of IoT devices, extending coverage to remote areas, and providing efficient connectivity between the device and the core network. However, its dependency on GSM networks and its relatively lower spectrum efficiency compared to newer IoT technologies could limit its scalability in the long run. Section 2.4 provides further analysis on EC-GSM's capabilities.

2.3.2.4. WiMAX

WiMAX (Worldwide Interoperability and Microwave Access) is a wireless communication standard designed to provide high-speed broadband access over a wide area. It is a wide-band based standard technology, operating on the SHF (2.3GHz to 5.8GHz) spectrum, and using IEEE 802.16 specification. The technology was launched in 2001 to form interoperability between different standards to provide a suitable alternative to high speed wireless LAN. It drove competition in the broadband market, potentially leading to better services and prices for consumers where it used viable broadband options for rural and underserved areas where traditional wired infrastructure was lacking or economically unfeasible [105]. Traditionally, WiMAX was envisioned as a means to provide last-mile broadband access and compete with traditional cable and Digital Subscriber Line (DSL) services [105].

The architecture consists of a physical layer, MAC layer and WiMAX's upper layers. It provides coverage for both LOS and non-LOS deployment where a non-LOS deployed is confined to 15 km from and to the nearest tower. The technology has been around for over two decades since it was first launched in 2001, and over this period of time, the throughput capability has increased many fold (2Gb) from what it was 30-40 Mb initially.

Pareit et al. [106] surveyed WiMAX with regard to its influence of IEEE 802.16 WG. The author looked at the early trends of WiMAX and compared that with the trends from 2011 onwards. That is, a sharp drop of interest is evident in research contributions using WiMAX beyond 2011. The reason is that the recent development under LPWAN has put WiMAX behind the row of popular mobile broadband technologies. Currently, the use of WiMAX (as a mobile broadband technology) is limited to the aviation sector only. The reason is the limited scope of WiMAX as new technologies such as 4G, and 5G are considered more suitable and feasible for deployment. The reasons include the following:

C**ompetition from LTE**: The LTE revolution has eclipsed the WiMAX standard based on higher data rates, lower latency and better support from major telecom operators.

Limited Ecosystem: While WiMAX ensured interoperability, the ecosystem of devices and vendors was smaller compared to the emerging LTE market.

Challenges with spectrum usages: WiMAX sometimes faced regulatory and licensing hurdles, limiting its global deployment.

Significant Infrastructure Cost: WiMAX infrastructure required significant investment, and in many cases, operators chose to invest in LTE instead due to its broader industry support and future potential.

2.3.3. LP-WPANs

LP-WPANs are a specialized form of private networks, designed for low-power, low-data-rate short-range applications, using the resource-constrained IoT devices. These networks can connect a variety of devices over short distances (typically, from 100 to 200 meters), while consuming minimal energy, and allowing devices to operate for extended periods on small batteries. LP-WPANs are known for timely data transfer, using cost-effective solutions that are easy to configure, though they may suffer from connection loss in dense urban areas due to interference, multi-path fading, and collision. LP-WPAN standards are particularly useful for home and industrial automation, enabling multi-hop networks that enhance range and flexibility to add more devices. This section provides a comprehensive review of popular LP-WPAN technologies and standards.

2.3.3.1. Z-wave

Z-Wave is a proprietary technology primarily developed by Zensys Incorporation [119], and acquired by Silicon Labs [57] in 2003. It offers robust short-range communication that is ideal for indoor applications like home automation [120]. For example, Z-Wave technology is employed in most devices such as smoke alarms and carbon monoxide detectors. Newer versions of Z-Wave offer ultra-low power networking solutions with an increased coverage range of 100 to 800 meters. These products are widely available online through retailers such as Amazon and eBay.

Z-Wave devices are extremely low power, battery operates sensors, that are designed to operate using a short range transceiver; an embedded chip. Upon detection, the devices form a mesh network fairly quickly, allowing seamless exchange of packets without a significant risk of interference and path-fading. This is because the devices operate in sub-1GHz bands within the UHF spectrum, which avoids interference with the commonly used 2.4 GHz spectrum occupied by co-existing networks like Wi-Fi, Bluetooth, and ZigBee. This separation minimizes overlapping frequencies and reduces potential cross-technology interference.

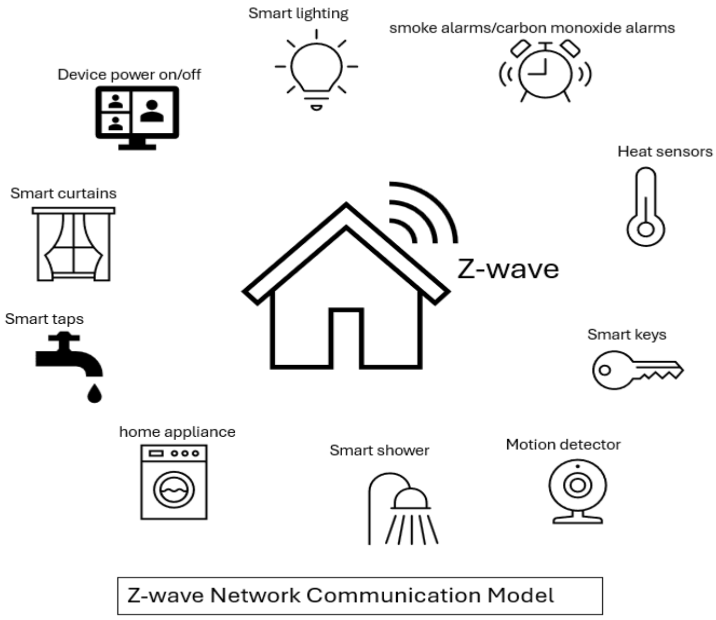

Figure 12. Z-wave network architecture

The networking model of Z-wave is shown in Figure 12 where a large number of dummy sensors and actuators are deployed for diverse use in indoor appliances. Notably, this includes *smart lighting*, *smoke detectors, carbon monoxide alarms*, *heat detectors*, *smart keys, motion detectors, smart taps* (used widely across the globe), *smart washing* and *showering sensors*, and several other devices. The Z-wave has a fully fledged communication stack comprising the following layers: Physical layer, MAC layer, Network layer, Transport layer and Application layer. The protocols used within the stack are proprietary and custom-designed and are only compatible with Z-Wave products. Currently the interoperability and standardization is managed by Z-Wave Alliances.

Z-wave offers many benefits over existing competitor technologies such as ZigBee, Thread, and Wi-Fi 802.11ah and one of its consolidated and promising feature is the increased life span of devices, which is tens of years. This capability is not easily to be challenged by the existing competitors. Apart from that, Z-wave offers secure-access, reliability communication and it is easy to install where each device comes with manufacture guarantees of several months.

As far as the shortcomings are concerned, the first and foremost is the high overheads, which are triggered due to meshed connectivity between Z-Wave-enabled devices. It leads to variations in data rate for two reasons: (a) devices are not IP-operable, (b) use of signaling constantly parting the short coverage. While other short range solutions such as ZigBee can offer throughput rate of 128 to 256 kbps, Z-wave's maximum throughput varies up to maximum of 100kbps, and with high overheads, it may be as low as 30- 40kbps [35]. This is another key shortcoming of Z-wave technology.

The Z-Wave products are available as per the domain of applicability where the latest specification is capable of providing a long-range transmission with new generation software and hardware. However, those platforms too are manufactured by different vendors so interoperability cannot be guaranteed. In terms of DL communication, Z-Wave is not optimized for tracking or monitoring on demand and it is more closely aligned with indoor home automation based applications only. Consequently; there are more suitable alternatives available in the form of standard technologies that are capable to provide seemingly a much higher data rate and extended range (see Table 2 for comparison).

2.3.3.2. Bluetooth Low Energy (BLE)

BLE [121] is a lightweight version of Bluetooth, which was first created in 2010 by Bluetooth Special Interest Group. It is a microwave-based technology that uses the IEEE 802.16 standard. The Bluetooth version 5 by default includes BLE as a built-in component, specifically tailored for M2M enabled IoT communication using mobile devices such as *wearables*, *smart phones*, as well as wireless ad-hoc networks.

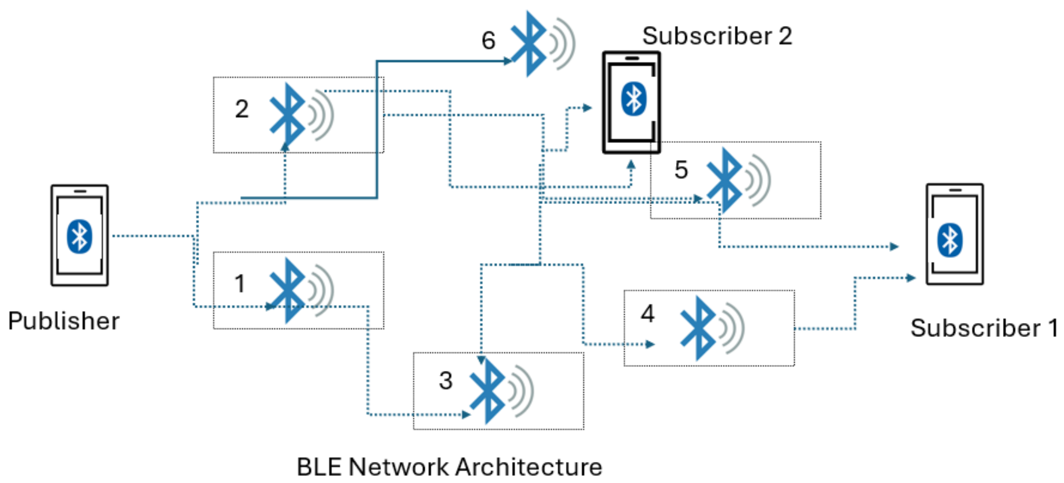

Figure 13. BLE network architecture

The architecture of BLE is presented in Figure 13. It is showing base-line connectivity with a BLE-enabled chip, along with a publisher, and subscribers. BLE was primarily designed to perform neighbor discovery using active and passive modes. For this purpose, it uses the *master* and *slave* communication model. The same strategy is also used by the standards Bluetooth technology except BLE has the flexibility to use *unicast* and *broadcast* mode of operation distinctively at a time.

Using the unicast-based communication model, the devices are scanned actively, and are acknowledged during *neighbor discovery (ND)*, whereas in passive scanning, a varying number of radio channels are used to receive data packets. With the supported BLE equipment, it can offer extended range, increased throughput, long battery life, and secure communication. The key application areas include monitoring, and tracking devices.

BLE unicast mode is a communication feature that allows a BLE device to establish direct connection and exchange data with a specific, single device. This mode is primarily used for applications that require a more personalized and secure interaction between devices. For example, device pairing and control (as a user wants to connect to and control a specific device, such as a fitness tracker, smart watch, or smart lock), data synchronization (syncing health data from wearables to smartphones or transferring files between devices), personalized notifications (for sending alerts and messages directly to connected phones ensuring privacy and security), smart home applications and game controllers to enable responsive gameplay and low-latency communication.

Under unicast connection, BLE-enabled can offer P2P interaction which is essential for applications that need a more direct, secure, and reliable communication between paired devices. Its ability to facilitate personalized interactions makes it a valuable feature in various domains, including health monitoring, smart home automation and personal electronics.

Using BLE's broadcast mode, it allows devices to send data packets to multiple devices without requiring a direct connection. This mode is particularly useful for a variety of applications including location-based tracking, asset tracking, environment monitoring, home automation and fitness devices (wearable fitness trackers can broadcast data such as heart rate, step count, or other metrics to nearby smartphones or fitness equipment for tracking and analysis). While the technology offers improved ND mechanism [122], it is not so precisely accurate as compared to other microwave-based technologies like UWB [123]. *Padiya et a.,* [124] highlighted some limitations of BLE in terms of MP2MP communication in addition to inaccurate discovery (a known challenge), and energy efficiency for outdoor environment. *Jeon et al.*, [125] highlighted BLE's shortcomings as being poorly scalable. Further the author highlights security and hardware-related limitations besides the high current consumption. The high power consumption and poor accuracy have been registered as open issues where BLE devices are employed in localization (for example mapping the location of the discharge in power grids or within the physical cables).

2.3.3.3. Ultra-Wide Band (UWB)

UWB [123] is considered as a small radar, which can stream media at a distance of up to 200 meters. UWB's *beam-like* connectivity has been a popular feature that integrates handheld devices (mobile devices) with the rest of the communication stack. It is yet another microwave-based technology that uses various specifications and amendments of underlying IEEE 802.16, IEEE 802.15 standards. With all supported features remaining active, UWB can locate the position of the device precisely by sending the pulse signals to the corresponding device (smart TV) via the frequency spectrum of 500 MHz (UHF). In this way, it calculates the round-trip delay in a precise, flawless, and contention-free manner. Currently, UWB is evolving with numerous specifications using Impulse Radio [126].

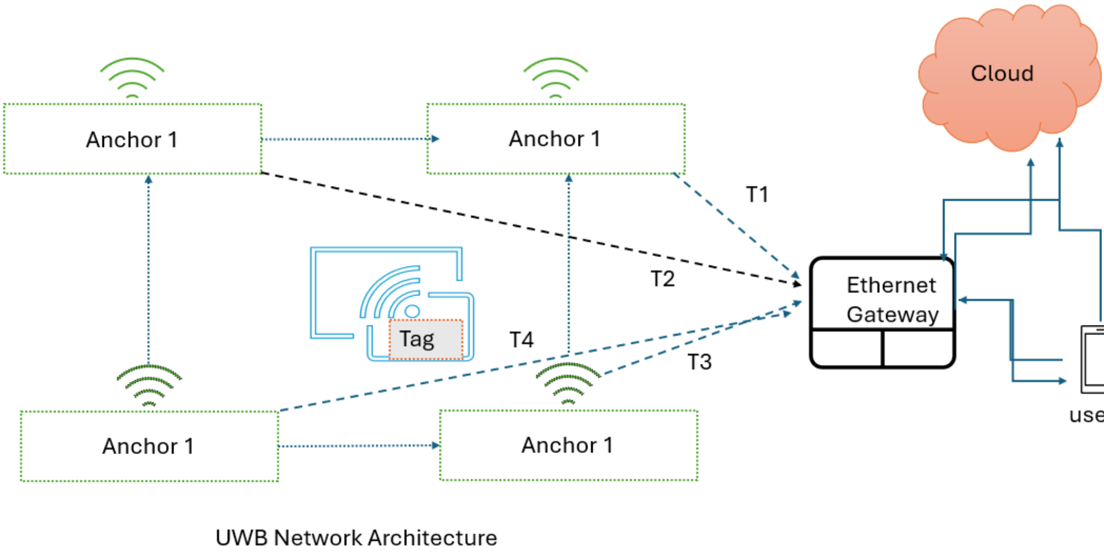

Figure 14. UWB simple network model using Two Way ranging.

Unlike traditional narrowband systems that used a continuous spread factor, the UWB transmits billions of very short, low-power energy pulses across a wide spectrum of frequencies. This approach provides high resistance to interference and other RF- obstacles, making it a suitable technology for tracking, and monitoring based applications. Since UWB uses a large proportion of the bandwidth available, the Tx power usage is regulated by the respective regional authority such as the Electronic Communication Committee (ECC) in Europe. Typically, UWB has been utilized in energy sector for leak or charge detention where it provides the location of the leak very precisely. Today, UWB is more commonly used across wide range of applications of which Multiple-Inputs and Multiple-Output (MIMO) is one example; with more antennas involved in communication, it benefits from multipath propagation using a wide range of channels. This technology incorporates three features towards tracking and monitoring precisely. These include Time of Flight (ToF), Time Difference of Arrival (TDoA), and Two-Way Ranging (TWR) [122]:

ToF measures the time it takes for a signal to travel from a transmitter to a receiver. This time is then used to calculate the distance based on the known speed of the signal (usually the speed of light for radio signals). This technique is prone to multi-path fading and it requires synchronization between anchor chips [123].

Time Difference of Arrival (TDoA) measures the difference in arrival times of a signal at multiple receivers. By knowing the locations of the receivers, the position of the transmitter can be triangulated. Here Multiple receivers record the time at which they receive a signal from a transmitter. The differences in arrival times are used to calculate hyperbolas on which the transmitter must lie. The intersection of these hyperbolas determines the transmitter's location. Despite being stateless (it does not require synchronization between Anchors), it suffers from challenges in the RF environment while the complex calculation of distance is susceptible to error caused by multi-path fading [123].

The third technique is **Two-Way Ranging (TWR)** [123], which involves bidirectional exchange of signals between two devices (transmitter and receiver) and measures the round-trip time to calculate the distance between them. Here, the initiating device measures the round-trip time of the signals and divides by two to estimate the distance, accounting for processing delays. Being highly accurate, it is widely used in mobile devices, TV, and so on. The key challenges is that it requires both devices to communicate to measure the round trip time.

The entire ecosystem for UWB encourages both chip-based (one-hop) and antenna-enabled transmission (multi-hop) deployment. Using IEEE 802.15.13a standard, it offers exceptionally high throughput, extended range, and precise neighbor discovery, which surpasses the performance of outgoing technologies such as Near Field Communication (NFC), RFID, and BLE.

As far as the challenges are concerned, QoS is difficult to achieve using too many specifications [127] and for each specification of radio standard technology, it requires a new modulation technique. Other limitations of UWB include eavesdropping in line of sight deployment. *Neimela et al.,* [128] concluded that UWB does not scale well due to poor security and global restrictions as it uses a diverse spectrum of licensed and unlicensed bands.

2.3.3.4. Near Field Communication (NFC)

NFC is specifically designed to facilitate extremely short-range communication in a secured manner. It uses both radio waves as well as *magnet-based* induction [129] at the distance of 1-3ft. The *touch-based* electromagnetic transmission (*magnet-based*) of NFC is reliable and secure whereas the output can translate into a maximum of 424 Kbps at nearest-distance. This capability of NFC originates from a *chip* that is using an extremely narrow band of spectrum (13.56 MHz).

Figure 15 illustrates the network model for NFC. It is comprised of *active* and *passive* tag devices where one of the devices is a *reader* and other is the passive device. The passive device is called '*Tag*', which is capable of storing limited amounts of information. An active device reads information stored with a tag device and exchanges data simultaneously with the passive device.

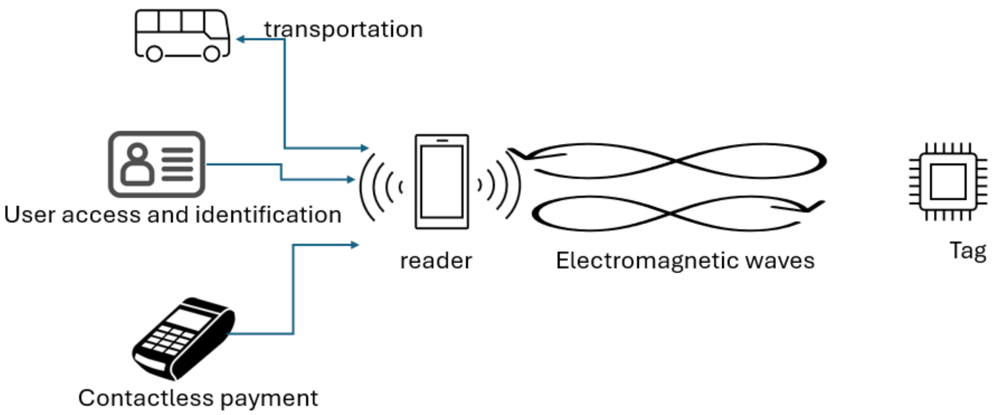

Figure 15. NFC network model.

Currently, NFC is being used as a secure platform for making contactless payment using mobile phone or chip-enabled bank cards. It is also used for various authentication-related services such as undergrounds door access, underwater mines and many other inhospitable zones. A complete list of applications of NFC is given in [130].

As to the relevant challenges, NFC devices are susceptible to physical damage or theft in addition to the fact that the technology is expensive to deploy in secured locations such as campuses, buildings, and other premises [130].

2.3.3.5. Radio Frequency Identification

RFID [131] is a chip-based communication technology that is intended to support M2M communication using *active* and *passive* devices.

It is an inexpensive technology that is currently deployed at a mass-scale for *identification*, and *tracking* purposes, thus making screening and merchandising hassle-free in the retail sector world-wide. The legacy RFID systems support both LF and UHF (such as 13.56MHz and 860-940MHz respectively); with UHF-enabled RFID systems, it can provide extended coverage and lower energy consumption though, the data rate is detrimental to the increased coverage using this technology [132].

The Architecture of RFID network is shown in Figure 16. According to this, RFID devices and Shelf-systems are positioned across both the left and right hand side of the diagram and the RFID Reader is located to scan these devices while maintaining a central position.

Generally, under M2M communication, RFID devices come attached to the product and get scanned upon being brought up to a point of sale system- a service point. The shelf system is fixed; in Figure 16 it is provided with a unique name incorporating the prefix 2348; this is only to distinguish it from other devices shown in diagram. After scanning the ED, the RFID reader sends data to the RFID network, which is further connected to a remote host. The data is archived at storage points.

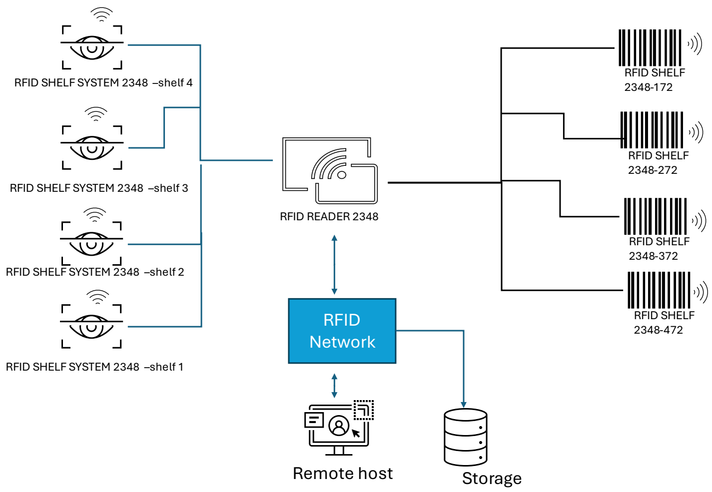

Figure 16. RFID network model.

RFID is not necessarily a "legacy" technology, but rather a mature and widely adopted one. It has been around for decades and continues to be used in many industries, including logistics, retail, healthcare, and industrial automation. While newer identification and tracking technologies such as BLE, UWB, and IoT-based solutions offer more advanced capabilities, RFID remains relevant due to its cost-effectiveness, reliability, and scalability.

Suresh et al., [133], and *Cheng et al.,* [134] have shown that extended coverage is possible using LoS deployment without loss of throughput. However the RFID network poses several vulnerabilities across low, high and ultra-high frequency bands. This includes safety (EDs can be physically abused or stolen and protecting each and every device is not feasible) and security of RFID deployment, energy consumption, poor data rate, limited coverage [135].

2.3.3.6. IEEE 802.15.4- Thread

Thread is an open-standard solution and one of the low-power, secure LP-WPAN technologies designed for battery-operated devices. It is a cost-effective and reliable solution for home usage [136]. Thread devices are based on IEEE 802.15.4 standard, operating on 2.4 GHz.

Based on IEEE 802.15.4, the devices form a mesh topology with the distance from each device is typically being less than 30 meters. Thread provides end-to-end encryption (AES-128), secure commissioning, and device authentication. Unlike ZigBee, Z-Wave, Thread is fully IPv6-compliant, making it easy to integrate with the internet. It Works well with DALI (Digital Addressable Lighting Interface) [137], KNX-IoT, Matter [57], enabling smart home and indoor IoT applications.

IEC 62386 is the international standard for Digital Addressable Lighting Interface, which is published in multiple parts [137]. DALI was originally developed for managing lighting systems, DALI covers a broad range of IoT applications, particularly being deployed in residential blocks (*Fluorescent lamps, low-voltage halogen lamps, LED modules, Switching functions, Color control, Supply voltage controller, conversion from digital signal into DC voltage*), and building automation (*load referencing, thermal gear protection, dimming curve selection , push button, light sensors, and many others*).

KNX IoT [138] is a leading standard used within home and building area networks under IoT domain. It leverages the advantages of IoT technologies to enhance the capabilities of building automation systems, enabling more flexible, scalable, and interoperable solutions.

Matter [139] is the unified standard for smart home devices and the Internet of Things (IoT) application that aims to improve interoperability between different IoT devices and ecosystems such as LTE-M, and NB-IoT, and various RF devices operating on 2.4GHz. The initiative is supported by the Connectivity Standards Alliance (CSA), formerly known as the Zigbee Alliance, and includes participation from major technology companies like Apple, Google, Amazon, and Samsung.

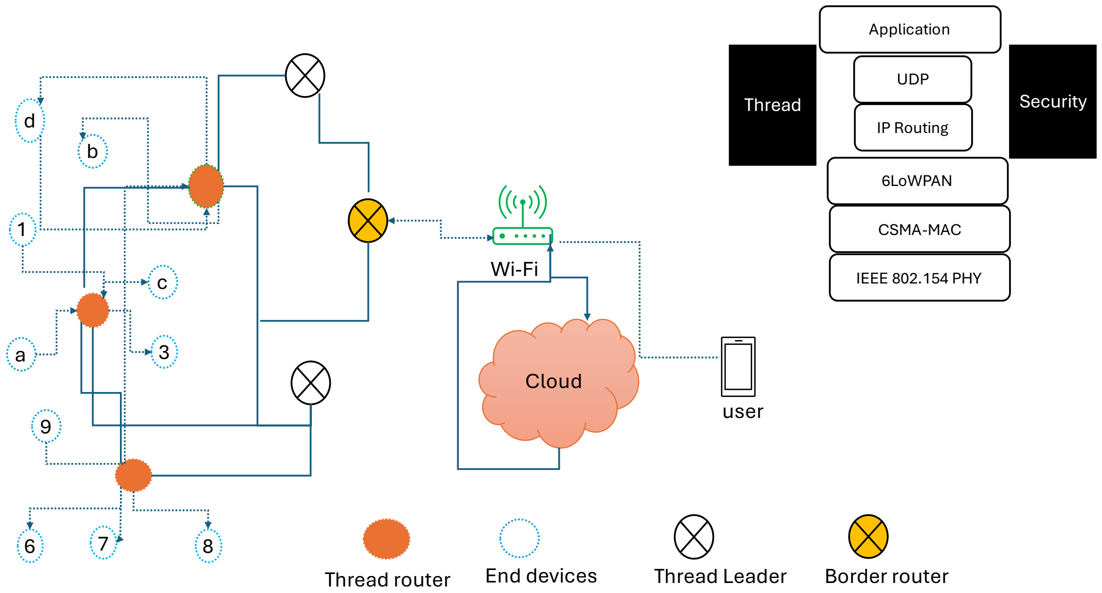

Figure 17. Overview of Thread Network Architecture.

The network architecture of Thread is shown in Figure 17. It shows varying types of thread devices under a single subnet. This includes EDs, used for data gathering. The collected data is relayed to the *leader* device via the nearest relay node. The role of leader is to forward the payload to the nearest Thread router and then the router is responsible for delivery of packets to the border router (network gateway router). The base-line deployment is sparse where each device forms a mesh topology.

Thread is distinguished from traditional LP-WPANs networks based on self-healing as it has a unique feature only introduced by the Thread technology. The relay nodes (leaders) are able to store a high volume of data in their reserves, acting as router. So, if a node fails to send a packet, it forwards the packet to another relay node (leader) which then locally computes a direct path to reach the node (ED) across all given links. The EDs do not offer routing capability.

At the right hand side of Figure 17, the communication stack is shown. Application layer protocols are described in Chapter 3 in detail. The application packet delivery is managed by UDP at the transport layer. The payload is protected with adequate security protocols. In terms of routing and scheduling, the standard relies on standard solutions (RFCs) from IETF and IEEE, aiding flexibility in the communication stack and connection to the internet is direct. That way, it can support various domains of application [140].

In terms of duty-cycle management, it can vary depending on the protocol specifications. For example, the compressed frame size requires smaller duration to transmit the packet, and the radio duty-cycle is naturally a lower share of slot duration. Conversely, transmitting the entire UDP packet takes longer and that way, the standard can adjust the duty-cycle accordingly. IEEE 802.15.4, by default, offers a limited MTU size where the payload adaptability is achieved using a compressed frame size using 6LoWPAN protocol. Many LP-WPANs follow this recommendation for the sake of a lower duty-cycle.

In terms of connectivity, Thread primarily uses Mesh Link Establishment (MLE) to perform joining operation (network). Each router therefore uses beaconing to maintain a link cost. The MLE beacon typically maintains one-hop connectivity. This is based on unicast or multicast between EDs thereby identifying, configuring, and securing links to neighboring devices in indoor environment. Each MLE instance contain information such as the channel in use, Personal Area Network ID (PAN ID).

As the nodes have joined the network, the routing within asynchronized model of Low Power and Lossy Networks (LLNs), is performed on demand using a multicast protocol [141]. It attracts a high volume of overheads and suffers from load-sensitivity. The coverage is subject to a cost imposed by overheads [140]. That is, each source node is required to undertake on-demand probing of link (multicast) and assessing the sensitivity of the radio for reliable path.

Because the distance is not significant between devices, so radio sensitivity may not be unrealistically lower (See Table 5). However, it depends on the deployment conditions: the influence of EIs present in the surrounding areas and multipath propagation can influence communication reliability. To avoid unrealistic links, a symmetrical bidirectionally path cost is maintained by the leader. To compute the path from source to destination, it uses a distance-vector routing protocol [16] but with a compressed frame size. That way, routing is performed locally using on-demand, and it uses a proactive routing protocol among the routers at global level, providing ND service within and across the subnets. For routing beyond the subnet, data packets are sent with a prefix that is maintaining PAN ID, and other necessary headers. This depends on the communication stack as some application prefer 6LoWPAN to ease the stress at the physical layer. The choice of headers and size can vary depending on the configuration of protocols in the communication stack. For example, the address configuration using IPv4 or IPv6 where IPv6 address is allocated through either using SLAAC (Stateless Address Auto configuration) or appoints a suitable DHCPv6 (Dynamic Host Configuration Protocol) server. The instance ID is referred to as PAN ID which includes addresses of BRs for routing beyond the meshed network.

Thread suffers from scalability challenges and while it is largely popular for offering seamless integration to the Internet without requiring 6loWPAN adaptation (possible option), the coverage per devices is limited to up to 30m, and there can be only 32 routers deployed per network; hence it is less likely to be considered suitable for Industrial automation.

2.3.3.7. Wi-Fi 802.11ah

Wi-Fi 802.11ah, also known as Wi-Fi HaLow, is an indoor technology designed to be offering reliable communication using sub-Ghz band (868 MHz). The devices are IP-operable and preferably form a one-hop network with the AP from a maximum distance of 1 km. The enhanced radio sensitivity, ranging from -110 dBm to -120 dBm, ensures the ability to detect a weak signal over an extended distance, while the devices follow asynchronous communication patterns to optimize power savings.

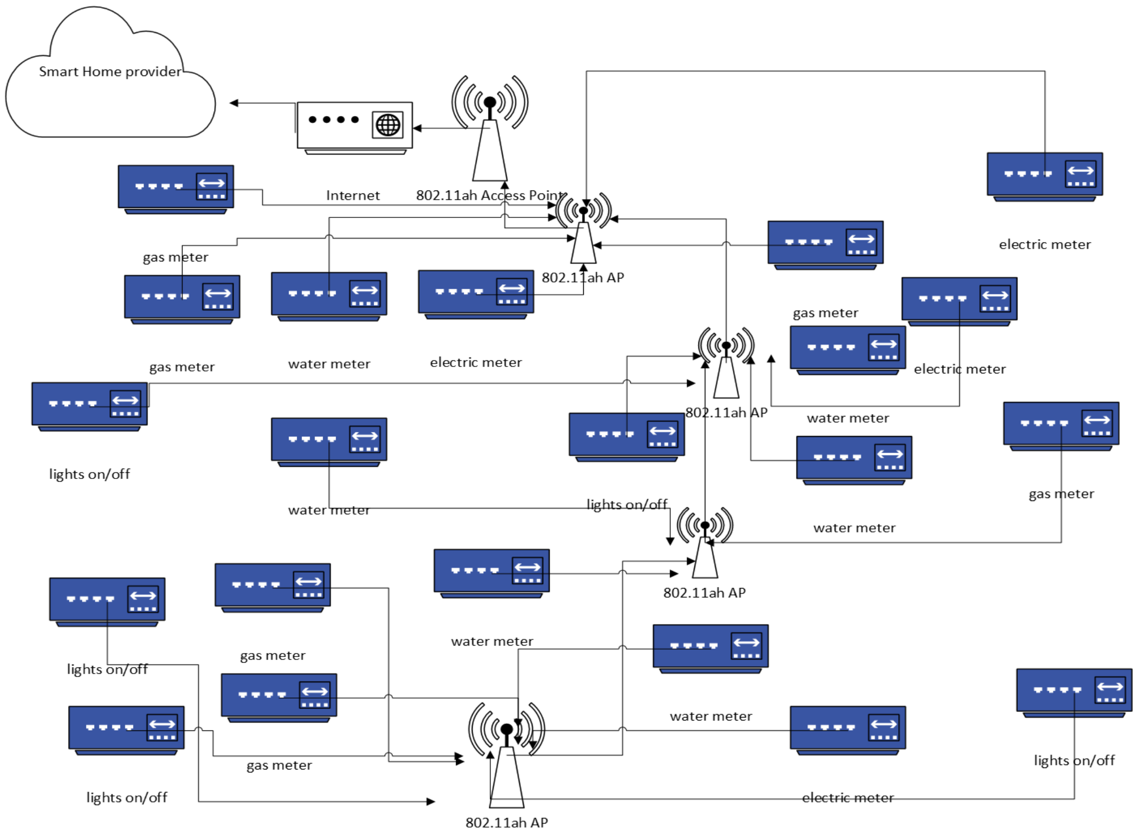

Figure 18. Wi-Fi Halow communication model

This model architecture of Wi-Fi 802.11ah shown in Figure 18 depicts a use case incorporating smart utility network [142] and home automation network [136]. The 802.11ah technology provides seamless integration of heterogenous IoT devices headed by one of more controller. The sensor devices form a star alignment with infrastructure mode in use and mesh topology is assumed under infrastructure-free mode. With infrastructure mode, EDs can communicate with the APs over extended transmission range of 1km. The data from the EDs is relayed through the APs to the internet and then to a central smart home cloud network, where it can be processed and managed remotely. Under the infrastructure-free model, the device can make a direct connection to another device without involving a centralized controller. This flexibility is due to the support from the mature eco-system of Wi-Fi.

With support for a wide range of protocols, Wi-Fi HaLow can offer a secure, and sustainable solution for indoor deployment. In terms of bandwidth availability, it uses 20MHz under 868 MHz, complementing massive IoT applications [68], while it is easy-to-install within infrastructure mode, qualified for industrial IoT applications and critical IoT systems [68].

In terms of spectrum usage and MAC-layer behavior, IEEE 802.11ah (Wi-Fi Halow) is radically different from existing Wi-Fi protocols [143]. Here, AP is in charge of making channel-access rules using three schemes called Restricted Access Window (RAW) [144], Traffic Indication Map (TIM) [144], and Hierarchical Association Identification (AID).

RAW is designed to minimize collisions and improve the efficiency of channel-access in environments with a high density of devices. It splits the channel access time into multiple time slots, allowing only specific groups of devices to transmit within each period. The half-duplex communication structure reduces the chances of collision. Under RAW, 802.11ah gateways are restricted to access certain slots while accessing the channel. Here, a smaller slot is offered for frequent transmission and longer duration for infrequent messaging [143].

TIM decides how long a device should be awake, using the buffered data at AP. Generally, AP wakes up all devices using an infrequent broadcast for data-aggregation where devices read the information from a broadcasting beacon and maintain their clocks accordingly. TIM is applied as a power-saving feature thereby informing each ED as to when they have buffered data waiting at the AP [143]. That way, the TIM mode of 802.11ah helps reduce power consumption by allowing EDs to sleep most of the time and wake up only when they need to receive data [145]. However, this mechanism requires synchronization between AP and EDs and multipath challenges can cause a signal loss; hence the communication fails. To avoid signal loss, it incurs a significant volume of beaconing between APs. Resultantly, it has an adverse impact on communication performance. That is, in addition to the fact that implementation of TIM is a complex procedure [144].

The Association Identifier (AID) mode is a unique feature assigned by the AP to each and every ED while joining the network for managing communication and optimizing scheduling efficiency when used alongside TIM mode of 802.11ah. It highlights which device has pending transmission or reception. The EDs enter sleep mode when there is no activity and wake up only when necessary, thus it not only enhances power-savings, but also aids resource management by enabling the AP to track and manage the schedule efficiently.

AID allow thousands of devices to be connected to the single AP. The hierarchical structure for AIDs not only improves scalability [38] but also reduces overhead. The key drawback of this mechanism is the requirement of tight synchronization between AP and the BS [146].

Currently, there are several variants of Wi-Fi standard available where 802.11ah is specifically designed for industrial-scale deployment, however, it does not provide resistance to indoor interferences due to multipath propagation [143] under the infrastructure mode and as more devices are added, the multipath propagation becomes too strong, causing path-loss. Contrarily, the infrastructure-free mode triggers a high volume of potential retransmissions due to signal loss [143]. The persistent multipath fading keeps the radio on for listening of payload for long time, one of the causes of slower market adoption; thus it is less suitable for industrial automation while there are alternative technologies which can combat multipath challenges using frequency hopping or frequency diversity techniques. For example 6TiSCH, WirelessHART, LTE-M [79].

2.3.3.8. ZigBee

ZigBee was developed by the ZigBee Alliance in 2002 as a short-range, low power, low-data rate wireless network technology. It is currently operating using two different radio specifications, enabling flexibility in communication and data transfer speed. The primary specification is based on IEEE 802.15.4, which is common among most LP-WPANs operating in the UHF, particularly, on the 2.4 GHz band. Under this specification, devices follow a synchronized communication pattern, where the maximum transmission unit (MTU) size is restricted to 127 bytes.

IEEE 802.15.4 amendment 2012 has two bands of frequencies where 2.4GHz is the secondary band (mode 1), used by most short-range deterministic networks where, by default, it uses Offset- Quadrature Phase Shifting Keying modulation (O-QPSK) with each symbol mapped to a 4 bits or 32 bits Pseudo-random sequence. The Pseudo- random Noise (PN) is used to spread the signal to wider bandwidth. The mode 2 (868MHz) of IEEE 802.15.4 amendment 2012 uses Binary Phase Shift Keying (BPSK) which uses 0s and 1s to represent the phase of signal arrival over time, mapping each symbol into 2 bits, that is 15 chips. The drawback of 15 chips is that it is not robust from a security point of view. Contrarily, a 32 chips with Pseudo-random noise, not only, spreads the signal widely but also prevent any correlation provoking jamming (eavesdropping or denial of service attacks).

The second specification of ZigBee is incorporated with BLE using IEEE 802.15.1 standard. This specification allows a slightly larger MTU size (250 bytes) and so the data rate can vary in between the mode of operations (it is reviewed under Subsection 2.3.3.2.). Notably, ZigBee ,by default, uses IEEE 802.15.4 standard and this is because of anticipated wake up of the devices is lower (30 milliseconds) compared to the BLE counterpart that can take up to more than one second to wake up.

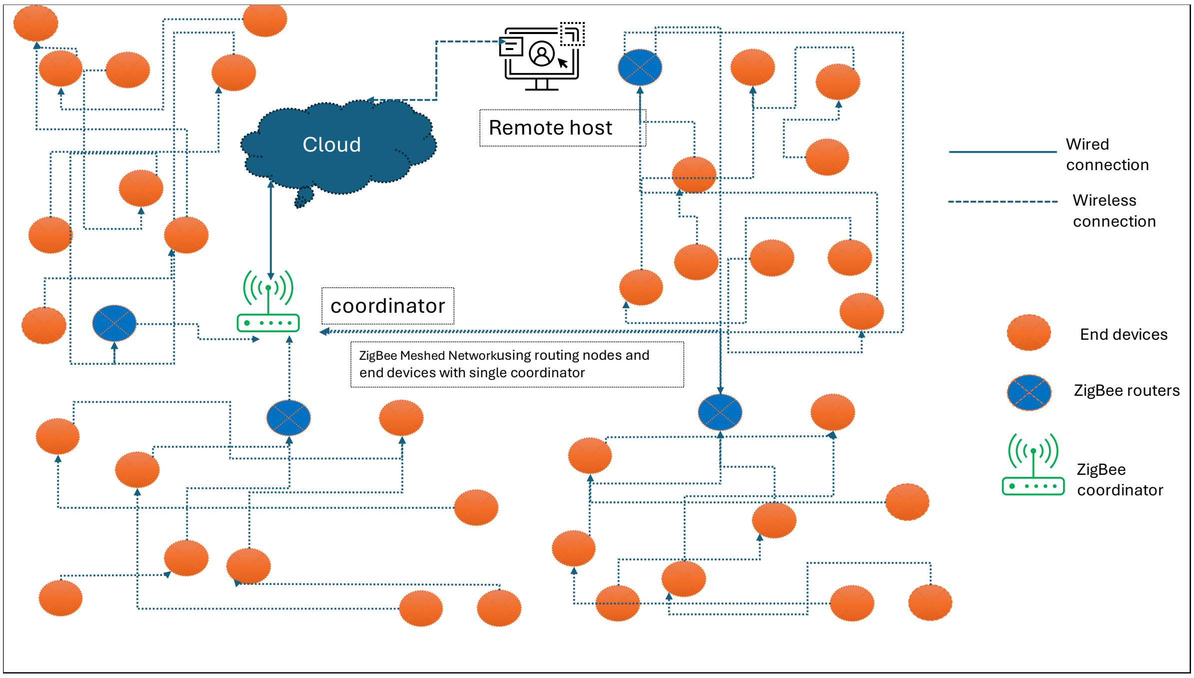

Figure 19. ZigBee Network model.

Figure 19 illustrates ZigBee architecture. The end nodes interact (shown in orange) with the ZigBee Router (ZR) where each ZR (shown in blue) can have multiple devices deployed; this deployment is not without site testing because there may be significant obstacles present that can impact link stability due to multipath effects. The impact assessment of path loss is usually performed before installation.

The connectivity from one ZR to another ZR takes place using a complex ND process where it is possible for a device from one ZR to send information to nodes under different ZR. The role of the **coordinator** (shown in green) is to manage its configuration and there is only 1 coordinator for the entire WSN. Using this model, ZigBee devices upload and download the data where the backhaul connectivity can be managed remotely via the Internet or Ethernet or cellular technologies(4G, and 5G).

The standard protocol stack of ZigBee using the IEEE 802.15.4 specification is flexible in terms of topological alignment where the network benefits from extended coverage by using multi-hop transmission as the transmission range of ZigBee sensors is constrained to few hundred meters only.

ZigBee has advanced significantly in both hardware and software, backed by a robust ecosystem of international standards and major manufacturers like Silicon Labs and Matter (discussed in Chapter 1). These developments enable ZigBee to adapt to new design objectives and expand its applications in home and building automation, solidifying its position as a leading LP-WPAN. Notably, ZigBee devices are allowed IP functions such as addressing and routing, enabling its use across diverse domains. While IPv4 limits scalability due to its insufficient address space, IPv6 overcomes this constraint, supporting ZigBee's growth and facilitating broader IoT deployment.

For a dense network, IPv6 is adopted with the 6LoWPAN protocol-suite by ZigBee providing payload compatibility. This is because the UDP payload is too heavy to be translated by the physical layer. Here, it is not being suggested that IPv6 doesn't support TCP. In fact, IPv6 fully supports both TCP and UDP, just like IPv4. However, IPv6 with TCP triggers a high volume of overheads compared to UDP, which is a simpler connectionless transport layer protocol that doesn't require guaranteed delivery per transmission. IPv6 supports UDP to facilitate applications that need quick, efficient data transmission without too many overheads. All transmission are scheduled using CSMA/CA as a default channel-access MAC layer protocol, traditionally used in wireless communication.

ZigBee is exclusively known for having a broader echo-system of protocols with RFCs and without RFCs, and the deployment follows a site test so that it could avoid any predictable obstruction. While it is a renowned standard for home and building automation, its ability to deal with wireless interference and multi-path challenges is poorly defined and recalibrating the device’s position in relation to existing RF barriers, both indoors and outdoors is not ideal for robust operation. Further, ZigBee lacks communication efficiency in terms of increased overheads from non-RFC protocols and poor reliability due to poor modelling of MAC layer capabilities.

As far as the other limitations are concerned, each ZR in ZigBee network is restricted to maximum of 30-50 devices. Beyond this limit, the network efficiency is negatively affected. The primary issue arises from *RF factors* and *payload incompatibility*. In a dense network with more than 30-50 devices, not only does the load factor increase, but the probability of interference from co-existing networks, such as Wi-Fi, also rises. The MTU size of IEEE 802.15.4 is restricted to 127 bytes, whereas a UDP packet may consist of several hundred bytes. A direct injection of a UDP packet for transmission can keep the radio engaged for a prolonged period, leading to an accelerated duty-cycle, and increased probability of packet loss due to existing RF factors such as EIs and multi-path challenges.

Additionally, in short-range, low-power, low-data-rate IEEE 802.15.4 networks, devices frequently interact and send data. A longer delivery time will keep the communication queue occupied until the packet is fully transmitted. This results in increased waiting times for other nodes trying to send or receive data, thereby affecting the network's overall reliability. In the worst case scenario, a single point of failure can trigger reconfiguration as there is only a single router for the entire network.

For internet integration, ZigBee relies on the IEEE 802.15.4 standard paired with 6LoWPAN for IP connectivity, and can also connect directly using IEEE 802.15.1. However, emerging solutions such as WirelessHART and 6TiSCH present more advanced options, addressing some of ZigBee’s limitations. These standards, operating on the same IEEE 802.15.4 physical layer, provide enhanced protection from EIs and multipath-fading, and are optimized for large-scale deployments. These standards manage bandwidth utilization more effectively, making them well-suited for load-sensitive applications.

2.3.3.9. WirelessHART (IEC 62591)

WirelessHART was first introduced in 2007 by the HART communication foundation [6] with the objective to provide secure, reliable communication for industrial automation (for protecting critical infrastructure within Oil Refineries) [147]; it was approved by International Electrotechnical Commission (IEC) as a standard for industrial networks in 2009. Currently, more than one specification of WirelessHART is available where IEEE 802.15.3 is sought for high throughput applications such as vehicular network and logistic management [148] and IEEE 802.15.4 is commonly used serving a low power, low data-rate based industrial IoT network.

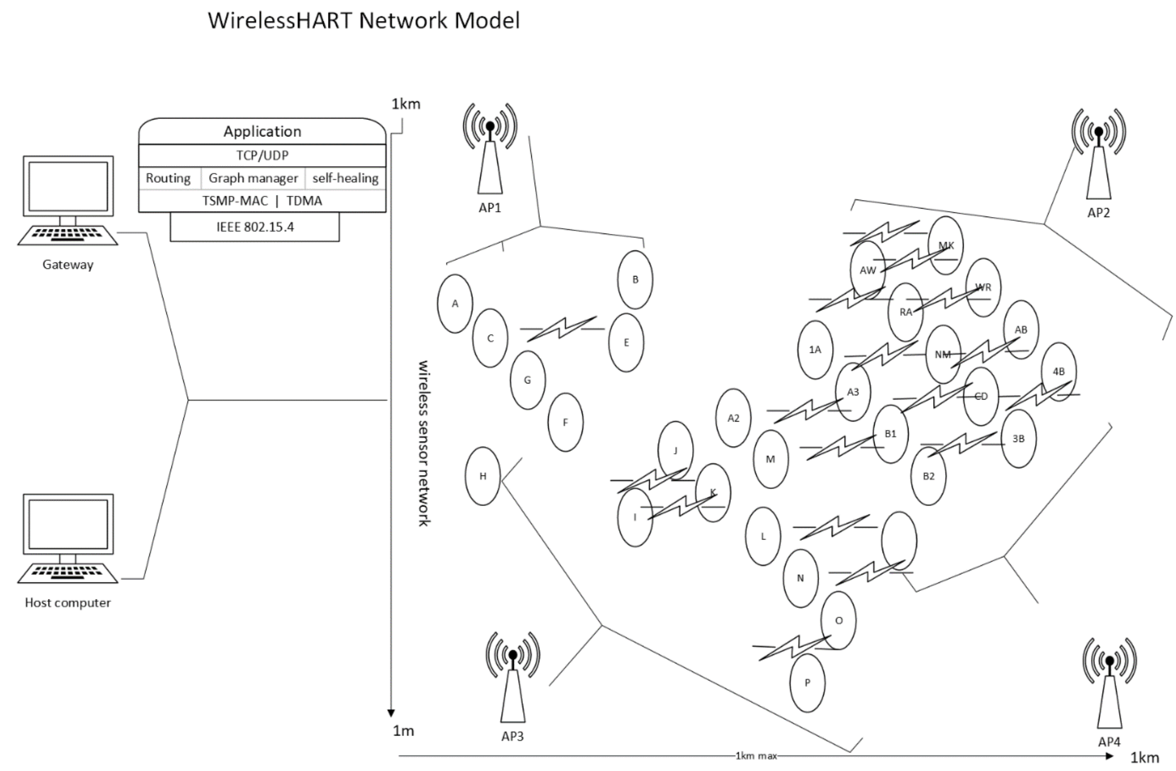

Figure 20. WirelessHART architecture.

The architecture of WirelessHART, depicted in Figure 20, comprises essential components tailored for industrial networks. At its core, a host computer connects to a gateway, which acts as a bridge between the base-line WSN and the host server. This gateway manages essential network functions such as data routing (graph management), and self-healing, ensuring continuous and reliable communication. At the base-line, multiple sensor devices form a mesh topology, with each device containing several wireless links leading to Access Points (AP1, AP2, AP3, and AP4). The APs, specification is crucial towards communication between the sensor nodes and the gateway for reliable transmission where TSMP (Time-Synchronized Mesh Protocol) [149] implemented by each device provides effective resilience to EIs and multipath challenges ensuring reliable transmission while switching frequency rapidly; thus reduces congestion over existing channels. Here, TDMA is alternatively utilized by other specification besides it is not capable to prevent path loss triggered by multipath propagation and EIs.

WirelessHART use a proprietary communication stack with TCP/UDP protocols, situated at the transport layer supporting a higher-level functions such as routing graph management. This is because the WirelessHART does not have a network layer. For routing, it employs a *Graph Manager* [6], which is responsible for configuration and maintenance of the optimal routing path, thus optimizing the network for reliability and improved performance: the graph manager replaces the IP functionalities provided by the network layer. However, this incurs a high amount of overheads and lack of IP support. Currently, the standard can operate with a maximum of approximately 8K EDs across all subnets [6].

The other limitation includes a high duty-cycle as devices takes longer to transmit a heavy payload via IEEE 802.15.4 in 2.4GHz band without using payload fragmentation and header compression for a lighter frame size. It incurs jitters since the MTU size of the underlying radio technology (IEEE 802.15.4) is several times lower than the UDP payload. Currently, one of the aims of IEEE 802.15 WGs is to develop a common standard that is interoperable with all low power, low data-rate technologies and standards [148]. However, it requires IP-operability, which WirelessHART architecture does not incorporate. This results in a scalability limitation challenge in terms of adding more devices to the network.

2.3.3.10. ISA 100.11a (IEC 62734)

The ISA100.11a is a global standard for industrial wireless communication networks, currently part of LP-WPAN [7]. This technology is designed to provide a real-time communication for delivering a time-sensitive traffic (deterministic latency). The devices are IP-operable and the standard communication stack has a network layer. For end-to-end delivery of data packet, it implements TCP/UDP protocols where UDP is preferred because it is a connectionless protocol and offers faster transmission by eliminating the need for establishing and maintaining a connection, as is required with TCP. For adaptation and compression of IP headers, it implements the 6LoWPAN protocol [9] to enable IPv6 communication over IEEE 802.15.4-based networks [150]. The MAC layer utilizes standard channel-access protocols such as CSMA and TDMA protocols where CSMA provides random access using a single channel and TDMA is used to provide a time reference while scheduling transmission by each device on a single channel.

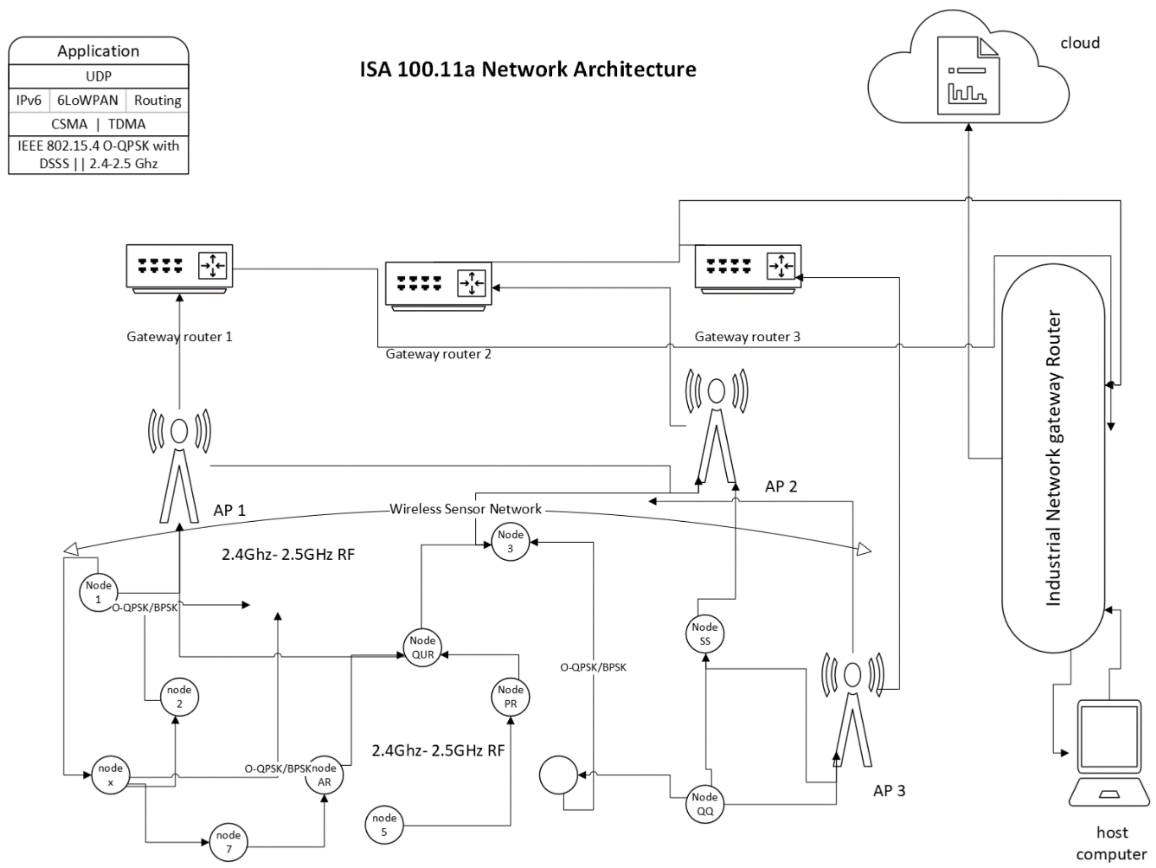

Figure 21. ISA 100.11a network architecture.

The network architecture of ISA 100.11a, is shown in Figure 21. It depicts a comprehensive deployment of industrial WSNs. At the core is the network gateway router that connects to the host computer and cloud, enabling data analysis, monitoring, and control from remote locations.

The WSN shown in Figure 21 is comprised of multiple sensor devices (Node 1, Node 2, etc.) organized into a multi-hop tree topology where each device operates with few under meters of transmission range using 2.4GHz. The industrial sensors deployed within the WSN communicate wirelessly through controller (AP 1, AP 2, AP 3) providing a decentralized access to network resources. The APs gather data from EDs and relay it to gateway routers (Gateway Router 1, 2, 3), which further direct the data to the industrial network gateway for cloud storage or further processing

The communication stack of ISA 100.11a is more flexible than WirelessHART as it can use existing standard RFCs and is fully IP-operable technology. However, customizing the protocol stack can pose new challenges, particularly in managing power consumption versus overheads. To search for a destination in the nearby subnets, it generates a huge amount of control traffic, causing rapid depletion of network resources and battery. Apart from high consumption, the technology is prone to multipath challenges and that too it does not implement channel-hopping technique at MAC layer. Consequently, ISA can not be proven reliable technology for IoT-driven industrial network.

Technologies	Coverage	Frequency	Data rate	Latency	Battery life	Applications
Z wave [120]	0- 800m [120]	868- 908 MHz [120]	0-30 Kbits/s [120]	very low [50]	5-7 years (AA type battery)	HA. Security systems such as fire alarm. Lighting control, energy management.
UWB [123]	up to 200m (indoor) [122]	3.1- 10.6 GHz [126]	4- 675 Mbits/s [126]	very low [126]	Few months (240 mAH Lithium coin cell) [126]	Indoor positioning, smart phone since 2019, navigation, keyless entry system ,retail, sports, safety and security
802.11ah [8]	1km [146]	Sub-1GHz [146]	100 Kbits/s [146]	varies on traffic [146]	5 years (rechargeable Lithium-Ion) [146]	Indoor monitoring, and tracking, smart homes, building automation.
BLE [121]	0-100m (start topology)	2.4- 2.485GHz	21 Kbits/s	6ms	2 years (2200mAh)	Health care medical devices, fitness and sports (tracking), smart home appliances, BLE-enabled cameras.
ZigBee [151]	0-100 m in star topology [152], 1-2 km (using BLE)	868-915MHz & 2.4 GHZ [152]	250 Kbits/s [152]	1s [152]	2 years (2200mAH) [152]	Smart home and building automation, navigation, and controlling.
WirelessHART [6]	200m- 1km	2.4GHz	250 Kbits/s	<4s over 80 bytes	5-10 years over 1 ppm (3000 mAH)	Oil refineries and industrial automation, retails, and warehouse operations.
ISA 100.11a [7]	200m-1km (multi-hop coverage)	868MHz-2.4Ghz	250 Kbits/s	<100-600ms	5-10 years over 1ppm (3000 mAh)	Oil refineries, and Process Automations

6LoWPAN (IEEE 802.15.4) [153]	0 - 200m (star topology), 1km (tree topology)	2.4GHz	256 Kbit/s	under 1s	2 years , subject to scale of operation (2200 mAH)	Smart Home, Environment monitoring, Asset tracking, Building automation
6TiSCH (IEEE 802.15.4) [15]	1-2 km in multi-hop tree [15]	2.4 GHz	256 Kbits/s	1s or less	2+ years, subject to scale of operation (2200 mAH)	Industrial Automation, smart homes, building automation, smart car parking [140].
Thread (IEEE 802.15.4) [140]	Up to 30 meter [140]	2.4GHz [140]	256 Kbits/s [140]	Very low [140]	2-5 years depending on traffic (Lithium-Ion) [140]	Smart Phones, Building Automation, Home Automation, Hotels.
NFC [154]	up to 3 ft. [154]	13.56 MHz [154]	424 Kbits/s [154]	0.05s or less [154]	NFC chip powered by device battery (smart phone)	Smart phones, and payment terminals.
RFID [155]	10cm-12cm	13.56, 865-868 ,902-928 MHz	100 Kbits/s	0.05s or less	RFID (for active mode, devices are powered by AA, forming air interface over several hundred meters), passive mode does not have any battery	Active devices used for signal jamming for open air operation, Retails, Warehouse, factory, and more commonly used in almost every small enterprise.

Table 4. Comparison of prominent LPWPANs Technologies and standards based on basic features.

2.3.3.11. IEEE 802.15.4-6LoWPAN

6LoWPAN was developed by the IETF working group in 2007 to improve performance in battery powered Wireless Personal Area Networks (WPANs) [9]. It uses a multi-hop transmission model with extended range and promises good interoperability as nearly all smart devices are identifiable with a 128-bit IPv6 address.

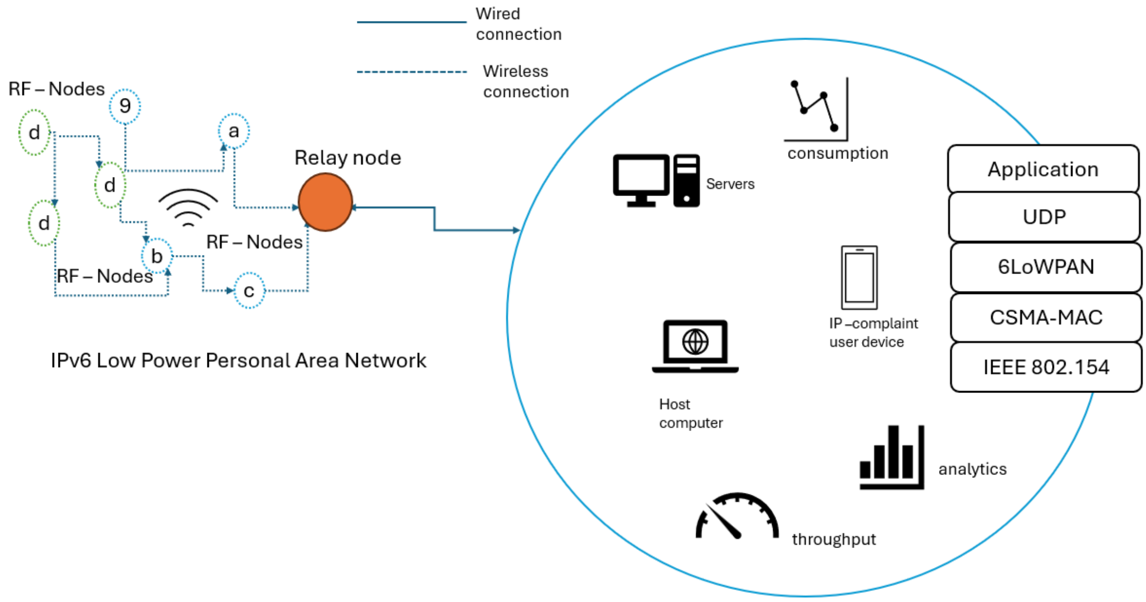

Figure 22. 6LoWPAN network model.

The 6LoWPAN architecture is shown in Figure 22. According to this, wireless sensors attached to the IoT device generate data, which is converted into a signal by the modulation scheme (IEEE 802.15.4 used by default with DSSS), carried by the UHF band, particularly the 2.4GHz.

For end-to-end delivery, UDP, a transport layer protocol, is employed (solely because it generates less overheads). The generated UDP payload is passed through the root (AP), which acts as a controller to a subnet and is not constrained to memory or processing capacity. The root is powered device that facilitate IPv6 addressing, RPL routing, and scheduling using CSMA as shown in the architecture. These protocols are reviewed in Chapter 3 briefly.

6LoWPAN protocol compresses the IP headers and divides the payload into fragments of manageable size so that these are translatable to the device's radio for smooth transmission [156]. The packets assembly mechanism on the receiver's end reassembles the payload to reconstitute the original packet. In existing IPv6 6LoWPAN architecture, the transmitter forwards packet fragment based on FIFO and waits for the entire payload to be received before forwarding a packet in the queue. Here, each fragment is given a IPv6 address containing source and destination prefixes, allowing them to independently access a shortest-best path, however this introduces the forwarding delay while it waits for entire packet to be received.

The inconsistency in payload assembly and queue utilization remains an open challenge in the 6LoPWAN network to date (it is further discussed in chapter 3 in relation to 6TiSCH which also uses existing IPv6 6LoWPAN architecture): once all fragments have arrived the original packet is formed, or all the fragments are dropped [157] due to inefficient recovery of a particular 6LoWPAN fragment.

Each fragment on the way to the destination wait for a contention-access, that is implemented by CSMA/CA where one of the its key shortcomings is longer waiting period and it provokes collision when two or more nodes are sending packets at the same time. Scheduled fragments are then delivered to the physical layer, which implements IEEE 802.15.4 standard and radio module is configured at 2.4 GHz for end-to-end transmission.

6LoWPAN standard has been evolving with various specifications of MAC layer standards. The current specification over IEEE 802.15.4 has attracted attention in terms of making 6LoPWAN reliable and scalable. Currently, neither specifications of MAC layer protocols include interference mitigation plan, which is vital for reliable transmission. Hence multipath-fading, and EI remain key challenges that are hampering the reliability of 6LoWPAN network. The other vulnerabilities include shorter range, poor ability to cope with load sensitivity in large-scale network [158].

2.3.3.12. IEEE 802.15.4- 6TiSCH

6TiSCH is a low power communication standard, operating at 2.4Ghz using IEEE 802.15.4. It was introduced in 2013 by IETF and IEEE as an extension to IEEE 802.15.4-6LoWPAN standard. It implements channel-hopping technique at the MAC-layer to combat interferences and mitigate multipath-fading effects. Additionally; it introduced a cross layer, situated just above the TSCH-MAC layer for efficient management of link-layer resources, while at the same time collecting network statistics due to its central position in the 6TiSCH stack (connecting the ends of the 6TiSCH stack). This is demonstrated in Chapter 3.

The 6TISCH standard [15] currently offers seamless connectivity with reliable transmission in a scalable multi-hop topology, and integration to internet via 6LoWPAN [158]. 6TiSCH can be deployed both indoor or outdoor as a private network, with or without internet connection. Currently, 6TiSCH has been standardized for both small scale and large-scale industrial networks, with network coverage per subnet is restricted to 1-2 km. The typical application of 6TiSCH include, factory automation [40],leak detection in gas-pipeline [159], plant automation, and smart agriculture [27], energy harvesting and smart grid [43], building automation [160], smart car parking[128], industrial IoT applications [128], etc.

In terms of communication patterns, 6TiSCH is only optimized for MP2P, and P2MP. The P2P communication using 6TiSCH suffers from poor reliability and lack of robust routing. This is because the sensor devices do not have sufficient buffer to store routing dynamics. At present, the routing metrics and path-computation is exclusively provided by the root, which is not constrained by storage, and processing capability, and may come with higher battery capacity or a pre-existing power source.

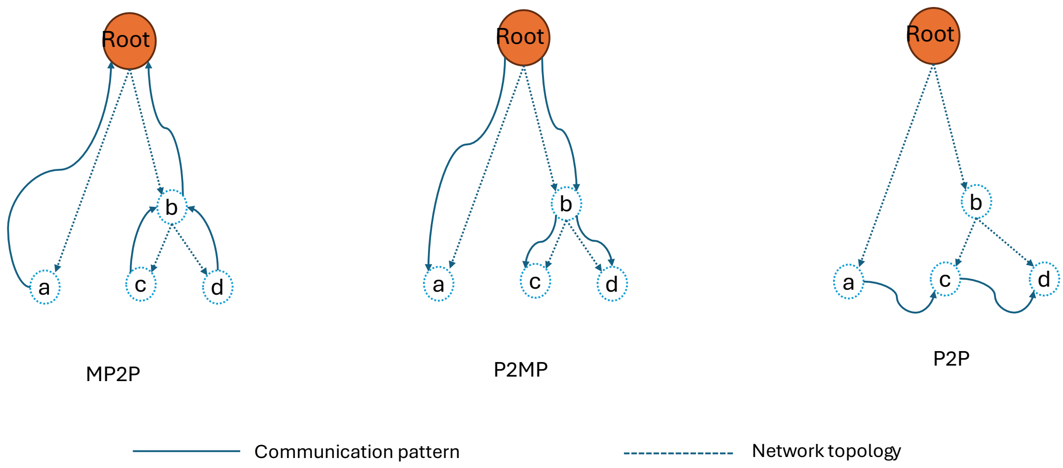

Figure 23. communication patterns in wireless sensor network using 6LoWPAN.

Figure 23 illustrates three communication patterns relevant to 6TiSCH networks:

1. **Multipoint-to-Point (MP2P)**: Data flows from multiple nodes (such as a, b, c, and d) to a node while forwarding the collected data to the root. This is the primary pattern employed for sensing based applications (gas leak detection, alarm system etc.)

2. **Point to Multipoint (P2MP)**: The root sends data to multiple odes, supporting use cases such as query forwarding or firmware updates. This is important to make devices to gather data based on the query propagation. It is also a preferred pattern to communication with a node via root. That is, nodes send data packets to the root first using MP2P pattern, then root decides the correct path to the destination using which the sender completes the transmission.

3. **Point-to-Point (P2P)**: A source node can communication with destination node without using root as common ancestor. This is achieved by signalling with intermediate nodes if the destination is not within the direct range.

IETF 6TiSCH is by default scalable up to 64000 sensor devices where multiple subnets can operate under single IPv6 6LoWPAN Border Router (6LBR). In the large-scale networks, the IPv6 address configuration focuses on two key aspects: autoconfiguration of addresses and ND services. The process for address configuration varies depending on the topological alignment: **‘Route-over’** and ‘**Mesh-under**’ topology.

In ‘**Route-over**’ alignment, IPv6 addresses are configured using RPL routing references. The 6LBR broadcasts Route Advertisement (RA) through a 6LoWPAN Local Router (6LR). Both the 6LBR and 6LR are network routers, but the 6LR operates only within the 6LoWPAN-enabled network and cannot directly exchange advertised information with a joining node. When a node joins the network in this topology, it first connects to the 6LBR. The 6LBR then sends RA to connected 6LR routers, including a prefix identifier. The 6LR router stores the advertised information and responds to the joining node. The 6LBR serves as a mediator between the joining node and the 6LR, which acts as a "joining proxy" (the node joining using single DoDAG is performed via nearest neighbour with superior link quality. It is further explained in Chapter 3) and assigns the appropriate prefix such as PAN ID or Context Id. This global prefix is then appended to the joining node's local address. Although effective, this process is somewhat complex.

in ‘**Mesh-under’** alignment**,** the address assignment uses the EUI-64 bit MAC address format, which does not rely on multicast or broadcast techniques for address distribution. This is because the network is typically small, and nodes operates with a one-hop advantage. In contrast, the Route-over topology is suitable for factory-level installation (large-scale deployment of thousands of devices) whereby the use of multicast and broadcast techniques can be reinforced. While setting up a 6TiSCH network with thousands of sensor nodes can be complex, and integration with internet is achieved through 6LoWPAN. this thesis focuses on single subnet with an aim to improve scalability.

2.4. Evaluation

IoT technologies are rapidly evolving with the key focus on the local impact. Their implementation in the industrial domain must guarantee communication accuracy and timeliness where a longer battery life is an advantage. Existing surveys categorically reviewed these technologies based on the scalability, market penetration, research challenges, standardization, suitability of applications, mobility and future development of standard mobile network such as 5G and 6G.

Gu et al., [161] and *Sinha et al*., [162] reviewed key LPWA and traditional short-range technologies. Both surveys advocate the use of LPWA’s low-power design and extended Tx range over short-range networks such as Wi-Fi, Bluetooth, and ZigBee. Here, the survey by author [161] overlooks their local impact in industrial sector where communication reliability and timely delivery are essential guarantees. Further, LPWA technologies, while not only lacking echo-system growth and standardization, but also do not gain the similar market traction. Apart from that, these surveys lack a systematic review evaluating their local impact with regards to spectrum-sharing and regional restrictions.

Raza et al., [54] highlighted that the key progress made over time by LPWA technologies within licensed and unlicensed RF spectrums is in line with the introduction of modern techniques at Physical and MAC-layer, not only to encourage the scalability but also to provide interoperability. The author highlighted the role of SDOs such as IEEE, IETF, 3GPP, and ETSI that are facilitating long range connectivity and interoperability across a wide array of mobile telecommunications technologies (such as 5G and LTE), and cybersecurity. In particular, ETSI has developed standards instructions for LPWANs, which includes the popular protocols for Sigfox and LoRa provided the two are the most popular LPWA solutions. ETSI also collaborates closely with other SDOs including 3GPP and IETF ensuring alliance between different vendors through mediation. However, the survey does not address the key limitations in terms of scalability for industrial networks.

Ayoub et al., [80] reviewed LoRa, Dash7, and NB-IoT based on their applicability in mobile IoT applications across diverse application scenarios including mobile wearables, connected cars, health equipment, smart cities, farming, and wildlife tracking. The survey addressed the deployment and management strategies of heterogeneous standards: LoRa was noted for using precise timing to enhance synchronization among the existing LPWA technologies and Dash7 is interoperable open standard supporting connectivity, with broadcast as a fallback for unicast failures. However, the study highlighted that neither technology consistently ensures reliability in critical, dense urban areas due to environmental and RF-related challenges.

Vaezi et al., [68] divided the IoT technologies into four categories based on operational models: (1) Massive IoT for large-scale M2M deployments with small, infrequent data transmissions over extended coverage; (2) Critical IoT, which prioritizes an ultra-low latency and high reliability; (3) Broadband IoT supporting high data volumes with low latency; and (4) Industrial IoT, emphasizing synchronized, timely data delivery. Each category was analyzed alongside CIoT, LPWA, and short-range networks (such as Wi-Fi, Bluetooth). Additionally, the discussion extended to 5G and 6G technologies, which found that the smartphones are less resource-constrained and their communication model could potentially benefit IoT applications besides the standard wireless technologies such as 5G/6G are not primarily designed for IoT communication and their different design goals are also different. Further, this survey lacks a systematic review of long-range wireless technologies with the primary focus on industrial-grade networks.

Chilamkurthy et al., [86] evaluated IoT technologies with a focus on power efficiency, range, cost, and technical barriers like interference and spectrum-sharing. However, a direct comparison with LP-WPANs was not aimed, leading to limited insight into feasibility of LPWA and CIoT for industrial use, especially in dense urban areas where these technologies often struggle with interference and path-loss challenges.

Buurman et al., [50] conducted a systematic review of long-range IoT technologies based on 6 key design objectives: *energy efficiency, long range, scalability, low cost, interference management,* and *integration*. This study explores LPWANs in line with their influence on various application. Here, the survey included 14 application scenarios, but it excluded industrial standards like WirelessHART, ISA 100.11a, and 6TiSCH which are dedicated to industrial-grade networks. The authors discussed key challenges in LPWANs including the lack of standardization, poor scalability, poor reliability, and less-advanced security, are further complicating their adoption.

Many existing surveys have examined LPWA, CIoT, and LP-WPANs technologies, neither has directly compared their design goals in the context of industrial networks sufficiently; through numerous emerging and existing technologies across all three categories are being introduced. Many prior surveys exclude short-range wireless technologies and standards that once dominated but are now less viable due to competition from modern IoT technologies. Furthermore, a direct comparison between LPWA, CIoT, and LP-WPANs is a complex process, as some technologies are no longer in active use while others lack advanced development, making it difficult to find relevant and up-to-date literature. For instance, WiMAX has become costly and unpopular, with limited advancements seen since 2011. Conversely, UWB, despite its complex implementation with multiple underlying radio standard used, each with varying set of protocols and modulation techniques, is a broader topic which is currently outside the scope of this thesis. The focus of this thesis remains on wireless ad-hoc networks where technologies such as Z-Wave, NFC, BLE, and RFID represents legacy solutions, through require a separate evaluation as these are currently not suitable for industrial networks.

Indicators	6LoWPAN	6TISCH	ZigBee	Thread	W. HART/ ISA	Wi-Fi 802.11ah	LoRa	Sigfox	Weightless-P	DASH 7	NB-IoT	LTE-M	EC-GSM	RPMA
Number of channels	16 at 2.4 GHz) [161], 1 (868 MHz)[[152], 10 (915 MHz)	16 (2.4-2.5Ghz), 1 (868 MHz), 10 (915 MHz) [163]	16 (2.4-2.5Ghz), 1 (868 MHz) [152], 10 (915 MHz) [152]	16 At 2.4Ghz [140], 1 channel at below GHz bands [132].	16 (2.4-2.5Ghz) [6], 1 (868 MHz), 10 (915 MHz) [6]	26(868M Hz) [163] (1MHz bandwidth 13(868M Hz with 2MHz bandwidth) [163]	3(433MH z) 8(868MH z)[[50], and, 64 at 915MHz [[50],	192 at (868 MHz) [50], 72 (915 MHz) [50],	64 868MHz [50], 72 between 914-928 MHz [50],	3 (433MHz) [50], 1 at 868 MHz [50],	2 PHY channels (divide into Up to 55 cellular frequenci es [50] [86],) (UL) and 4 for DL	Up to 14 channel s(700-900MH z) [50] [86]	124 (890-915MHz) [50], 374 (1880 MHz) [86], 295 (1930-1990 MHz) [50] [87], 16 (2.75G)	16 channels by default at 2.4Ghz [54], (IEEE 802.15.4)
Connectivi ty	Sync	Sync	Sync	Async	Sync	Async	Async	Async	Async	Async	Sync	Sync	Sync	Async
Duplexing pattern	Half-duplex [163]	Half-duplex ref] [163]	Half-duplex [39]	Half-duplex [163]	Half-duplex [163]	Half-duplex [163]	Half-duplex ref]	Half-duplex ref]	Half-duplex [50]	Half-duplex [50]	Half-duplex [86]	Half-duplex [86]	Half-duplex [86]	Half-duplex [54]
Operating frequency band	2.4 GHz, using IEEE 802.15.4 by default, 868MHz	2.4 GHz, IEEE 802.15.4 by default, 868MHz	2.4 GHz, using IEEE 802.15.4, 868MHz [39]	2.4 Ghz, 868 MHz, and 915 MHz	2.4 GHz, 868MHz IEEE 802.15.4, IEEE 802.16,	Sub-Ghz Bands 868 MHz [163]	433MHz 868MHz 780MHz 915 MHz	868 MHz and 924 MHz [77] [50]	433MHz 868MHz, and 915MHz [50]	433MHz 868MHz 780MHz, & 915 MHz [50]	700-900MHz Cellular Bands [86]	700-900MH z (Cellula r [86].	800-900MHz Cellular Band [86].	2.4 GHz, IEEE 802.15.4 [54]
Modulatio n	O-QPSK with DSSS	O-QPSK with [39] DSSS,	O-QPSK with DSSS	O-QPSK - DSSS (2.4Ghz) BPSK	O-QPSK with DSS 2.4GHz), BPSK	BPSK,, QPSK , 16-QAM,	CSS with SF7, SF8, SF9,SF10 ,	DBPSK (1bits) with FHSS	GMSK(1 bps), QPSK (2 bps) [50]	2-GFSK, DBPSK, BPSK	16-QAM for UL (Rel-17)	BPSK, 8, 16 QAM	GFSK (DL) (1bps) by default, and BPSK [86],	O-QPSK [54] (2bps) by default,

	(2.4GHz), [163] BPSK (868Mhz)	(2.4GHz), [163] BPSK (868Mhz)	[39], (2.4GHz) BPSK (868Mhz) [39]	for 868 MHz	with DSSS (868Mhz)	64-QAM	SF11,and SF12 [73]	(variable)		,GMSK [50]	QPSK for DL, also use BPSK, DBPSK [86]	(Rel-17), 64, 256 QAM [86]	QPSK, 16 QAM (UL) in UL, as per Rel-17.	and GMSK [54] (1bps).
Upward sensitivity	-97 to -110 dBM [27]	-97 to -110dBM [27]	-97 to -110dBM [39]	-97 to -110dBM [27]	-110-dBM [163]	-129 to -110 dBM [50]	-137dBM [50]	-134 to -142 dBM [50]	131dBM [50]	-97 to -110 dBM [50]	LTE tower sensitivity [86]	-132dBM [86]	GSM tower sensitivity [86]	-134 to 142 dBM [54]
Downward sensitivity	-85 to -103 dBM [27]	-85 to -103 dBM [27]	-87 to -103 dBM [39]	-87 to -103 dBM [27]	-110-dBM	-90 to -100dBM	-137dBM	-130 to -129 dBM	120 dBM [50]	-97 to -110 dBM [50]	-141 dBM [86]	-132dBM [86]	GSM tower sensitivity [86]	-121 dBM [54]
Signal width	2 MHz [27]	2 MHz [27]	2 MHz [39]	2 MHz [27]	2 MHz [50]	22 MHz [164]	7.8 500kHz [73]	100 Hz [73]	12.5kHz [50]	18-21kHz [73]	180kHz [73]	1.08MHz [50]	200kHz [87]	1 MHz [54]
Business model	Private [50]	Private [50]	Private [50]	Private [50]	Private [50]	Private [50]	Private, /telecom operator [50]	telecom operator	telecom operator [50]	Private network [50]	telecom operator [50]	telecom operator [50]	telecom operator [50]	Private [54]
TX power	10- 14mA [27]	10- 14mA [27]	10-14mA [39]	15- 25 mA [27]	14-25mA [27]	14-25 mA	28mA	10-50mA	49mA [50]	29 mA [50]	74-220mA [87]	380mA [87]	152-1228 mA [87]	750mA [54]
RX power	10 mA [27]	10mA [27]	10mA [39]	10mA [27]	10MA [27]	10-14mA	10.5 mA	10 mA	10mA [50]	10mA [50]	53.33 mA [87]	46 mA [87]	66mA [87]	300 mA [54]
Maximum Transmissi	+8 dBM [164]	+8 dBM [164]	10-14 dBM	8 dBM (802.15.4) [164]	8 dBM [164]	23 dBM [164]	14-30 dBM	14-30 dBM	15 dBM [50]	14- 27 dBM [50]	20 dBM [87]	20-23 dBM [87]	23-33 dBM [87]	36 dBM [54]

on power (dBM)														
Sleep Mode	0.1 µA [27]	0.1 µA [27]	0.1 µA [39]	0.5 µA [27]	0.1 µA [27]	1 µA	6 µA	1 µA	< 4 µA [50]	1-2 µA [50]	8 µA [87]	3 µA [87]	10 µA [87]	0.072 mA [54]
SNR	Low [27]	Low [27]	Low [39]	Low [27]	Low [27]	High	High	High	High [50]	Low [50]	High [87]	High [87]	High [87]	Low [54]
Coding schemes	16 bit CRC [27]	16 bit CRC [27]	16 bit CRC [39]	16 bit CRC, [27]	16 bit CRC (FCS)	FEC [50]	FEC [50]	FEC [50]	FEC [50]	FEC [50]	8,10,14 HARQ plus FEC (Rel-17) [50]	8,10,14 HARQ plus FEC [50]	8,10,14 HARQ plus FEC (Rel-17) [50]	FEC [54]
Deployment cost	Low	Low	Low [39]	Low	Low	Low	High	High	High	Low	Low	Low	Low	Low [54]
Battery capacity	2 * 2200 mAH [27]	2 * 2200 mAH [27]	2* 2831mAH [39]	2 * 2200 mAH [27]	2* 2400mAH	2* 2400 mAH	9 V	3.3 to 3.6 V	Coin-cell	Coin-cell or thin film [50]	5Wh [87] [50]	5Wh [87]	5Wh [87]	19 Ah (D-cell Lithium) [54]
Link Budget	Up to 20dB [27]	Up to 20dB [27]	Up to 20dB [39]	20dBM [27]	Up to 110 dB	121 dB	154-155 dB	163dB	154-155dB	140dB [50]	164dB (Rel-16, and Rel-17) [87]	155.7 dB [87]	164dB under Rel-17 [87]	168 dB [54]
Battery life (years)	2 (high Wi-Fi interference), [27] Many years (no	2 with high Wi-Fi impact, 6-7 years excluding interferen	2 years or less with EIs, <1 year 802.15.1 , [39]	Several years, Depends on duty cycle , and	2 years, many years without EIs [27] and using	5 years at most, Less than 2 years in dense urban areas.	10 years, depending on the EIs, and duty-cycle [73]	4 years (3.3 V) , 10 years (3.6V AA cell) [73]	3-8 years on coin cell, subject to EIs, and duty-cycle.	10 years on either coin cell or thin-film [50]	10 years on 5Wh , depending on distance of the	10 years 5Wh, based on RSSI &	10-14 years on 5Wh,depending on data rate and distance in	10 + years, Depending on RSSI, and TX

	interferenc e) [164]	ce, up to 3Mbps	Depends on traffic	traffic [27]	asynchron ous model.						deploym ent [87].	traffic [87]	built up areas [87].	power [54]
Channel-access	CSMA/C A, TDMA, ALOHA	TSCH mode of IEEE 802.15.4	CSMA/C A, TDMA, ALOHA	CSMA/C A, TDMA, ALOHA	TSMP, CSMA/C A, TDMA	RAW by default with AID support	ALOHA, LBT, TDMA, Random [165]	RFTDM A [165]	OFDMA [166]	Tag talk first (TTF) by default [50].	OFDMA [166]	OFDM A [166]	TDMA/FD MA	CSMA/C A, and TDMA [54]
Architectu re	Full stack	Open standard	Full stack	Full stack	Proprietar y stack	Full stack	Physical MAC layer	Physical layer	Physical and MAC layer [50]	Open standard [54]	Full stack [54]	Full stack [54]	Full stack [54]	Proprieta ry stack [54]
Packet size	127B (802.15.4)	127B (IEEE 802.15.4)	127B (802.15.4), 2027 B (802.15.4 g)	127 B (802.15.4 e)	127B (802.15.4)	127B (802.15.4)	Up to 250 B (802.15.4a)	12 B (802.15.4 a)	260 B, 514 B (GFSK and OQPSK) [50]	256 B [50]	2536 bits [50]	4008 bits [50]	128 B	260B (GFSK, 514B(O-QPSK) [54]
IP support and integration to Internet	Yes, provided within the stack	Yes, provided through 6LoPWA N	Yes, 6LoPWA N- based integratio n	Yes, direct integratio n to internet	No IP support, Integration to Internet via HART	Yes, direct integratio n to internet	No IP support at base-level (only backhaul)	No IP support at base-level	No IP support at base-level [50]	No, (only good backhaul connectivi ty) [50]	No IP support at base-level [50]	No IP support at base-level [50]	No IP support at base-level [50] (only backhaul)	No IP support at base-level [54]
Efficient operation per AP	30-50	> 50	30 -50	>50	30-50	30-50	Thousand s	Depends on use case	Thousand s [50]	Depends on use case [50]	High [50]	High	High	High [54]
Scalability	64K	64K	64K	250	500 devices	8K devices	50k per cell [167]	50 k per cell [167]	2 Millions [50]	2 Millions [50]	52,547-100 K [167]	80,000	50,000	50,000 [54]

Link stability	85% (802.15.4) depending on EI [164]	90% or higher over 16 channels with each 5Mhz apart, 802.15.4) at 3Mbps Wi-Fi ,	Deployment site test required (40% Ch. 26 prone to EI) [164]	40-85% depending on EI [164]	90% or higher over 16 channel, 802.15.4) at 3Mbps Wi-Fi [164]	40%, (non-orthogonal freq. each 7 MHz apart on 1, 6 , and 11 channel id	50%, subject to radio sensitivity and TX power	85% with frequency (192 channels) diversity mechanism	50% or lower subject to severity of EI , and higher [50] TX power consumption	Prone to EI since using 3 channels only [50]	Less Prone to EI due to high spread factor [50]	Less Prone to EI due to higher spread factor	Less prone to EI due to Cellular band , not contracted with Wi-Fi	High EI and high link retries, [164] [54].
Latency	1-3s	0.3- 2s	1-3s, varies on traffic	< 0.3s	4s , vary on traffic	Varies on traffic	10s [73]	10-14s [73]	8s	3-8s	10s [73]	10-15ms [73]	10-20s	< 10s [54]
N/W warm up time (minutes)	7- 25 depending on size and EI	7-25 minutes depends on size and EI	2s-10 minutes	2s minutes	7-25 minutes depending on size and EI	10-15 minutes	2-10 minutes [73]	2-10 minutes [73]	2-10 minutes [73] [50]	2-10 minutes [50]	1 minute [50]	Tens of minutes [50]	Fewer Minutes	7-25 minutes [54]
Set up cost	Low	Low	Moderate	Low	Moderate	Low	High	High	High	High	Very High	Very High	Very High	High [54]
Topology	Star, Tree Linear	Tree , Mesh	Star, Mesh	Mesh	Mesh	Start, Mesh	Star [73]	Star [73]	Star/Tree [50]	Star/ Tree [50]	Star [50]	Star [50]	Star [50]	Star/ Tree [54]

Table 5. Comparison of preferred IoT technologies based on technical specifications.

Section 2.4 evaluates the suitable IoT technologies based on the key performance metrics to explore a suitable option for industrial IoT networks, as follows:

2.4.1. Low-power efficiency

IoT devices consist of battery-powered sensors and actuators, integrated with a microprocessor, memory chip, and a radio module. These devices can operate through a switch within existing indoor systems or be wirelessly deployed in environments such as canopies, doorways, or street-mounted installations for monitoring and control applications.

Low-power sleep modes enable IoT devices to conserve energy by turning off their radio during periods of inactivity. The industrial sensors typically consume 4–20 mA or more. For deployments in nomadic or remote locations, battery replacement is often impractical [50] and existing energy-harvesting solutions such as solar panels face challenges related to energy storage, causing shortage. The key reason is that insufficient sunlight prevents battery charging. However, solar energy is not the only viable power source, vibration-based systems can also generate energy. In industrial settings, temperature sensors may need to operate within extreme temperature ranges from - 400°C to 850°C. In such cases, limitations in terms of energy storage can disrupt continuous industrial operations. This subsection evaluates IoT technologies in the context of low power consumption across multiple aspects, as follows:

- Connectivity:
- Radio sensitivity
- Duty-cycle
- Modulation
- Channel-access protocols

2.4.1.1. Connectivity

Connectivity is a crucial aspect of wireless networks. In IoT domain, connectivity can be categorized based on baseline and backhaul network operations. A baseline connectivity involves transmission of control beacons, allowing industrial sensors to perform *joining*; if the joining is successful, the device receives an established link (path) containing key information required for network synchronization. The EDs can be asked for joining each time upon being awake (frequently) under asynchronous communication mode whereas synchronization for a long period of time requires checking of connection infrequently in the network ensuring all links are valid and updated. The backhaul connectivity involves signalling between the core network (via a network gateway) and the baseline network. This category is used for supplying firmware updates or providing necessary instructions (commands) received from the application server. The thesis focuses on the baseline operation where sensor devices adhere to factory-level network settings in terms of connectivity. Apart from the factory-level settings, the core network is also responsible to provide key guidance in terms of Tx power usage, timer (activation period), and frequency-sharing.

LPWA technologies transmit a small amount of payload less frequently over a long distance [73]. These are asynchronous networks adhering the regional regulations while using the unlicensed RF bands with aim to provide wider coverage and long lasting network operation [168]. Mose of these technologies suffer from RF-propagation and constrained bandwidth where DL communication is more complex than UL because of the demand of tight synchronization. For a sufficient connectivity the deployed towers must allow a connecting device to get an average acceptable reception.

LoRa sends several unicast messages for establishing connectivity with network server via BS. The communication fails if there is insufficient signal strength. LoRa is a wideband technology where it uses a discreate range of channels where a spread factor provides resilience to physical interferences. In outdoor environments, LoRa can quickly perform a communication handshake, allowing sufficient reception in all areas within a good LOS conditions but the same is compromised due to multipath effect when devices are operating indoors. For localisation, TDoA is not an energy friendly technique and RSSI, while energy-efficient, suffers from multipath effect and EIs, lacking a precise mapping of the receiver's location. The delay can be more pronounced for indoor deployment.

Sigfox is a narrowband technology and its signals appear in a continuous wave format with minimal separating bandwidth due to which a signal from different device can arrive at the receiver within the same time and the phase, causing a momentarily gain in signal amplitude; consequently such a signal cannot decoded. As Sigfox devices do not transmit more frequently it must resist such overlapping, causing connectivity delay or no connectivity at all if the number of attempt to connect (per day) has exceeded the limit permitted. To improve connectivity, the technology implement FHSS, which provides a minimum separating width by dividing the medium into a number of carrier frequencies where channel-hopping combats multipath effects that each device is now provided with an acceptable reception in all areas.

Weightless-P do not use channel-hopping as it consumes an additional power and being a wideband solution it suffers from heterogeneous interferences where most of its devices are designed to operate outdoors. To protect itself from the interference, the devices use high Tx power and broadcasting technique for localisation, causing rapid battery consumption. However, the connectivity for indoor deployment can be far more critical than outdoor environment and it can take up to several minutes. To mitigate EIs and multipath effect, it proposed to relocate the sender device to a new location, which is not often practical from the point of long coverage range.

Dash7 use both wideband, and narrowband frequencies. It, by default, operates at 433MHz using broadcast mode, only if a unicast beacon goes unanswered. Dash7 is interoperable with most IoT vendors and is IP-operable. As a result the device can quickly connect using on-the-air updates, however the broadcast mode impedes power-savings. It gets worse under with multi-hop transmission where risk of collision between carrier frequencies cannot be ruled out.

RPMA suffers from multipath propagation and EIs where its devices can take several seconds to connect. Since it does not use channel-hopping to combat these barriers, the technology consumes superior Tx power compared any other IoT technologies. Increasing Tx power can improve signal strength and extend communication range, but it does not inherently solve multipath challenges. Multipath occurs when radio signals reflect off surfaces (buildings, walls, or terrain), creating multiple signal paths that interfere with each other at the receiver. Simply increasing Tx power (within 2.4Ghz) can sometimes worsen multipath effects by strengthening interfering reflections.

CIoT technologies (LTE-M, NB-IoT, and EC-GSM) are originated from 3GPP where these networks can switch from one carrier to another in on-the-fly manner, except with differential of services inactive during roaming. The reason is the lack of infrastructure support in those regions [166]. In terms of connectivity, a sensor device can experience higher delay due to poor signal quality or path-loss as the device moves away relatively from the hotspot.

LTE-M uses an increased Tx power penetrating physical objects such as hills, trees, etc. The effect of multipath propagation are mitigated using OFDMA, a MAC layer specification. A receiver device only asks for retransmissions if the BER is high enough (received signal quality is not acceptable) and that it is not possible for FEC alone to recover the corrupted bits in the data frame.

NB-IoT operates within the narrowband frequencies where it allows a distinct and non-overlapping channels carrying data frames to the receiver. It is achieved by OFDMA which provides channel-hopping characteristics, making collision less likely to occur. The downside is that the increased delay when connecting from core network to the baseline network.

In EC-GSM, the devices implement the primitive MAC-layer protocols, making collision imminent using the frequencies without channel-hopping. To deal with EIs and multipath effects, it compensates it with a higher Tx power.

3GPP standard offers new specification to facilitate efficient transmission. The HARQ mechanism is designed to recover corrupted bits by automatic retransmissions of the entire subframes (each subframe corresponds to portions of the payload received at higher abstraction layers [102]). Under release-17, this process has been exemplified with 14 HARQ transmission across UL and DL communication. This increment correlates a high data rate by allowing 16 QAM. The power consumption can vary where data rate is higher, offsetting the benefits achieved by the low power modes (PSW, and eDRX) within. Once connected, a device can stay synced for a long period of time (avoiding frequent reconfiguration).

LP-WPAN is comprised of short-range devices that appear and disappear during connectivity; a signal operating above the density of ground noise (-40dB) is struck by the physical objects, and get received over different time and phase. The overall signal loss can be higher than the sensitivity of the receiver making it hard to decode the signal. The path-loss caused by the destructive interferences including the interferences from coexisting networks.

Wi-Fi 802.11ah is an indoor technology using FEC for bits recovery. The multipath propagation is evidently strong for indoor deployment (comprising smaller and larger objects within the floor area). While relocating device frequently is not the practical solution to improve signal reception, Wi-Fi 802.11ah lacks channel-hopping. Consequently, the connectivity can be strained and may take several seconds in addition to delay occurred in waking up frequently in an asynchronous network, negating power-savings.

Traditional networks ZigBee, 6LoWPAN, Bluetooth, ISA100.11a also suffer from the multipath fading, making signal loss a key limitation of these technologies. Over time, new technologies have been introduced where the benefits of channel-hopping are exposed to them; 6TiSCH and WirelessHART implement this very capability to combat EIs, and multipath fading and these standards are more reliable than existing set of LP-WPANs. Notably, 6TiSCH as an advanced standard can connect all devices fairly quickly than the WirelessHART.

2.4.1.2. RSSI (Proximity)

RSSI is a power efficient measure, utilized by most IoT technologies. It allows receiver devices to adjust their sensitivity based on the transmitter's location in search for a good reception. However, RSSI does not provide an accurate estimate and that too it is prone to wireless interferences and multipath effects [169], necessitating relocation frequently. In contrast, a higher sensitivity does not affect the link budget as it reduces the need for relocation of devices or avoids Tx power acceleration when detecting a weak signal [170].

LoRa, Sigfox, RPMA, Weightless-P (a less popular wideband LPWA technology than LoRa and Sigfox [171]), LTE-M, NB-IoT, and EC-GSM exhibit a higher negative radio sensitivity, typically between -133 dBm to -142 dBm (as per Table 5 specifications). This sensitivity threshold enables improved signal propagation over wide-area coverage and provides a greater power efficiency.

Dash7 operates with a lower negative RSSI value, typically between -101 dBm and -85 dBm [172] making it’s coverage comparable to the asynchronous LP-WPAN technology such as Wi-Fi 802.11ah where the devices can sync over the maximum range of 1km: a lower negative RSSI compensates signal loss with a slightly higher Tx power. Notably, Dash7 is not an energy-efficient technology and its battery lifespan and QoS depends on the traffic conditions.

RPMA uses a higher RSSI [86] and superior Tx power to ensure end-to-end packet delivery, particularly within the congested 2.4 GHz ISM band [173]. It uses a higher chip rate that boosts the signal and provide long coverage (no other LPWA or CIoT has previously used 2.4GHz due to the trade off with power consumption and higher congestion). Many of RPMA's features are currently unknown since it is not standard technology like Dash7.

2.4.1.3. Duty-life Cycle

The duty cycle refers to the maximum duration within which a device is permitted to transmit its payload. A larger duty-cycle translates into a proportionally lower battery life. The duty-cycle can vary across unlicensed and licensed band; the unlicensed spectrum is freely available to all player where regional telecommunication authority can restrict the active period in line with spectrum-sharing rules.

IoT technologies operates with a maximum transmission capability per frame as illustrated in Table 5; if the payload from higher abstraction layers exceeds this capacity then the transceiver must transmit more frequently [73] having divided the payload into the subframes. Here, each subframe follow a sequence and the duty-cycle threshold.

Sigfox's throughput capability is constrained to 12 bytes at a time, with the number of transmissions per day not exceeding 6, as per imposed by regional authorities. In contrast, LoRa transmits less frequently, but it uses a rather higher frame capacity than the Sigfox (as shown in Table 5). In most cases, LoRa devices can last ten years with 1% duty-cycle limit applied. Beyond this threshold, subject to a specific class of LoRa device in use [64], the battery life can shirk to a shorter period due to a non-uniform distribution of charge. An effective energy consumption model is necessary to optimize the listening period, while the devices are using multitasking [64]. The remaining LPWA technologies (except Sigfox) use the fixed listening period [86].

In the wideband spectrum of LPWANs, Weightless-P provides the largest frame size (514 bytes) where the duty-cycle follows a uniform distribution, with each device to consume 49 mA approximately, is a twice higher estimate than LoRa's 28 mA and several times higher than Sigfox's 10 mA. With the number of bytes increase in the Tx buffer, the device transmits frequently, causing higher consumption. Further, Weightless-P can utilize the higher order modulation schemes (QAM) to meet the high data rate, followed by a proportionally high BER; Consequently a more frequent retransmission negatively affects battery savings. Typically, Weightless-P uses GFSK – a lower order modulation scheme yielding 1bps, leading to a proportionately lower BER (BER for low bits per symbol encoded is low as is consistent with all other technologies) [86]. As a result, the devices do not have to retransmit the frame.

Dash7 is a standard technology where its devices are using a relatively stable duty cycle, consuming around 29 mA, similar to LoRa's 28 mA. This capacity is independent of its frame size (dash7's frame contains maximum of 127 bytes compared to LoRa's 256). While the energy consumption shifts more towards dash7 due to lower-negative RSSI, it also triggers a goodput loss due high overheads. RPMA's battery life remains relatively compact despite superior Tx cost (750mA) where a larger input translates into lower battery life. This is because it uses comparatively a higher battery capacity: the enhanced battery capacity is needed in technologies that are less energy-efficient and for proprietary technologies, adding a designed block that holds bigger batteries is not a difficult task compared to standard solutions like Dash7.

In the web of CIoT, NB-IoT is a sensitive technology that makes certain compromises in terms of balancing energy consumption such as lack of support to emergency calling service. The upcoming release is aimed to optimise energy consumption while enabling additional features like media streaming, and VoIP for UL communication. Currently these features are not introduced because of constrained bandwidth under *In-band* (180kHz) and *Guard* band (200kHz) deployments where NB-IoT shares the same PRB as LTE-M. The standalone mode, while more capable, is less constrained, so these features can be implemented easily except the cost will also increase relatively. Notably, NB-IoT is a load-sensitive technology where the duty cycle per frame size is higher than the LTE-M and EC-GSM. The downside is the frequent transmission using limited frame size of 9-10 bytes. These devices are also likely to draw anywhere between 74 mA to 220 mA, subject to their distance from corresponding BS (the maximum link budget is set to 164 dB).

LTE-M has a much smaller transmission range than NB-IoT, but it is a fast and bandwidth-efficient supporting a large number of devices. It uses frequent payload transmissions with minimal delay (12 ms approximately). The frame size is approximately 15 bytes- a slightly larger than NB-IoT's 9–10 bytes. In dense urban areas, LTE-M devices may experience extended duty-cycle due to path-fading [64]. To improve reliability, it sends HARQ requests, with each consuming 380mA approximately. LTE-M suffers from an inconsistent duty-cycle [50]; for example, streaming media over a strained transmission range can slow transmission but won't halt it entirely, but it does accelerate battery drain. A higher Tx power can assist maintain smooth streaming and improves penetration through RF barriers, but this capability comes at the risk of a rather shorter battery lifespan [50].

EC-GSM connects rural and remote areas well, especially, where LTE-M, and NB-IoT technologies are absent. The sensor devices can communicate over wide area with enhanced tower sensitivity and can transmit up to 127 bytes with just 66*mA* per frame, is a notable advantage as it allows smaller duty-cycle compared to other CIoT technologies. However, the core network cannot easily support advanced features like emergency calling, media streaming, or Voice over IP without significant upgrades, limiting its popularity compared to NB-IoT and LTE-M.

Nearly all LP-WPANs (ZigBee, Thread, WirelessHART, ISA100.11a, 6LoWPAN, and 6TiSCH) consume a significant amount of battery charge in bootstrapping [170] and managing the network connectivity. The duty-cycle is roughly around 1% over 127 bytes being the default frame in IEEE 802.15.4. The unexpected surge in duty-cycle is caused by the EIs, and RF-challenges except for WirelessHART where charge consumption shifts towards inefficient payload manageability. In the web of asynchronous LP-WPANs, Wi-Fi 802.11ah use 28mA; the higher Tx power prevents signal quality degradation and offers resistance to EIs except it is not easier to predict the behaviour of the attached sensors as these may encounter multiple paths, causing poor reception. The site-testing is necessary to conclude the link stability, however it does not prevent unforeseen development in the near future. 6TiSCH does not require site-testing [27] and the devices can handle a heavy traffic using a fraction of 1% duty-cycle; the payload is divided into fragment where channel-hopping provides protection from EI, and multipath challenges. It further aims to minimize wastage, and controlling retransmissions caused due to fluctuation in traffic conditions using appropriate scheduling functions, which are explained in the next chapter.

2.4.1.4. Channel-access Protocols

IoT devices come in various shape and sizes (with one of more serial interfaces) where a large number of the devices are designed with consideration to hardware specification. According to this, the radio and other modules such as microprocessor and memory chips can be provided on the same board (SoC). This makes it easier to compute charge consumption during communication. IoT manufacturers adhere to spectrum-sharing rules following the radio module design objectives [174]. The channel-access protocols observe the available frequencies under the RF-module and provide a rule-based access, as per the MAC layer specification. Consequently, the battery life of a device is influenced by the way these protocols behave.

LoRa do not have a complete stack and the technology lacks standardization except it uses the LoRaWAN standard to define channel-access rules within its communication model [165]. Typically, a Lora device (under UL communication) offers poor efficiency due to fewer available channels under sub-Ghz bands; this translates into a potentially longer scheduling window, followed by a surge in its duty cycles, as the device contends for access. Though, DL communication requires a less frequent transmissions where a fewer channels can be sufficient. Typically, the duty-cycle implications may vary on classification of LoRa devices:

Class A (LoRa device) implements Pure-ALOHA [175] where it allows devices to send packets immediately upon receiving them, without checking for any possible collisions with other frequencies. Class B follows a time structure and the schedule, agreed by all devices, connected to the LoRa BS which is responsible to configure the schedule using TDMA protocol: each device follow a predefined

Tx and Rx window (extended listening is aborted) that is different channel for UL and DL communication; hence Class B is relaxed in terms of allocating a transmission window and the devices only transmit within agreed budget. The LBT scheduling approach implemented by Class C devices contrasts the latter two and emphasizes on selecting a collision-free channels ensuring a collision-free operation. The extended listening time results in poor energy-savings [54].

Sigfox employs RFTDMA [165]- a random channel-access solution without any contention involved. Using this protocol, the probability of collision is low as FDMA divides the available RF spectrum into distinct, non-overlapping frequencies, with each frequency is allocated to a unique device for communication. This enables steady, simultaneous connections across devices with low interference, however this requires a careful frequency management in the dense networks. Sigfox operates in an ultra-narrowband spectrum, where energy consumption do not shift significantly due to controlled number of transmission attempts per day, subject to regional constraints [86].

Dash7 uses advanced features like *wake-up* on demand, where devices remain in the REST mode and are only awake when data transmission is necessary. TTF-led channel-access (by the controller) allows devices to initiate communication whenever there is data packet to send, thereby reducing unnecessary power consumption and latency. This feature is particularly useful for scenarios where data needs to be transmitted sporadically. Since multiple Dash7 devices (Tags) can initiate communication simultaneously there is a higher risk of collisions and contention in the crowded RF bands.

Weightless-P employs LBT-based channel access mechanism that enhances communication reliability despite higher speed of data transfer compared to LoRa and Sigfox. However, continuous scanning across carrier frequencies encroaches batter efficiency of the device. Typically, weightless-P operates within a restricted bandwidth of just under 12.5 kHz where the narrow width of a channel stresses the duty-cycle (increased energy consumption). While Weightless-P sacrifices range and power both, it offers enhanced data rate. The trade-off can limit its adoption with strict power constraints [54] thus making it less versatile for monitoring-based applications.

RPMA implements CSMA/CA as MAC layer protocol, with each device to access the medium randomly using back-off timer [54]. While this protocol is energy-friendly, it can lead to poor goodput due to higher control frames pending in the soft Tx buffer, confined to a fewer kilobytes. Apart from that, it yields a lower SNR due to operating under 2.4GHz. Further, the noise floor can attenuate the signal. Evidently, a superior Tx power cannot ascertain sufficient reception in all areas [86].

LTE-M uses OFDMA [107] earlier used in CISCO Wi-Fi networks [176]. OFDMA divides the medium into the number of non-overlapping frequencies. Using OFDMA, CIoT networks can efficiently schedule their UL and DL payload. For example, LTE provides good reception to all devices connected to the LTE-M's packet core (high scalability). However, OFDMA is an expensive mechanism from the perspective of energy-savings and it consumes additional power [166] compared to the traditional protocols such as FDMA, TDMA, CSMA, etc [86]. The forthcoming release of 3GPP is envisioned to lower power consumption.

NB-IoT uses the three key modes where its deployment across standalone mode (in which it reuses the infrastructure provided) is critical to power consumption and cost-efficiency. The devices are available with various battery sizes and capacities. In this mode, its operation is not as constrained as in the LTE band itself, for example it reuses the bandwidth of the existing network (GSM or CDMA). In LTE core model, OFDMA is configured to use where it consumes between 74 and 220mA [166]. This is a lower estimate compared to LTE-M's 330mA. In contrast, its deployment within IN or Guard mode suffers from the constrained bandwidth (180 kHz- 200 kHz) that is the number of messages are exchanged per day are limited to 200 only and exceeding this limit or adding more devices will not only cause strain on scheduling resources (PRB), but also lower the capacity of the battery life proportionally.

EC-GSM is an optimised variant of GSM designed to support low-power wireless connectivity for IoT devices such as sensors, actuators, and machines. Unlike LTE-based technologies, it does not utilize OFDMA; instead, it relies on TDMA and CSMA, which are comparatively lightweight and more energy-efficient; the legacy GSM architecture cannot compete directly with LTE-M particularly in the emerging applications or new services (machine to machine communication, smart watches, smart cities etc) and reinforcing new services within EC-GSM would mean more investment, placing operators at a competitive disadvantage, especially when other carriers in the market offer these capabilities with greater ease. Consequently, EC-GSM demands substantial financial resources to implement advanced functionalities, making it less attractive in comparison to more modern cellular IoT solutions.

Wi-Fi 802.11ah is a standard benefited from the echo-system of Wi-Fi technology. It implements TIM as channel-access protocol, which allows devices to sleep for longer duration where AID mechanism offers resource management at AP. However, power-saving is critical while managing TIM efficiently for industrial networks in presence of internal interference. This triggers congestion and requires frequent retransmission to decode packet at the receiver's end.

ZigBee, Thread, Wi-Fi 802.11ah, 6LoWPAN, and ISA 100.11a utilize conventional protocols, which however offer low consumption in terms of scheduling and channel-access, but lacks the expected QoS. These protocols can face limitations in providing the consistent reliable performance (due to multipath propagation and EIs), required for many IoT and industrial applications. WirelessHART and 6TiSCH utilize the frequency-diversity mechanisms where WirelessHART uses TSMP and TSCH is used by 6TiSCH. These protocols, while sophisticated, are resource-intensive. Here, 6TiSCH is reliable and WirelessHART and ISA 100.11a (the two international standards for industrial networks) are completely reliable also the two also requires human-intervention over time [169].

2.4.1.5. Modulation and Data rate

Modulation is a physical layer technique that converts a digital data (data frame) into a radio signal and then back to the original data at the receiver's end. In narrowband modulation, the data is compressed into continuous, narrow pulses [166], concentrating power into a narrow frequency range (high amplitude). The receiver recover the original digital data where processing power can vary between the modulation schemes.

Typically, narrowband frequencies offer a lower data rate compared to their wideband counterpart where a signal is spread over a wider frequency range, depending on the spread factor. In this regards, a higher spread factor provides a wider coverage and with that it can avoid EIs on its way. There are many modulation techniques available in networking domain of IoT, each of which maintains an orientation in terms of data rate, energy-consumption, spread factor and antijamming features.

LoRa uses CSS, a wideband modulation scheme utilizing chirp-based spread factor. Using CSS, the devices are capable to provide extended transmission range, determined by the corresponding wavelength; A spread factor is declared separately which is anywhere between SF7 and SF12, with SF12 being less power efficient than SF11 and SF11 is less power efficient than SF10 [73] that way, as the wavelength increases, so does the power consumption. The study [177] incorporated LoRa's testing revealed that a higher spread factor benefits from less signal attenuation thereby avoiding physical objects. CSS-based modulation offers lower number of bits per symbol but offers significant advantages in terms of low power consumption compared to other schemes and is considered robust from the security point of view.

Sigfox devices transmit a very small number of bytes (12 bytes) using a distinct frequency using FHSS as essentially narrowband channels are not orthogonal that is the separating bandwidth is smaller and can cause overlapping with other signals [178]. Therefore it utilizes a coherent modulation scheme, which is different for UL and DL communication:

Notably, Differential Binary Phase-Shift Keying (DBPSK) [179] is a variant of Binary Phase-Shift Keying (BPSK) – an encoding scheme using binary data using 0 and 1 corresponding to two distinct phase shifts (typically 0° and 180°). DBPSK maintains a greater power efficiency where it is more suitable for UL as devices often follow adaptive streaming. Gaussian Frequency Shift Keying (GFSK) [179] is suitable for DL communication offering power efficiency with robustness in terms of thwarting jamming and eavesdropping and use a lower coding speed (1bps).

Dash7, RPMA, and Weightless-P- all of these commonly Quadrature Phase-Shift Keying (QPSK) [179] and Offset- Quadrature Phase-Shift Keying (O-QPSK)- a variant of QPSK offering enhanced power savings alongside a slightly better coding speed (2 bps) [50]. The spread factor is independently introduced to the device where a higher spread sequence consumes more power [68].

IoT is rapidly evolving where the choice of modulation scheme depends on the service requirement in the area. Typically, wideband modulation is more power-efficient, albeit it maintains a lower coding rate. In cellular bands, the spread factor is provided by default alongside other benefits (increased bandwidth and unrestricted duty-cycle).

NB-IoT is 4G-drivem and it uses O-QPSK for DL communication initially, mapping each symbol into four bits. As DL mode is more constrained than UL, the devices are benefited from using a higher order modulation except these rapidly drains the battery during processing bits. Alternatively, Gaussian Minimum Shift Keying (GMSK) with a low-pass Gaussian filter enables smooth signal transmission offering a more enveloped symbol with coding rate of 1 bps. It can be used across wideband cellular technology such as EC-GSM and narrowband technologies such NB-IoT.

Notably, modulation schemes offering a lower data rate are largely secure compared to a higher order coding modulation such as QAM- a modulation technique that combines both Amplitude Modulation (AM) and Phase Modulation (PM) to encode data; the data is transmitted by varying both the amplitude and phase of a carrier signal, enabling it to support higher data rate.

Under Rel-17 (3GPP specifications), LTE-M with 16 QAM, is capable to provide 1-2 Mbps speed, but the device must increases HARQ processes alongside BER. QAM is also utilized in Wi-Fi 802.11ah (LP-WPAN) for a higher throughput, but at an increased risk of energy consumption. This is because QAM is not an energy-friendly scheme and its usage in Wi-Fi 802.11ah does not go well with an increased demand for longer battery life (5 years); with QAM it can not achieve the same level of power efficiency as it can with the GFSK (five years), subject to traffic conditions [50].

Note that Wi-Fi 802.11ah is a short-range IoT technology that can coexists with IEEE 802.15.1 (ZigBee), IEEE 802.15.4 (WirelessHART, 6LoWPAN, and 6TiSCH), the risk of multipath signal loss and EIs is significant for indoor deployment regardless of RF selection (868MHz, 911MHz, 433MHs). O-QPSK offers a balanced data rate, enhanced power-savings, and improved security and no other modulation scheme can override these benefits. It implements Direct Sequence Spread Spectrum (DSSS) that introduces a spread sequence separately in 2.4 GHz. Table 5 specifications maintains that the reported average battery life of LP-WPANs using O-QPSK in IEEE 802.15.4 is approximately two years; though this may vary based on traffic rate and network size.

2.4.2. Latency

Industrial networks requires a prior service agreement where one of the key clauses is the minimal acceptable delay in communication [81]. Latency is a measured delay in data transmission from a sensor device to a receiver station (UL mostly) or vice versa (DL). The delay is co-influenced by a number factors including wake up time and synchronization accuracy, constrained bandwidth (larger network tend to share or reuse the bandwidth based on the contention-delay), transmission range, RF-propagation loss due to EIs and path-fading, congestion due to the spectrum-sharing, topological alignment (multi-hop requires routing efficiency which can be time consuming), communication modes (M2M, or network domain, which is infrastructure driven), payload size over a maximum acceptable number of bytes per frame and signal coding or decoding, parameterization, and MAC layer characteristics. The Physical and the MAC layer have a potential to optimize latency for industrial networks [81].

In LPWA segment, LoRaWAN take longer to communicate because of an on-demand synchronization delay where connection to the servers or BSs may take several seconds to establish, subject to device format (class type):

Class A uses pure-ALOHA [175] which sends packet without checking for collision on the carrier frequencies [165]; it keeps the Rx window open for two subsequent slots, if the acknowledgement is received within the first Rx window, then it removes the second window. The delay therefore depends on the time window or windows in which the acknowledgement is received.

In Class B, devices are allocated a fixed time slot to perform wireless activities. The delay is computable depending on the slots used before an acknowledge is received. Hence, the latency can vary up to tens of seconds.

Using Class C devices, the anticipated delay in channel-clearance and before a packet is sent is higher compared to Class A and Class B devices. Table 5 illustrates the number of channels available within each frequency range. According to this, a maximum of 3 channels are offered at 433MHz, 8 channels are available to use freely at 868MHz, 16 channels at 2.4GHz, and 64 channels at 915MHz RF band.

LoRa is a wideband technology where its devices benefit from the selection of a wide range of freely available frequencies across VHF and UHF. The 433MHz is considered a narrow frequency where the available bandwidth decreases as the number of channel are carved out that is likely to be lower unless further divided using FDMA. Here multipath propagation is present in all most all carrier frequencies. The lesser separating bandwidth provokes overlapping during transmission that too with a constrained bandwidth. In terms of the delay, with more channels availed, a device can perform communication with lesser delay; though, it may encounter a trade-off with power consumption [165]. Further, a single antenna in LoRa devices can only allow transmission or reception at a time, causing increased delay due to channel availability.

Sigfox divides the medium into a number of channels. The bandwidth depends on the wavelength of the frequency so the higher the bandwidth; thus more channels for communication. This includes 192 channels at the 862 MHz (Europe), 72 channels at the 928 MHz (United States), and fewer under specific frequencies depending on the geographical zones where the service provider must liaise with regional authority ensuring spectrum-sharing on freely available frequencies [180]. To mitigate the risk of signal loss due to overlapping and destructive interferences, it implements frequency hopping, separating each channel (with coherent bandwidth) that way sensor devices can switch the channel randomly across both time and frequency using RFTDMA [165]. As a result, the devices can broadcast payload of 8-12 bytes over distinct channel. In terms of latency, it exceeds several seconds using factory level settings of the device (equal to 1% of the duty-cycle, and it can send up to 6 messages, each with 8-12 bytes per day).

LBT has applications across all wireless technologies: Sigfox implementation in Japan and South Korea follow Sigfox uses the LBT as MAC-layer specification (determine channel-access) whereas in Brazil, Canada, Mexico, Puerto Rico, and USA, it follows RFTDMA. Frequency hopping is consistently used alongside the MAC-layer configurations. Here, using either channel-access, latency remains largely the same (10s).

Weightless-P uses LBT protocol too, causing a significant waiting period to avoid collision. While it uses a slightly higher bandwidth (12.5 kHz) than Sigfox, latency can take several seconds in a multi-hop network. The delay is worsen with primitive channel-access if not using LBT. The trade off is evident between latency, power consumption and the reliability. To better understand channel selection from the perspective of multipath loss, the technology leaves a room for a surge in latency due to poor localisation, and signal-loss due to poor channel-access rules. According to Table 5, the latency can translate into several seconds (8s).

Dash7 incorporates several types of antennas and it is flexible to use a variety of scheduling and channel-access mechanism available for a multi-hop networks, directly managed by controller. In this regards, TTF is a query-based scheduling that requires data aggregation precisely for reducing the communication delay. The EDs, by default, operate on 433 MHz with maximum of 3 channels. TTF therefore acts like ALOHA in scheduling packet as soon as possible using a single antenna, however the transmitting device can be exposed to larger waiting period, reinforced by the TTF where the latency can fluctuate depending on the delay in synchronization and relaying (routing). According to Table 5, the delay can be anywhere between 3 to 8 seconds. The downside is that when more devices are added to the network (using the same bandwidth) or the network is experiencing a frequent traffic [50] the latency can take up to ten seconds for the packets that were successfully received.

LTE-M uses a high bandwidth (1MHz- 5 MHz) with up to 14 channels, between the range of 700-900MHz. It offers extremely lowest latency (10ms) and a higher data rate, suitable for real-time applications like vehicular networks. However, in the areas with poor infrastructure support, it can compromise latency aided by poor flexibility to implement roaming and coverage issues. In terms of channel-access and the associated latency delay, OFDMA is an efficient non-primitive protocol where devices are benefited from channel-hopping; thus experience a minimal delay. The downside is that LTE-M is sensitive to the indoor interference and multipath propagation which can potentially influence the latency to rise where there is a poor reception; this delay can reach up to 1s or higher [50].

NB-IoT uses different mode of communication where the latency can vary depending on mode in operation: *In-band* operation within an LTE carrier can result in higher latency due to shared resources (PRB) and potential contention with LTE traffic. *Guard band* operation, while reducing interference with LTE, may still face delays due to lower priority in resource allocation [118]. In standalone mode, it depends on the underlying network infrastructure to meet ultra high coverage. The *standalone* mode is expensive as it reuses the resources provided by the existing network for example refarming GSM. Here, establishing a connection between the NB-IoT devices and the core network can introduce a delay via EPC, especially using the low power modes (PSM or eDRX). The device often needs to reconnect. The connection setup process can be as prolonged as Sigfox and it requires pre-authentication and resource allocation, which can introduce additional delays, beyond 10s. NB-IoT is not designed for latency-sensitive traffic and the projected delay can exceeds several seconds (10s).

EC-GSM utilizes existing GSM infrastructure. The devices takes several attempt to transmit the entire payload provided the bandwidth is roughly same as NB-IoT besides packet size may vary from 260 to 500 bytes, depending on the capacity of the device. With primitive scheduling and channel-access (CSMA/CA), the devices can take several rounds of waiting and thus the accumulated latency is roughly twice than the existing LPWA and CIoT technologies (10-20s).

RPMA employs highest Tx power (760mA) to accommodate longer coverage range in addition to the forming multi-hop connection that also influence overall coverage. The latency increases by each hop where data must pass through multiple intermediate nodes before reaching its destination, introducing delays at each hop and increasing overall latency, sometimes to tens of seconds [54], which gets worsen due to EIs and Multipath challenges as it uses CSMA/CA.

Wi-Fi 802.11ah uses RAW protocol for channel-access which restricts the access period (time) into numerous slots of different length. That's some devices are given more time to complete transmission than the others. The distribution of these slots per devices is a complex scheduling process, and prone to increased latency where a device has to wait for long to transmit. Additionally; indoor interference can further contribute to increased delay [8].

ZigBee, Wi-Fi, Bluetooth, 6LoWPAN, ISA, and Thread are prone to higher latency delay as these use primitive channel-access protocol which are somewhat power-efficient than non-primitive protocols. The delay can get worse off due to EIs and Multipath propagation, leading to transmission failure and congestion in the transmission buffer. In this regard, only 6TiSCH and WirelessHART use frequency-hopping, combined with TDMA. The channel-hopping eases congestion and prevents signal quality degradation. However, the latency can extend several seconds depending on traffic load and size of the Tx buffer used within the devices and the delay is more pronounced with WirelessHART devices which does not provide payload incompatibility and interoperability: the payload fragmentation is necessary to avoid longer transmission window which is prone to signal loss and IP-operability provide a unique address allowing devices to connect to the Internet. In contrast, 6TiSCH is IP-operable and it sends a small number of bytes (fragmented packet) frequently using a fraction of 1% duty-cycle, meeting the minimum latency threshold for industrial networks according to RFC 5673. However, latency can still increase due to bursty traffic conditions, and inconsistent scheduling by the overarching SF.

2.4.3. Interference

Wireless communication is susceptible to interferences, which can be categorized into two main types: Internal and External [181]. Internal interferences occurs when multiple devices simultaneously use the same carrier frequency, leading to network congestion. The key to mitigating this type of interference lies in efficient channel access protocols, which manage spectrum usage and minimize collisions. External interferences or EIs are caused by physical barriers affecting LOS and NLOS communication. In LOS conditions, the shortest-path signal is typically the strongest, whereas in NLOS environments, reflected or diffracted signals may dominate. Such interference causes data corruption, making received packets difficult to decode. This may result in outage events [181] due to an increased Packet Error Ratio (PER): A high PER often leads to communication failure [181].

LPWA technologies utilize a diverse range of physical layer implementations, each offering varying MTU capacity and bandwidth, depending on the RF module in use. Notably, packet size increases due to the impact of EIs and noise, which includes both ground noise and noise from the circuit-board, potentially leading to an outage event even when EDs are outside interference zones or miles apart, the environmental factors such as rain or dust storms can still further degrade signal quality [182].

LPWA technologies in the unlicensed spectrum rely on Tx power and RSSI to counteract EI penetration [182]. In contrast, licensed spectrum technologies is less constrained in terms of increasing the link budget to deal with the interferences and congestion due to spectrum-sharing: the Rule-based spectrum sharing ensures that certain frequencies experience minimal congestion from coexisting networks while utilizing a spread factor to enable wide-area connectivity and improve penetration through physical barriers like vegetation and buildings in different geographical zones [183]. However, access to licensed spectrum requires regulatory approval. Alternatively, unlicensed operators can introduce spread factors via modulation schemes, but Tx power restrictions may still compromise link quality over long-distance communication. The physical layer handles modulation, encoding, interference mitigation, and efficient payload management in wireless communication, while the MAC layer ensures reliable data transmission through channel access protocols.

Signal modulation plays a crucial role in detecting and managing EIs. These modulation schemes vary in their spread factor, where a higher spread factor generally improves resistance to interference. Each transmitted packet contains a unique code, allowing the intended receiver to decode it, while for other devices, the packet appears as noise. The code rate is closely linked to energy consumption, as the selection of a low or high code rate depends on the modulation scheme provided by the service provider. However, spectrum-sharing can complicate modulation, requiring adaptive techniques to handle EIs for both UL and DL traffic.

A received signal maintains a level of separation from ground noise, which is quantified as the SNR. A high SNR typically indicates a stronger signal relative to the noise, reducing the impact of wireless interference. This contributes to energy efficiency, as stronger signals require fewer retransmissions.

Sakauchi et al., [184] demonstrated the implementation of LoRa (Class B) with a dual-antenna setup in a bus tracking application. The study incorporated TDMA at the MAC layer to regulate channel access. Findings indicated that, with multiple channels, LoRa's Class B implementation enhances resistance to EIs. However, mobile devices require high localization accuracy; hence LoRa's effectiveness is more pronounced in fixed infrastructure deployments, particularly when operating on a single channel in less congested environments.

Sigfox counters the signal degradation by using narrowband. It uses frequency hopping to deal with EIs and multipath fading since the narrowband signals are not orthogonal it has to apply frequency division separately. The overlapping of signal (trough to crest) can result in destructive patterns causing signal degradation. However, the exact number of frequencies to be configured is decided by the network operator.

Yamazaki et al., [185] tested Sigfox in an agricultural field within a small deployment area aimed at plant protection. The study found that transmission reliability was significantly lower due to poor signal reception, which worsened as more devices were added. Additionally, vegetation obstructed signals, leading to multipath effects and variations in link quality. To improve reception, the study suggested allocating extra bandwidth, which in turn required the deployment of additional servers. Furthermore, it was necessary to mount devices at higher elevations to minimize interference from vegetation within the deployment zone.

Wireless communication is generally less restrictive with open-standard technologies such as Dash7, which benefit from a variety of modulation techniques [80]. Both Dash7 and Weightless-P operate within the 868 MHz European standard and 915 MHz ISM bands. By default, these technologies utilize GFSK, a secure modulation technique that employs a Gaussian filter, characterized by an impulse response following a Gaussian function. These filters smooth data transmission, act as low-pass filters (1 bps), and enhance resistance to EIs by removing high-frequency components [50].

Dash7 further incorporates data whitening with FEC [186]. Data whitening is a coding scheme [187] that uses a 9-bit pseudo-random generator (PN9 encoding) to ensure balanced bit transitions and reduce transmission errors. In the context of internal interference, each transmission window is pre-assigned by the controller using TTF as channel-access protocol, allowing data whitening to function without additional beaconing. However, Dash7 is limited by a maximum of three channels over the 433 MHz RF band, making collisions unavoidable in industrial-grade networks. This limitation persists regardless the higher Tx power.

Weightless-P relies on high Tx power and elevated RSSI values. However, it remains vulnerable to EIs, leading to a higher BER, particularly when using higher-order modulation schemes and larger frame sizes.

RPMA use spreading code consists of a sequence of bits known as chips. The chip rate is much higher than the data rate, resulting in a spread spectrum signal. For example, if the data rate is 1 kbps and the chip rate is 10 kbps. The ratio of the chip rate to the data rate is known as the spreading factor. For spreading the signal in to a wider bandwidth, RPMA employs DSSS- a commonly used technique with O-QPSK modulation in IEEE 802.15.4 standard. According to this the original signal is multiplied by the spreading sequence, providing spreading across a wider frequency band. In terms of transmission, the signal is resilient to EIs provided the device will be required to keep the radio on at a higher Tx power usage (760mA) while operating in 2.4GHz band. RPMA is benefitted from wider bandwidth (1-20 MHz) and additional security. The downside is single carrier-access (CSMA/CA) [157], therefore it is rather more suitable for leak detection in gas and oil industry with a medium-range coverage [188].

LTE-M is a scalable technology allowing each device a sufficient amount of bandwidth. It has increased protection from internal interferences where devices access channel using OFDMA. With the higher encoding rate per signal, network can achieve higher spectral efficiency, and a higher SNR is crucial to for avoiding outage at receiving end. *Ikpehai et al.,* [188] evaluated LPWAs and CIoTs where EIs including temperature, humidity, etc can cause path-loss and signal attenuation via multipath propagation. The author found that the impact of EIs is higher for indoor deployment compared to the outdoor; the signal may reflect off the physical objects such as furniture, window, toaster, etc that affects the devices synced with LTE-M as it moves around in the defined zone.

NB-IoT operates in more than one RF bands, allowing superior coverage than existing technologies. With higher RSSI, it can detect the weak signal at much higher distance without boosting the Tx power. In terms of EIs, NB-IoT's flow is unlikely to be affected by the co-existing wireless networks except it is sensitive to high BER triggered by higher order modulation scheme, yielding higher number of bit per symbol modulation (16-QAM for UL). To deal with internal interference, NB-IoT use OFDMA, which provides frequency diversity and improved goodput. The latest release (Rel-17) emphasized on the fair increment of HARQ to lower data corruption only when using 16 QAM. The DL traffic is as usually directed through O-QPSK, which is resilient to BER to a greater extent.

EC-GSM uses existing GSM tower's sensitivity by default and is benefited from existing infrastructure therefore adding more devices is an advantage. While, EC-GSM can deliver higher data rate, but it is poorly equipped to prevent signal loss due to multipath-fading using the mobile devices and internal interferences (OFDMA is expensive for new devices). Compared to LTE-M and NB-IoT, it is less versatile in adopting advance features that are only available with LTE-M and NB-IoT. EC-GSM necessitates a high SNR and the devices are prone to frequent connection loss in dense areas. EC-GSM suffers from heterogeneous interference, causing higher BER, and signal-loss.

Note that most LPWA and CIoT technologies implements FEC encoding to reduce retransmission and prevent packet corruption caused by collisions on carrier frequencies, ensuring packet length remains consistent. However, spectrum-sharing enables different radio standards to coexist and this can still lead to increased packet lengths at the receiving device. LP-WPAN technologies generally rely on Cyclic Redundancy Check (CRC) for error detection. While CRC adds redundancy, it does not correct corrupted data, necessitating retransmissions. Here, IEEE 802.11ah is not restricted from employing FEC, resulting in a lower retransmission rate compared to other short-range networks.

Wi-Fi 802.11ah exhibits a slightly higher negative sensitivity than most LP-WPANs. This trade-off has relaxed transmission coverage, while other LP-WPANs operate within an RSSI range -97 to -101 dBm and support lower transmission distances approximately 100–200 meters. CIoT and LPWA technologies follow distinct design objectives and have established infrastructure to deal with variations in synchronization accuracy using the varying means of localization. For Wi-Fi 802.11ah to become as effective as CIoT and LPWA, it must match the infrastructure disparity.

LP-WPANs primarily operate under 2.4GHz, or sub-Ghz band (868MHz) when using IEEE 802.15.4 standard. Recently, many emerging standards (Thread, ZigBee) have used the 868 MHz band in IEEE 802.15.4 facilitating M2M communication, for example: Apple AirTags. Among LP-WPANs, only WirelessHART and 6TiSCH can claim to be reliable where the performance of WirelessHART remains contingent on scalability and traffic density. Notably, 6TiSCH deployment does not require site-testing unlike those conducting site-testing to assess the impact of heterogeneous interference, with higher

RSSI values being crucial for resilience. 6TiSCH further ensures minimal data collisions and corruption by integrating TSCH and a cross-layer scheduling mechanism that passively monitors link stability while efficiently allocating network resources. As a result, 6TiSCH stands as the most advanced and suitable standard for industrial standard employing IPv6-based WSNs, whereas other LP-WPAN technologies have not achieved the same level of robustness.

2.4.4. Low Power Scalability Analysis of IoT Technologies

Traditionally, scalability is described as an impact on communication performance while the network size grows. Today, it can be described in more complex way, from the point of increased network coverage allowing increasingly populated network with varying load sensitivity [50]; therefore scalability can be assessed as per the business models: (1) An organization benefit from an existing subscriber-base where a user has to pay a monthly premium depending on the tariffs and services offered. The downside is the limit of how many devices more can be added to the same connection and lack of network control. (2) A manufacturing based model allows a user to setup its own private network, however this model is feasible when there are not many choices available (cost and benefit analysis).

LPWA technologies are mostly proprietary technologies evolving with a varying capabilities as per their design objectives. Generally; these technologies cannot offer a guaranteed reliability, but are focused to solve a particular problem in IoT landscape using frequencies that are freely available to use. Here, adding more devices to an existing network is contingent on the underlying technological specifications and the spectrum utilization. The narrowband spectrum of frequencies offer a higher coverage but poor data rate in contrast to the wideband spectrum. The collaboration between these players is potentially beneficial to enhance scalability, allowing device to connect ‘over the air’ with different networks while out of the reach from its home network. In terms of scalability, the capacity of a server or BS ultimately dictates the network’s expansion.

LoRa achieves a wideband connectivity with higher spread factors. Recent tests of LoRa over ISM 2.4 GHz have demonstrated a poor link stability (PDR) compared to coexisting short-range technologies this means a wider bandwidth does not solve the propagation issues alone; the ISM 2.4 GHz band offers higher bandwidth (1- 20MHz), however the signal loss is more pronounced in the band. To improve signal strength, more BSs must be deployed [50]; this will also provide synchronization accuracy ensuring all devices operate in a timely manner,

The narrowband spectrum is utilized by Sigfox where spread factor is by default available and a signal suffers minimal loss over long distance since narrowband frequencies are not commonly used in the web of standard wireless networks such as Wi-Fi, 5G, 4G etc [77]. However, a narrowband signal might fade particularly when the devices are improperly mounted avoiding physical objects, causing multipath propagation. The resulting signals might reach at the receiver with an increased BER and Sigfox is already constrained in terms of data rate. The path loss will be even more persistent with mobile devices. In the stationary devices, scaling (adding more devices) depends on testing where LoS and NLoS scenarios are evaluated in advance in line with coherent bandwidth and coherent distance. Under LoS, a single device will be sufficient providing 100km coverage if mounted appropriately with each implementing frequency hopping to avoid multipath propagation.

Dash7 follows a multi-hop mesh alignment and provide a stable reception and an improved data rate. Here, each sensor device is free to connect to any network via OTA switching. Notably, Dash7 does not enforce a default security key (but application developer may implement pre-shared security keys for authentication depending on their need). Clearly, Dash7 technology is a leader among LPWA segment offering improved connectivity compared to LoRa and Sigfox. Further, network scaling does not fade the signal as long as there are existing networks present in the area that way it can allow millions of devices to be configured within the same network hierarchy. As far as the multipath loss is concerned, the sensitivity of *tag* devices (Dash 7 sensors) is an equivalent to the RSSI range proposed for short-range technologies (-85 to -110 dBM); hence the risk of unstable links cannot be ruled out where the distance between the EDs is significant (>5 km); Dash7 can communicate at a higher distance with the same RSSI threshold but with the higher Tx power.

Weightless-P using wideband frequencies sacrifice coverage for higher data rate [61]. It uses both higher Tx power and a higher negative RSSI value (allowing devices to remain far apart using multi-hop alignment). Tx power and RSSI are commonly employed in deciding the coverage and efficiency of a long range wireless network. Devices take longer to sync and may suffer greater signal loss from multipath propagation [86]. In terms of scalability, Weightless-P offers sufficient bandwidth allowing millions of device connected to the core network where goodput loss is evident due to poor performance that is poor ability to deal with the RF-challenges where it does not use frequency hopping to mitigate path-fading [50]. Consequently, such networks cannot be a suitable solution for industrial automation where reliability and timeliness are paramount.

A licensed cellular band, by default, an increased capacity, allowing millions of devices due to higher bandwidth.

LTE-M is a core standard, allowing network scaling while adding millions of new devices under it's coverage zone (to the same hotspot) besides, the user will have to pay a monthly fee. LTE-M with massive bandwidth (The PRB is fairly larger than NB-IoT, and EC-GSM) offer higher data rate across UL and DL communication (16-QAM modulation offer higher order of coding), but it suffers from poor transmission coverage and requires more BS by every 10-11km [50] where a single BS can support up to 80,000 devices with improved security (it is higher number compared to NB-IoT). In terms of signal loss, LTE-M's performance can be inconsistent under high load conditions due to EIs and multipath propagation, making it less feasible for real-time automation applications rather, it is more suitable technology for monitoring applications where high throughput is necessary with minimal latency; for example a vehicular IoT networks.

NB-IoT's coverage is superior that can easily meet 100 km under LoS conditions and 50 km under NLoS. Here, each BS can accommodate approximately 52547 devices, however with an increased distance between EDs and BS, the signal strength of a mobile device can fluctuate [189]. NB-IoT uses narrowband spectrum of frequencies where it operates using the three key modes; nearly all use OFDMA to provide channel-diversity avoiding wireless interferences, and the multipath losses. The downside is that it is expensive to be used as a standalone mode and other two modes (IN band and Guard band) lack data rate (but it is certainly higher than Sigfox); the data rate for IN and Guard band is about 200 messages per day, through the number of messages exchanged per day are substantially higher compared to old releases (Rel-13- Rel-16). The release-17 demands implementation of higher order modulation schemes to further enhance the data rate, however it needs to evaluate the charge drawn in implementing 16-QAM, which is expectedly higher than those with lower order modulation schemes. Consequently, the forthcoming release (REl-18) is focused to reduce the energy consumption as the data rate increases. Currently, neither releases of NB-IoT seem to prioritize latency (10s or higher) and the industrial networks necessitate a lower minimal delay of 1s or lower (RFC5673); hence the design objective of NB-IoT are not aligned with industry 4.0.

EC-GSM offers 15 km or less in the urban areas and greater than 15 km in the rural area. In terms of scalability, it poses challenge as the capability of BS is met with 50,000 devices. EC-GSM lacks hosting new services which are currently possible for both LTE-M and NB-IoT to implement, for example emergency calling, media streaming, etc. This is because the existing GSM infrastructure is outdated where connection loss can occur despite being in the range of BS or over relative distance to the other devices [190]. EC-GSM does not prioritize latency like NB-IoT and registers goodput loss using mobile devices; thus it can not be considered scalable for industrial-grade networks.

LP-WPAN follows the manufacturing based model, allowing user to have an independent private wireless network. The scalability can vary depending on the underlying technologies:

Thread it is poorly scalable technology, as it can only configure maximum of 32 routers [140]. According to the latest release it support maximum of 256 routers, this means it can now allow proportionally higher volume of devices added to the same hotspot than the previous enhancements. In terms of scalability, it is practically impossible to accommodate hundreds of sensor devices under single router despite the registered surge in the capacity of the router that too the transmission range of each sensor device is confined to 30 meters approximately.

WirelessHART is an international standard designed to support both indoor and outdoor communication where it utilize channel-hopping to mitigate EIs and multipath signal loss. To what extend it is possible to combat these depends on the coherent bandwidth and coherent distancing rules, which is further evaluated in [11]. Evidently, *Park et al.,* [191] finds signal loss are still evident within indoor spaces due to multipath propagation. In terms of network expansion, the WirelessHART forms a mesh network which can extend up to maximum of 1km per subnet and, with each subnet router it can configure up to 500 devices. The communication fails when devices are taking significantly longer to transmit a heavy payload of 127 bytes.

Wi-Fi 802.11ah can offer direct connectivity over several hundred meters where it can configure a maximum of 8K devices; when adding more devices indoors it causes signal loss in some areas due to multipath propagation. Apart from this, the connectivity in 802.11ah is an overhead-laden process where additional routing and scheduling overheads consume a higher share of the bandwidth, causing goodput loss as per the findings of *Ahmed et al.,* [192].

Yunis et al. [193] finds that 802.11ah suffers from the *hidden terminal problem* that occurs when two or more controller devices (APs) that are out of range, or transmit simultaneously. The author finds that the primitive channel-access protocols are responsible for poor scalability.

ZigBee and 6LoWPAN are benefited from IPv6, supporting up to 64,000 devices, with each device can cover up to 100-200 meters under sparse deployment. Using multi-hop transmission model, these technologies can often form a densely populated network at a relatively low infrastructure costs. However, their load scalability is compromised due to RF-challenges.

6TiSCH integrates IPv6 over the TSCH mode of IEEE 802.15.4, enabling the deployment of up to 64,000 independent sensor devices within a single industrial WSN. Each subnet optimizes IPv6 address compression and adaptation, reducing transmission overhead. The IPv6 addresses are further compressed into a prefix for local interactions, allowing ND with the compressed header, making communication less stringent on IEEE 802.15.4. Despite the integration of 6LoWPAN with TSCH mode over IEEE 802.15.4, 6TiSCH renders a fairly compact and lightweight payload for transmission. The channel-hopping contributes to network reliability by mitigating path loss [164] due to multipath propagation (discussed in Chapter 1). Additionally, the control layer plays a crucial role in traffic management, further enhancing network performance and scalability. 6TiSCH can meet the extended coverage requirement by forming a multi-hop network architecture. Currently it is used across various domains, including factory automation [40], smart agriculture [27], smart grids [43], and smart buildings [75]. The downside is that managing communication beyond its subnet remains a complex procedure as it does not connect to the Internet directly in case a use requires remote access. This thesis will focus on 6TiSCH as a desired solution for industrial networks.

2.5. Summary

A wide range of IoT solutions integrate LPWA technologies, most of which operate in sub-1 GHz frequency bands, with fewer solutions utilizing frequencies above the 1 GHz. These solutions face key challenges, including low data rates, high latency, constrained bandwidth, and frequent connection losses due to RF propagation issues. Industrial networks prioritize reliability.

LPWANs are constrained networks, transmitting small amounts of data over long distances. However, signal degradation occurs due to attenuation, wireless interference, and rudimentary channel-access mechanisms. Receivers often require retransmissions to recover corrupt bits in received frames. While many LPWANs are proprietary and non-standard, their customized physical layer designs offer advantages, such as extended battery life and specialized hardware (manufactured with custom SoC certificates).

Beyond physical constraints, interoperability among LPWA standards remains a major challenge, significantly impacting operational costs. Typically, LPWA subscription costs range from $2–$5 per month, excluding setup costs, which depend on deployment conditions. Furthermore, vendor-locked devices and scalability issues increase expenses, as adding more devices often results in higher tariffs. Improved interoperability would enhance connectivity, reduce costs, expand the subscriber base, and foster ecosystem growth. However, regional regulations impose limitations on RF band operations, restricting broader adoption.

LPWANs require further advancements to meet industrial network demands, particularly for real-time, autonomous operations. Their deployment in closed-loop, mission-critical monitoring and control systems remains problematic, as potential automatic shutdowns pose operational risks. Consequently, LPWANs are not yet viable for industrial applications requiring high reliability and minimal delay.

CIoT technologies are currently evolving. Their deployment vary globally, depending on infrastructure support and spectrum-sharing regulations [86]. Subscription cost as a key barrier that differ by region and service requirements. Among CIoT solutions:

- LTE-M supports high data rates (≥1 Mbps) but has a limited coverage range (11–15 km in urban areas), necessitating additional base stations for extended coverage.
- NB-IoT offers higher UL data rates in Release-16 and achieves ultra-wide coverage (up to 100 km per BS). However, its data rates remain inconsistent across releases, failing to meet industrial requirements such as low latency and reliability.
- EC-GSM also falls short of industrial network demands and faces significant investment barriers, limiting its adoption in the evolving IoT landscape.

While CIoT networks support mobility, their resilience to EIs is limited, particularly in urban areas, where multipath propagation weaken signal strength. Despite operating in licensed RF bands (which generally experience less interference than unlicensed UHF bands), poor reception persists, especially in non-habitable or obstructed terrain. Signal loss due to shadowing (caused by hills, tall buildings, etc.) remains a challenge.

Deploying new towers is often infeasible, making LTE-M the only viable standard offering low latency, high throughput, and extended coverage. Many industrial systems require a guaranteed minimum and maximum delay for reliable data transmission, even under non-critical event-based monitoring. Other CIoT solutions lack the capability to meet these demands effectively.

Traditional LP-WPANs such as ZigBee and Bluetooth suffer from the multipath fading, and EIs, causing signal strength degradation over short distances. Over time, many new technologies have emerged where only handful of them are proven reliable (using channel-hopping) for industrial LLNs. The evaluation has found that each suffers from particular type of challenges, hindering their adoption as a suitable solutions for the industrial LLNs:

- Wi-Fi HaLow
  - Suffers from connectivity complexity due to high susceptibility to fast-fading within indoor environments.
  - Asynchronous network
- ZigBee, ISA 100.11a, and 6LoWPAN
  - Highly susceptible to EIs and multipath fading in dense environments.
  - Scalability and reliability concerns arise when managing large numbers of devices under high traffic loads, adversely affecting performance.
- Thread
  - Operates within a 30–300m range, offering a low data rate.
  - One of the few LP-WPANs supporting self-healing alongside IP operability.
- WirelessHART
  - Lacks a network layer, complicating integration to Internet.
  - Puts strain on Physical layer resources due to lack of payload fragmentation and bulky headers.
- 6TiSCH
  - Provides network coverage of up to 2 km in urban and dense environments.
  - No site-testing required as channel-hopping can mitigate multipath-fading issues and EIs.
  - Smooth payload transition from source to destination with compressed and fragmented packets.

- Effectively mitigates RF barriers and demonstrates high reliability with potential through optimized scheduling at the 6top (control) layer to further improve scalability.
- Fully IP-compliant specification.
- A deterministic network that unanimously meets QoS for industrial applications.
- A superior but a more lightweight solution promising improved power consumption.
- Deployment complexity limits its current scope to industrial IoT applications only.

Among both new and traditional LP-WPAN technologies, 6TiSCH has emerged as the most suitable standard for industrial IoT networks. Its scalability is inherent within the IPv6 6LoWPAN stack, allowing thousands of sensor devices to operate in a coordinated manner while connecting to one or more 6LRs (AP). These APs, in turn, connect to a single 6LBR (Gateway Router), which can provide connectivity to the Internet, depending on the gateway settings. This setup enables the collected data to be made remotely accessible for further processing beyond the baseline network hierarchy.

Currently, 6TiSCH provides scalability through a multi-hop transmission model under a single 6LR, making it well-suited for small industrial networks. For large-scale operations, 6TiSCH can interconnect several LLNs using 6LRs, allowing the configuration of thousands of devices for industrial monitoring [26] [194].

6TiSCH is an open standard for industrial networking, supporting a broad range of IoT applications, both industrial and non-industrial. These applications include closed-loop monitoring and mission-critical operations, which can function independently of human intervention. Examples include home automation [194], building automation [164], smart agriculture [27].

Over the past five years, 6TiSCH has witnessed significant improvements in communication performance, including secure joining, packet reassembly, optimized latency, enhanced network responsiveness (especially in node's failure scenarios), improved goodput, and optimized configuration settings. These enhancements solidify 6TiSCH as a strong candidate for low-power, wireless industrial networks.

This thesis will focus on 6TiSCH, with the next chapter providing a comprehensive review of its capabilities based on the 6TiSCH architecture reference model (communication stack), where each corresponding layer and its associated technologies are described in detail.

3. 6TiSCH

Industrial IoT networks require a stable connection with reliable signal reception within the coverage area, enabling sensor nodes to perform data gathering based on the domain requirements. These requirements include query-based detection, periodic data collection (at specific times of the day), and event-based detection. This thesis primarily focuses on event-based monitoring applications, where sensor devices remain continuously synchronized and transmit data packets immediately upon event detection. Chapter 2 identified IEEE 802.15.4-6TiSCH as a suitable technology due to its ability to provide communication reliability across a multi-tiered network hierarchy. Moreover, 6TiSCH can establish multiple such hierarchies to extend coverage, with a single hierarchy covering up to 1–2 km.

3.1. Review of 6TiSCH Architecture

The network architecture of 6TiSCH [15] is comprised of layers where each layer represents a set of lightweight protocols used for communication.

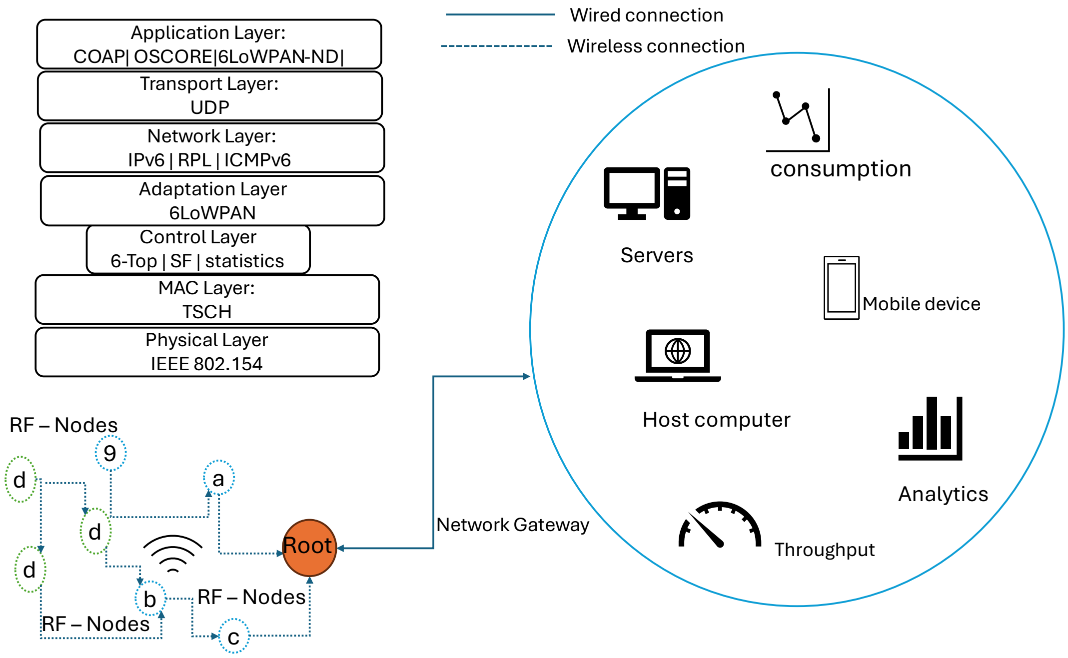

Figure 24. 6TiSCH network architecture.

The architecture reference model of 6TiSCH, illustrated in Figure 24, depicts a small IPv6 subnet consisting of seven RF nodes (battery-powered sensor devices), commonly referred to as ‘motes’ or ‘nodes’. Each node is alphabetically labelled and arranged in a hierarchical tree (RPL topology), with a single root node at the top. The root node is also known by various names such as sink, 6LR, subnet controller, or access point (AP). It is responsible for managing network connectivity to a gateway router, also called the border router (6LBR). From the border router, the network can be extended to the Internet using a wired connection (Ethernet) or a wireless medium (Wi-Fi or cellular networks like 4G and 5G).

The backhaul connectivity supports a variety of applications, including data analytics, utility metering (monitoring consumption and throughput), and industrial automation [195]. This section provides a coherent description of the communication stack of 6TiSCH.

3.1.1. Application Layer

6TiSCH Application layer is comprised of standard messaging protocols allowing interaction between devices within the IPv6 subnet (LLN). Each protocol follows a different communication strategy, and use some form of security mechanism protecting the application-generated payload. These protocols are briefly described in this subsection:

Message Queuing Telemetry Transport (MQTT) [196] messages are lightweight and can operate on smaller microcontrollers such as 8-16 bits Microcontroller Unit (MCU). It uses *publisher* and *subscriber* model offering bidirectional communication while using broadcasting between devices to cloud and cloud to devices [196]. MQTT is flexible to adopt modern security protocol for encryption and by default the payload is protected using existing Transport Layer Security (TLS), a mechanism designed for protecting data sent over the internet.

Constrained Application Protocol (CoAP) [197] is a lightweight version of Hypertext Transfer Protocol (HTTP) [198] used for device to device communication under IP subnets, where IoT devices can rest and send data upon scheduled wake up. CoAP is designed for extremely lightweight operations and can run on the tiny sensor platforms. Object Security for Constrained RESTful Environment (OSCORE) is introduced as standard security protocols for resource-constrained IoT devices. RFC 8613 extends CoAP library of functions to protect data packets exchanged via request and response message [199].

Data Distribution Service (DDS) [200] is a publish/subscriber-based messaging protocol, which is interoperable with other technologies too; it can be used in conjunction with various communication protocols and web services such as Representational State Transfer (REST), MQTT, Advance Message Queuing Protocol (AMQP), and can be further extended to support custom data types. DDS provides a robust framework for real-time, high-performance data distribution within distributed systems. Its flexibility, QoS controls, and scalability make it a popular choice for industries that demand low-latency, reliable communication between systems. In terms of payload security, it uses TLS. However, it is not as lightweight as CoAP and MQTT as it incurs overheads.

AMQP [201] is built around the concept of messaging, which enables systems to send and receive messages asynchronously, decoupling the producers of messages (senders) from the consumers (receivers). This is useful in distributed systems where components may not be available simultaneously. CoAP would be the better choice due to its lightweight nature. AMQP is more appropriate for scenarios where reliability, security, and advanced messaging features are needed, but it is not as lightweight as CoAP.

Extensible Messaging and Presence Protocol (XMPP) is based on Extensible Markup Language (XML) that enables near real-time exchange of structured data between clients on a network [202]. It is Originally developed for instant messaging. XMPP has since then evolved to support a wide range of applications including online collaboration, IoT, gaming, and RESTful APIs (to help better utilize the device's resources in terms of real-time communication and throughput maximization). It, by default, uses TLS for payload protection. The downside is that XMPP is an expensive protocol compared to CoAP.

The 6TiSCH nodes prefer to use the CoAP [197] because of its lightweight nature, minimal overheads, and by default support of OSCORE [203] for payload security. Using the CoAP, nodes exchange messages frequently.

The application layer also include 6LoWPAN Neighbour Discovery protocol (6LoWPA-ND) [204], which is responsible to assist with node tracking beyond a subnet and provides required compression and adaption to make messaging seamless between devices in different subnets. This capability is driven originally from the 6LoPWAN protocol, operating at a different layer in the stack. Notably, 6LoWPAN-ND protocol is an alternative to classic IPv6 based Neighbour Discovery, using prefixes for efficient tracking of nodes while at the same time, it reduce multicasting and broadcasting towards prefix distribution in a multi-hop network.

3.1.2. Transport Layer

The transport layer utilizes User Datagram Protocol (UDP) to deliver CoAP packets. UDP is a stateless transport protocol that does not require acknowledgement for each transmission. It manages end-to-end delivery of CoAP packets efficiently for power-constrained networks where each CoAP packet is assigned with an unique network address by the IPv6 network layer, with no routing information stored under non-storing mode of RPL.

3.1.3. Network layer

The network layer consists of key protocols, including IPv6 for addressing, RPL for routing, and Internet Control Message Protocol for IPv6 (ICMPv6) can be implemented at different levels of the stack, but at this layer, it is primarily used to handle routing and addressing-related exceptions.

The IPv6 protocol is responsible for addressing, allowing each and every node within the subnet to have an unique IPv6 address. An IPv6 address is 128 bits long or 16 bytes or 32 hexadecimal characters. It is typically written in hexadecimal notation, separated by colons into eight groups of 16-bit blocks. The root node maintains a complete view of topology where these addresses are compressed into local prefixes and later appended to the packet's header as source path [205].

3.1.3.1. RPL Layer

The RPL as RFC 6550, is a lightweight routing protocol specifically designed for Low-Power and Lossy Links by the ROLL WG. The following subsections provide a brief overview of key processes including *control beacons*, *objective functions*, *operation modes*, the *trickle timer* mechanism, and *downward routing*.

3.1.3.1.1. Control Messages

The RPL is designed for deterministic networks, while organizing the topology based on Destination Oriented Dynamic Acyclic Graph (DoDAG) Cluster Tree [206]. It uses the *rank* metric as weight assigned based on the underlying propagation model. It is initially computed by Objective Functions (OFs) based on the link quality metrics such as RSSI, and PDR. The rank value which is a two byte long counter increases and decreases following the changes in the physical environment. Further, it depicts distance in terms of number of hops to the root.

Once the root is configured, it is initiated with rank zero. To keep the topology operational the protocol uses three types of control beacons: DIS (DODAG Information Solicitation), DIO (DODAG Information Object), and DAO (DODAG Advertisement Object) or DAO-ACK (DODAG Advertisement Object Acknowledgement). At first, RPL broadcast DIO containing the *rank value* of *root* and IPv6 address of the gateway router. As new node joins the network, it connects to a parent node and then derive the rank from the parent's rank, which is an increment based on the maximum rank increase threshold (256). The role of DIO is to keep network topology up to date, which is expected to be broadcasted at a defined probability (a value from 0.0 - 1.0).

DIS beacons are used by the joining node for information solicitation prior being assigned a rank. DAO messages are used by source node to propagate or advertise path information upward through the root using unicast messaging. DAO-ACK is used by sender to acknowledge delivery of DAO message.

3.1.3.1.2. Objective Functions

An OF is a core program used for topology building. It is primarily responsible for calculating a rank value or cost from combination of link metrics. Using this rank value, it organize the DODAG tree by enabling preferred parent. There are mainly two OFs provided in standard RFC 6550: Objective Function Zero (*OF0),* and Minimum Rank with Hysteresis Objective Function (*MRHOF*).

OF0 governs route selection based on the rank value, computed by RSSI metrics, and distribution takes place in manner that the nodes located far away from the root, will be assigned higher rank and lower rank for nodes aligned closer to root in the DoDAG topology. Conversely, MRHOF does not consider '*hop-distance'* as a primary routing metrics. It rather stresses on path cost and avoids longer path by calculating accurately the link quality. In [207], the author evaluated the two OFs assessing their credibility in strained transmission range. In which, the author concluded MRHOF is a superior function than OF0. However, OF0 is a default implementation of RPL because it generates low overheads.

Existing surveys [208] and [209] found that OFs in RPL suffer with three key challenges: (1) The first challenge is poor *load balancing*; once a shortest-best path is found, all packets are directed through that path. This process impedes resources of nodes attached to that route. On the contrary, multi-path routing is not admissible as it causes high amount of overheads leading to memory overflow. (2) The second challenge is *under specification of link metrics.* RPL does not explicitly define as to what set of link metrics should be optimal to calculate the rank value based on which route selection and optimization is carried out [171]. (3) The third challenge includes *quality of links and the impact of hop counts*, which implies whether a path is longer or shorter, thus the quality of links must be checked to avoid the low performing nodes on the way to the destination. Under performing nodes can potentially cause an asymmetrical path, leading to packet loss. In RPL, MRHOF evaluates link quality more precisely using Expected Transmission Count (ETX) [12]. ETX is an expensive link metric that monitors all incoming and outgoing packets.

3.1.3.1.3. RPL Mode of Operations

RPL operates using one of the two pre-defined MoPs. These are, called *Storing* and *Non-storing* MoPs. Under storing mode, nodes are allowed to store routing information about the topology. The routing is performed using proactive or reactive manner where the reactive routing is currently out of scope for 6TiSCH; simply because it requires frequent broadcasting leading to a high volume of overheads. A proactive routing is ideal besides node can encounter memory overflow as the network grows, leading to network bottleneck.

Under non-storing MoPs, nodes are not required to store routing information and all packets are first sent to the root using forwarding rules (preferred parent) to enable source routing. Root is thus capable to store a large amount of routing information and can perform path computation using standard algorithms as used in standard wireless network. The routing nodes are however required to update their status over a regular interval of time to maintain path accuracy. This approach has limitations as longer path translates into a larger source header, which is to be inserted to the header of the packet itself before making a journey downwards in the routing hierarchy. Currently, interoperability between MoPs is also a challenging aspect [210].

3.1.3.1.4. *Trickle Timer*

Trickle Timer [211] is distinct function of RPL, introduced by IETF for *Suppression of overheads* and *Manipulation of Expected Duty Cycle* [212]. In RPL, several instances of same DIOs are created in an attempt to keep network tightly synchronized. These beacons are transmitted in the multi-hop setting where propagation delay is often proportional to number of hops it takes to reach the target destination [209]. Apart from this, duty-life cycle suffers due to disproportionate amount of transmission by nodes provided some node transmits more beacons that others. As a result, overlapping can takes place when some neighbors those are already put to sleep. The Trickle timer mechanism is only suitable for synchronized networks because in the asynchronized networks the DIOs are sent less frequently, making suppression unworthy. However, it can be argued from the perspective of proportion of DIOs to be suppressed as suppressing over 70% DIOs can render the routing topology unstable [209].

3.1.3.1.5. *Point to Point Routing*

Downward routing is often complicated than upward routing in IoT networks. A downward flow of traffic using 6TiSCH refers to scenarios where data packet is travelling from root to nodes (P2MP) or node to node(P2P). For that matter, RPL's success rate is roughly 98% under P2MP [209] and it further decreases to 74% approximately under P2P [212]. Notably, 6TiSCH is not optimized for industrial networks that follow a critical close-loop supervisory application where downward messaging must be reliable. To put it simply, controlling, and tracking on demand can be less popular than monitoring-based applications. There are multitudes of reasons behind the poor downward performance, including poor route discovery, lack of accurate path formation, and loop formation (when a packet is forwarded in the wrong direction).

3.1.4. Adaptation Layer

Once a IPv6 packet is fully configured, it undergoes adaptation and fragmentation where the 6LoWPAN layer is responsible to compresses both UDP and IP headers [213] (roughly 40 bytes long) and divide a heavy UDP payload (1024 bytes approximately) into smaller fragments based on the MTU size of the IEEE 802.15.4 (127 bytes). 6LoWPAN layer filter this into approximately 8 - 10 fragments depending on the capacity of the assembly buffer; the assembly buffer stores each 6LoPWAN fragments at transmitter's end and is responsible for reassembly of the original UDP packet at the receiver's end.

Prior 2020, fragmentation and assembly was carried out where a node had to wait for the entire packet to be assembled before forwarding new fragments to the next hop neighbor. This caused an unnecessary delay in forwarding an IPv6 packet. Virtual Reassembly Buffer (VRB) [RFC 8930] is a technique introduced in 2020 by *Bormann et al.,* [157]. According to this, at least 2-3 VRB tables are sufficient for assembly of packets in hop by hop manner using single subnet, so that the nodes are sending data packets without having to wait for the entire payload to be assembled and this contributed to reduction in queuing and packet forwarding delay.

The downside is that this technique is critical to constrained assembly buffer (at a time, the assembly buffer can store maximum of 2 UDP packets), packet loss when more than one nodes are sending packets concurrently, causing *hidden terminal problem*, and poor fragment recovery, which is currently an open issue. According to this, if the missing fragment is not received, the entire packet is dropped. A fragment can go missing due to not been provided an IP header as it is only attached to the first fragment, making fragment sequencing problematic and the retransmission causes an unnecessary traffic in the network; thus, managing packet assembly and sequencing is a critical process where each packet type encounters delay based on queuing priorities: typically, the first packet should enter first, however, which packet to be allowed in the TX queue first is subject to priority attached to the TSCH cell type. Consequently, a node can drop the packet if the transmission delay is significant [214].

As far as the compression is concerned, IPv6 header compression (HC) is a complex process, which requires node's local addresses (specific to connectivity within the subnet) to be compressed into prefixes, then to be discovered across the subnet [215]. The compression at the local level (within the subnet) is carried out with the help of signaling, however, with signaling, it is counter-productive to perform ND outside the subnet using the local addresses (prefixes). That way, compression technique must be coherent and context-driven. A context ID is thus attached as a part of the node's address through Internet Protocol Header Compression (IPHC) header. Here, all local addresses are fully compressed during joining and once the node has become a part of a global IP (provided by 6LBR), the local address is replaced with global IP address for connectivity to the Internet.

6TiSCH supports multiple subnets whereby locating a node in the different subnet is a complex task. It requires efficient routing across multiple subnets. To do so, 6TiSCH proposed tunnelling [216] between IPv6 subnets, which places the routing header in the tunnel header (above base-level hierarchy). However, routing via tunnelling generate extra overheads and it even translates into longer source path, which is one of the key weakness of source header-based RPL routing under the non-storing mode of operation [171].

IETF sponsored working groups, such as 6lO [217], 6LoRH [218], ROLL [205], and 6TiSCH WGs have recommend compression of the RPL artifacts through the header and reuse the space reserved for optional fields in IPv6 header (such as RPL instance ID), and as provided in the MAC frame (the complete view of the IEEE 802.15.4 frame is provided in [214]). This is currently defined as 6LoRH specification. ROLL WG [205] is currently working towards specifications towards upstreaming traffic beyond the subnet via efficient internet connection.

3.1.5. Control Layer

The 6LoWPAN fragments are relayed to the 6Top layer [14] for storage after compression and adaptation. The 6top layer is responsible to collect network statistics passively and implements SF that way each packet is provided a transmission and reception window corresponding to the departure and arrival time using random channel-hopping capability. 6P [219] is a replication of 6Top, designed to provide flexibility within the various TSCH-led scheduling designs: The following commands are used by 6Top to support TSCH operation:

1. *ADD*: It is used to add a TX /RX cell based on the node's request.
2. *DELETE*: Cells are deleted when requested by SF or when nodes are changing parents.
3. *RELOCATE*: This commands removes a TX/RX cell from the node's buffer due to collision. Once removed ,the cells are brought back into slotframe and activated after quarantine period, which can be explicitly defined by SFs.
4. *COUNT*: It is used to count a cells categorized by cell type (shared, dedicated, or minimal broadcast cell). For example, to find out how many dedicated TX cells are currently being used in the network for transmission, COUNT at the complexity of O(N) provides the precise value.
5. *LIST*: It is used to list available cells in the slotframe
6. *SIGNAL*: It is placeholder for SF, used to assist various functionalities of network such as synchronization, negotiations, resource allocation.
7. *CLEAN*: It clears scheduled TX and RX at a particular node. The command is also used as placeholder to deal with scheduling inconsistencies.

6Top is vital component of 6TiSCH, that connects the upper and lower end of the 6TiSCH stack. It acts upon the instruction from the SF, and stores network dynamics to facilitate scheduling decisions. The SF manages the state of the device's radio (*sleep, transmission, reception*) by providing instructions. The next subsection 3.1.5.1 discusses the current specification of scheduling algorithm, also known as generic SF for the standard 6TiSCH stack.

3.1.5.1. Generic Scheduling Function

6TiSCH implements MSF (RFC 9033) as a generic solution, which use centralized scheduling design for managing topology using shared cells and traffic adaption is carried out with distributed scheduling using dedicated cells. That way, there are more than one slotframes used where each TSCH cell is scheduled in a half-duplex manner: a node can either transmit (Tx) or receive (Rx) at a time and different SFs used the scheduler to tune up the performance to meet specific goals. These solutions are reviewed in the next section.

MSF uses three consecutive slotframes. The first slotframe is exactly 1 timeslot long, of which the 0^{th} slot is considered to be used for propagating Extended Beacons (EBs) in the network, allowing nodes to join the network. Nodes can learn about the shortest-best path to root by deciphering EBs. The 2^{nd} slotframe comprises of autonomous unicast cells (Rx and Tx), computed per node basis. These are unicast cells, added and deleted frequently and most importantly, to be accessed on contention-basis. Finaly, the 3^{rd} slotframe contains the dedicated unicast (Tx and Rx) cells that are not shared with other nodes. These are used for adapting traffic on the nodes.

MSF follows a prolonged **bootstrapping** process which begins with a compatibility check between different devices under a subnet and ensuring interoperability based on the pre-configured Pre-Shared Key (PSK) [220], leading to a secure joining process. PSK is a security solutions, often used within lightweight protocols, but if a node wants to skip this stage then it is possible provided there are no pre-configured security implemented. Once the radio is switched on, it chooses a *frequency* from the available channels and then starts *listening.* This allows a joining node to explore existing neighborhood and choose one of them (neighbors with stable link characteristics) as its Join Proxy (JP). The next task is setting up the *autonomous* cells with the help of a hash function, which then computes both channel and slot offset from an Extended Unique Identifier (EUI-64) of node, as follows:

*Slotoffset = 1+ hash (EUI64, Length(slotframe-1)-1)……(**2**)*
*chOffset = hash (EUI64, ChannelDesity)…………………..(**3**)*

After the selection of a JP, the node sends a 6Top request for the installation of an *autonomous* Tx cell at the chosen parent. TSCH is half-duplex, so it must first remove any autonomous Rx cells immediately before initiating the 6P_ADD command. The parent node uses the configured Tx cells for sending out the response and then requests a 6P_DELETE to removes the autonomous Tx cell immediately that way the child node can receive the response using autonomous Rx cells. However, if the 6P transaction is unsuccessful, the joined node continues repeating the same steps until an *autonomous* TX cell is installed at the chosen parent.

The next step determines the frequency of broadcast beaconing such as EBs and DIOs (both are broadcast-based advertisement beacons) based on the probability distribution model for the sake reducing energy-consumption. MSF uses 0.33, and 0.01 as an optimized limit for sending EBs and DIOs [221].

Finally, the node has synchronized, is using correct keying mechanism prescribed for the link layer, has a PP, to whom it has installed a Tx and Rx cells, is able to forward the oncoming data traffic, and is capable to allow other nodes to join the network by becoming the JP. Once joined the network, the node is then able to decipher DIOs, compute its own rank, and change PP to align itself with shortest proximity to the root.

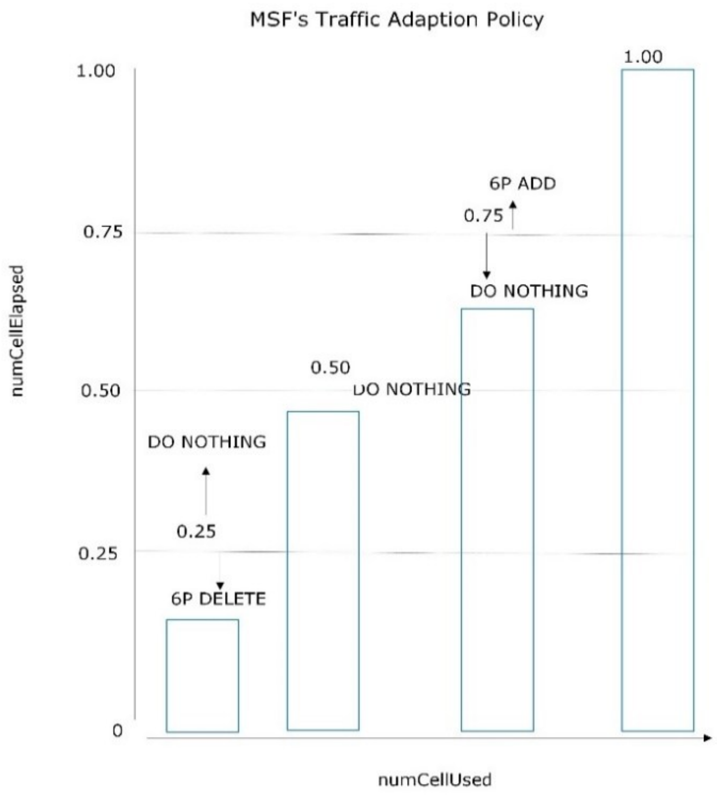

Figure 25.MSF traffic adaption mechanism.

The graph shown in Figure 25 illustrates the Traffic Adaptation Policy of the MSF. This policy is designed to adapt the allocation of dedicated cells from 3rd slotframe based on traffic demand, helping the network balance resource utilization with current traffic conditions. The X-axis (*numCellUsed*) represents the proportion of scheduled cells that are actively being used by a node and the Y-axis (*numCellElapsed*) shows the proportion of scheduled cells that has elapsed regardless of success or unsuccessful transmissions.

MSF operates through set of thresholds: when the *numCellUsed* value falls below 0.25, the policy initiates a 6P_DELETE request to remove unnecessary cells, as the traffic load is low. When the *numCellUsed* value is between 0.25 and 0.75, no action is taken, maintaining the current cell allocation. However, as *numCellUsed* exceeds 0.75, MSF triggers a 6P_ADD command to add one more cell and support the increased traffic demand. By dynamically adjusting the number of cells, the MSF policy aims to manage link-layer resources in response to traffic fluctuations in dynamic topology.

MSF's traffic adaption delay is generally a fixed value represented by MAX_NUMCELL and given hysteresis (*numCellUsed* and *numCellElapsed*) are used a counters, increases based on the cell usage.

For MAX_NUMCELL = 4, a high volume of 6P transactions are triggered [222] . This improves latency but increases consumption and provoke packet loss over *Tx-queue* being full whereas, a higher value can also lead to an increased latency and provoke congestion. Clearly; it is not an latency-centric SF, instead, the focus is placed on reducing overheads, mitigating collisions, which is subject to how cells are selected. Cell selection by MSF is a 3 fold process provided it uses 3 consecutive slotframes:

(1) in *minimal slotframe*, channel selection is contention-driven as the broadcast cell is shared with other nodes in the network. Despite the reduced probability of EBs, the collision can still occur in advertisement cell. A *backup* mechanism is provided by default in IEEE 802.15.4 to deal with it.

(2) As far as the *autonomous cells* are concerned, MSF uses a hash function to compute these identifier where probability of collision is very rare as TSCH scheduling is half-duplex. Further, In *autonomous slotframe,* allocation is fairly static. MSF monitors collision using link-quality metrics: a cell is collided where it exhibits poor PDR, as a result; the collided cells is removed and deactivated for 5 minutes, is called quarantine period decided by MSF. However, if the topology is static and there is no movement or change in network condition (children nodes are prohibited to obtain a Tx cells), the number of 6P_CLEAR are likely to be triggered over and over as the slotframe repeats itself, leading to increased energy-consumption.

(3) In *negotiated* or dedicated slotframe, The cells are not shared and therefore, collided cells can consume high energy based on the radio activity. MSF's housekeeping policy is designed to check collision in dedicated cells based on the link quality of the receiving node, it relocates the cell immediately to avoid poor performance.

The queue assignment follows the priorities assigned to each cell type by the MSF that means a broadcast cell has the highest priority than the autonomous cells and the autonomous cells have priority the negotiated cells, which executes in the end. Tx buffer follow such admissions based on the attached priorities. Towards packet assembly and forwarding rules, MSF implements the VRB which then dictates the forwarding rules; though managing this is not straight-forward, especially, with the old packets, sitting for long in the queue, while waiting for their retransmission; this can trigger congestion, leading to increased admission delay for new packets. MSF has several weaknesses where some of these are to do with the design itself; for example adding more than 1 cell at a time causes higher execution delay, leading to problematic sequencing (fragments). As a result, the sequence counter is necessary to be reset more often. A longer delay in transmission can trigger packet removal from the Tx queue due the expiry of timers, which are set to avoid idle-listening and energy-wastage (this is discussed under energy-consumption model in Subsection 3.1.6).

3.1.6. MAC Layer

TSCH is a MAC-layer protocol that combines time with channel-hopping exercise, allowing sensor device to communicate efficiently. The TSCH scheduler is half-duplex and it is implemented with flexibility by various scheduling designs laid by 6Top. The responsibility of TSCH is to manage *time cycle* and *channel-hopping* capability. TSCH operation is described in broader detail in the beginning of chapter 1 using an example in Figure 1.

3.1.7. Physical layer

Physical layer determines modulation, encoding, selection of frequency band (number of antennas), etc. The IoT devices are manufactured by different-2 companies so the hardware design and configuration may vary from one device to another. Typically, all have some limitation in terms of limited memory, processing, and battery capacity. These devices must to IEEE 802.15.4-complaint and must operate on 2.4GHz frequency band.

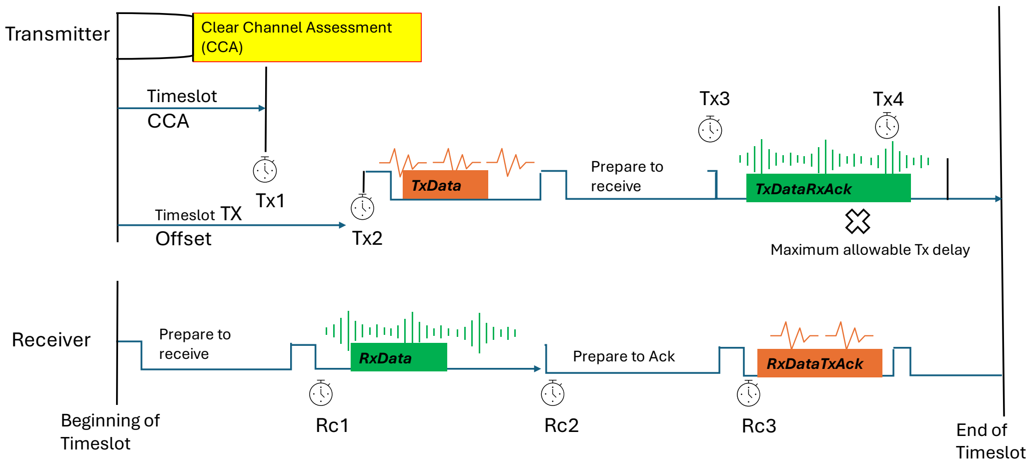

Figure 26. IEEE 802.15.4 TSCH transmission model from [169].

Figure 26 demonstrates a simple end-to-end transmission and reception using a sender and receiver with each implementing TSCH mode of IEEE 802.15.4 [169]. The sender transmits a data frame to the receiver. The first stage is to check for a clear channel using Clear Channel Assessment (CCA). This is necessary to avoid any sort of collision before transmitting data, but this is an optional feature. The second stage enables transmission (*TxData*). Once the packet is relayed, the sender then awaits an acknowledgement (*TxDataRxAck*), which is the third stage. If an acknowledgement is not received, a guard timer designed to suitably terminate listening after a fixed period, turns the radio off forcefully, is the 4th stage at transmitter's end [169]. TSCH state machine implements these timers to avoid adversaries in terms of high duty-cycle. As TSCH is half-duplex, the Tx cells is removed from the sender.

On the receiving side, the 1st stage determines that the radio is tuned on. If the packet is lost then it concludes the duration of period the radio to continue remain active as often there is no packet to be received (*idle-listening*), is the 2nd stage, but if a packet has arrived, the receiver performs reception using Rx cell, is the third stage. The last stage (4th stage) ensures that an acknowledgement is sent to the sender of the packet [169]. For each radio activity shown in Figure 26, the node follows maximum energy consumption limits (guard timers). This process depends on the *board specification* and *specifications per each slot type*, for example a system-on chip (SOC) specification has both microcontroller and radio module and other specification do not have these components on the same board this means the energy consumption is computed as the device enter different module (slot) registering change of state of MCU and radio.

Vilajosana et al., [169] provided an energy consumption model for 6TiSCH network where the author provides a breakdown of charge consumption based on the testbed experiments using OpenWSN [223]. OpenWSN is testing tool, emulating the capabilities of multiple hardware platforms. In this experiment, author [169] used two key platforms that could run following TSCH-MAC implementation [223]. Both platforms (GINA and OpenMote-STM32) [169] are IEEE 802.15.4 compliant besides featuring different processing capabilities (MCU), but uses the same radio module, manufactured by Atmel (AT86RF231 radio). GINA is assembled with MSP430F2618, a Texas instrument following a 16 bit MCU whereas OpenMote-STM is equipped with 32 bit MCU using the same radio instrument as GINA.

Platforms	TxDataRxAck	TxData	RxDataTxAck	RxData	Idle	Sleep
OpenMote-STM 32	161.9 μC (microcoulombs)	119.1 μC	217.0 μC	154.8 μC	101.1 μC	8.2 μC
GINA	92.6 μC	69.6 μC	96.3 μC	72.1 μC	47.9 μC	4.9 μC

Table 6. Measured charge drawn per slot type using both hardware platforms from [169].

Table 4 provides a breakdown of energy consumption in microcoulombs (μC) across various states for two IoT platforms: OpenMote-STM32 and GINA. The consumption varies across states of radio and depending on the number of bits processed by MCU. The estimates provided in Table 4 are representative of the testbed results mentioned in [169]. The purpose of this to provide a rich picture concerning the energy consumption by the devices. For each activity, OpenMote-STM32 generally consumes more energy compared to GINA. For example, in the TxDataRxAck mode, OpenMote-STM32 uses 161.9 μC compared to 92.6 μC for GINA. Similarly, OpenMote-STM32 consumes 119.1 μC for TxData, while GINA uses only 69.6 μC. The differences highlight that OpenMote-STM32 consumes a higher power across all operational states because of higher processing capability, with both platforms drawing minimal energy in their Sleep state (OpenMote-STM32: 8.2 μC, GINA: 4.9 μC).

6TiSCH follows the realistic energy consumption model based on the radio activities (states). The author [169] included these *states,* reflect the consumption by each platform. The energy consumption is therefore the sum of consumed current in these states by a device based on the total energy consumed in state. To put it simply that each state's contribution across TSCH is computed separately for the period the node has been actively used. The sum of these contributions provides the total energy consumed. The author describes consumption across 6 different states, used in TSCH slotframe by IoT device for wireless communication:

(a) In *TxData* slot, no acknowledgement is received.
(b) *TxDataRxAck* allows transmission of data and receive an acknowledgement for successful delivery.
(c) *RxData* is used for reception without acknowledgement.
(d) In *RxDataTxAck* , a radio device receives packets and send acknowledgement.
(e) A device listen for data when there is no data expected is called *idle* slot.
(f) Finally, *sleep* slot indicates no radio activity and that radio is not hearing any communication under this stage.

The energy consumption modelling is a complex process and it can vary from one technology to another irrespective of IEEE 802.15.4 standard, which is not exclusively adopted by 6TiSCH alone as underlying physical layer specification.

In terms of modulation scheme, IoT device uses O-QPSK (this is described in detail under Section 2.4) where DSSS is used to provide the spread factor in dealing with Eis, and other RF-challenges. The modulation scheme offers *2bps* coding, allowing devices to maintains an acceptable data rate. Further at this layer, each hardware device is required to keep synchronized using a common clock where the guard time determines how long can a device remain desynchronized. There are two types of hardware (crystals comes attached to the MCU in OpenMote and other devices too) utilized to monitor the clock accuracy:

(a) A high speed crystal, attached to the board using 20MHz frequency and it only turns the radio on where there is some communication activity to be performed. The drift is maintained at 40 parts per million (ppm).

(b) A constantly powered 32kHz crystal attached to the MCU, which is also known as low speed crystal, maintains a speed of 30ppm. The drift is caused by both imperfect assembly and manufacturing, and external environmental (temperature, power supply, and device's age). For a detailed information about factors causing drift are summarized in [214].

This thesis primarily focuses on the functionalities of the 6Top layer, particularly in providing specific scheduling instructions to regulate network traffic and enhance overall communication performance. While accommodating 30-50 devices within a subnet with providing high reliability with acceptable QoS is not limited to 6TiSCH, as the other industrial standards such as WirelessHART, ISA 100.11a, and Wi-Fi 802.11ah, ZigBee can also offer the same, 6TiSCH distinguishes itself by addressing scalability challenges. The goal is to enable each AP to support a dense network with hundreds of nodes, including multiple relay and leaf devices. To meet these scalability requirements, various SFs across centralized, distributed, and hybrid design have been proposed for 6TiSCH networks. This section provides a comprehensive review of 6TiSCH scheduling capabilities based on the existing scheduling algorithms, offering key insights into their methodologies and performances. The goal here is to identify the potential areas in scheduling that can contribute towards enhancing communication efficiency of the 6TiSCH standard ensuring scalable communication.

3.2. Review of TSCH-led SFs for 6TiSCH Networks

TSCH has been added as a default mode in the recent amendment of IEEE 802.15.4 and is now a widely adopted MAC layer protocol. Other standards, such as ZigBee, ISA 100.11a, and 6LoWPAN, can also leverage its capabilities to enhance network performance. This section will review many SFs compatible with 6TiSCH networks.

Hermeto et al., [18] highlighted importance of channel-hopping for low power IoT networks in terms of eliminating EIs, and combating multipath challenges. The author evaluated roughly 50, providing insights pertaining scheduling issues such as link stability and traffic conditions. The literatures presented divided SFs based on centralized, distributed, and hybrid scheduling category where the author characterized scheduling efficiency based on *schedule compactness*, *end-to-end reliability maximization*, *parent change*, and *performance trade offs*. This survey concluded with the open issues: lack of self-healing in 6TiSCH networks, interference model (to avoid collisions), asymmetrical links, scalability limitation, and poor mobility support. Since 2017, 6TiSCH scheduling has evolved, however many of these open challenges remain the same; most importantly the scalability limitation.

In 2018, *Mohamadi and Senouci* [224] surveyed SFs focused on the 6TiSCH networks, however, the author reviewed a smaller number of contributions (SFs) and did not propose any taxonomy.

In 2019, *Kharb and Singhrova* [225] provided a new taxonomy based on algorithm execution models (centralized, distributed, autonomous, and hybrid) aligning each category with different goals; this includes centralized & distributed category to be more suitable for the latency-centric applications, autonomous scheduling for low power efficiency allowing overhead reduction, and finally the hybrid scheduling for improved reliability and scalability. However this survey overlooks the scheduling design where distributed execution (SFs) can provide a low latency and reliable communication. It is scalable as long as control overheads are managed efficiency. Notably, the autonomous execution model (SFs) is not completely overhead-free [226].

Elsts et al., [227] proposed a taxonomy based on autonomous scheduling where the author focused on the niche concepts such as *cell allocation, channel allocation,* and *re-allocation*. Literatures presented were reviewed repeatedly under each category, making classification distinct; however it introduces redundancy, making the survey unnecessary lengthy. Apart from that, routing-independent TSCH scheduling solutions are out of the scope of 6TiSCH. Other than these two, the sample size is fairly small because autonomous scheduling was introduced in 2015 by [228]. The author however reviewed the key solution published between 2015 and march 2020. The autonomous scheduling have evolved since 2020. For example, MSF was introduced in 2021 as internet-draft (genetic solution), using autonomous scheduling to manage topology.

Righetti et al., [226] provided a focused review of autonomous scheduling solutions with emerging focus on adaptive autonomous scheduling (traffic scenarios) where the author initially covered key solutions published between 2015 and by the end of 2021. Because the autonomous SFs were not as many as distributed and centralized SFs (in terms of their sample sizes), and scalability has remained an open issue, a very less number of SFs were examined that too it was carried out theoretically, providing quantitative comparison based on adaptive traffic scenario. It does not address scalability in the sufficient detail.

Urke et al., [229] was published in 2022 showcasing a comprehensive review of a large number of SFs. The author presented taxonomy based on four main categories: *centralized, decentralized, static,* and *hybrid*. The decentralized category is further divided into *autonomous*, and *collaborative* (distributed). The author further divided *collaborative* scheduling into three sub categories called *Local*, *Recursive*, and *End-to-End*. The *local* class reflects on *negotiation for a cells between neighbors* and *recursive* class describes *on the fly* reservation of cells along the path using signaling, and finally, the *end-to-end* scheduling is described as a pre-computed number of cells allocated per link basis. The downside of this survey is that each category is extreme deduction across each category; though each subcategory is presenting a unique concept, but with a narrow sample size, it fails to capture the general applicability required to assess scalability under diverse scenarios. Apart from that, inconsistent renaming such as *collaborative* scheduling, which is hardly referenced in existing literatures.

Senouci et al., [195] is the latest survey that systematically aligns each SF based on the taxonomy presented: *approach specific traffic-aware*, *traffic-specification category*, *network characteristics*, and *adopted methodology*. The approach-specific category included *centralized*, *distributed*, & *autonomous* under execution model where schedule specification points to *cell allocation, design goals* as per QoS requirements of 6TiSCH applications. The link directions put this into context where traffic-awareness metrics such as *queue, cell usage*, *traffic flow,* or *hybrid* are described in depth. The traffic models (periodic and event-driven traffic) were also covered under traffic-specifications, which is 2nd category under the taxonomy provided by the author. Under *network characteristics* classification, the author reviewed SFs based on the underlying topologies, size of network, and mobility supported solutions. The existing solutions were reviewed based on these three traffic-awareness metrics, suggesting insights as per network characterization however, it did not sufficiently review these solutions addressing scalability limitation as an open challenge. The *adopted methodology* is the fourth class of the survey, which is comprised of problem solving methods followed by SFs, and evaluation methodologies such as simulation, analytics, testbeds. The survey shows neither SFs related to 6TiSCH follow an analytical based evaluation. It is vital survey from the point of selecting a suitable evaluation methodology. The downside is that the author reviewed SFs, which were repeatedly appearing throughout the review and it does not particularly address scalability in sufficient detail, instead being more focused on traffic-aware scheduling.

Currently, scalability is an open challenges for 6TiSCH networks and existing literatures ignore this key limitation of 6TiSCH standard. 6TiSCH has been tested using varying number of network sizes, ranging from 20 - 50 nodes and showed good performance; through, this advantage is not exclusive to 6TiSCH as other technologies such as Wi-Fi 802.11ah, and ZigBee can also offer the same advantage at even lower cost and are less complex than 6TiSCH in terms of deployment.

This thesis provides a structured review, using related SFs within the scope of IETF 6TiSCH. The study introduces a unique taxonomy based on 6TiSCH scheduling research, selecting popular SFs allowing a better understanding of their contributions towards improving the communication performance of 6TiSCH networks. These SFs are divided into three main categories:

1. **Centralized:** Scheduling decisions are made by controller (root), which can offer schedule compactness, optimization based on routing paths but faces scalability issues in larger networks due to frequent signalling.
2. **Decentralized:** Scheduling is handled by individual nodes using negotiations, without a central controller. This category is further divided into:
    - **Unicast-based Decentralized SFs:** Involve a direct, one-to-one cell usage in the TSCH slotframe maintaining half-duplexity, and it is typically designed to ensure that individual node being scheduled in a collision-free manner.
    - **Broadcast-based Decentralized SFs:** Use one-to-many communication, enhancing scalability by allowing nodes to share TSCH cells with multiple neighbors in a half-duplex manner.

3. **Hybrid:** Combines both centralized and decentralized scheduling approaches, aiming to balance scalability and energy-efficiency (reduced 6Top overheads).

This taxonomy is tailored to meet the key objective of the thesis - **scalability improvement; hence** by keeping scalability in the centre, the related SFs are aligned providing a more nuanced review that highlights the suitability of different SFs for different network sizes and application requirements.

The existing surveys have used different strategies in past and have laid taxonomy accordingly. The adoption strategy of this thesis is driven from the most used keywords: "6TiSCH scheduling" through google scholar. **Figure 27** presents classification based on the taxonomy provided.

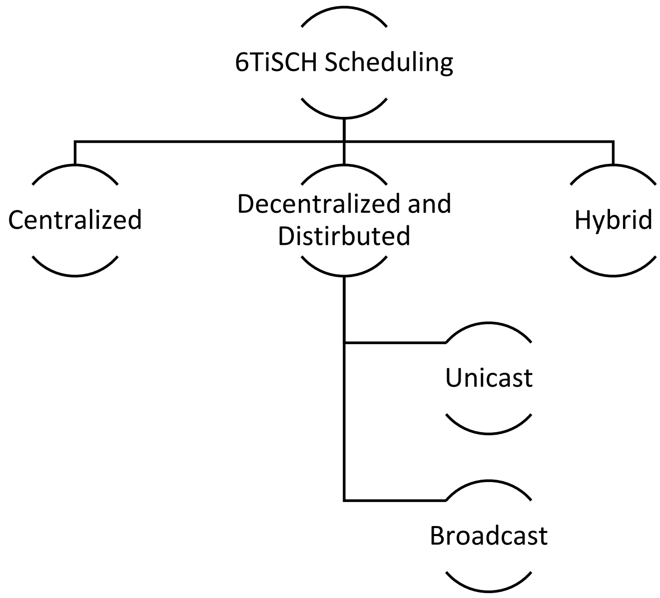

Figure 27. 6TiSCh Scheduling classification.

In 6TiSCH scheduling, predicting the complexity of SFs accurately is challenging due to the varied design objectives and scheduling approaches. This section of the thesis introduces a taxonomy of scheduling approaches and organize these contributions categorically using the diagram provided in Figure 27. The goal here is to provide a brief review of what each SF offers to enhance scalability in 6TiSCH industrial networks, aided by performance comparison based on several essential performance indicators. **Table 7** compares SFs based on these key performance metrics:

- **Reliability**: It is a presented as a ratio of the packets sent by a node over the received volume of packets. As a key performance indicator, it determines how effectively an SF can support network to maintain a dependable communication.
- **Latency**: The delay between the initiation and completion of communication by a node, which is crucial for time-sensitive applications.

- **Energy Efficiency**: An effort by a node implementing a certain qualities towards reducing energy consumption so that the node using a single charge can operate for a longer duration.
- **Scalability**: The ability of an SF to handle network expansion at varying traffic levels without significant performance degradation.

Table 7 presents a theoretical comparison of SFs, evaluating their effectiveness in terms of reliability, latency, energy efficiency, and scalability. The analysis is concise yet informative, focusing on the most relevant aspects of scheduling schemes in performance assessment. This evaluation provides key insights into the strengths and weaknesses of each SF, helping readers identify scheduling inconsistencies and potential research gaps.

3.2.1. Centralized Scheduling Functions

Centralized SFs enjoy the one-hop connectivity and benefits from improved slotframe management where a node can add or delete cells directly by signaling and that way it is easier to update schedule in presence of recurrent changes in the routing topology. This section will review key centralized SFs considering scalability limitations.

Palattella et al., [230] introduced the Traffic-Aware Scheduling Algorithm (TASA). It is the first centralized solution introduced for 6TiSCH network and a most cited approach across published contributions related to the 6TiSCH scheduling. TASA organizes nodes in a star topology where scheduling is performed by signaling. It uses color-matching pattern through the graph where each node directly engages with root to add or delete a cell to deal with the traffic condition. Despite the one-hop advantage, TASA has failed to address packet loss under a densely populated network of 100 nodes [195]. The reason is that it generates a heavy volume of signaling overheads, which not only limits the throughput, but also affects bandwidth utilization, causing poor scalability.

Choi & Chung [231] introduced Quick Setup Scheduling (QSS) technique, which follows centralized approach besides it is a broadcast-based centralized SF that allocates and deallocates schedules with the controller; hence it is using shared cells, allowing contention-based access to the schedule prepared by the controller. The cells are added based on the RPL rank. Here, rank-based allocation treats the network with a distinct advantage, however, it translates into a longer routing path while a shorter path is available instantly [18]. The cells are allocated and deallocated based on the traffic experienced and during the parent-change event. Notably, broadcast-based scheduling, by default, offers an improved propagation, the downside of which is the rapid battery drain as has been commonly witnessed [226]. Apart from this, shared cells are indeterministic, so collision is imminent, causing communication failure after an exhausted retransmissions [226].

Faras & Dujovne [232] introduced a Path-based Computation Engine (PCE) scheduling, which incorporated a model with multiple RPL instances generated concurrently. This approach provides a pre-computed schedule where each node is directed by the central entity regarding the specific timing and channel allocation for Tx and Rx activity, derived from the existing routing entries and path information stored at root.

PCE statistically measure allocation while comparing slotframe usage by nodes based on their routing positions. Notably, PCE-based scheduling exploits a linear relationship between the topology depth and slotframe occupancy as an efficient allocation strategy, indicating that as the network depth increases, the number of occupied slots grow proportionally. Such a pattern is effective for adjusting to traffic variations within the network. Each node receives a schedule in advance with a number of reserved slots and channel offsets. Limitations arise due to the high signalling overhead and increased change events, if this happens, the node has to relocate the amount of cells to its new parent especially when the routing topology is not static. As nodes require additional cells to handle temporary traffic, they must frequently signal the root, which leads to an increase in control traffic. Since, overprovisioning isn't incorporated in the PCE-based scheduling, the connected nodes may struggle with temporary traffic surges as each request for any additional cell requires a separate signalling. This leads to potential bandwidth consumption and limits the protocol's adaptability to bursty traffic. The high overheads from continuous signalling restricts scalability too. Thus, PCE-based solutions are only suitable for networks with stable routing topologies.

Huyun et al., [233] extended the PCE-based scheduling using Approximate Dynamic Programming (ADP) approach, while proposing a solution that incorporates an opportunistic forwarding mechanism. This mechanism uses a *Markovian* model [233] to dynamically interpolate radio frequencies (channels). The model allows the SF to adapt to network changes more fluidly than PCE-based static scheduling. However, it shows significant scalability constraints. For example: as the network grows beyond 40 nodes, the routing overhead increases sharply, causing straining in terms of resources allocation. Secondly, this mechanism struggles to handle bursty traffic effectively as the adaptive channel selection doesn't fully account for dynamic traffic demands, resulting in frequent signalling. These limitations are heightened in balancing adaptability with overhead management in dynamic and base-line network expansion.

3.2.2. Decentralized Scheduling Functions

Distributed/Decentralized scheduling is a popular category that holds the most contributions arrived over the past 5-7 years. A large number of SFs have come from this category alone [226]. Existing surveys [18] [229] [195] have reviewed these SFs across several categories where a further classification of decentralized SFs was meaningful through unicast-based, and broadcast-based decentralized SFs.

3.2.2.1. Unicast-based Scheduling Algorithm

The term '*Unicast*' in scheduling refers to one-to-one communication where one cell is equal to 1 node. Such cells are dedicated to particular nodes and can not be shared with any other node in the network. A dedicated schedule is contention-free where the node can either transmit or receive in a single timeslot. Several dedicated cells can be scheduled at a time by using channel-hopping whereby a node enters negotiations between other nodes to place a bargain for free cells and that way the unicast-led SFs have advantage of collision-free access and timely delivery.

Unicast SFs maintain the TSCH slotframe with at least one cell configured as a broadcast cell; it is needed for managing the network topology [195]. The remaining cells are accessed on half-duplex manner. Nodes allocates a bundle of cells or a single cell that are free in the slotframe locally; though it is sensitive to overheads and energy-consumption. A common myth about unicast SFs is that when the slotframe occupancy is higher, it triggers a network bottleneck due to collision. Many algorithms have failed to avoid the recurrent wastage of cells as TSCH frame repeats itself over time. Apart from that these algorithms also ignore the trade-off with other QoS controls such as latency, energy consumption. The following contributions are observed in this category:

Dujovene et al., [234] proposed *Scheduling Function Zero* (SF0)- Internet-draft, which provides extra cells to nodes based on the link quality (PDR). The physical layer provides two key link quality metrics including RSSI and PDR. RSSI can change over increased distance and PDR lies as a ratio of volume of packets sent and volume of packets acknowledged. SF0 allocates schedule based on link metrics performance while monitoring each link passively (prior to providing extra cells). However, SF0 is load-sensitive and drops packets under heavy traffic conditions. Consequently, this SF underestimates the number of cells required by a node to progress one-hop or shortest-path possible as most packets are sent via single-best path (queue implements FIFO, leading to congestion due to poor traffic adaption).

Watteyne et al., [20] extended SF0 by allowing a fixed volume of cells to be added and deleted as overprovisioning criteria, which sits just above the SF0. The downside is that OTF causes recurrent wastage of cells under higher threshold limit and triggers proportionally higher volume of collided cells. Conversely, the lower value of threshold also packet loss due poorly predicted traffic on the node. Hence, OTF potentially under-over-estimate slot distribution. The only benefit here is the low complexity and an easy to use solution. It has attracted a larger number of contribution towards optimization of scheduling resources.

Chang et al., [235] proposed Low latency Scheduling Function (LLSF) that uses the *daisy-chaining mechanism,* allowing connected nodes to schedule transmission soon after reception. The allocation policy is the same as OTF besides it filters for a specific low-latency slots out of the slotframe. These are distant slots from the next slotframe cycle. However, if a node fails to add slot or there is no free slot available to add, it disrupts the entire scheduling process. Additionally, it does not scan for poor performing links, where longer links are prone to increased delay [18]. Since TSCH slotframe repeats itself, LLSF causes recurrent wastage due to fixed overprovisioning cells given each time a node wants to add additional slot [195]. This process exacerbates cell consumption under heavy traffic conditions, leading to fewer slots for the other nodes to add in the slotframe.

Daneel et al., [236] enhanced LLSF using Recurrent Scheduling Function (ReSF) with an aim to address recurrent wastage using a separate traffic management algorithm. This algorithm reserves a series of slots along the path the root and that way it can predict the success or failure of packet being received in advance. However, this could not be accomplished without active monitoring of queue, and link-quality metrics allowing such models to accurately predict the relay between node and it's neighbours. While it solved the recurrent wastage problem, the energy consumption remains at a same level as SF0 [234]. Additionally; the approach suffers from high control overheads and packet loss under challenging traffic conditions [195].

Soua et al., [237] divided the slotframe into waves where the root is responsible for scheduling by triggering waves. The root node maintains a list of transmitters for each slot and channel offset that is available for allocation. However, it underestimate the interfering nodes using the same offsets in the slotframe. This algorithms introduces a wave of control overheads which rapidly accelerate radio activities in the network.

Duy et al., [19] presented an Enhanced SF0 (ESF0). The proposal use the '*best portioning'* approach. According to this, it divides the slotframe length into a number of equal-sized portions corresponding to the size of the Tx buffer. Each portion then maintain a density value relating to the maximum number of free slots in the portion. The slots are selected randomly out of each portion where probability of collision is a non-zero value. To avoid simultaneous channel-access, the author introduced a channel-change algorithm that randomly switch the channel to avoid packet loss. For this reason, it continuously monitors the link quality to detect collision on specific channels. When a channel exhibits sustained interferences it is flagged for potential replacement. However, packets are dropped under challenging traffic scenarios because dedicated slots are limited and ESF0 does not adapt traffic dynamically. ESFO is also criticized for inadequate portioning of the slotframe as it does not add up to a process where some nodes are given higher slots than the others. In fact the schedule allocation is same as OTF where it uses a lower threshold.

Prieto et al., [131] is another threshold-based scheduling function inspired by Proportional-Integral-Derivative (PID) controller. PiD controller is a widely used feedback control mechanism in automation and engineering, especially in systems that require precise control, such as industrial machinery, robotics, and temperature regulation. In the context of 6TiSCH scheduling, the author incorporated this mechanism to calculates an error value as a difference between actual traffic and expected traffic, and adjusts allocation of cells based on the error rate over time. While, it led to improved resilience, the algorithm does not provide an interference-free communication over given channels [195]. This is because of interference arising due to overlapping with channels between 6TiSCH network and other networks such as Wi-Fi 802.11 [164]. In addition, monitoring queue conditions actively incurs a trade-off with energy consumption and transparent allocation [195].

Wang et al., [238] proposed Enhanced Distributed Scheduling Function (EDSF), which focuses on cell selection based on the transmission capability assigned by EDSF on per cell-basis by using the stored 6Top statistics. This is another way of predicting traffic through the slotframe [195]. EDSF uses PDR as link metrics to assign a transmission probability value per cell. EDSF relies on dedicated cells for both managing traffic and network topology. Hence collision can still occur due to poor synchronization with two nodes accessing the same cells during high slotframe occupancy. EDSF therefore requires a more frequent housekeeping to avoid network bottlenecks in terms of challenging traffic conditions. The author [238] did not test scalability for dense and larger networks.

3.2.2.2. Broadcast-based Scheduling Algorithms

6TiSCH offers an open access plan [194] to replace wired-like connectivity with a densely populated multi-hop IPv6 WSN. This is achieved by using Decentralized, Broadcast-based Scheduler (DeBRaS) [239]. It ,by default, offers an improved propagation as single broadcast cell wasn't enough for a network-wide coverage [239] and poor propagation means fewer routes to the destination. However, collision can occur frequently under DeBRaS-led operation due to clock drift [18]. If this happens, the network will not collapse straight-away instead it will show packet loss to a greater extent. The key limitation of DeBRaS-based solutions is that when more broadcast cells are added, nodes rapidly consume battery current [239], leading to a shorter battery life. Currently, energy consumption is an open issue [239]. For the sake of preventing rapid battery drain, *Municio et al.,* [239] has come up with an optimal limit (3 cells). Many contributions are observed under this category:

Accettura et al., [240] proposed Decentralized Traffic Aware Scheduling Algorithm in 6TiSCH Networks (DeTAS). DeTAS is an extension of TASA (a centralized SF). It introduced a unique approach towards traffic management whereby each node must observe the even-numbered slot for outgoing traffic and odd-numbered slot for incoming traffic, making important distinction between oncoming and relaying traffic. In DeTAS, traffic bursts are generated locally, while packets are upstreamed through DeBRaS scheduler. This reduces dependency on root. However, DeTAS faces criticism due to high volume of collided cells and superior volume of overheads, which stem from insufficient gaps between transmission slots. Consequently, overlapping prevails within frequencies due to congestion, triggered by adding more devices to the network; hence DeTAS is an effective solution for smaller to medium-sized networks with lower traffic volumes [241].

Soua et al., [242] proposed Distributed Scheduling Converge cast in multichannel Wireless Sensor Networks' (DISCA), an improved version of '*Wave*' [237]. DISCA is a lock-based scheduling approach [18] which computes node's schedule locally (using negotiation-based scheduling). This algorithm follows a step by step iterative scheduling process: the sender has to notify its interfering neighbors through a *cellist,* maintained by sender so that it can select a particular Tx and Rx slot, locked in the neighborhood. It does so to avoid any conflict of interest between nodes. To avoid collision, it uses flooding techniques while making a reservation to a particular cell bundle. The key limitation of DISCA is that it underestimates the conflicting neighbors under broadcast-based scheduling scenarios in the working slotframe, and compensates throughput [243].

Aijaz & Raza. [241] proposed a Decentralized Adaptive Multi-Hop Scheduling Protocol for 6TiSCH Wireless Networks (DeAMON). It is a decentralized, broadcast-based scheduling algorithm that uses a data-centric query. The query is broadcasted in the network ensuring that the payload (traffic) is forwarded in advance. This SF supports both MP2P and P2MP mode of RPL operation. The evaluation of the SF confirms that it is reliable and efficient solution for mobile-friendly networks. However it registered shortcomings in terms of poor propagation: the query to reach the distant nodes incurs a high volume of signaling overheads. This thesis follow the RPL-based routing that is as per the non-storing MoPs where path to destination is provided by the root before the nodes make their journey downwards in the routing hierarchy. DeAMON is an expensive SF for a densely populated network which consumes a large proportion of bandwidth, leading to fewer collision-free cells for other nodes [229].

Kralevska et al., [21] proposes a graph-based approach that organizes the routing topology into a graph enforcing *G= {VE}* where *V* represents the set of nodes and *E* the connecting edges. While the graph theory may still be seen as complex, these are amongst the best performing approaches exploiting multipath delivery.

Local Voting divides traffic load equally amongst the nodes to perform load balancing. It does so to minimize the peaked latency by simply monitoring queue length (number of packets in queue) of the parent node; that is to monitor associated links with a parent node. It gives an estimate of packets in buffer of each node and if the load is unequal, it adds or delete cells based on the connecting edges (E). Packets take multiple path while reaching the root as the ultimate destination. Generally, the queue length for all nodes is set to 100 packets: each node maintains an extended Tx buffer [40].

Theoretically, queue balancing contributes to improved resilience, and shorter delay. The author of LV [21] did not specify an overprovisioning limit dealing with uncertain traffic (overprovisioning). In the extended version of LV [244], the author proposed a fixed threshold-based overprovisioning limit (the assumed maximum limit is 10 cells). The algorithm can add cells whenever requested by the nodes. However, neither version of LV is scalable as the pre-estimated load sharing provides no concessions toward optimizing bandwidth consumption (it is evident with LV's reaction to changing topologies in Chapter 6). Additionally; it uses unreliable, and poor links, which may have been present in the routing topology causing a longer path and a higher latency.

Righetti et al., [245] proposed an Extension of OTF (E-OTF). It is used in both unicast and broadcast-based scheduling operations. E-OTF, instead of allocating cells to an individual nodes, it uses links, that translate in to a combination of nodes. The algorithm schedule cells per link-basis which translates the traffic prediction along the root in advance. While taking into account the factors like each node's duty-cycle (with respect to the slot occupancy), and queue status with congestion bonus, the author poorly defines these measures necessary to address temporary peaks of traffic along to the root. Apart from these, E-OTF does not scan the unrealistic links while making reservation of cells along the root.

Wang and Fapojuwo [246] proposed Hysteresis-Free-OTF (HF-OTF), a decentralized and broadcast-based solution using OTF without any fixed threshold limit (to meet traffic demand in the network); it autonomously compute overprovisioning cells per node-basis, however, the proposal monitors queue occupancy to predict cells required by a node to successfully dispatch its payload. HF-OTF is not as popular as OTF or E-OTF where it inherits the common shortcomings in terms of energy-efficiency because the charge consumption does not shift significantly even though it is allowing a fewer cells to some nodes than the others.

3.2.3. Hybrid Scheduling Functions

Hybrid scheduling incorporates more than one scheduling designs towards solving a novel problem. It allows each scheduler to maximize it's competitive advantages (something that it is has been proven worthy for); The autonomous scheduler offers a competitive advantage in terms of reducing overheads. This includes EBs and routing beacons). On the other hand, the negotiation-based decentralized scheduler performs traffic adaption efficiently. These algorithms are reviewed under this category:

Morell et al., [247] proposed an idea of using Generalized Multiprotocol Label Switching (GMPLS) for TSCH scheduling networks; the standard protocol (RFC 4328) [248] augments Multiprotocol Label Switching (MPLS) to support 6TiSCH scheduling. The proposed SF divides the slotframe to manages network schedule and cell reservation separately as there are different labels for data packets and control packets available for reservation, which takes place per link basis. The author used Resource Reservation Protocol-Traffic Engineering (RSVP-TE) [249] for managing reservation of cells per node where LSP (label switched path) are installed to connect nodes in the network. Each LSP is pre-configured in the network where connected nodes are tagged with a label based on the switching rules of LSPs.

A label is comprised of time slot and channel id forming a TSCH cell and the cell or label has association with link metrics following the node. GMPLS uses this information for managing labels where it can detect the weak and unrealistic links in the network ensuring the success or failure of LSP-based transmission in advance. Notably, RSVP-TE protocol is expensive and it generates a high volume of signaling overheads towards reservation where in the algorithm it is used alongside the label distribution mechanism provided by GMPLS.

In term of collision, the probability of this happening is low as each path translates into a unique time slots and frequencies, for example, if node A is 2 hops away to node C and the node C is 2 hops away from node D, The GMPLS processes time slots as labels that increase chronologically from Node A to Node B and Node B to Node C. The path from Node D to Node E and Node E to Node C uses a higher time slots chronologically that way each label represents a series of cells that are preconfigured. As far as the drawbacks of this approach is concerned, it uses a set of fixed labels with a complex scheduling design, triggering a high volume of signaling overheads in relaying the traffic. The proposed solution has been tested with over 25 nodes only and the impact of traffic condition is analytically modelled by the author, so there are no further evidences available for this being a scalable solution for a densely populated network. Additionally, it assumes a static topology where LSPs are pre-computed ensuring symmetrical bidirectional flow.

Duaquennoy et al., [228] proposed *Orchestra*, which uses an all time active (autonomous) slot, computed on per node basis. As negotiations are expensive, the autonomous cells are allocated to the nodes based on Tx and Rx traffic. Currently, it is a much preferred approach for managing network dynamics for a load-sensitive IPv6 subnet, extended by a number of approaches including the MSF itself [250]. However, there are some common weaknesses of this solution that disqualifies it for the industrial operation where energy-efficiency, and acceptable low latency is a critical requirement [251]. Orchestra is radically different solution compared to centralized and negotiation-based SFs and it has a broader scope (beyond this thesis) since some of its extensions are well aligned with the *Storing* MoPs where the nodes are using reactive routing.

Pratama et al., [252] proposed a Reinforced Learning (RL)-based SF which is a machine-learning solution designed to maximize communication performance through many outcomes. It extends the autonomous-based TSCH scheduling design where RL-SF studies the Tx slots with the lowest transmission failure rate and select only those slots with a high PDR for the next series of packet to transmit. The solution monitors the pre-computed cells, continuously active in every slotframe, whether it is used as a Tx or Rx cell is not relevant. The Q-leaning algorithm that it uses demands the accuracy of previously used slots (communication exchanges) and that way it assumes a fairly static network conditions, ignoring the sudden changes in traffic conditions based node's displacement in routing table and parent-change which triggers relocation of the entire cell bundle [195]. Apart from that RL-SF is not an energy-efficient solution [195].

Chang et al., [117] proposed MSF (RFC 9033) that adopts autonomous slots with state-of-art OTF (a unicast-based distributed SF that uses a fixed threshold-based overprovisioning limit). MSF is not sufficiently scalable for large-scale networks and neither has it satisfied the key QoS considerations of the 6TiSCH network unanimously (latency, reliability, battery performance, etc.). It has been thoroughly studies in Section 3.1.4.

Chang et al., [253] extends MSF to addresses traffic adaption scenario by proposing a strategy that can add or remove multiple cells simultaneously. This leads to minimum delay as 6Top exchanges are fairly bulky and sometimes communication fails when these are taking unexpectedly higher time, causing radio to force stop the process. With more cells added at the same time, demanding nodes are relieved from triggering frequent request for addition or deletion of a cell unless the estimate is biased. This proposal provides key recommendation in terms of tuning the application traffic based on the adaption delay, represented by MAX_NUMCELLS in MSF (refer to chapter 5 where these acronyms are frequently used). Notably, AMSF for bursty traffic proposes MAX_NUMCELLS= 4 and for steady traffic, the delay must equal to 32 cells (MAX_NUMCELLS= 32). These limits, once declared, do not interpolate over run time; hence scheduler follows these limits throughput the time, causing mismatch against actual traffic, which is difficult to predict in the dynamic topology (It is evident in chapter 5 where the impact of fixed adaptation delay over periodic traffic is not advantageous). Clearly, a fixed threshold does not provide any advantage.

Hamza and Kaddoum [254] proposed Enhanced Minimal Scheduling Function (EMSF) which is yet another extension of MSF **incorporated** *Poisson* distribution for traffic prediction. It predicts amount of traffic generated in the network of *n* nodes based on the previous estimates of slotframe (packets generated by each nodes per slotframe). By assuming that all links are symmetrical, the nodes are generating packets on event-based with randomness applied, the value of number of slotframe to be taken in account prior aggregation and before the algorithm executes could predict the accurate volume of packet that a node may experience (β) is custom-defined. The simulation-based experimentation assumed β=10. The author also defined periodic traffic generation mode where the connected nodes generate traffic at a certain time slots, acquired through enhanced beacons. For robustness of results, it integrates both periodic and event-based as combined throughput. The challenges with this learning-based algorithms is that when queue monitoring is ignored, the prediction-based model to learn about the traffic through aggregated statistics over a certain slotframes can only take from 10- 100 slotframe cycle where the network *worm up* period can vary; this can potentially mislead the actual traffic that an individual node may experience in a dynamic network topology if worm time is shorter [195]. The overprovisioning can take place violating the half-duplexity constraint, necessary to avoid instant packet loss. EMSF contributes towards significant overheads reduction, however it is not a scalable solution.

Tapadar et al., [255] proposed IMSF, aimed to achieve slotframe optimization by monitoring queue occupancy per node-basis. Based on this near-accurate estimate, this SF predicts the traffic volume expected against the cells needed for nodes. Here, queue-monitoring is a resource-intensive process that triggers control overheads, separate from the routing beacons. The results indicates that IMSF triggers fewer 6P transactions by adhering a transparent allocation plan but it is not scalable considering a large-scale operation. The reason is that some nodes may experience a temporary surge in traffic volume and IMSF does not use overprovisioning, necessary as an alternative allocation plan.

Tanaka et al., [256] proposed YSF as an extension of MSF with regards to reducing the latency. It followed a top-down allocation of cells to minimize latency, however, it alone does not solve the traffic adaption which is an open issue with MSF. By providing slots close by in the slotframe the proposal can lead to collision due to high traffic loads; hence, more work is needed to make sure that YSF to remain reliable with varying load-sensitivity under a large-scale industrial network.

Kim et al., [257] proposed Autonomous Link-based Cell Scheduling (ALICE) which performed allocation of cells on a link-basis. By doing so, it surpassed the performance of *Orchestra* significantly. In terms of traffic adaption, ALICE assesses traffic conditions based-on the changes happened in routing topology and that way by it finds a sub-optimal number by which it allows a node to add or delete extra cells in line with the demand, however, how many cells are sufficient is not defined by ALICE. Clearly, traffic conditions are difficult to be judged in the dynamic topology especially with higher load-sensitivity where this approach suffers from poor reliability under variable traffic conditions due to the pre-allocation [258].

Righetti et al., [226] proposed Autonomous Link-based Cell Scheduling-Frame Pending (ALICE-FP), which is an extension to ALICE. This solution provides nodes to exchange their *frame pending* bit (it is mostly unused throughout the MAC frame) to address requirement to add or delete more cells meeting traffic demands on the corresponding nodes especially those carrying more traffic from the sending nodes (relay nodes). The proposal employed the *piggybacked* technique and is not completely an overhead-free solution. Apart from this, it lacks efficient traffic adaption despite assisting nodes which experience peaks of traffic. The piggybacked technique is further exploited by other SFs addressing a temporary peak of the traffic; this technique is less complex than performing recurrent negotiations.

Jeong et al., [258] proposed Traffic Aware Elastic Slotframe Adjustment **(TESLA),** which further exploited *piggybacked* technique. TESLA uses a receiver-based mode of *orchestra* with adjustments in the slotframe based on incoming traffic: each node exchanges control packets and transmit packets to the next hop neighbor. The cells are added based on the piggybacked mechanism attached to the data stream. The downside is that this approach is not an overhead-free approach; the autonomous scheduling algorithms has utilized this alongside the negotiation-based approaches using the 6top layer or 6P protocol [219].

Tanaka et al., [259] extended MSF in the context of reducing a joining delay. The author called it SF-Fastboot and it is inspired by MSF. This solution exploits the asymmetry between the root and industrial sensors following the *SmartMesh IP* design [260], allowing different beacon interval for different nodes. SF-Fastboot is implemented at root because nodes do not have sufficient storage and processing capabilities required for the execution of this algorithm. The overheads generated at root are ignored because root is assumed to be a powered device.

According to this algorithm, a joining node will hear more frequently from root as it is given a higher priority towards frequent beaconing, allowing nodes to decipher DIOs sent and reverted back using DIS messages sent by the nodes. The DIS beacons are further categorized into unicast and broadcast mode of operation whereby an unicast DIS is sent as response to DIO received and the broadcast DIS is sent to reset the *trickle timer* informing about some inconsistencies in the network.

SF-Fastboot faces notable challenges in network management as it scales up to 100 nodes; more specifically, with the trickle time mechanism of RPL. 6TiSCH operates on ISM 2.4GHz band with limited bandwidth where an heavy influx of DIOs in the network can risk available broadcast channels to be overlapping. If this SF uses broadcast cells to propagate DIOs, the scalability depends on how many of these cells are allocated in the slotframe as nodes often require sufficient resources to respond using DIS messages whereby a frequent unicast transmissions necessitate cells to be frequently added and removed (upholding the frequency-diversity), causing limited throughout due to straining link-layer resources.

As additional nodes are allowed to join the network using the unicast beacons, the joining can take longer and the opposite is assumed in the case of broadcast-based joining. Further, the broadcast-based is prone to frequency overlapping where collision is likely to occur when the joined nodes starts sending packets subsequently after the radio is turned on, could lead to early packet-loss due to insufficient link probing. The risk of packet loss is more pronounced at the early stages of network formation, which is further exacerbated by SF-Fastboot. This SF faces limitations in terms of resource consumption and network scalability.

SF name	Description	Reliability	Latency	Energy efficiency	Scalability
TASA [230]	• Synchronized end-nodes with one-hop alignment [230]. • Slotframe maintenance with color-matched traffic.	• Reliable for 30-50 nodes [230]. • High collision risk and buffer congestion in large networks. • Registers packet loss beyond 100 nodes [23].	• Latency fluctuates with high traffic and poor buffer utilization [18]. • One- hop access. • Poor load sharing lead to higher latency delay.	• High consumption due to frequent reconfiguration. • Using dedicated cells. • High signaling overheads to adapt traffic. • Frequent battery replacement	• Poor scalability for large networks and multiple sinks [23]. • Frequent signaling leads to high control overheads. • Poor bandwidth utilization
QSS [231]	• Broadcast-based, Centralized SF. • Slotframe divided into rings (stratum), cells shared across rings. • Multi-path propagation, alternative paths for nodes.	• Prone to collision under heavy traffic due to inappropriate slotframe partitioning [18]. • Risk of collision across different rings • Reliability affected by heavy traffic and signaling overheads [231].	• Latency Increases under heavy traffic due to high signaling overheads [226]. • Evaluation tool used does not accurately model EIs as it may have impact on latency.	• High cell consumption [226] • Increased retransmission cost. • Frequent housekeeping and signaling overhead. • Not an energy-efficient SF.	• Scalable with lightweight traffic. • High overhead limits node longevity. • Frequent interference from neighbors. • Evaluation tool does not model EI accurately.
PCE-Based scheduling [232]	• Seeks linear relation between RPL topology & slotframe occupancy. • Schedule computed by root node using path elements.	• Reliable for medium-sized networks (30-50 nodes). • Poor neighbor discovery under subnet interactions [233]. • Slotframe compactness. • Random channel allocation [233].	• Optimal routing path provided by controller. • Latency fluctuates with traffic load. • Impact of EI not known on latency. • Lower acceptable Latency under medium sized subnet.	• High signaling overhead due to lack of self-healing [233]. • Poor awareness of link stability causes idle listening [233]. • EI impact unknown as default random channel allocation is used.	• Supports multiple sinks: limited scalability beyond single subnet [233]. • Packet loss is likely due to asymmetrical links. • Not suitable for dynamic topology [233].
Huyun et al., 2017 [233]	• Extension of PCE-based scheduling ADP for traffic adaption [233]. • channel selection based on Markovian model. • Traffic-aware scheduling approach	• Benefitted from optimal path and slotframe compactness. • Channel-selection to improve adaption of traffic for dynamic topology. • Radio is pre-programmed and it turns on frequently due to high overhead.	• Impact of EI not known on latency. • Latency fluctuates depending on the availability of queue space for new packets • Collision from nearby nodes under high traffic conditions under sparse deployment.	• Frequent 6Top request to add and delete cells by nodes • High routing and signaling overheads making frequent radio activities. • The impact of EI from other networks unknown.	• Imposes scalability concerns beyond 40 nodes [233]. • Not suitable for dynamic topology [233].. • Assumes a fairly static topology in terms of cell allocation.

	• Use PCE- to compute optimal cells against predicted traffic.	• Failed to meet theoretical optimum predicting traffic accurately.		• No over provisioning of cells due to being traffic aware.	• Flexible to be used across more than one subnets with no guaranteed packet delivery.
SF0 [261]	• Distributed SFs, allocating cells based on link PDR. • Node-based cell allocation. • Randomized cell selection. • Cells are allocated using negotiation between nodes.	• Scheduling performed locally. • PDR upheld to be over 50%. • No extra cells to nodes. • Random time slot and channel does not guarantee a collision-free schedule. • Improved bandwidth utilization. • Can detect *unrealistic links* [18].	• Latency increased with increased traffic. • Extended hop distance with lower volume of cells, leading to higher latency [20]. • Node to get all fragment before forwarding the payload next hop, triggers additional delay. • Poor Traffic smoother (50-50) between oncoming and outgoing packets.	• Lower cell consumption • All scheduling and network beaconing carried out over dedicated cells. • Increased retransmission cost. • Monitoring link-metric triggers overheads. • Idle listening [236]. • Frequent cell assignments [236].	• Poor queue utilization as no extra cells provided to deal with bursty traffic. • Incurs performance trade-offs with latency. • Stable performance under steady traffic as more nodes added to the network. • Network collapses due to high collision under heavy traffic burst.
OTF [20]	• Extension of SF0 • Generic solution with various implementations. • Distributed negotiation-based scheduling • testbed available across dedicated and shared cells implementation.	• A fixed threshold to misjudge actual traffic. • No link metric monitoring; cannot detect weak nodes enroute. • Triggers idle-listening [236]. • Packet loss due to high bandwidth usage, fewer routes, congestion, and retry exhaustion [20].	• Latency vs. reliability trade-off in large-scale setups with dedicated cells. • Distant nodes trigger reconfigurations, causing quick battery drain. • Latency varies with OTF overprovisioning levels. • On-the-fly cell allocation adds delays.	• Battery consumption follows linear pattern with cell consumption (See Chapter 4). • Low 6Top overhead with high volume of cells follows uniform distribution. • High 6Top overheads with lower threshold, requiring frequent cell allocation. • Dedicated cells are expensive, and Shared-cells trigger collision.	• Inefficient traffic adaption • Performance trade-offs with latency and reliability. • It inherit drawbacks of RPL based RSSI metrics. • Evaluation suggests varying level of resilience and packet loss under heavy traffic beyond 60 ppm, and as the network grows beyond 50 nodes.
LLSF [235]	• A daisy chained based time slot selection. • Distant slot from next slotframe	• Schedule allocation is same as OTF.	• Typically, latency fluctuates between 3-5s under adverse traffic condition in just 50 node networks.	• Recurrent wastage of cells attributed to high energy consumption.	• Network collapses due to frequent collisions in the network.

	• use pure dedicated cells in distributed fashion • randomized channel selection. • Unicast delivery	• High collision as slots are closer at one side of the slotframe. • Not reliable under heavy traffic conditions [236]. • Failing to add a low latency cost, or having low performing nodes can break the chain.	• Latency maintains trade-off with reliability and energy consumption. • Implementation with shared-cells is subject to addition contention delay.	• Does not check for unrealistic nodes along the root. • High 6top overheads • High cost of managing topology	• Suffer from packer loss under heavy traffic condition and longer path. • Not scalable [195]. • Poor load balancing, • Simulation-based results do not predict interference.
ReSF [236]	• Reserves cells in advance to each link using traffic manager. • Queue-aware SFs • Link-based scheduling using series of dedicated cells.	• Pronounced delivery of packets in advance. • Improved reliability over 67 nodes using 12 packers per minute [236]. • Monitoring overheads, • Traffic manager considers unrealistic links on the way. • Overlooks collision	• Entire-path is reserved in advanced using the model. • Latency fluctuates under heavy traffic load. • Impact of EI unknown • The Traffic Engineering (TE) model does not include real-time and sudden changes in the topology and that way it ignores a low link cost.	• Resolved recurrent wastage problem. • Energy consumption is roughly same as SF0 for larger networks. • High control overheads towards monitoring queue status. • Use dedicated cells for both managing data traffic and network topology.	• Simulator used in the experiment does not model EI accurately. • Not sufficiently scalable as scarcity of cells can not only impeded sustainability but also results in severe packet loss. • Failed to address heavy traffic periodic traffic witnessed by a node.
Wave [237]	• Slotframe fragmentation into waves. • Root decided when each node is to be awake for transmission or reception. • PCE-used for selecting optimal path [237]. • Traffic-aware SF	• Nodes periodically receive beacons to activate radio for transmission; scheduling is critical if links are unstable, as distant nodes may miss timely beacons [237]. • Collisions may occur from nearby nodes, unaware of potential slot and channel conflicts.	• Low latency as long as there is no conflict [237]. • Impact of EI is unknown as the nodes are assumed to be operating in sparse-meshed network. • Asymmetrical links, leading to higher latency under severe traffic conditions. • LBT-based channel selection triggers addition delay.	• High overheads as each node is required to be served with set of beacons by root [237]. • Under shared cells, consumption is significantly higher using unicast delivery links. • Impact from nearby Wi-Fi is not known over energy consumption using larger networks. • Not an energy-friendly SFs.	• More evidence needed as simulation results lack proof of scalability [229]. • Controller-led scheduling is scalable only with stable topology; long-term node survival isn't guaranteed [195]. • High cell collision rates as nodes dynamically seek shortest path to root.

ESF0 [19]	• Extension of SF0. • Divides slotframe into equal portion against queue size • Each portion maintains density value, the higher the better • Channel-change implemented separately	• Reliable than SF0, OTF, and ,several unicast based SFs, besides under less challenging traffic. • Inadequate portioning does not aid declining reliability due to cell shortage and poor queue utilization [18]. • Poor traffic adaption • Channel-change is crucial to avoid collision.	• Typically low with high volume of OTF threshold, and higher with low overprovisioning. • Fluctuates based on heavy-traffic load, and while slotframe is highly occupied. • Trade-off with reliability and it continues to behave like OTF from there on[15]. • Impact of EI is not known on latency.	• Low cell consumption • Low collisions • Poor bandwidth utilization • Improved energy savings than SF0, LLSF, OTF, and ReSF when RSSI is not lower than the given range (-97 an -101dBM). • Larger network may trigger high consumption where ESF0 follow uniform distribution.	• Reliable up to 100 nodes but has not been tested for worsening traffic conditions. • Portioning does not guarantee low latency or slotframe compactness. • Poor load balancing. • Lacks real-time testbed experimentation. • Poor traffic adaption
PiD-based [131]	• PiD controller which provides minimal optimized volume of cell per node using Error rate. • Implemented on top of OTF. Cell selection is same as OTF.	• Ignores collision and scanning of unrealistic links on the way to the root [15]. • Optimizes occupancy by nodes, as dedicated cells are limited. • Queue monitoring is compulsory to generates error rate using PiD algorithm [131]. • Reliability subject to traffic conditions.	• Low latency due to minimization of queuing delay. • The impact of challenging traffic in is unknown. • Delay caused by propagation across distant nodes. • Latency can fluctuates under heavy traffic but less likely cause cell outage. • Latency increases due to lack of overprovisioning.	• High signaling and negotiation-based overheads impede energy-saving. • It relies on actively monitoring of the TX buffer. • Low cell consumption. • Dedicated cells are limited where it used these cells for all kinds of traffic. • High complexity of the solution.	• Lacks standardization. • A complex mapping of traffic through buffer occupancy. • Analytically evaluated SFs, • Lacks efficient modelling of EI and collision between nodes [195]. • Poorly address change events in the routing topology. • Poor propagation presents risk of synchronization.
EDSF [238]	• Predicts traffic by monitoring link statistics, based on TX probability. • Higher transmission success increases allocation of cells to nodes. • Does not allocate extra cells to nodes.	• Reliable for medium-sized networks under low traffic conditions F [238]. • Monitors cell stability in slotframe, detecting poor links on the way to root. • Impact of EI is overlooked.	• Latency fluctuates based on traffic load. • Cells with high Transmission ability can produce lower minimal latency besides dedicated cells are not enough for large-scale operation • Not an latency-friendly SFF [238].	• Same as SF0, • Evaluation is led by an older version of the 6TiSCH simulator which does not model EI accurately hence actual battery consumption estimate over long duration is needed to reach any estimate.	• EDSF's impact on scalability is unclear, as testing involved only a limited number of nodes and low packet volume • Unreliable for large networks requiring high bandwidth. • Lacks specification for handling temporary bursts.

		• Packet loss can take place due to scarcity of cells with good Tx probability.		• Low overheads as it solely depend on cell‘s TX assessment.	• Lack testbed evaluation as the solution is based on link stability.
Municio and Latre [239]	• DeBRaS scheduling using SF0 for schedule adaption. • Random cell selection. • All nodes use a common TX buffer which is 100 packet [239]. • Cells reservation performed locally within the hierarchy.	• Reliable up to 100 nodes under challenging traffic. • Packet loss and congestion during bootstrapping. • Collision due to conflict of interest between nodes. • Aggressive slotframe utilization [239]. • contention-access at local level. • Impact of EIs is unknown for dense network.	• Packet assembly hop-by hop causes delay as the node do not relay packets until all fragments are received. • Latency is high in the beginning due to congestion and then it remains flattened, depending on traffic conditions [239]. • Shared cells are deterministic and may cause delay in forwarding payload to next available hop.	• Extremely higher as most SFs under this category use at least 3 broadcast cells for efficient propagation. • High consumption [239]. • High 6Top overheads due to high rank-churn [239]. • Impact of EI is not known. • High volume of collision hence housekeeping in slotframe is frequently required.	• Scalable but risk a short lived network [195]. • Behaves like a smart mesh IP networks with hundreds of meters of bidirectional coverage. • High rank-churn and a highly flexible topology with tight synchronization [242]. • Ideal with powered batteries and increased buffer size.
DeTAS [240]	• Extension of TASA. • Using even and odd to distinguish traffic. • Slotframe utilization DeBRaS scheduler.	• Improved reliability compared to TASA. • Frequent reconfigurations [240]. • packet loss due to temporary peak of the traffic on nodes [240]. • High collisions [240].	• latency increases as per traffic load and network density [240]. • Shared cells are accessed on contention-based [240]. • Housekeeping delay. • Frequent collision in shared cells. • Requires higher TX buffer.	• Inherits common drawback of DeBRaS-led scheduler. • High 6top overheads. • Impact of EI not evaluated. • Retransmission cost attributed to frequent collisions.	• Poorly scalable and risks a short lived network. • Propagation leads to heavy toll of EBs generation. • Ideal for large-scale network where batteries can last long. • Other solutions can offer better performance.
DISCA [242]	• Extension of *wave* [242] • DeBRaS scheduler. • Controlled flooding to avoid conflict of interest • Negotiation-based Distributed scheduling. • Priority-led forwarding.	• High reliability under regular traffic [242]. • Poorly estimate the conflicting nodes within the network [195]. • Shared cells are indeterministic [240]. • Complex scheduling to meet variable traffic demands [195].	• latency, subject to traffic load/congestion. • Shared cells are accessed on contention-basis. • Frequent reconfigurations [241]. • High control overheads. • Collision triggers retransmission, adding to congestion.	• Not an energy friendly SFs, • Produces a high volume of overheads due to multiple broadcast cells. • Impact of EI unknowns. • Sub-optimal traffic adaption triggering frequent 6Top requests. • Retransmission cost.	• Poorly scalable due to high volume of overheads • High congested slotframe • Risk a short-lived network. • Other approaches such as [241] offers improved resource usage.

					• Further evaluation required using testbed.
DeAMON [241]	• Extension of DISCA. • Query forwarding-based scheduling [241]. • Using distributed and decentralized scheduler, • Can address downward scheduling traffic including P2P [241].	• Poor assessment of conflicting nodes as query advertisement slows down across distant nodes. • Query propagation incurs delay and overheads. • Implementation using *storing MoPs.* • Path is reserved in advance using query-propagation.	• Latency subject to successful reaching out of propagated beacons across the depth of the network. • Poor assessment of conflicting neighbors • Contention-access delay. • On demand probing of path attributed to increased delay.	• High signaling overheads [241]. • Generally, high in DeBRaS scheduling implementations, • Controlled 6Top transaction. • Use RPL's storing MoPs which is sensitive to existing challenges in 6TiSCH network [241]. • Retransmission caused by collision, triggered by poor query forwarding.	• Risk a shortly lived network • Query propagation is poor across the leaf nodes • Generates superior volume of control overheads. • An expensive SF under non-storing MoPs [229]. • Primitive channel-access as poorly synchronized node can collide over same RF.
LV [21]	• A load balancing SF for low latency. • graph-based scheduling • schedule is locally computed by allowing participation from nodes. • Initially, it does not offer overprovisioning. • Use higher buffer capacity.	• Reliability suffers from equal distribution of packets without any extra cells given. • A high volume of collided cells. • risk buffer overflow with amount of 6Top overheads generated. • Packet loss occurs under challenging traffic condition is not the only jitter here.	• Latency is generally high due lack of overprovisioning and equal distribution of traffic. • Packets are taking unnecessary longer path as a result, causes limited-rank churn (see Chapter 6). • Delivers packet at delay even with less congested buffer of nodes. Packet assembly is subject FIFO. • Impact of EIs not evaluated.	• It does not add no new cells to the nodes unless the available cells are less than the required cells. • Limited control messages. • High 6Top transaction for adding cells frequently. • High consumption is due to DeBRaS-based operation which is using minimum of 3 broadcast cells.	• The latter version provides bandwidth reservation. • Efficiently manages traffic through queue and allow faster delivery of packets. • Suffers from collided cells • The latter version is threshold-based, allocating extra cells out of maximum OTF threshold limit.
E-OTF [245]	• Extension of OTF using DeBRaS scheduler. • Link-based scheduling • End-to-end path reservation. • Assumes symmetric path from node to destination.	• Traffic adaption is derived from slot usage, and congestion bonus (see Chapter 6). • E-OTF uses hysteresis similar to OTF which over and under-estimates the bandwidth allocation.	• Typically, the latency is recorded low by E-OTF but can vary based on threshold used, and as per traffic conditions. • Impact of EIs not evaluated. • Latency is lower for the higher threshold limit and opposite is considered with lower limit under heavy traffic conditions.	• Consumes a slightly less volume of cells using base-line threshold of 0 cells. • Use more than one broadcast cell. • It too is not an energy-friendly solution provided DeBRaS-led scheduler.	• Complex process to find an optimal threshold for application as it incurs trade-off with latency and reliability. • Reliable than most DeBRaS led SFs.

		• Yet a reliable and superior solution than LV, and existing decentralized SFs		• A high volume of 6Top transaction recorded with low threshold limit.	• Not sufficiently scalable without overprovisioning (see chapter 6).
HF-OTF [246]	• Extended version of OTF. • Uses queue monitoring instead for accuracy of traffic prediction. • Maintain TX success rate for each cell to avoid poor performing links [246]. • Hysteresis-free SFs	• High reliability in a smartmesh Ip like network, maintaining several path for traffic to be forwarded. • Impact of EI is not known as the solution is evaluated using simulation. • Suffers from high collisions across shared medium.	• Latency is subject to traffic conditions, and contention-access. • Triggers frequent 6Top transaction to meet traffic demand. • Subject to deployment conditions. • Further evaluation requires using testbed as the algorithm does not consider scalability as key requirement.	• Triggers a high volume of monitoring overheads. • Energy-consumption does not shift so significantly compared to E-OTF or other related SFs because of DeBRaS based operation. • Not an energy-friendly SFs , using cell status monitoring.	• Reliable depending on less challenging traffic conditions. • It does not unanimously meet all demands of the network such as latency, and reliability. • Expensive SF.. • Risk short-lived network.
Label-switching [247]	• Each traffic flow containing nodes on the way to destination is represented by a unique LSP. • It allows LSP based scheduling where each parent node is aware of cell requirement of the children.	• Only been tested with 25 nodes and no further evidence available today to prove this being a scalable solution • Follows LSP based control planes where data packets are treated with different labels. • A complex mechanism relying static LSP towards traffic mapping.	• Latency depending on the traffic conditions and impact of EI. • Latency is higher as the hop distance from root to node increases. • Currently tested in *sparse mesh IP* network within limited coverage. • Only tested with 25 nodes so far.	• The algorithm computes both link metrics : PDR and RSSI • Cell consumption is low as it is pre-computed using RSVP-TE with GMPLS being used to support switching between different traffic flows. • The colliding node will have increased inferences hence lead to poor *RSSI*. • High signalling overheads.	• High signaling overheads to relay traffic to root • Complex solution • Reliable for small network of 25 nodes [247]. • Fixed label assignment is suitable for static topology. • Evaluated using testbed-based experimentation. • Not scalable for larger networks due to poor bandwidth usage.
Orchestra [228]	• Single auto TX and RX cell, computed using a hash function[172]. • Nodes use this cell to transmit payload in connection-access manner. • Support storing MoPs .	• Reliable depends on routing MoPs as orchestra has been implemented with SFs using storing MoPs[172]. • Single cell for propagation of EBs[172].	• Latency is higher under normal traffic condition and it can further deteriorate depending on the traffic conditions[172] . • High contention delay • Latency fluctuates based on the distance from the root.	• No 6Top negotiations to meet traffic requirements on the fly. • Allocated autonomous cells are all time active. • Not an energy-friendly SF [172]. • Triggers Idle-listening [172].	• Low communication overheads[172]. • Poor reliability as the network size increases or traffic conditions are worse enough [250].

		• Poor traffic adaption using single auto cell			• Support storing mode (indeterministic networks).
RL-SF [252]	• Machine Learning-based solution [252]. • Q-learning based SF that relies on the performance of previous slotframe. • Feedback-based scheduling [252].	• It is not a suitable solution for dynamic topology where nodes change parents frequently [195]. • Poor traffic adaption. • It studies TX slots to lower failure rate [195].	• Lower contention-access delay since cells are active at most time. • Latency can increase depending on sudden event leading to temporary traffic on nodes [195]. • Impact of EIs unknown [195].	• Not an energy-efficient solution as the cell is continuously on for every transmission. • Idle listening. • High retransmission cost due to inconsistent pattern for scheduling [195].	• Pre-computed schedule to all nodes. • Lack testbed evaluation. • Not scalable for industrial networks as traffic conditions can be unpredictable [195].
MSF [250]	• Standard, generic solution recommended for 6TiSCH stack [250]. • Allocates one cell per node at a time [250]. • Random assignment of cells negotiated distributed slotframe. • Pre-computed schedule for managing topology [250]	• Poor propagation makes leaf nodes to frequently appear and disappear. • Poor traffic adaption like OTF [255]. • Lengthy 6top transaction. • An asymmetric path checked. • Poor fragment recovery [255]. • Problematic sequencing of packets in VRB buffer.	• Delay in adaption has significant impact on latency. • Increased latency due to Congestion, • Traffic adaption on RX leads to higher delay. • The delay in between RX and TX can influence latency. • Sub-optimal traffic adaption. • Fewer routes for nodes.	• Energy consumption varies upon MAX_NUMCELLS. • Hysteresis-laden SF that places several counters to monitors node's ability to deliver packets keeping autonomous cell busy. • Energy consumption does not shift significantly under low periodic traffic. • Triggers idle listening [253].	• Several inconsistencies in schedule [253]. • Prone to longer path under random deployment [255]. • Sub-optimal traffic adaption. • No tuning for adaption delay(MAX_NUMCELL) [253]. • Poor propagation risk synchronization, leading collision [195].
AMSF [253]	• Extension of MSF, deciding when should a node start traffic adaption [253]. • link metrics PDR checked node's efficiency [253]. • MAX_NUMCELLS = 4, for bursty traffic. • MAX_NUMCELLS = 32, for steady traffic.	• Packet loss due poor propagation [253]. • MAX_NUMCELLS = 4, does not benefit reliability under random deployment [253] (see chapter 5). • MAX_NUMCELLS = 32, triggers congestion, leading to packet loss anyway [253] (see chapter 5). • Unrealistic nodes checked on the way to root.	• Shorter the slotframe, the lower the latency [250]. • Contention-delay can increase latency. • Lower traffic adaption delay reduced latency significantly. • Average latency under heavy periodic traffic is higher than both SF0 and OTF [253]. • Gap between packets received and packet scheduled for transmission.	• No significant change in energy-savings than MSF. • Hysteresis-laden SF. • Energy consumption does not shift significantly under low periodic traffic. • Wastage of cells when nodes do not have any packet to send • Higher adaption delay causes frequent 6top transaction.	• Not scalable as it does not add more than 1 cells. • Poor estimate of traffic leads to several inconsistencies. • Poor propagation and lengthy node joining and synchronization. • Early packet adaption can negatively affect joining and synchronization delay [195].

	• Can add only 1 cell at a time.				
IMSF [255]	• Regarded as extension of MSF. • Monitors queue condition of each and every nodes to accurately predict traffic. • Does not use overprovisioning cells.	• Improved transparency over traffic conditions for a more regular traffic [195]. • Not responsive to frequent changes in routing topology. • No overprovisioning towards handling collided cells.	• Additional signaling required to monitor queue condition. • Fewer routing path as extra cells not provided for nodes to independently probe surroundings. • High latency due to no extra cells are provided to nodes	• Despite significant reduction in frequently occurring 6top , consumption does not shift significantly [255]. • Additional overheads turns radio on and off frequently to assess traffic.	• Not entirely a threshold-free approach [255]. • It does not provide extra cells, leading to a high influx of packets in Tx buffer. • Poor reliability as hundreds of nodes added to the subnet.
EMSF [254]	• Predict cells required per node using predictive learning based on *Poisson* distribution. • Use data aggregation. • Does not require queue monitoring.	• Poor knowledge of topology as nodes changes path frequently [255]. • Assume a symmetric link from root to node and node to root. • Threshold-based aggregation does not predict the influence of EIs.	• Latency varies depending on the size of slotframe [255]. • Fluctuates based on the traffic demands as EMSF does not use overprovisioning [255]. • Critical deployment where some nodes may not appear due to poor propagation [255].	• Low overheads [255]. • Energy-consumption does not shift significantly due to several active slots configured using pseudo random sequence [255]. • Poor duty-cycle utilization as traffic is pre-computed on nodes [195].	• Poor traffic adaptions risk packet loss [195]. • Risk synchronization due to poor propagation [195]. • Ignores low performing nodes leading to asymmetric path to root [195].
YSF [256]	• The focus is on cell-selection to minimize latency and allow faster transmission as soon as packet enters queue. • Uses same hysteresis as used for MSF for traffic adaption.	• Ignores traffic adaption , and it is same as MSF. • Provokes collision under heavy traffic conditions. • Provide a compact topology [229].	• Higher contention-access delay since nodes are allocated cells closer together. • Latency may register increase under high slotframe occupancy • Impact of on Packet assembly through VRB is inconclusive.	• Energy-consumption is same as MSF. • Autonomous cells are all time active. • High volume of 6Top mulling the slotframe compactness [195].	• As slots are assigned adjacent to each other, that is nodes are in closer vicinity risks. • On ground link-stability unknown . • Simulation-based experimentation.
ALICE [257]	• Extension of orchestra which uses link-based allocation [257]. • Nodes are given a pre-computed schedule	• Orchestra-like scheduling, allowing more cells to meet heavy steady traffic per link, • Poor ability to predict changing patterns to adjust the cells [226].	• With high volume of cells, the latency reduces, depending on the traffic conditions. • Links can be asymmetric in large network [226].	• Accelerated cell consumption as more cells are added per link [226]. • Increased retransmissions. • Follows a static schedule and ignore change events.	• Traffic demand may shift in the network. • Not scalable • Not an adaptive approach.

	• Adapt schedule in advance [257].	• Cells is pre-computed [257].	• Latency subject to contention-delay [226].	• Reduced overheads [257].	• Channel conditions not assessed as more nodes are added [257].
ALICE-FP [226]	• Is an extension of ALICE [226]. • Utilize frame-pending bit a 1 byte long counter to detect the extra traffic on the node [226]. • Does not use dedicated cell.	• Traffic adaption as per frame-pending bit. • Extra autonomous cells added using piggyback bits per data frame [229]. • Packets are reliably upstreamed to root.	• Latency fluctuates depending on the link length where a short path registers lower latency [229]. • Added Jitters as FP, causing extra delay on selective nodes. • Delay triggered by change events [229].	• All time monitoring of FP attached to each packet. • Shared cells consume most energy. • Fewer overheads while exchanging FP. • Not an overhead-free solution [222].	• Adaptive traffic-flow predicting sudden change accurately using FP [229]. • Failed to meet bandwidth demand without a compromise. • Collision due to nodes in interference range [170].
TESLA [258]	• Extended orchestra using RX-based allocation [258]. • It adjusts the size of slotframe on the fly [258]. • Employed pending bits to meet traffic adaption.	• Monitoring each and every node for traffic patterns [258]. • It uses autonomous cells for exchange messaging where it fails to add more than one cells to adapt traffic [195].	• Average latency can vary depending on traffic conditions [229]. • Contention-access delay on selective node, can further drive latency up to several seconds [195].	• Heavy influx of control packets in the network. • High cost of beaconing to keep the network operation. • Energy consumption does not shift significantly [258].	• Not sufficiently scalable under challenging traffic conditions [195]. • Does not evaluate collision in the slotframe • Poor propagation can risks synchronization [195].
SF-Fastboot [259]	• Is designed to reduce network formation time. • Extends *SmartMesh IP* design using unicast and broadcast beaconing. • It uses extra beaconing by root t allow nodes to FastTrack joining.	• Packet loss during worm up time. • Nodes triggers interaction straight after joining, causing congestion. • Ignores the buffer condition of nodes, and bandwidth utilization.	• Lower joining delay, though, is not representative of the delay caused by MSF. • Increased contention-access delay in the beginning causes a superior latency.	• An increased influx of DIOs and DIS lead to a increased consumption. • Consumption vary based on configuration and deployment setting. • SmartMesh trigger several connections in the network.	• The impact of EI unknown. • Bandwidth limitation due to increased control overheads. • Raises conflict with existing trickle-timer, used to control redundant messages. • Packet loss in the beginning.

Table 7: Comparison of 6TiSCH scheduling solutions.

3.2.4. Evaluation of Popular SFs

Section 3.2.3 analyzed key contributions across multiple categories, with Table 7 offering a detailed comparison based on performance indicators. This analysis was necessary identify scheduling inconsistencies like suboptimal traffic adaptation, controlling overheads, bandwidth utilization, selection of timeslots and channel offset, collision in different types of scheduling modes, congestion in Tx queue, and dynamic routing topology.

Centralized SFs leverage one-hop alignment with PCE-based scheduling, efficiently mapping traffic conditions based on routing elements. However, achieving theoretical optimality is challenging, especially when nodes frequently change their routing parent to align more closely with the root. This frequent reallocation of cells from an old routing parent to a new one leads to increased resource consumption. In LLNs, sensor nodes continually seek additional bandwidth, striving to find the shortest path to the root.

TASA's assignment of Tx and Rx slots is based on the color-matching criteria [230]. While this technique can reduce the probability of collision between nodes accessing the same cell simultaneously, with more nodes in the vicinity the overlapping is imminent provided TASA does not scan the ongoing transmissions by default.

Centralized SFs offer slotframe compactness aligning slots closer together on the either side of the slotframe where channels are added randomly. The risk of collision in these slots prevails and neither centralized SF can guarantee a collision-free scheduling (channel access) due to the poor performing nodes, caused by the inappropriate suppression of control overheads. This trade-off arises when the higher volume of control message negate a node's throughput, caused by unavailability of outbound Tx cell.

Routing topology plays an important role in scaling the performance of centralized scheduling solutions where a more stable global view of RPL topology is preferred for optimal bandwidth usage [231] [232]. *Huyun et al.,* [233] exploits the relationship between the changing routing dynamics and bandwidth utilization where the *Markovian* model aid channel-access. The channel access process used by the author is expensive in terms of cell consumption as it demands frequent signaling, which is undesired for scaling battery life. Consequently, centralized SFs suffer with limited scalability [195].

Distributed scheduling performs allocation based on negotiation where various traffic predictions measures are used by the popular distributed SFs. Some of these solution incorporated *queue* monitoring and the others used the physical link corresponding to Tx and Rx cells [261]. As nodes use negotiations between parent or the neighbouring nodes, the accuracy in traffic adaption remains a challenging task: SF0 utilizes link metrics such as PDR to assess allocation per node, yet nodes can still experience sudden burst of traffic for which it provides no overprovisioning (extra) cells [261]. Overprovisioning can take place for individual node, or a link. It is essential to deal with unexpected traffic burst and for the timely forwarding of payload to the corresponding next hop, however a fixed distribution (node-based in OTF or link-based in E-OTF) often results in an inconsistent measurement between actual and predicted traffic, causing bandwidth wastage. Alternatively, predicting traffic based on monitoring (queue conditions or cell status in terms of Tx and Rx) involves intensive signaling: The error rate by PiD-based scheduler [131] and cell list used monitoring by EDSF [238] are key SFs that use monitoring towards scheduling where these offer a near precise estimate of cells, but a the cost of straining the source header, and high consumption. Here, straining source header is not beneficial if the frame size is fairly too small (127 bytes). Conversely, passive monitoring fails to capture real-time topological changes, making neither approach suitable from the point of scalability in 6TiSCH networks [229].

Many distributed SFs prioritized a low latency, and energy efficiency over scalability [236]. These include the daisy-chaining implementation by LLSF [235], aimed to add the low latency slot in a series that often incurs a trade-offs with reliability because distant slots are limited in the slotframe [229]. These proposals overlook cell selection for a short-term gain. YSF [256] using top-down alignment provides an improved reliability and lower latency by allowing slots to be closer together towards the top-left of slotframe. YSF uses a hybrid scheduling design where the probability of collision is low concerning data traffic adaption (different types of cells for control packets, and data packets). *Wave* achieved a shorter delay where scheduling information is advertised by the root to all nodes: each node is aware of other node's schedule. However, poor propagation of EBs can raise a conflict of interest where more than one nodes can end up using the same cell, leading to collision.

Broadcast-based distributed scheduling rapidly consumes the dedicated cells in the slotframe, making such solution more better aligned with shared cells whereby a node can access them on the contention-basis. Notably, the DeBRaS-led solutions offer more alternate routing paths, allowing nodes under common ancestor to participate in negotiation with improved propagation, leading to a higher success rate of acquiring cells locally and a more compact topology [239].

DeBRaS-based scheduling approaches have attracted a significant number of contributions [195] where neither SF implemented the VRB in terms of packet aggregation. VRB optimizes forwarding delay. Nearly all DeBRaS-led solutions implements FIFO where nodes have to wait for the entire packet to be assembled prior forwarding. VRB is comparatively a lightweight solution that however drops the entire set of fragments received if any one of the fragment is missing, leading to a frequent retransmissions; hence the fragment recovery is still an open challenge. Notably, DeBRaS scheduler ignore VRB because of the extra Tx buffer provided for nodes, making sequencing less problematic and with more alternate routing path, DeBRaS ,by default, contributes toward load-sharing. Thus, VRB is not used by these SFs (DeTAS, DISCA, LV, E-OTF, and HF-OTF).

In terms of scalability, DeBRaS-led solutions have shown improved reliability beyond a 50 node network but struggled with extremely challenging traffic loads and a high volume of control overheads. This situation has resulted in higher bandwidth consumption on top a shorter battery life [195].

Hybrid scheduling is a popular design using both centralized and distributed scheduler in a combined manner. The core advantage lies in separating these two schedulers based on the flow-labels. Label-switching mechanisms [248] has exhibited that each traffic flow can be distinguished effectively [247]. The hybrid scheduling utilizes different slotframes for distinct traffic types.

Autonomous scheduling manages network functions effectively with pre-computed ALOHA, accessed on contention-basis by the hybrid scheduler; this isn't completely an overhead-free approach. For example, MSF is unsuitable for latency-centric applications where reliability depends on the traffic adaptation model. Those extended MSF (IMSF, AMSF, EMSF, YSF) have contributed little towards improving scalability. Other SFs using autonomous scheduling alone (such as ALICE, and ALICE-FP) provides static allocations, and are not well-suited to handle temporary traffic peaks on nodes without incurring overheads. The energy-consumption increases rapidly when cells are accessed frequently by nodes [227]. Overall, hybrid solutions require improvement in terms of balancing performance objectives and lower power management.

This evaluation concludes that unicast-based scheduling is well-suited for a lightweight traffic offering better energy efficiency and longer battery life with minimal strain on network resource. Broadcast-based scheduling is ideal for a dense network and is more feasible where batteries can be easily replaced. Hybrid SFs pose poor balance of objectives and energy consumption. In addition, the complex design makes it difficult to modify.

For scalability-sake, DeBRaS-led scheduling solutions have advantages, but risks faster battery depletion. The Hybrid scheduling, although complex, provides spectral-efficiency as sufficient bandwidth for managing control beacons and application data, however, it requires a balance in terms of reducing frequent prediction, and queue optimization. Thus, scalability-limitations remain an open issue. Additionally, experimental setups often overlook the impact of EIs as many testing platforms do not accurately predict the physical environment. The evaluation methodologies are discussed in the following section.

3.3. Evaluation methodology

This section focuses on the selection of appropriate evaluation method for testing the proposed solution. In this regard, existing surveys [195] have highlighted available methodologies (simulation, analytical, and testbed evaluation) where key insights are gained by comparison between these methodologies in terms of testing a TSCH-based scheduling function. According to the existing surveys, A larger number of SFs followed a simulation-based testing, which is reliable, easy to configure, quick, cost-effective, and can be beneficial for testing for application-specific scenarios incorporating scalability [195].

Currently, there are various open source implementations provided to test communication performance of 6TiSCH networks. These systems include OpenWSN [223], 6TiSCH simulator [262] [263] Contiki-NG [264], TinyOS [265], NS-2 [266], RiOT [267], and TOSSIM [268]. Each implementation is run over a designated Operating System (OS), but are specific to platform settings (emulated hardware capabilities), making these systems independent and interoperable at different PlugTest (PG) event [269] recorded to date. PGs are interoperability testing events organized by standardization bodies such as IETF and IETF to verify the compatibility and interoperability of different implementations of a standard. These events contributes towards building a reliable and efficient ecosystem for industrial IoT applications. Different PGs are carried out for different standard at different time. The IETF *PG* events were carried out mainly on the three hardware platforms including OpenMote CC2538 [270]. The other devices also used for testing IPv6 WSN includes I3Mote [271], Analog LTP5902 [272], IoT Lab M3 [273], IoTeam Dusty [274], Nordic NRF51822 [275], OpenMote CC2650 [270], Telos-B [276], and Zolertia Re-Mote [277].

Currently, a small proportion of solutions are evaluated using real-time testbeds whereas the testbed-based scalability tests requires hundreds of IoT devices to be deployed. Notably, most SFs have been tested with 10- 50 hardware devices per subnet. On the contrary, simulation-based evaluation is cost-effective for testing scalability of a 6TiSCH network using a larger number of emulated nodes. As a result, the majority of testing is performed using the simulation tools. In this regards, *Senouci et al.,* [195] states, 'approximately 50 SFs have been evaluated using simulators'. The downside of the simulation-based experiments is that these experiments does not accurately reflect the impact of physical environments, which includes wireless interferences, radio propagation, node mobility, and other related challenges. There are several open-source simulators available for testing a wireless IPv6 networks where a fewer of these are specifically engineered for testing TSCH- based IPv6 WSN. Table 8 highlights the key differences between these software packages based on complexity level, scalability, topology with full or partial implementation of 6TiSCH stack, coding platforms, traffic patterns, interoperability, and the diversity of hardware platforms in use.

The author [195] provided an estimate based on the usage of these tools where 6TiSCH simulator is used by 40% of the total TSCH-led scheduling solutions and that too it is possible to have each solution evaluated across different tools that means a solution tested using 6TiSCH simulator could also have been tested using OpenWSN and Contiki-NG: MSF is generic solution, implemented by various simulators including 6TiSCH simulator, and other testing tools like OpenWSN, and Contiki, with diversity of emulated platforms.

Vilajosana et al., [214] provided a rich summary of these software projects, used with regards to 6TiSCH evaluation. Among these, NS-2, TOSSIM, and RiOT are rarely used for testing scheduling performance of 6TiSCH networks; NS-2 implements a IPv6 stack, but lacks support for TSCH and this is one of the reasons it is rarely used. The OpenWSN, and Contiki-NG are equally popular as the 6TiSCH simulator. According to the survey [195], a little less than 20% of the total simulation-based testing of TSCH-led solutions is carried out by Cooja, which is a component of Contiki-NG (OS). Cooja simulator supports a variety of proprietary devices including its own software platform called *Contiki motes,* where these nodes are organized into a *Grid topology*. Cooja is a complex simulation tool, constrained by the *collection view* (a module that supports various KPIs) this means extra lines of coding will be required to add a new indicator without ignoring the buffer limitations.

OpenWSN [45] is 3rd most popular testing tool used for both simulation and real time testbeds evaluation. The communication stack of OpenWSN, by default, offers support to various applications. The repository of OpenWSN contains several projects implemented using OpenWSN for testing key SFs. If implemented with simulation mode, it is possible to run testing using a diverse number of emulated platforms including Telos-B [276], IoT-labs [273], OpenMote-B [270], and many other proprietary devices. OpenWSN, by default, implements OpenMote CC2835 as an advanced prototype.

In terms of network sizes and execution environment (windows OS, Linux), Cooja can only operate on *Ubuntu* OS; whereas OpenWSN is flexible across both Microsoft Windows and *Ubuntu* OS. SFs require long lasting operation to check the network stability along with the pre-defined KPIs; Cooja encounters limitations like buffer overflow over long duration in experimentation [278]. OpenWSN-led experiments can last several hours (long duration), however OpenWSN is a complex solution for testing scalability in comparison to the 6TiSCH simulator.

The 6TiSCH simulator is specifically designed for testing IPv6 WSN comprising a larger number of nodes incorporating various deployment strategies and traffic conditions, making it the most popular simulation-based testing tool. The downside is that it does not accurately predict the physical environment compared to an IoT testbeds. The concept IoT virtual labs is gaining attention where a third-party allows distributed access remotely to run experimentation using predefined base-lines setup. These experiment are focused on the controlled environment that however considers physical environment characteristics, but not as freely as it is used in commercial deployment. Further, it involves third-party that facilitates the access to existing infrastructure: for an instance OpenWSN can run on installed devices at the IoT-Lab [273] and this add a value to the solution, but at the same time, this type of adjustment is not suitable for testing large-scale dense network comprising hundreds of nodes per subnet [278]. Apart from this, the risk of privacy and copyright-related issues cannot be ruled out for remote experiments, being facilitated by a third-part infrastructure.

The third type of evaluation method is based on mathematical models. These models are based on theories and have limitations in term of poorly predicting performance of devices using assumptions [195].

The simulation-based experimentation is a feasible and reliable method for testing scalability where the 6TiSCH simulator is the most popular tool and an ideal candidate for testing 6TiSCH SFs. It is an open access software that emulates the behavior of OpenMote CC2538. The older most version of it emulated Telos-B, which is no longer being used due to poor hardware capacity such as memory size, and processing capacity and the other platforms such as OpenMote CC2528 can offer better features, leading to enhanced capabilities. Furthermore, The 6TiSCH simulator is a dedicated, scalable, lightweight standalone tool for testing scheduling solutions for 6TiSCH networks using an event-driven model; it is a valid tool [278] that does not incur buffer overflow due to scaling or over extended length of time.

The work in this thesis is evaluated using a discrete python-based simulator developed by a member of IETF WG. The 6TiSCH simulator is quick, yields valid results [195], and it implements both distributed and hybrid scheduling algorithms that way it is easier to compare results. The current version is capable to emulate hardware functionalities and can run for over extended period of time. The experimentation is carried out in the next section.

Tools	Hardware	Complexity	Topology	Code	Scalability	Stack	TSCH	Interoperability	Traffic Flow	MSF
NS-2 [266]	Proprietary Analog LTP5902 [272], Nordic NRF51822 [275],	High [266]	Multiple	C++, Python	Average	IPv6 Stack	No [195]	Support libraries and models [195].	All	No
Contiki-NG (Cooja) [264]	LTP5902 [272], Zolertia [277], IoT Lab M3 [273], OpenMote CC2538 [270],Telos-B [276].	High [195]	Grid [195]	Java, C	Low	Full 6TISCH stack [195]	Yes [195]	Supports full 6TiSCH libraries and models, and different routing MoPs.	MP2P P2MP	YES
TOSSIM [268]	Mica2,MicaZ [214], Telos-B [276] CC2420 [270], iMote 3 [271]	Medium [195]	Multiple	Python, C++	High	Full 6TiSCH stack	No [195]	Supports full 6TiSCH stack	MP2P	No
OpenWSN [223]	LTP5902 [272], IoT Lab M3 [273], OpenMote CC2538[265], Telos-B [276], OpenMote-B [270].	Moderate [195]	Mesh and Linear	Python and C++	Average	Full 6TiSCH stack [195]	Yes [195]	Yes, but byte-accurate	MP2P P2MP	Yes
6TiSCH simulator [262] [263]	Telos-B [276], OpenMote-B [270], OpenMote CC2538 [270]	Low	Multiple [195]	Python only	High	Full 6TISCH stack [263] [195]	Yes [195]	Yes, an event-driven lightweight tool implementing full 6TiSCH stack and libraries.	MP2P P2MP	Yes
RiOT [267]	IoT Lab M3 [273], OpenMote CC2538 [270], Telos-B [276], OpenMote-B [270]	High [195]	Multiple [195]	C, C++	High, but cause high overheads	Full 6TiSCH stack [195]	No [195]	Support a large number of IPv6 libraries [195] just like OpenWSN.	All	Yes, but mostly on demand [279]

Table 8. Summary of evaluation tools.

3.4. Experimentation of Existing Scheduling Functions

This section focuses on experimentation of scheduling solutions using the 6TiSCH simulator. The simulator has six built-in modules, placed around the 6TiSCH container- a layered protocol stack implemented by each *mote* (module), configured with TSCH mode over IEEE 802.15.4. Currently, 6TiSCH does not support mobility; hence the nodes are not mobile devices. It follows MP2P pattern with each node or mote sending data packets upwards using an event-based reporting model. The simulator incorporates several event-based traffic generation models emulating realistic network traffic. As far as the homogeneity across nodes is concerned, nodes (IoT devices) are homogeneous and must follow uniform configuration across the network. This ensures that each node behaves in a similar manner which can be crucial for evaluating the baseline performance of 6TiSCH network protocols and configurations. Further, homogeneous configuration provides a controlled environment to evaluate the baseline performance of a network where the uniform settings make easier to identify and isolate issues in the network. It also helps in understanding how the network scales with an increasing number of nodes.

The simulator used in this thesis include *Periodic Steady Traffic,* and *Bursty Traffic model,* currently provided for testing network performance. The steady traffic model generates packets at a regular interval and it is commonly used for monitoring-based applications, sending data regularly over time. The connected nodes can find out about their schedule for packet generation in the propagated beacons. This model can be implemented by setting a fixed time interval between packet generations, is denoted by *packet generation period* or *packet period*, measured into seconds, for example *packet period= 1s* translates into 60 Packets Per Minute (ppm). The value is explicitly defined across configuration parameters as per the objective of the experiment. It is then applied to each and every connected nodes in the network as a need to generate packet at a scheduled time. The Bursty traffic model generates traffic in bursts, where a certain amount of packets are sent in a short period, followed by periods of low or no activity; this can be used to simulate scenarios like *alarms* or *event-triggered* reporting.

All scheduled requests are processed through the '*SimEngine*' responsible to manage the bidirectional flow of information from and to the container (stack). Here, all pending *action* queries are processed based on the scheduled event. Individual layers can also communicate with this module to perform specific action. The Module called '*SimStats*' contains the logs of scheduling metrics. The last two modules are '*Topology'* and '*SimSettings',* whereby *SimSettings* defines initial setting of deployment parameters and constraints, which are linked through the container and the '*Topology'* module, allowing a specific topology to be added as scheduled action via *propagation* module. This module is responsible to simulate/emulate the IEEE 802.15.4 functionalities and predict the physical environment. In the recent version of the simulator, propagation module has been replaced with *connectivity traces,* described in Chapter 5 where the current scheduling draft is evaluated against the proposed solution. Finally, this next section reproduces some possible results of OTF [20] using 6TiSCH simulator. OTF is a distributed SF using reservation-based scheduling. It is a widely cited SF across the literatures focused to 6TiSCH scheduling that way relating back to the problem at hand, the analysis will highlight the potential issues in scheduling.

3.4.1. Reproducing some of the results from OTF using 6TiSCH simulator

OTF was published in 2016 by Watteyne et al**.** [20]. In this paper, the author tested varying threshold limits provided for overprovisioning using the 6TiSCH simulator. This section aims to reproduce some of the results from this paper [20] except that the version of the 6TiSCH simulator used is an evolved one that means it may or may not generate exactly point to point results. Moreover, a large number of 6TiSCH scheduling solutions (SF0, LV, DeTAS, E-OTF) including some of the most recent ones (EDSF) [238] have been tested using the same version, making benchmarking easier and effective.

Each experiment simulates the functionalities of OpenMote CC2538 [280], a popular platform actively used in base-line radio communication. It embeds *temperature sensor*, *motion detector* and *light sensor*. The brain of the device is 32 bit Cortex-M3 microcontroller, using clock frequency of 32MHz with the maximum drift time being 40ppm (parts per million) [280]. In terms of memory profile, OpenMote cc2538 is equipped with 32 kB RAM, and 512 kB of flash memory. The battery capacity is 2200 milliampere-hour (*mAh*) and each device is provided with at least two *AA*-sized batteries. Further, the device is compatible with IP, and TSCH mode of IEEE 802.15.4 standard, operating in ISM 2.4GHz band. The TSCH slotframe is configured with 101 time slots where maximum channel density is 16. The configuration parameters used in the chosen paper are provided in Table 9, below:

Name	**Parameters**	**Name**	**Parameters**
Deployment Area	[2*2] km	PDR	0.5 or 50%
Communication pattern	MP2P	Battery capacity	[2200] mAh
Node's buffer	[10] packets	Radio sensitivity	[-101] decibel-milliwatts
Packet Forwarding	FIFO	Number of nodes	50
Slot duration	[10] ms	Topology	Linear
Maximum available channels	16	Slotframe Length	[101] slots
OTF Housekeeping period	[1]s	Number of runs	100
RPL's Objective Function	OF0	Packet generation period	[1,10,60]s
DIO's interval	[1]s	OTF threshold	[0,4,10] cells
DAO's interval	[10]s	RPL parent size	[3] neighbors
Broadcast Beacon probability	0.33	Max MAC retries	5
Keep Alive (KA) messages	[10]s	RPL minHopIncrease Limit	256

Table 9.Simulation Parameters as per **[20]**.

In the beginning the root is configured which then triggers transmission of EBs, and DIOs allowing new nodes to join. A joining node initiates listening at a randomly chosen channel after receiving EBs from the nearby nodes (from root when there are no other nodes in the network at this stage). The joining node selects one of the neighbors with a stable link quality as Join Proxy (JP) to which it synchronizes its clock with and initiates joining process.

The joining process requires the node to follow the *secure join* procedure. Here, a joining node first exchanges unicast messages containing security information. Once authenticated, it sends a DIS messages to solicit DIOs from the chosen RPL neighbour and deciphers the DIOs to acquire a preferred parent's rank information. Finaly, the joined node is due to add at least one Tx cell with the corresponding parent; this request is initially carried by EBs.

Once the topology configuration is complete, the Keep Alive (KA) beacons are scheduled every 10s ensuring routing path accuracy across a tightly synchronized network. In this regards, the behaviour of IEEE 802.15.4 standard is described in Section 3.1.7.

OTF follows the design principles of RPL (RFC 6550) where it uses the *non-storing* mode, by default provided in the simulator. The sensor nodes forward each received packet upward first and once it is received at the root via PP mechanism the root populates path information in the outgoing packet's header leading to a downward trajectory to reach the chosen destination; there is no requirement for a node in DoDAG topology to store an entire set of routing entries instead, a single entry to the corresponding Direct Acyclic Graph (DAG) parent is sufficient. This is because the nodes are the memory-constrained devices. The full set of routing entries are only stored by the root which is also responsible to compute the shortest-best path to the destination; this mechanism is supported by DAOs and DAO-ACKs unicast messages sent periodically by the non-root node in the topology. The DAO message contain downward routing entries and are marked valid upon a timely receipt of DAO-ACK. If the destination is not found, the entire packet is dropped. In this regards, following scheduling restrictions are imposed by OTF:

- All source nodes follow RPL's non-storing routing mode of operation.
- A sensor node follows a half-duplex communication.
- Parents and children can transmit and receive a packet using the same TSCH cell.
- Source nodes are not mobile.
- Each node generates packets using periodic packet generation period.
- TSCH slotframe contains 0^{th} slots as advertisement and rest are all dedicated slots.

The simulator generates a new topology for each simulation run where this experiment uses 100 simulation runs in total; each run depicts two key functionalities: (a) generating a new topology, and (2) studying the network performance for a given period of time: each run is comprised of 100 slotframe cycles (time) and each slotframe cycle last roughly 1 second, with each slot out of 101 slot, is equivalent to 10 milliseconds and 100 slotframe cycles are equivalent to 100 seconds approximately. The results are averaged and plotted using 95% Confidence Interval (CI). **Table 9** contains a complete set of configuration parameters used by OTF. These parameters are justified for industrial-scale monitoring based operation as provided within RFC 5673 [26]. The positioning of devices follow RFC 5673 [26]. The maximum area for deployment is 2 square kilometers where 50 devices (nodes) are deployed. Each device is placed randomly ensuring there is sufficient connectivity for routing and is connected to at least 3 nodes whose link PDR >= 0.5. Here, PDR is a value between *0.00 and 1.00*, calculated on the basis of RSSI and as per the propagation model incorporated in the simulator [281]. The RSSI value justifies proximity between two sensor devices. Typically, the PDR for most link is constant and stable, however it may fluctuate in the event of collision. The receiver converts the RSSI into Signal to Interference-plus-Noise Ratio (SINR) and then it is converted into PDR using the RSSI and PDR table, provided in [281]. An RSSI value of -101 dBM translates into 1% PDR (with ability to detect the weak signal at distance without boosting transmission power). The radio sensitivity for synchronized LP-WPANs typically remains between -85 dBm and -101 dBm for both upward and downward communication.

Each node follows a fixed limit concerning MAC layer retransmission (max retries = 5). After that, the packet will be removed from the Tx queue. OTF performs traffic adaption based on OTF housekeeping triggered every second, leading to addition/deletion of cells based on the OTF threshold applied- a pre-defined range between 0 and 10 cells.

The 6Top housekeeping runs in background by root checking duplicate as well as collided cells in the slotframe, which is another important task ensuring timely maintenance of TSCH schedule. RPL's housekeeping is triggered by root to dispatch broadcast beacons based on the given probability value (0.33). A slotframe is comprised of 100 slots and 16 channels by default on ISM 2.4GHz: the total number of cells per slotframe can not exceed 1616. *Tx* cells are used for transmission and *Rx* for reception or listening to incomings payload. The channel-hoping operation is described in Chapter 1.

The reproduced results are essentially an average values, computed with 95% CI and it is as per the configuration parameters listed under Table 9. Each sensor node generate traffic over time using steady patterns with probability of earliest generation of packets is 50%. This means, a node may at earliest generate packet at ½ of the defined packet generation period or packet period.

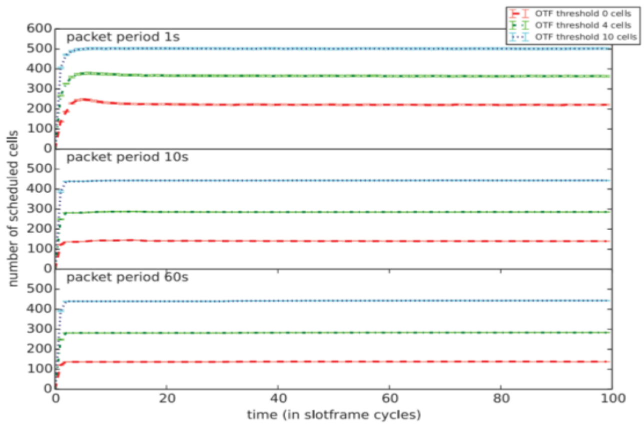

Figure 28:Fig 7 From [20]

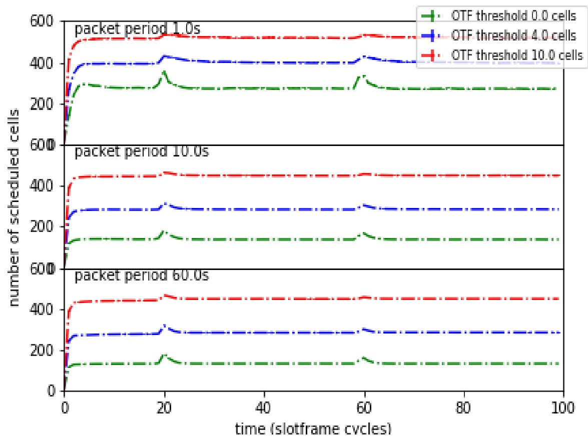

Figure 29.Reproduced results.

In Figure 28 and Figure 29, the impact of different OTF thresholds (0, 4, and 10 cells) on resource consumption is evident across packet periods (1s, 10s, and 60s), highlighting how varying the threshold can influence the number of scheduled cells and therefore the network's bandwidth usage. The graphs reveal, with an OTF threshold of 0 cells, the network maintains the lowest volume of scheduled cells for each packet period, showing minimal resource consumption. For example, with a 1s packet period, the scheduled cells stabilize around 200–300 in both figures, indicating a consistent allocation.

At an OTF threshold of 4 cells, cell consumption increases moderately across all packet periods. In both figures, the 1s packet period results in roughly 300–400 scheduled cells, a noticeable increase from the threshold of 0 cells, reflecting the OTF's traffic adaptation to handle an increased traffic load.

An OTF threshold of 10 cells, however, leads to the highest cell consumption. For a 1s packet period, the number of scheduled cells stabilizes around 400–500, showing the most substantial resource allocation to accommodate frequent packet transmissions. Even with less frequent packet periods, such as 10s and 60s, the threshold of 10 cells results in a higher baseline of scheduled cells compared to lower thresholds.

Overall, increasing the OTF threshold raises the scheduled cell count, demonstrating how higher thresholds consume more cells scheduled to enhance traffic-handling capacity. Figure 28 and Figure 29 reveal that the consumption intensifies with shorter packet periods and higher OTF thresholds, underscoring the balance required between resource allocation and actual traffic demand.

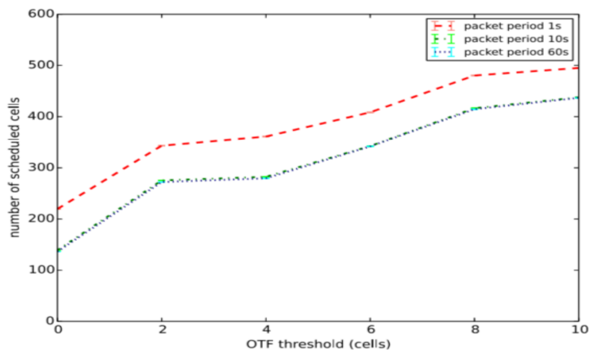

Figure 30:Fig 8 From [20]

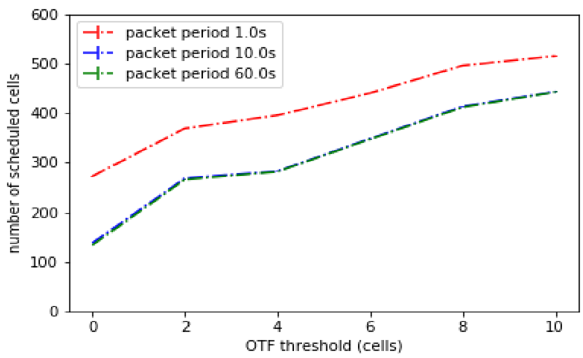

Figure 31:Reproduced Tx cell Vs Threshold.

Figure 30 and Figure 31 illustrate the relationship between the OTF threshold (in cells) and the number of scheduled cells over varying traffic conditions, denoted by packet periods (1s, 10s, and 60s) using steady traffic patterns. As the OTF threshold increases, the number of scheduled cells rises across all packet periods, reflecting a direct correlation between the threshold setting and schedule allocation. For a packet period of 1s, the number of scheduled cells climbs steeply, reaching over 500 cells at the highest OTF threshold (10 cells) in both figures. This indicates significant resource consumption, as shorter packet intervals require more frequent scheduling of cells to accommodate the traffic demand.

In comparison, the packet period of 10s, and 60s shows identical base-line for a moderate increase in scheduled cells with the OTF threshold, levelling off just under 400 cells in both graphs. Overall, these trends highlights that shorter packet periods aligned with higher OTF thresholds lead to higher resource consumption in terms of scheduled cells, while longer packet periods mitigate the effect of increasing OTF thresholds on meeting application needs. This demonstrates how both traffic conditions (packet periods) and OTF threshold settings influence resource consumption in the network.

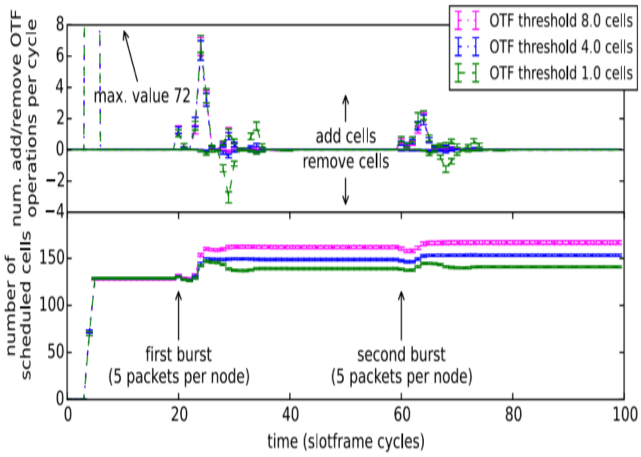

Figure 32: Impulse response of OTF from Fig 10 From [20].

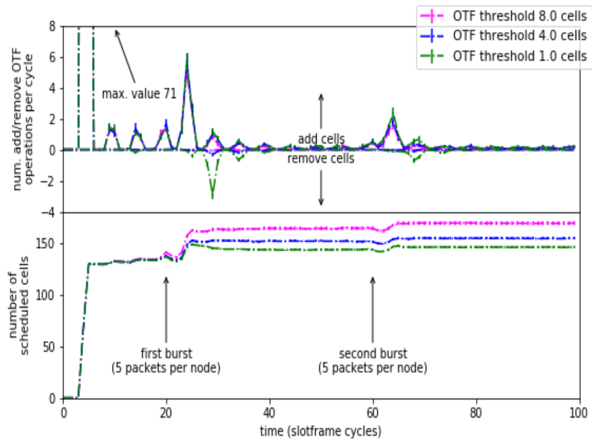

Figure 33: Reproduced Simulation Results 6top Activities.

Figure 32, and Figure 33 show the impact of bursty traffic on network performance. The simulator injects 5 packets at given time (20, and 60 slotframe cycles). Both figures show a similar structure, depicting OTF scheduling activities over time (slotframe cycles) under different OTF thresholds (8.0, 4.0, and 1.0 cells).

In the top subplot, which tracks OTF operations per slotframe cycle, both figures display high initial spikes in cell adjustments (adding and deletion). Comparing the two graphs reveal subtle minor differences in scheduling consistency over time. This is because, in the Figure 33, the maximum operations per cycle over given time reaches 72, slightly higher than the 71 in Figure 32, indicating marginal adjustments during the initial setup.

In the bottom subplot, both figures show a gradual increase in the number of scheduled cells in response to two traffic bursts, with the network stabilizing after each burst. The total number of scheduled cells by the end of the simulation is similar between the both graphs. This suggests a more consistent scheduling response, with fewer fluctuations in the number of scheduled cells. The gaps between the scheduled cells for different thresholds (8.0, 4.0, 1.0 cells) are consistent across both figures too, reinforcing the pattern that higher OTF thresholds lead to more scheduled cells overall.

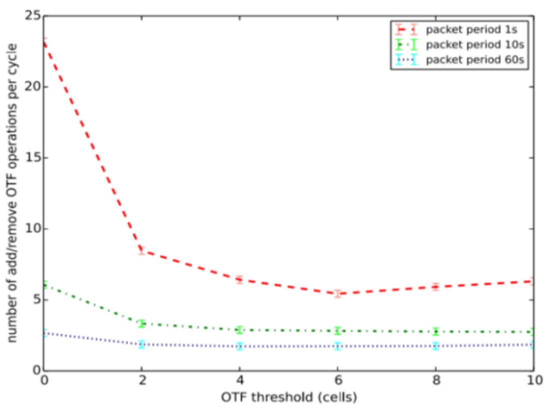

Figure 34: OTF threshold vs 6Top from Fig 9 From [20].

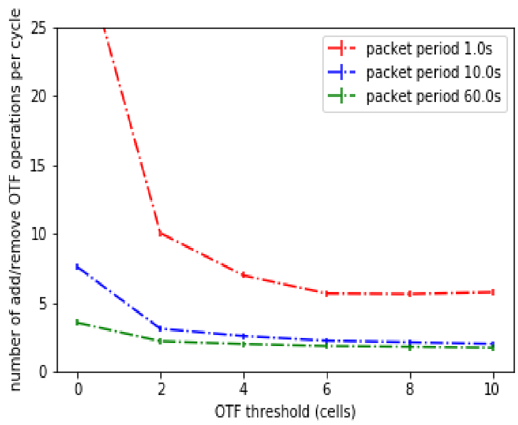

Figure 35:Reproduced Results OTF threshold vs 6Top.

Figure 34 and Figure 35 illustrate the effect of the OTF threshold on the average number of add/remove 6Top operations per cycle using steady traffic, with different packet periods (1s, 10s, and 60s) represented by distinct lines. The X-axis shows the OTF threshold as volume of cells, where lower thresholds trigger increased number of 6Top transactions, making the scheduler to add cells on recurrent basis to meet traffic demand. Conversely, higher thresholds reduce 6Top overheads. The Y-axis represents the frequency of 6Top operations, indicating the overheads involved in adjusting overprovisioning cells. For the lowest packet period (1s), the network sends most packet and triggers a higher volume of 6Top cycles for OTF-based operation. As the threshold increases, the number of 6Top cycles decrease sharply, though it remains higher than for the other packet periods (10s and 60s). With a 10s packet period, OTF is triggering 6Top operation less frequently, which is decreasing gradually with the threshold. For the longest packet period (60s), the network performs the fewest 6Top operations, remaining low across all threshold values, reflecting the lighter traffic load. Overall, both figures demonstrate that while lower thresholds increase 6Top operations, it also raises overheads. Higher thresholds reduce these overhead but may limit the network's ability to adapt quickly to traffic changes, suggesting that threshold selection should tune up with the accurate traffic load, which is difficult to be predicted based on the fixed overprovisioning.

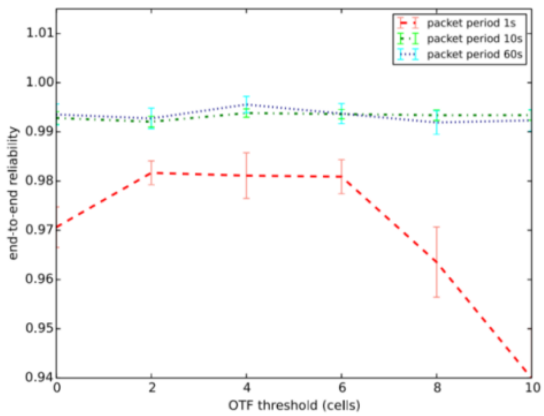

Figure 36: Reliability Vs Threshold [20].

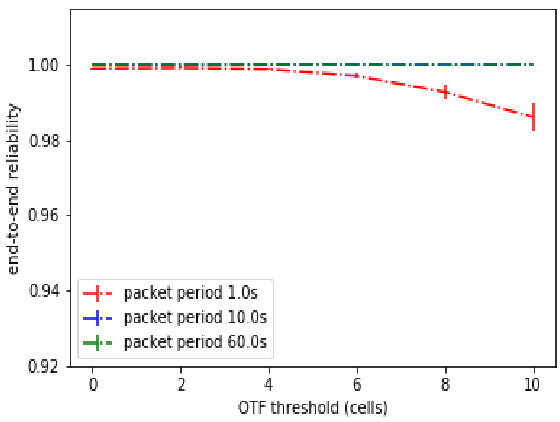

Figure 37:Reproduced Reliability Vs Threshold

In Figure 36, the reliability under heavy traffic (packet period 1s) declines to up to 94% over OTF thresholds, which in contrast to reproduced result in Figure 37 is trailed by approximately 4%.

As per the author [20], the reliability is affected by four key reasons: (1) No outbound TX cells, (2) Max Retries Expired, (3) Congestion , and (4) No Source Route. Besides, the author does not show the proportion of packet loss due to individual packet loss scenarios.

Further, as the traffic conditions becomes incrementally less challenging (packet period 10s, 60s), Figure 37 indicates zero packet-loss, compared to marginal loss shown in Figure 36. This is because, the reproduced results are slightly efficient because of the implementation of OTF through the slightly evolved version of the 6TiSCH simulator and that the difference reported is negligible while comparing both figures.

3.5. Summary

This chapter comprehensively described the 6TiSCH architecture reference model, provided a brief literature review of 6TiSCH scheduling approaches, evaluated testing tools, and reproduced some of the key results (of OTF) using the chosen evaluation methodology. The activities covered in this chapter are as following:

- Section 3.1 provided an in-depth examination of the primary components of the 6TiSCH stack, including 6LoWPAN, IPv6 layer, 6Top layer, TSCH at the MAC layer, and the IEEE 802.15.4 Physical layer. This section aimed to clarify key concepts such as packet fragmentation and reassembly via 6LoWPAN protocol, RPL-based routing, scheduling function (MSF) and 6Top layer functionalities, as well as the key characteristics of physical layer (energy consumption, end-to-end transmission, and synchronization in 6TiSCH network).
- Section 3.2 reviewed key literatures, and evaluated core SFs using a proposed taxonomy. Table 9 compared existing scheduling solutions based on KPIs (reliability, latency, energy consumption, and scalability) providing insights into the scalability issues in 6TiSCH networks.
- Section 3.3 discussed various evaluation methods and identified the most suitable testing tool for evaluation. This selection was based on a careful examination of each tool's strengths and weaknesses in relation to the aim of this thesis.
- Section 3.4 presented reproduced results from OTF using the 6TiSCH simulator. Although, no significant differences were found between the actual graph from the paper and the reproduced version, except the reproducing exact point to point results was challenging due to the use of an older simulator version in the original work (OTF). The results indicated that fixed, hysteresis-driven overprovisioning fall short in accurately predicting network traffic demands, leading to frequent cell additions and deletions when estimates are too low. Additionally, OTF highlighted specific causes of packet loss, which will be examined further in the next chapter alongside proposed solutions.

In summary, the lessons learned from reproducing OTF results underscore the need to address the challenges identified in this review to enable meaningful performance assessments of 6TiSCH.

4. SCALABLE SCHEDULING RESERVATION

SSR is a scheduling function, implemented at the 6top layer of 6TiSCH. The proposal provides bidirectional handshake between sensor nodes using 6Top commands (as illustrated in Section 3.1.5 in Chapter 3). The implementation of SSR is carried out using TSCH-based scheduler where sensor nodes acquire Tx and Rx cells locally in the network. The propagation of EBs is channeled through advertisement cell, called '*minimal cell'*, located in the beginning of the TSCH slotframe at the 0^{th} slot (Figure 1 in Chapter 1). Proposed SF is initially aimed to improve scalability of 6TiSCH network using a model presented in Figure 38. The proposed solution deals with existing scheduling challenges and provides an efficient use of link-layer resources.

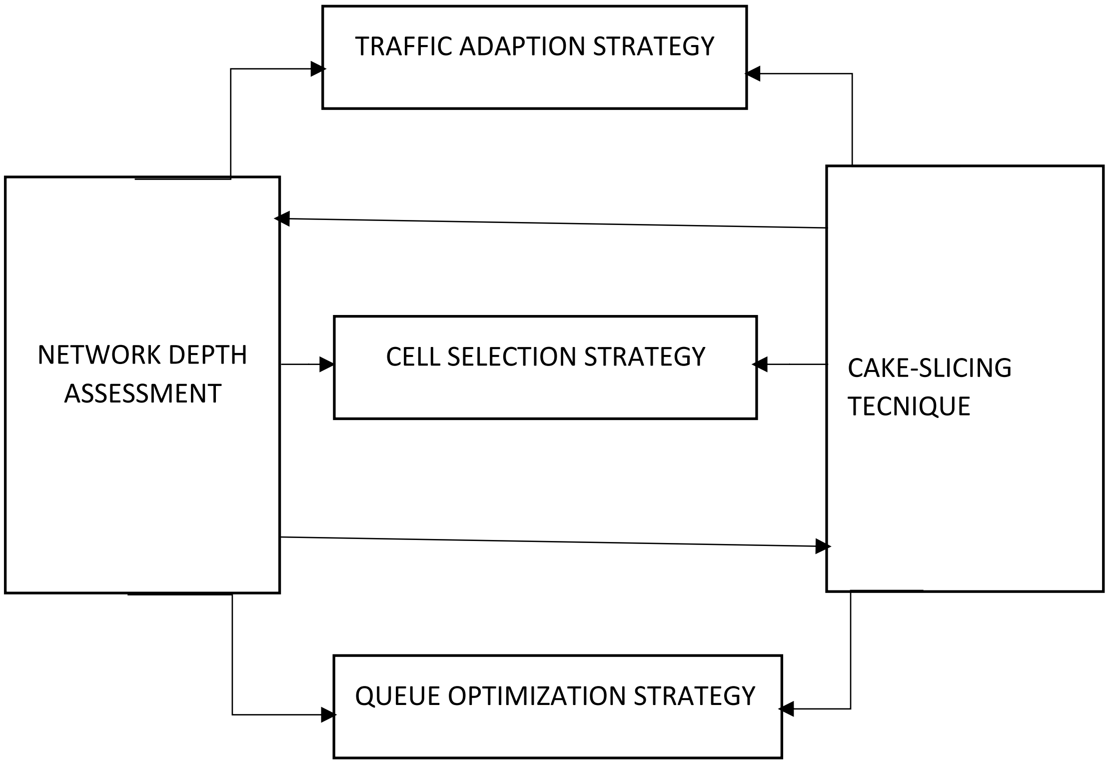

Figure 38. SSR using distributed scheduling model.

The diagram in Figure 38 illustrates a new model for improving communication performance of 6TiSCH networks where each component serves a specific purpose optimizing the network performance. The model is flexible with its deployment across different schedulers (centralized, or decentralized, or hybrid). This chapter proposes to use distributed scheduling as a popular category in terms of improving network performance while handling most network-related activities using dedicated cells. The proposed SF is called SSR, introduced in this chapter as core model where each strategy (components of the model) is tested for its impact on network performance, with each one disabled and enabled. Notably, the role of the cake-slicing technique is central providing key distribution pattens required for optimization of scheduling processes, when used with an appropriate strategy designed; each strategy is a unique process designed to address key challenges, subject to implementation and choice of scheduler.

1) **CAKE-SLICING**

   Cake-slicing is a key component of the model, ensures that the link-layer resources are used based on the corresponding topology depth (according to [20] the simulator yields the topology depth of 8 hops), and maximum length of TSCH slotframe. The outcome of which is then utilized appropriately by corresponding scheduling strategies.

2) **NETWORK DEPTH MEASUREMENT (NDS)**

   NDS provides a value corresponding to the number of hops it takes to reach the root. It is utilized differently across the different scheduling design. Chapter 4 and 6 follows a fixed values (maximum rank increase) towards increasing the hop distance and Chapter 5 uses the cake-slicing additives to increase hop distance that way it regroup the nodes into the scheduling hierarchy.

3) **DYNAMIC TRAFFIC ADAPTION (DTS)**

   To ensure dynamic traffic adaption follows an adaptive overprovisioning (extra cells per node), DTS implements the cake-slicing technique and the NDS so that the nodes located at a certain corresponding hop-distance are given appropriate number of extra cells to deal with traffic conditions. This decreases an average estimate of cells scheduled in the network and improves reliability without triggering any trade-offs with latency or energy-consumption.

4) **QUEUE OPTIMIZATION STRATEGY (QOS)**

   Nodes forward packets from one hop and another towards the root using PP mechanism. QoS assumes that some nodes forwards more packets than the others using shortest-best path and with fewer routes this process can become aggressive, leading to increased traffic load on the nodes that are forwarding most packets upward. Packet aggregation strategy (PAS) is a part of QOS, allows balancing the queue conditions under extreme traffic conditions. It utilize the cake-slicing technique and the NDS together; thus nodes closer to the root can avoid potential packet loss due to congestion in the Tx buffer (queue).

This section describes the design of the proposed solution to improve scalability of 6TiSCH networks.

4.1. Cake-Slicing Technique

Cake-slicing is an analytical measure used resolving a particular problem related to the distribution of resources in resource-constrained networks. For example, bandwidth allocation in an adaptive manner. In the context of 6TiSCH networks it allows effective distribution of bandwidth to the connected nodes in advance adapting the unforeseeable traffic conditions, triggered by various factors, while at the same time avoiding recurrent wastage by connected devices. As the routing nodes change their PP frequently searching for a more efficient and direct path to the root; it is led by the link quality metrics responsible for triggering additional control overheads to avoid packet loss; with these limitations of RPL, this technique cannot completely rule out the overhead-count.

This algorithm is implemented at the root level, enabling easy access to entire routing table. For efficient computation, input parameters must be coherent and so can be computed easily by the root node without additional processing. The key statistics produced as output by the cake-slicing technique is then acquired by 6Top layer whereby the connected nodes can access the output generated passively. While cake-slicing is in use, the proposal does not need to monitor queue conditions, or cell list, or any other node's critical reserves for assessing traffic conditions. The technique simply divides a number (assumed to be maximum slotframe length excluding advertisement slots) into multiple portions. These portions are utilized in a hop by hop manner. The network depth (distance from root from the node with highest rank) is initially set to 4 and this is because, in the beginning, the *rank* value per node is an infinitely high. As more and more nodes join the topology, rank values follow a normal distribution; the distance of node from the root increases or decreases depending on the rank value. Once a network is fully formed and the nodes are synchronized, the network depth becomes a function of average maximum rank divided by the sum of default RPL rank increase factor and rank interval. The default rank increase factor of RPL is 256, and rank interval, set by SSR, is 127. The algorithm shown in Figure 40 follows an example, corresponding to Figure 39 where slotframe length= 100, and network depth= 4.

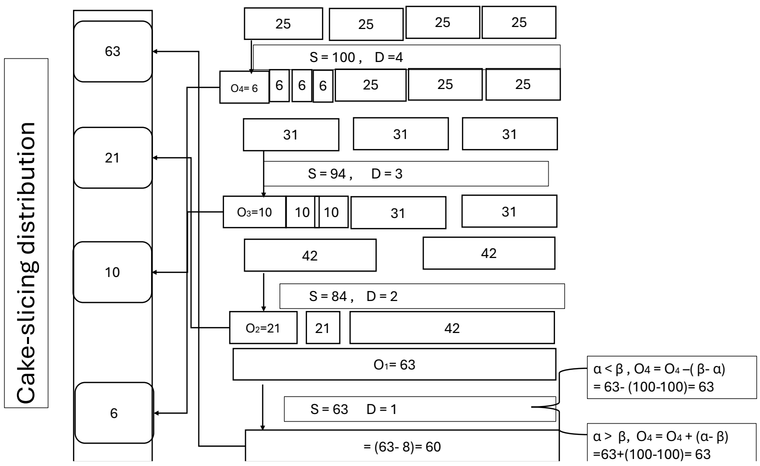

Figure 39. example of cake- slicing technique.

Algorithm 1 Cake-slicing

SLICER(S N)

$T \leftarrow N$, $\alpha \leftarrow S$

while T > =1 do

$O_t \leftarrow | S / T^2 |$

$S \leftarrow \{ ((1 – 1/T) * S) + ((S/T) - O_t) \}$

$T \leftarrow T–1$

end while

$\beta \leftarrow \beta + O_i$ **for** (i < = 1,…,N)

if $\alpha < \beta$ **then** $O_t \leftarrow (O_t - (\beta – \alpha))$

otherwise $O_t \leftarrow (O_t + (\alpha - \beta))$

return O

Figure 40. Cake-slicing algorithm.

The algorithm provided in Figure 40 demonstrate an example of the cake-slicing technique based on the assumptions (*S* as the maximum length of the slotframe and *N* as network depth). *T* is a function variable reflects the network depth as well but it decreases more frequently unlike N. The variables follow the acronyms used in algorithm that way it is easier to articulate the example (Figure 39).

Initially *S* is divided by T^2 and the results are stored through 'O' (It is a list that stores the output). The remaining share of 'S' is brought forward along with the unused portions; for example when 100 is divided by 16 as T^2 initially, the outcome is rounded to a number, and stored through 4th position in the list O or O_4. After that, the algorithm recomputes 'S' for each iteration as a function of **((1 – 1/T) * S)** + **(S/T - O_t)=** ((1- 1/4) * 100) + ((100/4)-6)) = 94. That way, S after 1st iteration becomes 94 and T = T-1=3.

In the 2nd iteration, 94 is divided by 3^2, where a resultant value (O_3= 10) is stored. The S becomes function of **((1 – 1/T) * S)** + **(S/T- O_t)=** ((1- 1/3) * 94) + ((94/3)- 10)) = 84 and T= T-1= 3-1= 2.

In the 3rd Iteration, O_2= 21, and S= ((1- 1/2) * 84) + ((84/2)- 21) = 63 and T= 2-1 =1

The 4th Iteration, which is to be the last iteration as per the given limits, considers O_1= 63 and S= **((1 – 1/T) * S)** + **(S/T- O_t)=** ((1-1) * 63) + ((63/1) -63)) = 0.

As given in the algorithm, the sum of all elements in O, denoted as β, must be equal to original slotframe length (denoted as α). In the beginning α= 100 and β has now become 100 by adding all values in O. Such that β= 6+10+21+63= 100. The if condition checks for any variance between the two and amend the T_{th} element of O. In the current example there is no variance found between α and β; hence the O_4 remains the unmodified. The variance may occur based on the probability of obtaining a non-integer value after division. Figure 41 illustrates several key patterns of cake-slicing output as follows:

S	D		Hop 1	Hop 2	Hop 3	Hop 4	Hop 5	Hop 6	Hop 7	Hop 8	Hop 9
100	2	=	75	25	X	X	X	X	X	X	X
100	3	=	67	22	11	X	X	X	X	X	X
100	4	=	63	21	10	6	X	X	X	X	X
100	5	=	60	20	10	6	4	X	X	X	X
100	6	=	59	19	10	6	4	2	X	X	X
100	7	=	58	19	9	5	4	3	2	X	X
100	8	=	56	19	9	6	4	3	2	1	X
100	9	=	56	18	9	5	4	3	2	2	1

Figure 41.Demonstrating multiple configurations of cake-slicing with varying network depth (D).

Figure 41 depicts a negative-linear distribution using the example of cake-slicing where the value of S is a constant (100), and D increases per row by 1 (variable). It shows the difference of weights assigned in hop by hop manner where hop 1's weight is almost 3 times more than that of hop 2 and it is true for all 9 cases listed. Here, nodes towards the bottom (away from hop 2 and 3) get an extreme share and it continues to decrease. The cross (X) sign in Figure 41 indicates a *null value* and is used as a filler showing that the network depth is less than 9 hops while S and N are both non-zero. SSR adapts to the *cake-slicing* technique to improve scheduling performance.

4.2. Network Depth Strategy

NDS is utilized for computing the distance into number of hops to the root. It is a function that returns an integer. The role of NDS is crucial towards across each strategies incorporated in the model.

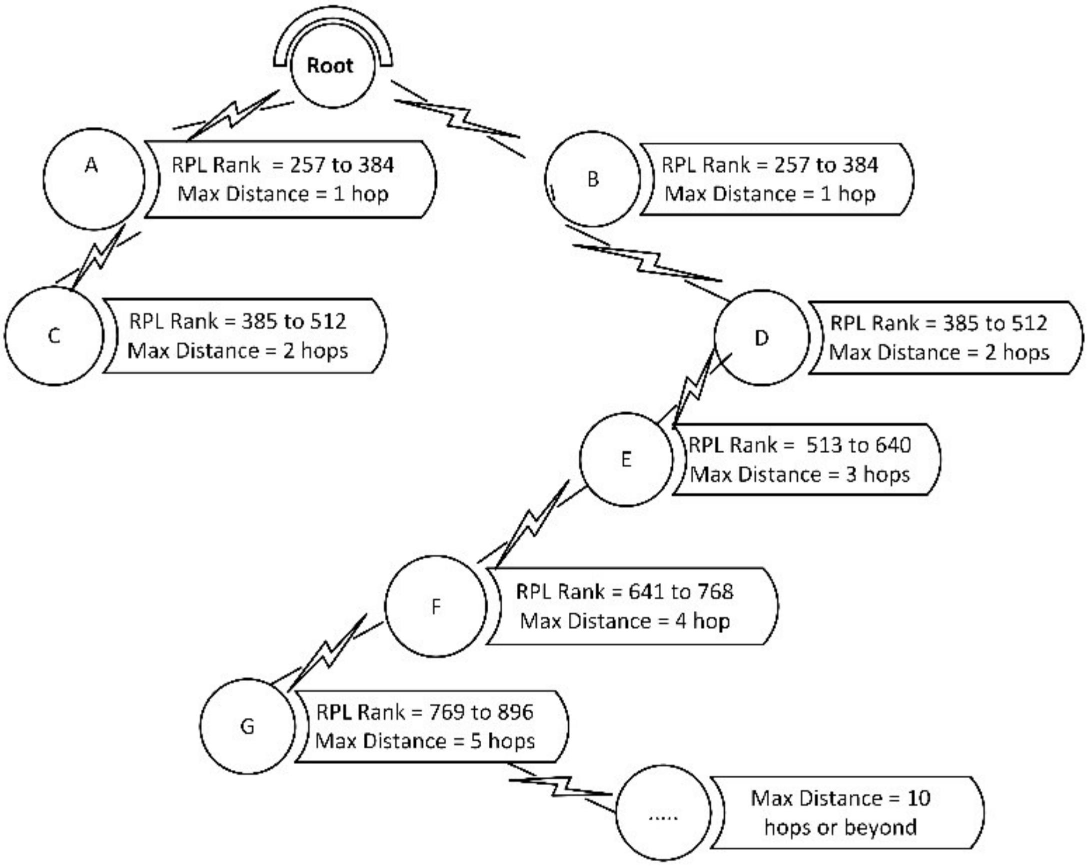

Figure 42. Example of SSR's Network Depth Strategy.

The diagram in Figure 42 presents a RPL topology in which the nodes labelled as A, B, C, D, etc, are located in the circle (shown in the diagram above). These nodes form a scheduling overlay that branches out from the root, with each node having a rank that corresponds to its routing position (hop-distance). These nodes are then organized based on NDS, using RPL rank determining the number of hops to and from the root. For example, Nodes A and B have rank values, ranging from 257 to 384 positioned 1 hop away from the root. Moving further from the root, nodes C and D, with RPL rank value between 385 and 512 are located 2 hops away. The rank increases using a fixed rank interval (127) and as this happens, so does the distance from the root; Node E, Node F and others falling into higher rank category such that Node E has a rank between 513 and 640, placing it 3 hops away, and Node F, with a rank between 641 and 768, is positioned 4 hops from the root. These pattern continues with Node G as well which has a rank between 769 and 896, so is considered 5 hops away. This systematic alignment extends further into the network potentially reaching 10 hops or higher, allowing for scalable NDS distribution.

4.3. Dynamic Traffic Strategy

A dynamic threshold is the difference between actual and predicted traffic per node in the topology. This section briefly describes DTS and it's core features in terms of assessing traffic conditions on each node in advance based on the NDS. This process is repeated until all nodes are adequately scheduled with required extra cells.

Algorithm 1. SSR Allocation Algorithm

```
Procedure SSR ALLOCATION (S, R, T)
        S ← Number of available cells
        R ← Number of requested cells
        D ← Network Depth Interval
        Slices← GetSlicer(Slotframe, Max Network Depth)
        T← Slices[D]>>3                              => DTS threshold

    if R > S and S >=0 then
        if R > 0 then
            S= R - S + (T+1)/2                       => add cells
        else
            S= 1                                     => add a single cell
        end if
    else if R< (S- T)   then
        S= S- R - (T+1)/2                            => remove cells
    else
        S= 0                                         => do nothing
    end if
```

Figure 43. SSR's schedule allocation algorithm.

The schedule allocation proposed by DTS is shown in Figure 43. According to this, a new 6Top cycle will not occur if the value of '*R'* (required cells) is roughly around the value of '*S*' (available cells). However, it is not possible to completely get rid of 6Top transactions as the traffic conditions may vary in a dynamic topology. Figure 44 presents an example of DTS. The example of DTS uses a particular row from Figure 41 where S= 100 and N=D= 5 and Figure 42 (NDS) to measure hop distance in the network topology.

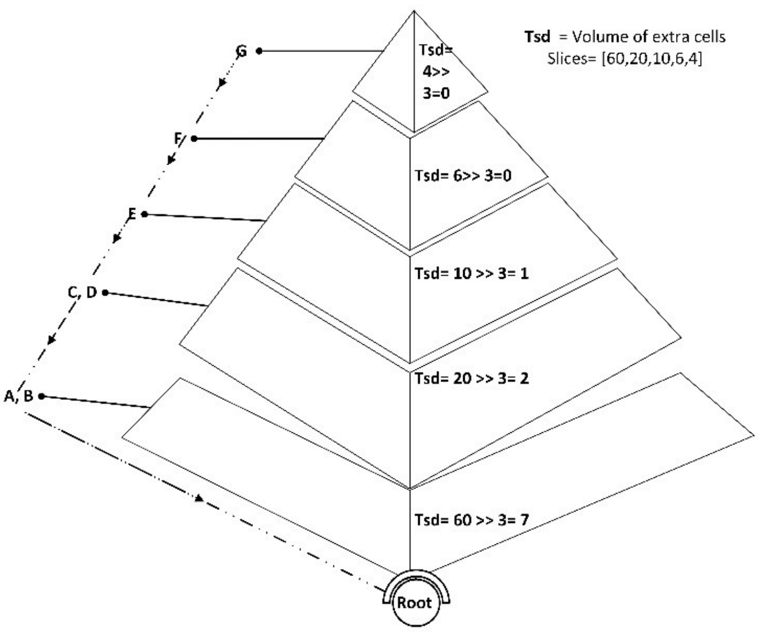

Figure 44. Example of SSR's DTS using 5-hop RPL topology.

The example in Figure 44 arranged nodes in a leaf format with the root being positioned at the bottom. The alignment to the left-hand side indicates connected nodes and the computation of DTS threshold (T_{sd}) takes place on the right-hand side- a representative of amount of cells to added for dealing with adverse traffic. To compute T_{sd}, DTS shifts 3 bits to the right using a bitwise operator (>>) that is applied against the corresponding cake-slicing portion (60, 20, 10, 6, and 4) following the distribution provided in Figure 41. For example, Node A and B gets T_{sd}= 7, which is the highest value. Node C and D get T_{sd}= 2 each, that is about 3.5 times less than the value of T_{sd} assigned to the nodes situated at hop 1 and is as per the scenarios displayed in Figure 41. Finally, Node E, F &G situated at hop 3 get T_{sd}= 1, T_{sd} = 0, T_{sd} = 0 respectively. With these estimates being supplied on the run-time, SSR replaces unform distribution of fixed cells on recurrent basis. The implementation of DTS may vary as per the scheduler. The schedule allocation algorithm is deployed on root, and scheduled at the same time as housekeeping time.

Case 1: R=1,S=0,T=0 - Status: ADD 1	
	• R>S and S=0, so we move into the first condition.
	• Since R>0, we add a single cell. **S becomes 1** (Added 1 cell).
Case 2: R=0, S=1, T=0- Status: DELETE 1	
	• R<(S−T) since 0<(1−0).
	• So we move into the condition to delete cells: S=S−R−(T+1)/2=1−0−(0+1)/2=1−0.5=0.5 We round down to zero, so **S becomes 0** (Deleted 0 cell).
Case 3: R=0,S=0,T=0- Status: Do nothing	
	• S=0, no action is taken, so **S remains 0**.
Case 4: R=1,S=1,T=0 - Status: Do nothing	
	• Since R=S, there is no need to add or delete cells.
	• **S remains 1**.
Case 5: R=1,S=0,T=1- Status: ADD 2	
	• R>S, so we add cells using the formula: S=R−S+(T+1)/2=1−0+(1+1)/2=1+1=2 **S becomes 2** (Added 2 cells).
Case 6: R=0,S=1,T=1 - Status: Do nothing	
	• R<S−T, but the difference is 0, so **no action is taken**.
	• **S remains 1**.
Case 7: R=2, S=1, T=2- Status: ADD 2	
	• R>S, so we add cells: S=R−S+(T+1)/2=2−1+(2+1)/2=1+1.5=2.5 Rounded up, **S becomes 2** (Added 2 cells).
Case 8: R=1,S=2,T=2 - Status: Do nothing	
	• R=S−T, no cells are added or deleted.
	• **S remains 2**.
Case 9: R=1, S=1,T=2 - Status: Do nothing	
	• Since R=S, **no action is taken**.
	• **S remains 1**.
Case 10: R=2,S=2,T=2 - Status: Do nothing	
	• Again, since R=S, **no action is taken**.
	• **S remains 2**.
Case 11: R=2,S=0,T=2 - Status: ADD 3	

• R>S, so we add cells: S=R−S+(T+1)/2=2−0+(2+1)/2=2+1.5=3.5 Rounded up, **S becomes 3** (Added 3 cells).
Case 12: R=0,S=2,T=2 - Status: Do nothing
• No action is taken as S=2.
• **S remains 2**.
Case 13: R=3,S=1,T=7 - Status: ADD 6
• R>S, so we add cells: S=R−S+(T+1)/2=3−1+(7+1)/2=2+4=6 **S becomes 6** (Added 6 cells).
Case 14: R=1,S=3,T=7 - Status: Do nothing
• No action is taken as R=1 and S=3.
• **S remains 3**.
Case 15: R=3,S=3,T=7 - Status: Do nothing
• No action is taken as R=S.
• **S remains 3**.
Case 16: R=1,S=1,T=7 - Status: Do nothing
• No action is taken as R=S.
• **S remains 1**.
Case 17: R=1,S=0,T=7 - Status: ADD 5
• R>S, so we add cells: S=R−S+(T+1)/2=1−0+(7+1)/2=1+4=5 **S becomes 5** (Added 5 cells).

Table 10. DTS Table of thresholds and possible 6Top scenarios.

Table 10 illustrates key scenario following DTS implementation, leading to variations in adding and deleting cells. It illustrates various scenario by manipulating values of *R* (required cells), *S* (available cells), and *T* is as per the example shown in Figure 44. The illustration in Table 10 provides a rich context to DTS-based schedule allocation for 6TiSCH network.

4.4. Cell Selection Strategy

The CSS algorithm divides the slotframe width into several slices or portions based on cake-slicing technique, with each slice representing a specific range of slots in the slotframe. The boundaries of these slices are determined by defined starting and ending points, ensuring compactness of TSCH schedule.

Algorithm 3 Schedule selection

```
SELECTION (SR)
        D← PREDICT (D)
        T← SLICER (SD)
        R← REQUIRED CELLS
        INDEX← NULL
        do
                SELECT FREE CELLS X ? S_INDEX
                COUNTER ← COUNTER + X
                INDEX ← INDEX + 1
        While INDEX >= D or  COUNTER < R
         if  COUNTER >=R then
                return X
        otherwise
                SELECT FREE CELLS X ? S
                 Return X
```

Figure 45.SSR's Cell Selection Algorithm.

The CSS algorithm shown in Figure 45 **is** deployed at root level where each node is informed of their respected scheduled events in the slotframe. According to this algorithm, SSR scans through each retained slice of slots (*Slices*) for free slots. These slices vary in size, when checking each slotframe slice, the algorithm ensures steady withdrawal if the maximum number of free cells (*counter*) in the corresponding slice is greater than or equal to the required number of cells (*R*). However, when all slices are exhausted, the TSCH scheduler implements *random* selection and drops packets if the required volume of slots (*R*) is not matched. If the selection is successful, then it proceeds to channel allocation. SSR use channel-change approach, initially proposed by Duy e*t al.* [19], selecting channel(*Ch*), to minimize the risk of collision in *Tx* slots.

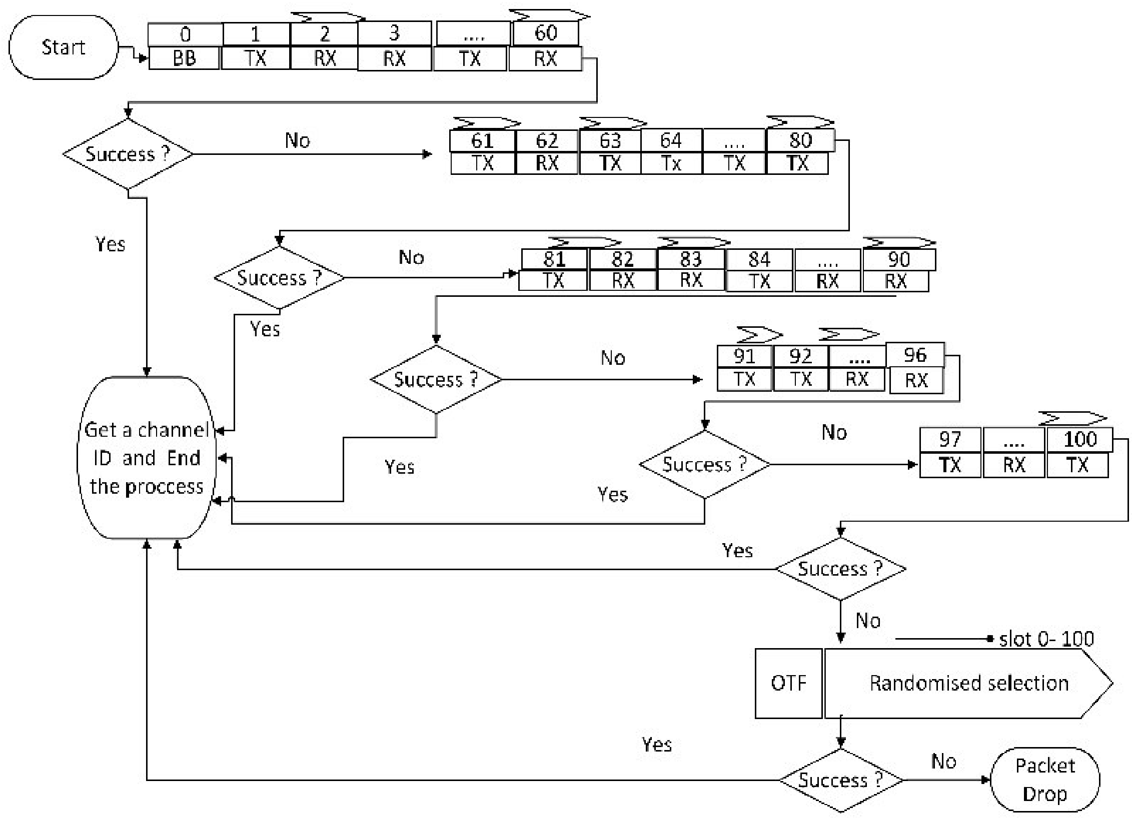

Figure 46. Example of SSR's CSS using S=100 and N=5 hop RPL topology.

In Figure 46, an example of CSS is given where the first slice is representing the largest volume of slots, spanning from the 0th slot (the starting point) to the 60th slot (the endpoint); here the 0th slot is a broadcast schedule used for network functions such as node joining. The primary objective of CSS distribution is to ensure that slot allocation remains contiguous, thus avoiding unnecessary slotframe scanning during normal operation: CSS treats each corresponding slice as a slotframe, which is then scanned thoroughly by nodes for free slots until the demand of requested cells is met. The next slice is 20 slots long, hence, the 2nd slotframe starts from 61 and ends with 80. That is, exactly 20 slots. The rest are shown in Figure 46 where the scheduler allocates most slots to the left in the slotframe under normal traffic conditions. However, if the occupancy of a slotframe (slice) reaches 100%, the scheduler chronologically uses the next available slotframe (slice) and this process continues until the demand is met. However, if all slotframes are scanned and the occupancy is high, SSR opts for a randomized selection and drops packets upon failure to locate the sufficient volume of free cells.

4.5. Queue Optimization Strategy

Queue optimization is a function of minimum *queuing delay* and *resilience*. In 6TiSCH, a priority-based aggregation of packets in Tx queue is used by several SFs including OTF, differentiating between the forwarding and self-generated traffic. However, it provided a sub-optimal output, not matching with the condition of the queue of each node.

SSR reacts to varying traffic conditions in the network and adapts special provisions in terms of queuing policy. That is a sensor node located closer to the root is assumed to be attracting a larger volume of incoming payload than the self-generated stream. It should collects packets from the nearby neighbors to a greater extent using a threshold limit, which is inversely proportional to the percentage of self-generated packets added to the Tx queue. However, the proposed consideration prioritizes the self-generated stream of packets over forwarding packets since distant nodes have comparatively fewer forwarding packets than their own. To bring these considerations into practice, Packet Aggregation Strategy (PAS) is defined. The aim of PAS is to overcome congestion and avoid concurrency risk, with multiple nodes sending packets to the same destination. SSR incorporate PAS in line with traffic forwarding priorities.

Traffic Prioritization: Nodes closer to the root receive a larger proportion of incoming packets, and generate comparatively less to their own packets (SELF). Conversely, distant nodes are expected to attracts much larger stream of traffic on their own (SELF). As the hop distance increases, nodes are programmed to allow most of the incoming payload straightaway and add lesser of SELF payload as per the PAS threshold. PAS threshold utilizes cake-slicing heuristics.

PAS Threshold Calculation: Each hop in the routing topology employs PAS Threshold (T). This threshold represents a varying percentage share of the portions in (O), indexed by hop_id. The algorithm adjusts the threshold dynamically according to network conditions and traffic load. The algorithm shown in Fig. 47 computes 'T' for each hop_id. This threshold is them applied for adapting queue conditions.

Algorithm 5 SSR Packet Assembly Strategy

SSR_PAS (PP, hop_id, S, D)
  D← PREDICT (D), O_T← SLICER (S, D)
  IN← PKT.RX, FWD← PKT.TX, SELF←PKT.GEN
  T← $\frac{(\boldsymbol{O_{hop\_id}})}{\mathbf{100}}$
  do
    Assert node is not root
    $\boldsymbol{TX_{QUEUE}} \leftarrow \boldsymbol{FWD} + (\boldsymbol{SELF} \times \boldsymbol{T}) + (\boldsymbol{IN} \times \mathbf{1} - \boldsymbol{T})$
  While TRUE
  Return PP. $\boldsymbol{TX_{QUEUE}}$

Figure 47.Queue optimization strategy algorithm.

Further articulation of PAS is shown using an example in Figure 48: Node A and Node B at *hop_id* 1 must relay the 40% incoming payload (IN) and 60% from their own (SELF) that is inversely proportional threshold. Since SELF payload may consist of beacons used to maintain clock synchronization and keeping topology operational hence it is vital to prioritize such payload at this level (closer most to the root). Additionally, nodes at *hop_id* 1 have high priorities in DTS algorithm.

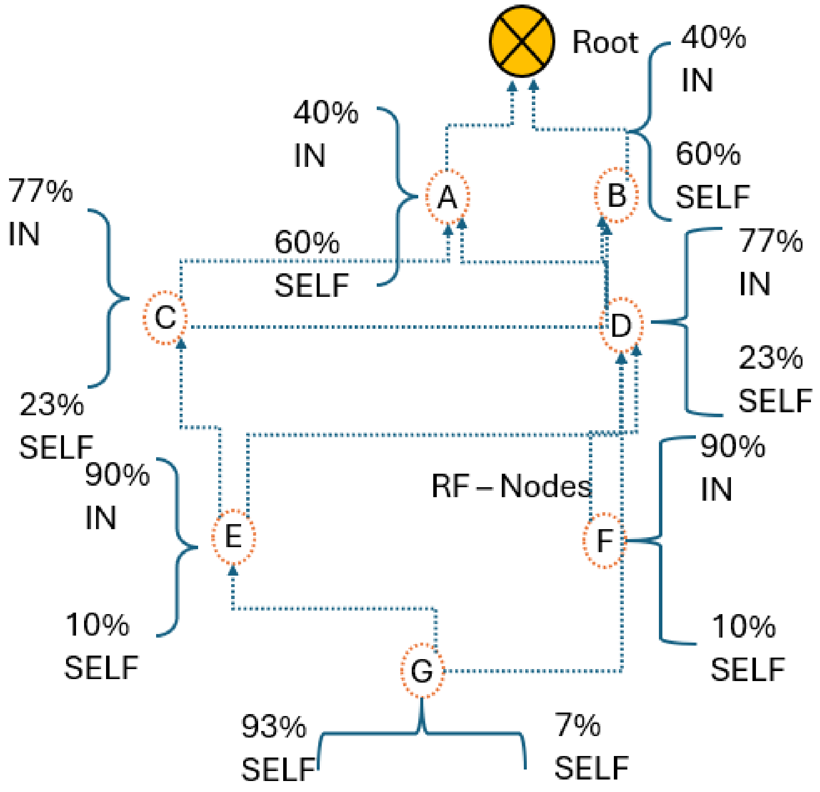

Figure 48. Example of Packet Aggregation.

Node C and D relay 77% of IN packets and 23% of their SELF. The topology is more populated and dense at this stage and nodes are benefited from uniform schedule allocation. The nodes E and F at *hop_id* 3 may receive the broadcast at delay compared to the Node C and Node D, therefore resetting the clock more frequently to avoid collisions, which is a non-zero probability.

Node E and Node F relay 90% of their IN packets and 10% of their SELF packets. The SELF may constitute to the unicast beacons in addition to the data packets. Lastly, Node G is the distant node, which moves less frequently in the topology because of increased distance to the root. Node G may have to reset its clock each time it is leaving the network and rejoining with distant nodes being it's parent (Node E, Node F). This happens because of poor propagation (using single broadcast cell). At this hop level, PAS desires to upstream 97% of IN packets compared to 7% its SELF payload (distance nodes are mostly spending time listening to oncoming beacons to keep their clock synchronized).

4.6. Evaluation of SSR

This section provides valuable insights into SSR's performance under various network conditions and topologies. Each experiment simulates the functionalities of OpenMote CC2538 when using the 6TiSCH simulator. Table 11 presents the configuration parameters, with parameter values sourced from [20]. These values are updated based on the aims and objectives of each experiment, ensuring tailored testing for individual scenarios, following RFC 5673 [26]. Additionally, Section 3.4.1 of Chapter 3 provides a brief description of these configuration parameters. The deployment assumes sufficient connectivity for routing and propagation. The proposed solution is evaluated using the same older version of the 6TiSCH simulator referenced in Section 3.4.1.

Name	**Parameters**	**Name**	**Parameters**
Deployment Area	[1*1] km	EB's Broadcast probability	0.1
Communication pattern	MP2P	Keep Alive (KA) messages	[10]s
Node's buffer	[10] packets	Packet Delivery Ratio	0.5
Packet Forwarding	FIFO	Battery capacity	[2200] mAh
Radio Frequency Band	[2.4] GHz	Radio sensitivity	[-101] dBM
Channel density	16	Number of nodes	[40,50,60,70,80,90,100]
Housekeeping period	[2, 5]s	Topology	Linear
RPL's Objective Function	OF0	Slotframe Length	[101] slots
DIO's interval	[1]s	Number of runs	[100, 200]
DAO's interval	[10]s	Packet generation interval	[1.0, 2.0,5.0,10.0]s
DIO's broadcast probability	0.33	minHopRankIncrease	256

Table 11.Configuration parameters for industrial network (RFC 5673).

The deployment area has shifted to *1* Square kilometers where root is centrally positioned. The sensor nodes are aligned in linear topology, with each connected node being provided with at least 3 neighbors whose link PDR is a value between 0.5 and 1.0. The RSSI values is set as per the propagation model, assuming 1% PDR. The control beacons such as DIOs and DAOs are adequately scheduled using 1s for and 10s interval, which are further utilized towards suppression of duplicate messages by Trickle timer. As a node joins the network, ranks are computed based on the minHopRankIncrease: the original rank of PP + the minHopRankIncrease (which is set to 256). The simulator generates a new topology on each run, and this experiment uses appropriate setting where number of runs can vary from 100 to 200, with each run comprised of 100 slotframe cycle. The length of slotframe cycle is *1s* approximately and each slot lasts for 10 milliseconds.

The experiment follows steady packet generation using the given packet generation intervals (packet periods): 1s, 2s, 5s, and 10s, corresponding to 60, 30, 12, and 6 packet per minutes respectively. These settings of packet generation can vary from one experiment to another similarly the size of the network is defined as per the requirement of each experiment through next Subsections. The performance evaluation may choose the number of nodes per installation appropriately besides each node's distance is as per the connectivity metrics and propagation model provided in the simulator.

The deployed nodes have smaller Tx buffer (10 packet) and aren't mobile devices; through this should not be mistaken in the case of routing where routing nodes can move up and down the hierarchy without affecting the base-line physical deployment plan. At the base-line deployment the expected PDR is considered stable. SSR triggers allocation of cells based on the 6Top housekeeping timer, which is set to 2s, and 5s; with 2s, each node will be frequently assessing their cell allocation, and at the same time housekeeping will be performed. Most of these parameters are explained in Section 3.4.1 of Chapter 3 besides the values may vary depending on the scenarios to be tested. Subsection 4.6.1 tests resilience against traffic variability using appropriate tuning of the parameters presented in Table 11. The simulation-based results depict the average value, presented with 95% CI.

4.6.1. Resilience to traffic variability

In this experiment, SSR's resilience is evaluated against the impact of traffic variability, following the industrial network scenario, outlined in [20]. The configuration parameters are the same as shown in Table 11, except that the packet generation interval is set to 2 seconds (30 ppm). The housekeeping interval is set to 5 seconds by default, which dictates that the allocation of excess cells for each node depends on the housekeeping delay, contributing to power-savings. The experiment follows the unicast-based scheduling rules.

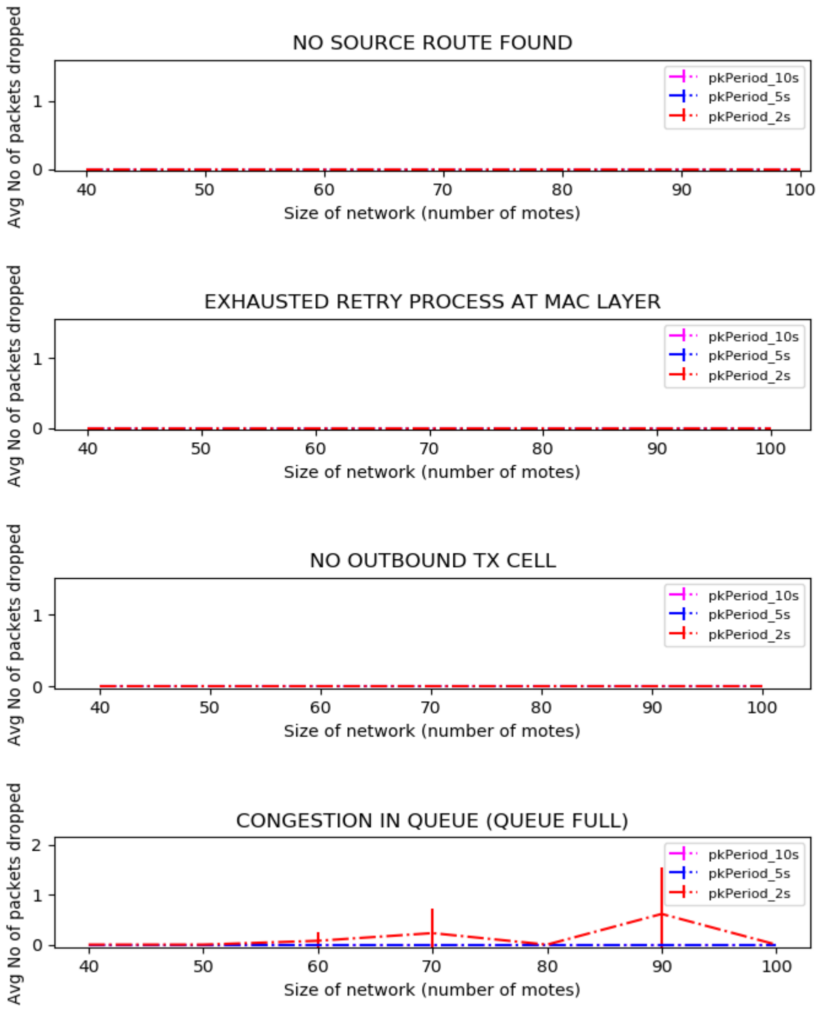

Figure 49. SSR's resilience to existing packet-loss scenarios over given setting.

The results presented in Figure 49 are based the average trend, presented with 95% CI. The data analysis process involves the following steps:

1. **Data Capture**: Each slotframe cycle, approximately lasting one second, generates a single value. Over 100 slotframe cycles per simulation run, this results in 100 values per run.

2. **Data Aggregation**: For 200 simulation runs, each list of 100 values is converted into a single average value. This process yields a total of 200 averaged values, each corresponding to one simulation run.

3. **Result Presentation**: The average values for each run are further analyzed to compute the 95% CI. These values are then plotted on the Y-axis of the subplots in Figure 49, presenting the variability of results for each experiment. This approach ensures a statistically valid representation of the simulation outcomes.

First subplot from the top shows that the *unavailability of a source route* is not directly related to scheduling but rather inherent to RPL routing, often caused by poor propagation of EBs or invalid unicast DAO beacons. As a result, the first subplot shows no packet loss due to the absence of a source route when all traffic is directed upward. This observation holds true across all network installations.

2nd subplot focuses on packet retransmissions due to exhausted MAC-layer retries; the second subplot confirm that SSR experiences no payload loss due to failed retransmissions (exhausted retry process).

The 3rd subplot similarly reports no dropped packets due to the unavailability of outbound TX cells. This is because sensor nodes were given sufficient Tx cells to complete end-to-end transmissions under SSR.

The 4th subplot depicts average packet loss due to congestion in the queue. SSR effectively prevents congestion by leveraging the node's hop distance as critical measure incorporated within NDS. Unlike other SFs, SSR does not waste network resources on congestion notifications or selective packet recovery. The results demonstrate that SSR is resilient to the given traffic patterns, with only a slight spike in packet loss at 70 and 90 nodes network, which is attributed to changes in topological alignment during simulation runs provided the simulator generates new topology each time.

4.6.2. Significance of SSR's Strategies

This subsection evaluates the influence of SSR strategies on network performance by enabling and disabling each strategy individually over given settings (Table 11), and by following the same data representation technique.

When NDS is disabled, scheduling follows a uniform distribution, making it universal to all nodes. When DTS is disabled, no extra cells are allocated, as the DTS threshold is turned off. If CSS is disabled, cells are randomly selected from the slotframe. Lastly, when the QOS is disabled, PAS will aggregate traffic equally, with 50% dedicated to forwarding traffic and 50% to self-generated traffic.

This experiment uses the same packet generation period as detailed in Section 4.6.1. All other parameters also remain consistent with those defined in Section 4.6.1 and as shown in Table 11. The experiment evaluates key network performance metrics such as resilience, latency, consumption, collision, and reliability to assess the impact of the SSR strategies.

Figure 50 illustrates the contribution of SSR's four scheduling strategies with respect to resilience against packet loss across four key scenarios. The results indicate that transmission of unicast beacons, such as DAO, is negatively impacted when nodes are not allocated extra cells, leading to fewer valid paths.

The 1st subplot shows an average packet loss of 1-2 packets due to the absence of a source route under varying network densities when the dynamic traffic strategy (DTS) is disabled. None of the other strategies contribute to packet loss, which suggests that without extra cells, nodes have reduced flexibility to explore new routes.

The 2nd subplot highlights packet loss due to the "Exhausted retry process at the MAC layer". This shows the critical role of NDS in managing packet success rate, especially in networks with more than 70 nodes. As network density increases, so does the number of packets; meaning some nodes require a higher proportion of excess cells to handle both incoming and self-generated traffic. When NDS is disabled, overprovisioning follows a uniform distribution with higher threshold limits for all nodes, leading to cell shortages. Consequently, packet loss becomes more likely as some nodes cannot cope with temporary traffic over time. This negatively affects resilience, particularly in the "No Outbound Tx cell" scenario (in 3rd subplot), with packet loss rising to 2 packets in networks of over 90 nodes, as shown in the third subplot of Figure 50.

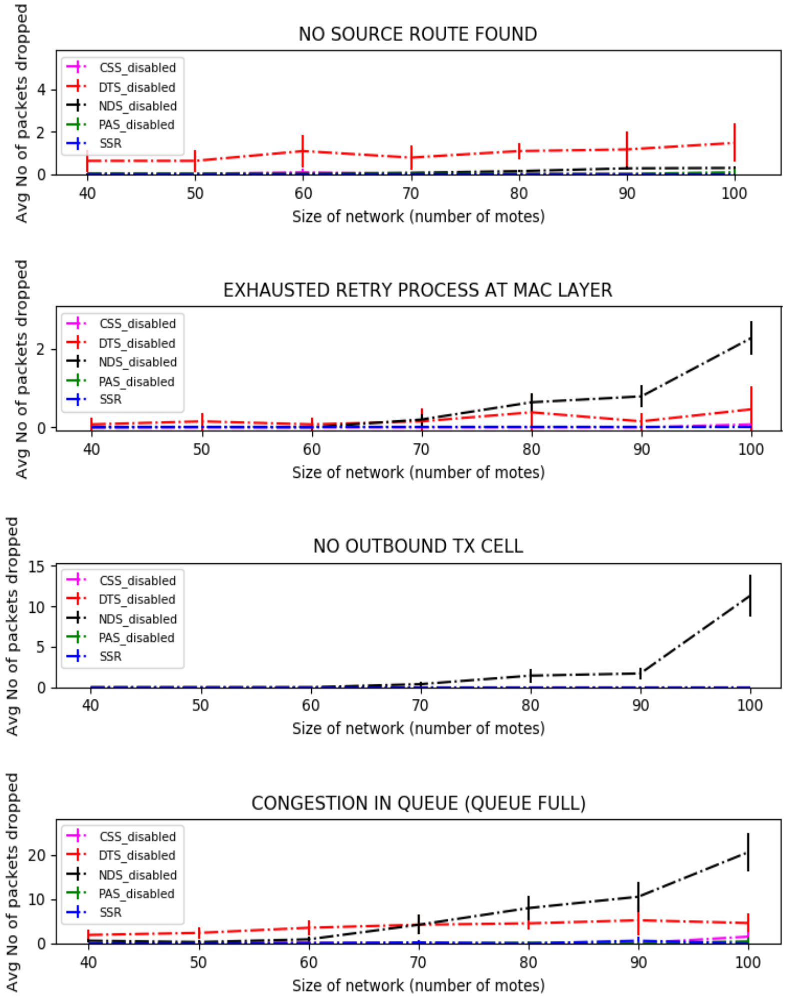

Figure 50.Poor resilience following the deactivation of NDS and DTS.

The 4th subplot in Figure 50 depicts queue congestion, demonstrating the importance of NDS and DTS. While the impact of DTS is less pronounced, it affects networks of all densities. Disabling NDS results in a linear increase in packet loss, particularly starting from networks of 70 nodes, then rapidly increasing up to 20 packets over 100 nodes networks. In this scenario, the influence of the CSS and PAS is minimal, as these strategies have a greater impact under heavy traffic or extended network densities beyond 100 nodes.

Next, latency is analyzed. Latency is typically measured as the total time taken for a packet to travel from a source node to the root. With more excess cells available, packets can often take a one-hop route, reducing latency. Figure 51 shows a trade-off between energy consumption and increased latency of 5 seconds (500 slots) when DTS is disabled. DTS mitigates this trade-off by allocating more Tx cells to a smaller number of nodes, based on their hop distance to the root. The other strategies, CSS, and PAS, do not significantly impact latency.

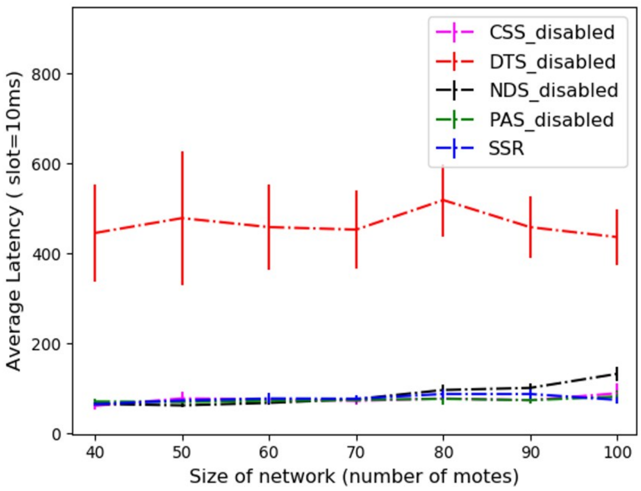

Figure 51.SSR's latency as a function network density.

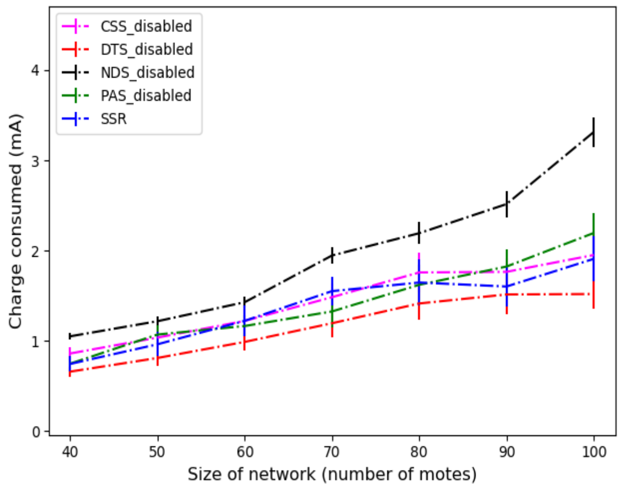

Figure 52. SSR's strategies with regards to charge consumption.

Figure 52 illustrates charge consumption as network densities increase. For most scheduling metrics, charge consumption follows a linear trend; as more cells are scheduled for network-related activities, charge consumption rises correspondingly. The interaction between NDS and DTS significantly influences consumption due to the under- or overestimation of required cells.

When NDS is disabled, a higher number of extra cells are scheduled per node following a uniform distribution, while disabling DTS results in no additional cells being scheduled. This effect is clearly depicted in Figure 52. Conversely, when the other strategies are disabled, the consumption level remains the same as SSR.

A poorly synchronized network can lead to frequent collisions; when multiple nodes are scheduled on the same cell, resulting in a decline in the PDR at the receiving node. Additionally, collisions can escalate as consumption increases. When NDS is disabled, consumption reaches an upper bound.

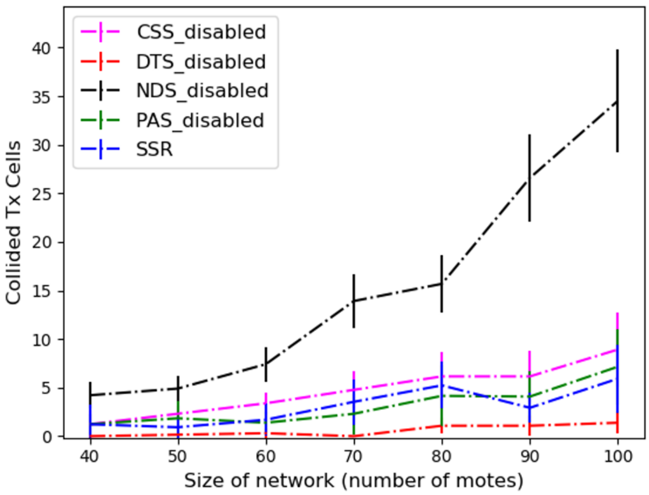

Figure 53. SSR's strategies with regard to collision.

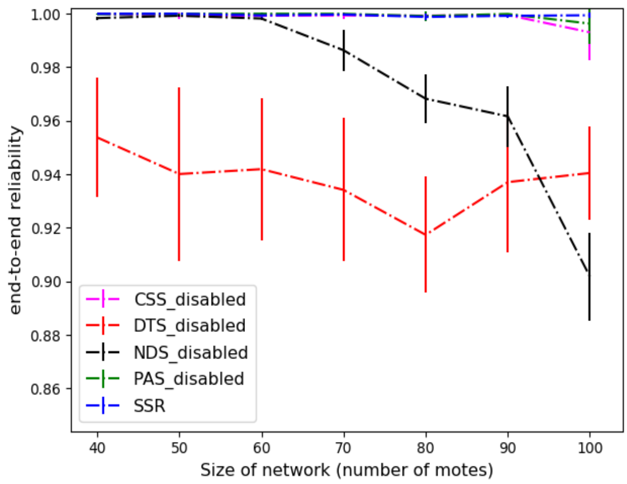

Figure 54. SSR's strategies influence on End-to-End Reliability.

Figure 53 demonstrates that the number of collided Tx cells increases linearly as the network is growing, Thus, reaching approximately 35 cells in a 100-node network due to the disabled NDS. In terms of reliability, Figure

54 indicates that performance is co-influenced by both DTS and NDS. DTS generally contributes to a drop in reliability when disabled, while a more pronounced decline is witnessed starting from networks of 60 nodes when NDS is disabled. Apart from these, CSS does not show significant difference in performance besides, a slight decline witnessed with 100 nodes network, trailed by disabled PAS, through, the differences in performance are not significant especially; with PAS, which will require a further investigation.

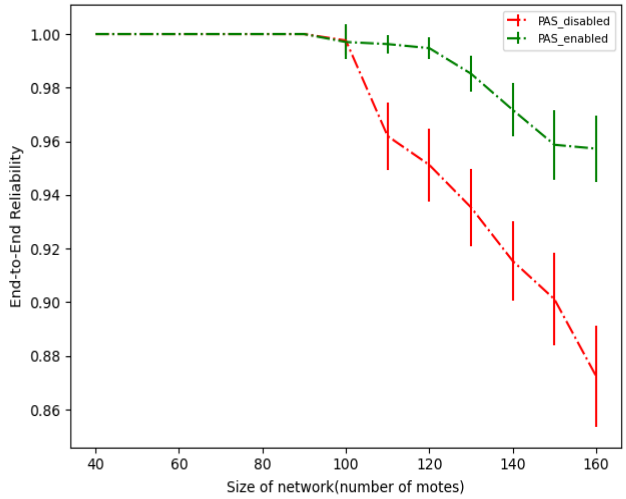

Figure 55.The evolution of PAS with extended network size.

To evaluate the performance of PAS, an additional experiment was conducted by increasing the number of nodes in the network, scaling up to 160, while keeping all other simulation parameters consistent with those listed in Table 11. The results, as illustrated in Figure 55, reveal that PAS plays a critical role in maintaining reliability in larger networks. Specifically, the reliability demonstrates a steep decline when PAS is disabled, particularly as the network size surpasses 100 nodes. This emphasizes the necessity of PAS for ensuring reliable communication by easing congestion in high-density networks.

4.6.3. Comparing SSR with Popular SFs

This section evaluates the performance of SSR against other prominent SFs, focusing on KPIs such as latency, reliability, battery life, and collision. The experiment is conducted under identical parameters outlined in Table 11, except the packet generation interval (packet period) is adjusted to 2 seconds. This adjustment allows for a fair and consistent comparison across the SFs while observing their behavior under less challenging traffic conditions.

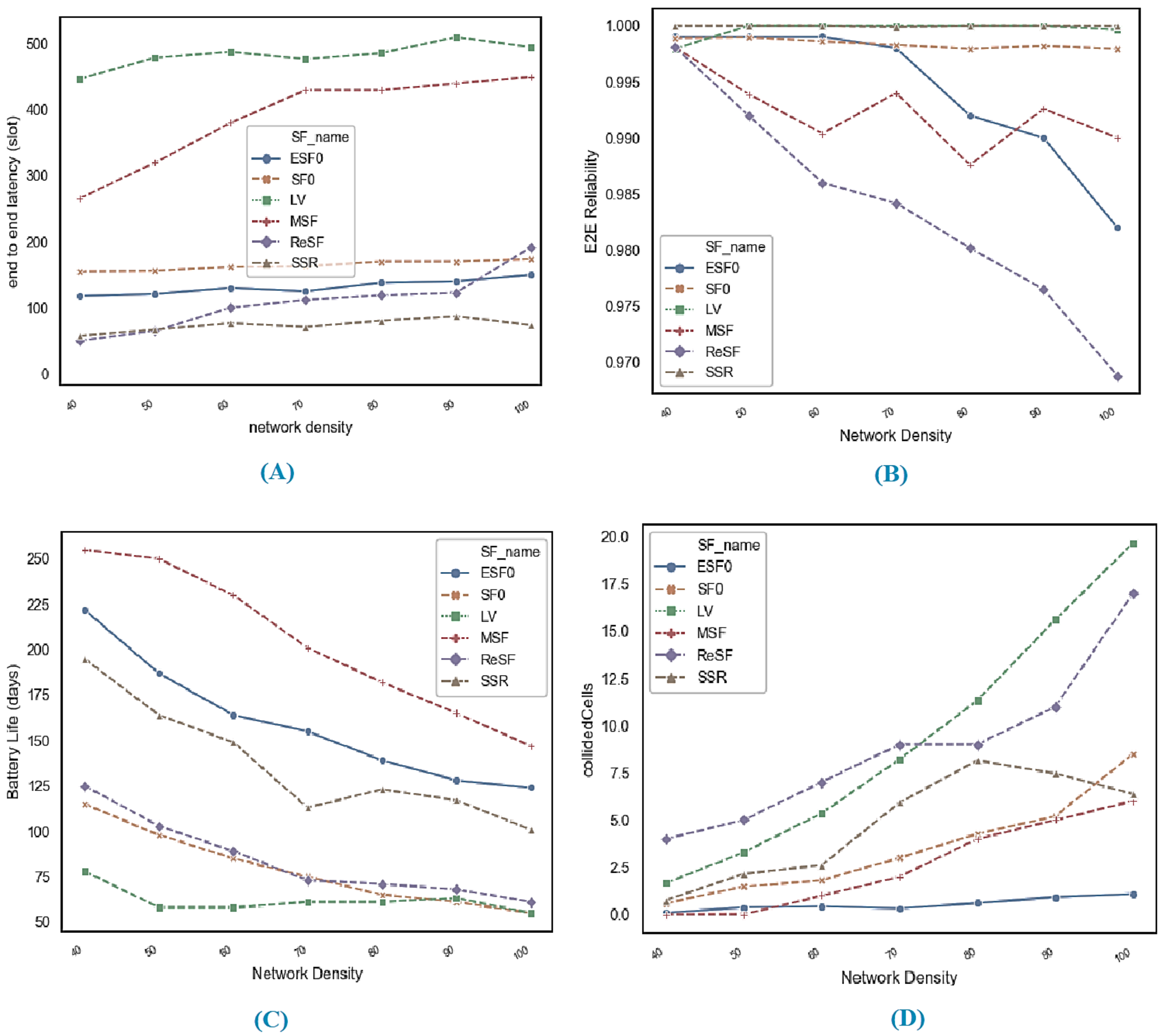

Figure 56. benchmarking results of SSR against other key SFs.

The four subplots (A-D) in Figure 56 provide a comparison of solutions (ESF0, SF0, LV, MSF, ReSF, and SSR), based on KPIs under varying network densities:

1. **(A) End-to-End Latency:** Latency increases with fewer cells awarded to the nodes in 6TiSCH network, leading to a trade-off with slotframe consumption and number of hops to the root provided all packets are sent to root. SSR demonstrates the lowest latency, consistently remaining under 1 second for network sizes up to 100 nodes, due to its adaptive and efficient scheduling strategies. In contrast, MSF and LV exhibit higher latencies; MSF struggles with poor traffic adaptation, while LV divides traffic equally but fails to allocate extra cells for path-probing and ignores poorly performing nodes as well leading to a longer path while a shorter one could have been discovered by nodes. SF0, which does not add extra cells, averages a latency of 1.5 seconds. ESF0 and ReSF achieve slightly better latency through distinct mechanisms: ESF0 places cells closer together in the slotframe for lesser delay, and ReSF uses queue mapping, and signaling to accurately predict cell requirements ensuring delivery in advance by allocating

cells per link-basis. SSR outperforms all other SFs by maintaining lowest latency even as network density increases.

2. **(B) End-to-End (E2E) Reliability:** Figure 56 (B) illustrates end-to-end reliability as network density increases. SSR and LV maintain near-perfect reliability, with LV showing slight packet loss initially but stabilizing quickly. In contrast, other solutions like ESF0, ReSF, MSF display a negative linear trend in reliability as the network scales up to 100 nodes. This decline is attributed to poor traffic adaptation, which results in packet drops due to the inability to accommodate increased network demand effectively.
3. **(C) Battery Life:** Battery life reduces as network density increases. MSF outperforms all other SFs by maintaining the highest battery life, followed by SSR. MSF is radically different from other SFs as it focuses on reducing consumption of dedicated cell. SSR, on the other hand, use dedicated cells for both managing control overheads and data packets, causing increased consumption, but it is comparatively lower than SF0, and LV, with LV being the worse energy-friendly SF. Though, ESF0 show a slightly higher battery life than SSR, it triggers a trade-off with reliability as can be seen in Figure 56 (B).
4. **(D) Collided Cells:** As the number of scheduled cells increases, particularly in dense network of 100 nodes, the collisions also increases proportionately, leading to more frequent housekeeping in the network and if retransmission continues with the same cell, leads to packet-loss. This is evident in Figure 56 (D), which compares different solutions with regards to collision in Tx cells. It reveals that collision increases with network density for all SFs. SSR has the fewest collisions because nodes awarded with higher cells form a compact topology, leading to small gap between slots; though it does not affect reliability as the nodes in closer routing proximity have extra cells, with these, alternate paths to relay the payload can be used. This advantage is not available to ReSF, while scheduling follows link-basis allocation, ignoring poor links and change events, leading to higher collisions, compared to SSR. ESF0 and SF0 also perform well where SF0 use smaller portion of cells, and ESFO use overprovisioning of 1 cell per node, allowing gap between the slots, and with channel-change, nodes are less likely to encounter collision unless all portions are fully occupied.

SSR outperforms most SFs in terms of latency, and reliability, and collision avoidance, making it well-suited for dense IoT networks. However, MSF leads in battery life, and ReSF offers competitive latency too but faces jitters with reliability. ESF0 leads with improved collision avoidance, but drop packets.SF0 is less effective overall, particularly for dense networks.

4.6.4. SSR vs OTF Under Adverse Traffic Conditions

This section benchmark results of OTF and SSR using a slightly challenging traffic condition. The packet period is reduced to *1s*. That is each node generates 60 packets per minute on its scheduled time. This experiment is divided based on the scale of network operation. The simulation parameters are as shown in Table 11, except the 6Top housekeeping timer is reduced to 2s, meaning that the node's status will be reviewed more frequently.

4.6.4.1. SSR vs OTF Evaluation in Medium-sized Network

This subsection will evaluate a 50 node network over 200 slotframe cycles. Each slotframe cycle last approximately 1 second. Therefore the entire duration of experiment is set to 200 seconds. This is as per the propagation model employed. Increasing the number of slotframe cycle using this version of 6TiSCH simulator results in repetition of the results. The results will be focused on *KPIs such as Latency, consumption of cells, collisions*, and *6Top overheads.* The reliability is plotted in the next section with even wider range of networks.

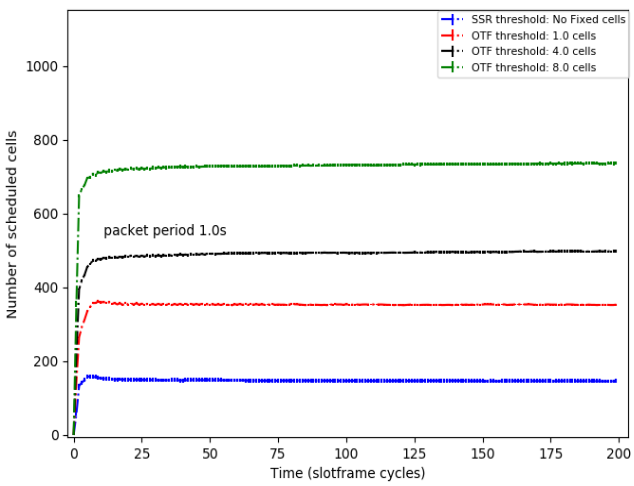

Figure 57.Cell consumption over time, 60 packets per minute.

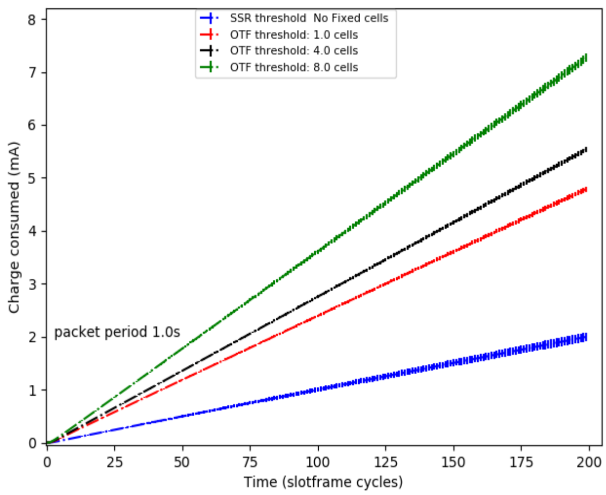

Figure 58.Charge consumption(mA) over time, 60 ppm.

Figure 57 shows, OTF with multiple thresholds is scheduling more cells than SSR. The different threshold limits in OTF seem to result in linear growth over cell consumption.

Charge consumption is calculated on a per-node basis and expressed in milliamperes (mA), as shown on the Y-axis. This reflects the recorded consumption over 200 slotframe cycles, averaged across 100 simulation runs. The 6TiSCH simulator accounts for changing topologies in each run, resulting in an average charge consumed by nodes across various network activities over these 100 runs; individual assessments for each topology are not considered.

In Figure 58, the charge consumption for OTF appears to depend on cell consumption. As overprovisioning increases, OTF consumes more current (mA) due to idle listening caused by a higher volume of extra cells allocated to the nodes. Consequently, consumption is higher with a greater threshold for OTF and lower with a reduced threshold.

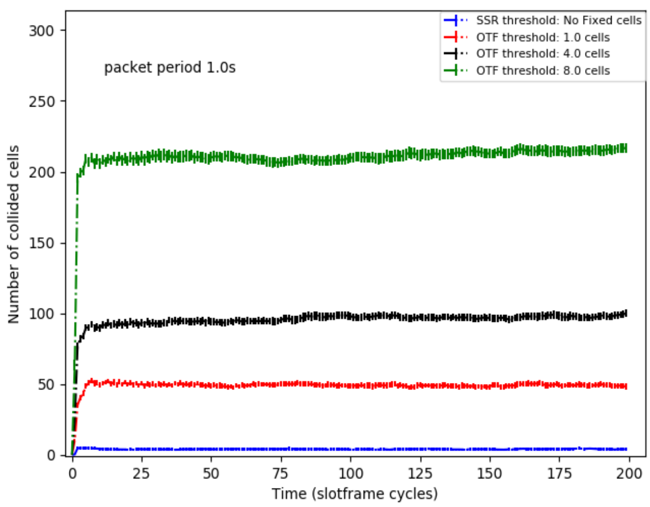

Figure 59.Collision in Tx cells over time, 60ppm.

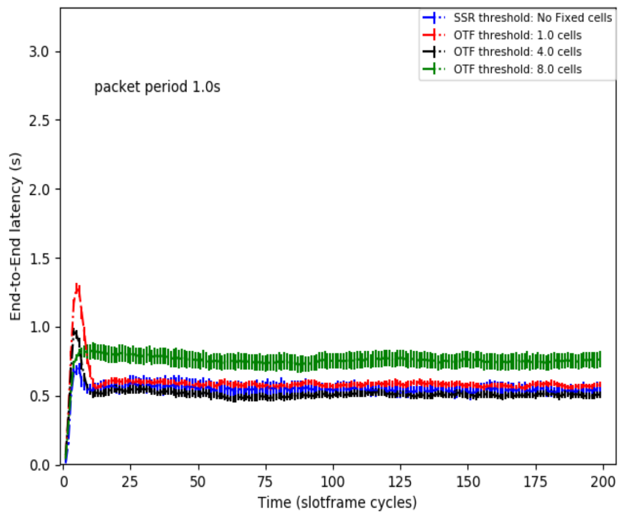

Figure 60.End-to-End latency (s) over time, 60 ppm.

A high number of collisions can significantly impact network stability. Figure 59 illustrates that every fourth or fifth cell scheduled by OTF experiences collisions. Consequently, a fixed threshold limit proves ineffective, as it may under- or overestimate the number of over-provisioned cells relative to data volumes. In contrast, SSR demonstrates nearly zero collided cells. The results of SSR, presented in Figures 57, 58, and 59, do not exhibit trade-offs with other metrics evaluated in this experiment. In terms of consumption and collisions, dynamic overprovisioning effectively mitigates the conflict between high consumption and collisions, as employed by SSR.

Figure 60 illustrates end-to-end latency over time, showing that latency initially increases between timestamps 0 and 20. As most nodes successfully schedule TX cells and join the network, more routes are discovered, facilitating shorter paths to the root and easing congestion through the availability of multiple routes. The latency for both SFs stabilizes around 1 second or lower, with SSR and OTF (using a lower threshold of cells) exhibiting the same minimum delay, which is roughly 40% less than the delay experienced by OTF using 8 cells (a higher threshold).

This outcome contrasts with expectations, as one might anticipate lowest latency with a greater number of cells allocated to all nodes. However, congestion arises when more nodes lead to one-hop convergence toward the root. As most nodes utilize the single best path, congestion becomes challenging to manage, causing packets to wait prior entering the Tx queue along the busiest routes.

Regarding SSR's performance, it experiences an initial spike in latency to 1 second (lower than the spike caused by lowest threshold of OTF) between the first 0 to 20 slotframe cycles but then settles at a lower latency comparable to OTF using 1 and 4 cells, with 4 cells per node yielding a slightly lower latency than SSR. This demonstrates that SSR operates without the trade-offs observed with OTF.

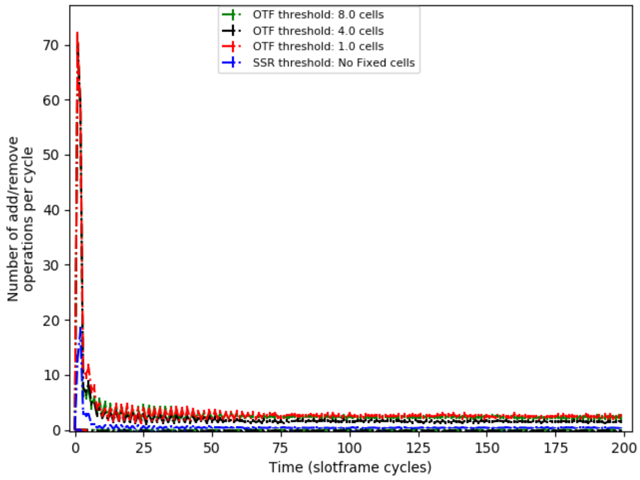

Figure 61.ADD/DELETE activities over time, 60 packets per minute.

Figure 61 describes the frequency of *ADD/DELETE* transactions over a period of time. The scheduling function instructs 6Top to manage cells for sensor nodes at run-time. Thus, a lower bound is preferred. **Figure 61** shows a pattern in OTF, as the threshold limits advance, the number of 6Top a*dd/remove* activities decreases.

This pattern is opposite to the consumption pattern shown in Figure 57, Figure 58, and Figure 59. Hence, OTF causes a trade-off between consumption and the 6Top activities where the SSR appears to maintain a balanced view in this regard.

4.6.4.2. SSR vs OTF Evaluation in Larger Networks

SSR is evaluated against OTF with varying threshold limits in networks up to 100 nodes but under challenging traffic condition: the simulations parameters are provided in Table 11 where this experiment follows packet generation interval= 1s (60 ppm), and the housekeeping timer is set to 2s. In the subsection 4.6.4.1, the results were plotted over time using a 50 node network using packet period of 1s besides the performance was analyzed over time. This experiment takes average value, presented with 95% CI, grouped by OTF threshold (cells). The scenarios looked into this experiment include cell consumption, collision, latency, battery life, and reliability.

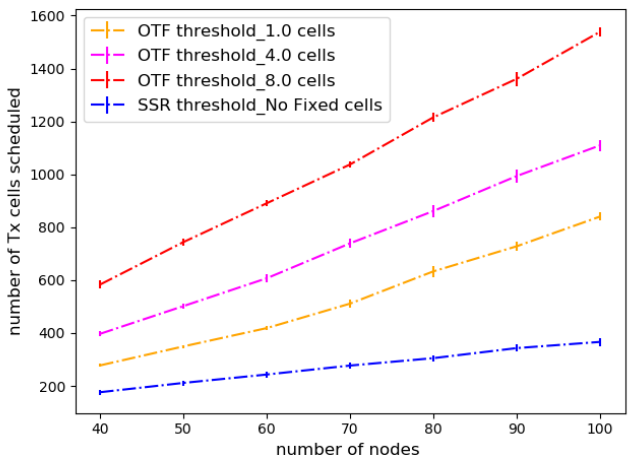

Figure 62: Volume of TX cells scheduled by SSR and OTF.

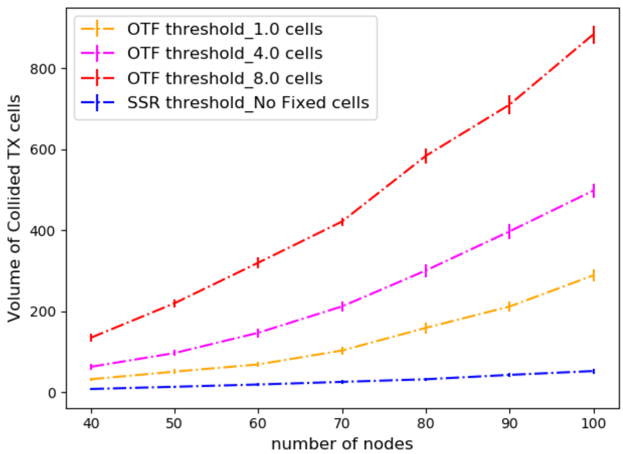

Figure 63: Volume of cells collided by SSR and OTF.

In comparing the number of collided Tx cells to the volume of scheduled cells across each configuration, Figure 62 and 63 shows significant differences for each grouping variable (SFs):

For **OTF Threshold 1.0**, the scheduled cells increase linearly with the number of nodes (Figure 62), and while the volume of collisions also rises (Figure 63), it remains relatively low compared to higher thresholds. This configuration achieves better control over collision, indicating moderate efficiency, though not as effective as SSR. The proportion of collided cells to scheduled cells is smaller, showing a balanced scheduling strategy that avoids excessive collisions.

With **OTF Threshold 4.0**, both the number of scheduled and collided cells increase noticeably compared to the 1.0 threshold. Although the volume of collided cells grow, it is still lower than the highest OTF threshold of 8.0. This suggests a moderate level of efficiency, as the OTF scheduling permits collisions regardless the random selection (slots and channel id).

For **OTF Threshold 8.0**, the volume of scheduled cells is the highest, but it comes with a significant trade-off. The collision volume also reaches its peak, indicating a high inefficiency in densely populated networks. The high ratio of collided cells to scheduled cells suggests that with this threshold, the scheduling method fails to manage bandwidth effectively, leading to frequent and costly collisions. In contrast, **SSR** consistently maintains the lowest number of scheduled and collided cells across all network densities. Collisions remain minimal as a fraction of the scheduled cells, even as the network scales up. This highlights SSR's strength in optimizing cell scheduling and avoiding collisions effectively, showcasing its efficiency in high-density networks.

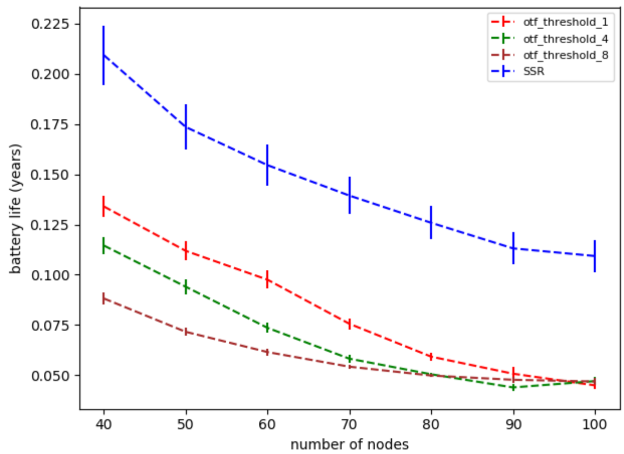

Figure 64: Battery life of both SSR and OTF using 60ppm.

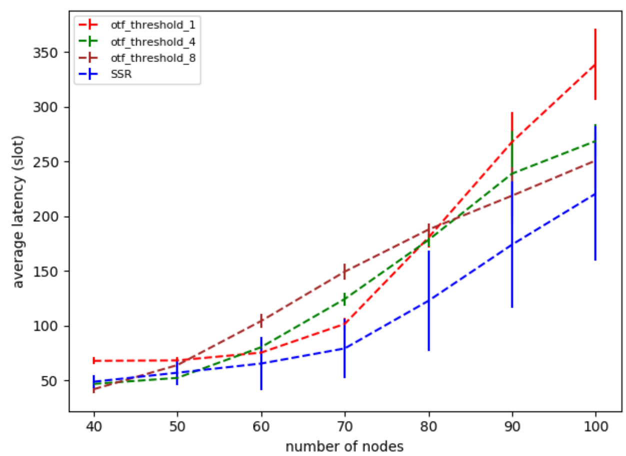

Figure 65: Average latency for both SSR and OTF.

Figure 64 illustrates the impact of high consumption by both SFs on the battery life of the network. It reveals, when the network exceeds 90 nodes network, the difference in battery life of SSR and OTF becomes significant, with OTF levelling off at approximately 0.06 or about 20 days. In contrast, SSR offers a considerably longer battery life at higher network densities, with the battery lasting roughly 45 to 50 days, is about 50% improvement over OTF for networks with 90 to 100 nodes. This occurs when each node generates 60ppm over regular period of time, and housekeeping is performed every 2 seconds, ensuring node's status is checked more frequently.

Battery performance can improve significantly with fewer nodes, particularly in the 50–70 range, under favourable traffic conditions besides there are other indicator that may have considerable impact on performance while further reducing the cell scheduled by SSR. This includes latency where sufficient extra cells helps the nodes progress to shortest path to root.

Figure 65 illustrates the average latency (in time slots) as the number of nodes in the network increases, comparing the performance of OTF configurations with thresholds of 1, 4, and 8, and SSR. As network density grows, the latency rises across all configurations, with the OTF Threshold 8 experiencing the highest latency, reaching over 350 slots (3.5 second) at 100 nodes. OTF Threshold 1 and 4 show moderate latencies, though they still increase significantly with network size.

SSR demonstrates the lowest latency, maintaining a steady and lower growth rate, which indicates better scalability and efficiency. This suggests that SSR is more effective in handling increased traffic loads with reduced latency compared to OTF configurations, making it advantageous in scenarios where lower latency is critical for industrial scenarios..

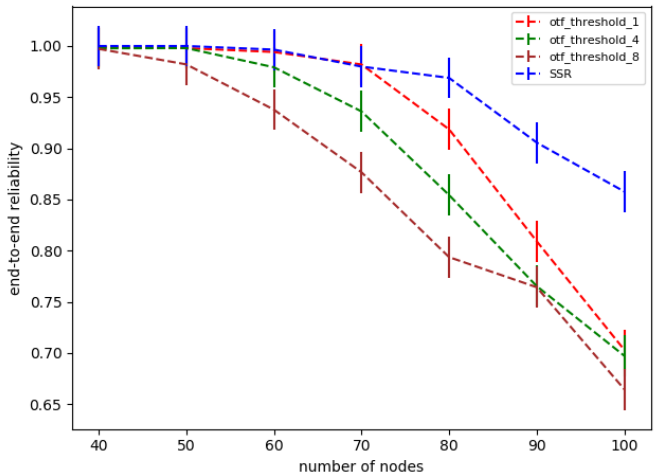

Figure 66. E2E reliability using packet generation period 1s (60 packets per minute).

Figure 66 shows that SSR is outperforming OTF for all tested network sizes. Indeed, its advantage is growing with the size of networks. While SSR declines with an increase in network density as well, it does so significantly more slowly than OTF. To further improve SSR and meet application demand, high node-churn is required where the network depth strategy will require a tuning up through the existing *rank* interval used and DTS needs to be updated so that poor performing nodes are avoided from being given cells.

4.7. Summary

The Section presented a novel distributed scheduling function (SSR) implementing TSCH-MAC over IEEE802.15.4e standard for improvement in scalability of 6TiSCH networks. SSR assesses various scheduling needs dynamically using a *four-pillar* model. In particular, the *slicing* operation is considered the core logic assisting faster delivery of the time-sensitive traffic in a dynamic 6TiSCH topology. SSR is therefore an improvement to SF0, OTF, and ESF0.The performance of SSR was assessed through simulation run over increasing networks of up to *100* nodes. Using a varying packet generation period of *2s*, *5s*, and *10s*, SSR achieved high resilience to packet loss.

In the analysis of SSR's scheduling strategies, the results confirmed that all four strategies play a key role in improving the scalability of the 6TiSCH network. The comparative analysis using a packet generation period of *2s,* has shown that SSR can upstream a packet to root in just under *1s* while having achieved 99.9% reliability, a lower collision rate, and reasonable battery life.

Finally, SSR's performance was assessed against OTF with varying threshold limits under an incrementally challenging traffic scenario (packet period *1s*). The results showed that SSR outperforms OTF in all the tested scenarios, however, it incurs a steady loss of reliability beyond 60-70 nodes. The key reasons include poor proliferation of information in the network, with fewer routes available for nodes to take to reach destination and these the routing does not eliminate poor links, and manage load under unicast-based scheduling.

5. SSR USING HYBRID SCHEDULING DESIGN

Chapter 4 evaluated SSR under a heavy traffic stream of 60 packets generated over a regular period where each node generated approximately 60 ppm. The results showed the shortcomings of SSR in terms of steady decline in reliability due to scaling and high control overheads. The dedicated cells are utilized by SSR for both for managing topology and adapting traffic are limited in the slotframe. Consequently, the availability of free cells depends on how frequent the radio is on for performing network-related activities. Although, SSR used the lowest form of charge consumption, maintains a linear association with cell consumption.The steady fall in performance was due to poor propagation, leading to fewer alternative paths and the capacity of the Tx queue is constrained (10 packets). A frequent demand (to add and remove cells) by a node that is already experiencing a higher volume of traffic due to poor load-balancing triggers congestion [256], is responsible for performance degradation.

Hybrid scheduling can overcome these inconsistencies by separating control packets from data packets. It is designed overcome the frequent need to add more dedicated cells for each and every node by using centralized execution model for all non-data traffic (autonomous cells). These are the shared cells that are accessed on contention-basis. For data packet, distributed scheduling is found suitable. The implementation of SSR in the hybrid scheduling design can benefit from overheads reduction and improve scalability of 6TiSCH network. MSF is a generic hybrid solution reviewed in Subsection 3.1.5.1 in Chapter 3.

This section outlines key changes to SSR's model in order to adapt hybrid scheduling design; this requires meaningful selection of SSR's strategies prior their implementation within the skeleton of MSF. For performance evaluation, the latest version of the 6TiSCH simulator will suffice as it can assess performance over extended period of time based on 'K7' connectivity traces (the propagation characteristics are explained in this chapter).

5.1. NDS for Hybrid Scheduling

NDS is one of most influential strategy assisting resource-allocation based on the routing dynamics of RPL. The implementation of NDS may vary depending on applicability and scheduling design. There are necessary changes proposed to the NDS implementation. The enhanced version of NDS is articulated in Figure 67 for readability-sake and the actual algorithm is shown in Figure 68. According to the algorithm, the variable, 'Rankinterval (*R*)', is initially set to 512 and it increases by 256 with each iteration. The standard library of RPL ,by default, gives the value of ***maximum rank*** and the rank of a particular node if at all exists in the subnet at then time. The variable called $prev_{hop}$ is used to store initial rank intervals of previous hops so that comparison can be meaningful against the node's current rank value, ensuring current rank of a node is greater than the $\boldsymbol{prev_{hop}}$ where the $\boldsymbol{hop_{id}}$ is initially set to 1 and it increases iteratively.

For articulation of the enhanced NDS, we retain slotframe length (S)= 100, and network depth (D)=4. Using these values, the cake-slicing function provides a distribution (O), which is equal to {63,21,10,6}.

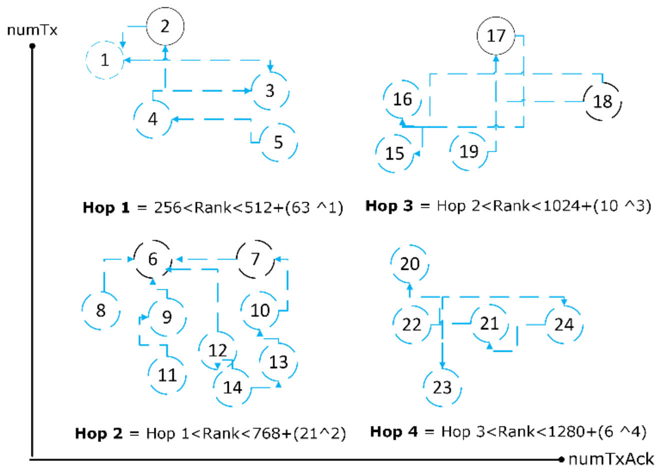

Figure 67. Evolution of NDS following hybrid scheduling.

Algorithm 2 Network Depth Strategy

NDS (node_id)
  $\boldsymbol{rank} \leftarrow$ RPL.OF0.getRank(node_id)
  $\boldsymbol{maximum\ rank} \leftarrow$ RPL.OFO.getMaximumRank()
  $\boldsymbol{R} \leftarrow 512$, $\boldsymbol{hop} \leftarrow 0$, $\boldsymbol{prev_{hop}} \leftarrow 256$
  Do
  if $\boldsymbol{prev\_hop} < \boldsymbol{rank} < \boldsymbol{R} + (\boldsymbol{O_{hop_{id}}})^{\boldsymbol{hop_{id}}}$
    Break
  Otherwise
    $\boldsymbol{hop\ increases\ by\ 1}$
    $\boldsymbol{R}$ increases by 256
    $\boldsymbol{prev_{hop}} \leftarrow \boldsymbol{R} + (\boldsymbol{O_{hop_{id}}})^{\boldsymbol{hop_{id}}}$
  endif
  while $\boldsymbol{R} < \boldsymbol{maximum\ rank}$
  return $\boldsymbol{hop}$

Figure 68. Network Depth Strategy Algorithm.

According to the example in Figure 67, the enhanced NDS assume a node being 1 hop away from the root if the corresponding rank of the node falls within the range 257 and (512+63^1). Here, the *rankinterval (R)* is 512, and $(O_{hop\_id})^{\wedge hop\_id}=63^1$. For ‘hop 2’, *rankinterval* increases to 768 that is the sum of rankinterval and maximum increase allowed; hence the rank condition becomes hop1 < rank<($768+21^2$). Note that 21 is the 2nd element (value) in the list O denoted by O_{hop_id}. Similarly, for hop 3 and hop 4. The rank becomes hop 2 < rank < ($1024+10^3$), and hop 3< rank<($1280+6^4$) respectively. Note that 10 and 6 are the 3rd and 4th consecutive elements in the list O (O_{hop_id}). The algorithm terminates as the rank of a node is located with these conditions applied, determining the node’s appropriate depth in the routing topology.

5.2. CSS for Hybrid Scheduling

CSS stresses on selection of timeslot being allocated closer together towards the top-left side of the slotframe; this strategy causes reduction in queuing delay as a difference of time a packet has arrived and the packet that left the queue. In the hybrid scheduling model, CSS can provoke collision in shared cells because more than one nodes can end up using cells that have minimal gap, causing the selection less dynamic and more predictable. A random selection mechanism is more suitable here rather than CSS, with Rx cells not allowed to be reactively adjusted by SSR.

5.3. DTS for Hybrid Scheduling

DTS ensues extra cells are provided to nodes to adapt traffic efficiently. It is utilized in hybrid scheduling based on NDS and the cake-slicing technique, unaltered. According to this, the nodes with closer proximity to the root (such as at hop 1) are given more cells than the nodes located further away from the root and have higher rank value (such as at hop 2,3,4…N). In hybrid scheduling, traffic adaption is performed based on the condition where MAX_NUMCELLS = NUMCELLSELAPSED this means when the adaption delay (MAX-NUMCELLS) meets total volume of 6Top transaction by a node for the given slotframe cycle; hence the traffic adaption becomes functionally dependent on the value of MAX_NUMCELLS.

The proposed approach distinguishes from existing traffic adaption approaches of hybrid scheduling based on the prediction of overprovisioning cells that a node can be provided, is purely a statistical exercise. The algorithm of DTS is shown in Figure 69, followed by a coherent example describing DTS in Figure 70.

Algorithm 4 Schedule allocation

SSR_ADAPTION (hop_id, S, D)

$O_T \leftarrow$ SLICER (S, D)

X$\leftarrow$ NUMBER OF CELLS TO ADD/DELETE

If $\frac{NUMCELLUSED}{NUMCELLELAPSED} > \frac{(S-O_{hop_{id}})}{100}$ **then**

$\mathbf{X} \leftarrow \frac{(O_{hop_{id}}) \ll 3}{2}$ => add Tx cells

endif

if $\frac{NUMCELLUSED}{NUMCELLELAPSED} < 0.25$ **then**

$\mathbf{X} \leftarrow \frac{(O_{hop_{id}}) \ll 3}{2}$ => delete Tx cells

endif

return

Figure 69. Traffic adaption using SSR under hybrid scheduling design.

The traffic adaption algorithm in Figure 69 shows the value of X is computed if the comparison between Tx utilization (NumCellUsed/NumCellElapsed) and DTS threshold, computed by subtracting the corresponding element of **O_{hop_id}**, from **S**, divided by **100**. The algorithm use O_T as a list variable containing the output of cake-slicing function called SLICER.

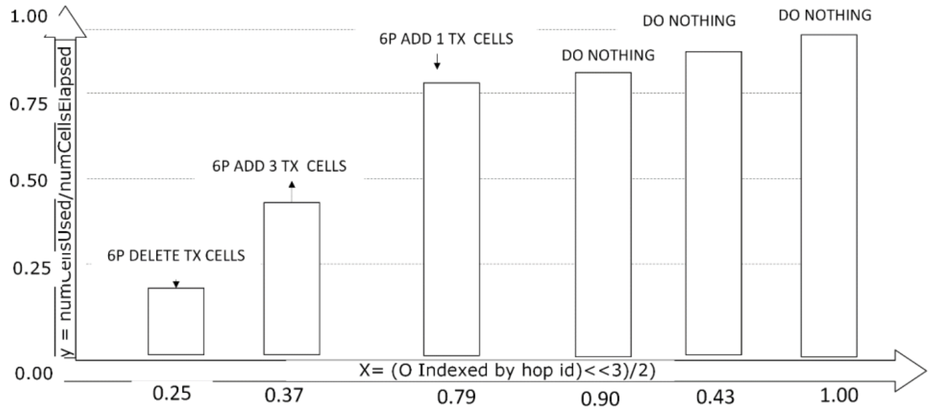

O indexed by hop_id	Hop_id= {1,2,3,4}	X	Vol. of numCell ADD/DELETE
63	1	(100-63)/100= 0.37	(63<<3) /2= 3
21	2	(100-21)/100= 0.79	(21<<3) /2= 1
10	3	(100-10)/100=0.90	(10<<3) /2= 0
6	4	(100-7)/100= 0.94	(6<<3) /2= 0

Figure 70. Articulation of enhanced DTS for hybrid scheduling.

The example shown in Figure 70 follows cake-slicing projections such as $O_{T=}$ {63,21,10,6} provided S=100 and D=4. Figure 70 is divided across two objects (graph and a tabular structure). The graph depicts traffic adaption and relevant statistics are recorded in the structure below for the sake of making description less complex.

Further, the DTS threshold is compared against the Tx utilization threshold as can be seen at the Y-axis in graph in Figure 70**.** If **t**he TX utilization is higher than DTS threshold, then **X** is computed based on O_{hop_id} by shifting 3 bits to the right using bitwise operator and then the outcome is divided by 2. The structure below the graph in Figure 70 exhibits relevant values.

The rationale behind DTS comparison with TX utilization threshold is such that the value of NUMCELLSUSED counter is generally much lower compared that of value of NUMCELLSELAPSED [253], and Tx utilization varies at different levels in RPL topology simply because some nodes forwards more packets than the others.

Here, nodes located closer to the root, with DTS threshold being 0.4, are not given extra cell by DTS if Tx utilization is below 37% or 0.37. However, if the volume of NUMCELLSUSED increase beyond this threshold and Tx utilization increases beyond 0.37, then the nodes are given 3 Tx cells, assuming frequent transmissions due to being in closest proximity to root, and there can be more than 1 node predicted in this periphery**.** Contrarily, if the DTS threshold = 0.79 and nodes are in the periphery of hop_id 2, SSR assumes there more than 2 nodes presents to forward traffic and unanimous distribution of high volume of cells can lead higher volume of 6top transaction. That way, 1 extra cell is sufficient per node**.** Further, DTS threshold increases within the periphery of Hop 3 where neither nodes are given extra TX cells due to the risk of increased hop-distance between forwarding nodes in routing topology. A detailed analysis based on the varying DTS threshold is provided with the outcome in Figure 70.

5.4. QOS for Hybrid Scheduling

Queue optimization strategy is adopted as it is implemented in Chapter 4.

5.5. Performance Evaluation

This section provides valuable insights into SSR's performance under various network conditions and topologies. For benchmarking, MSF is used, by default implemented in 6TiSCH simulator. The simulator implement OpenMote CC2538 with all key modules such as board configuration, RF modules, and other features [214].

The current version of 6TiSCH simulator is crucial from the point of testing network stability over long time. It implements the full set of 6TiSCH protocols along with the ‘K7 connectivity trace’ [263] (derived from several real testbed results) which replaces existing propagation model. It follows the duty-cycle limits proposed by [169] following each possible radio activities (see Chapter 3). With connectivity trace, it offers more realistic results over extended slotframe cycles and performs well in terms of simulation speed and scenario testing. In terms of traffic generation, it provides two models, which are discussed in Chapter 3. After the end of each slotframe cycle, the battery consumption is computed based on a equation, by default implemented by programs given under 6TiSCH simulator. This equation is as follows:

$$\frac{AA_{mAh} * 10^3/'avg_{current'_{uA}}}{24.0 * 365} \ldots\ldots\ldots\ldots\ldots\ldots..\ldots\ldots\ldots.(4)$$

AA_mAh represent battery capacity and $avg\_current_{uA}$ represents average current consumed per node and it may varies depending on the many indicators included through the analysis.

Network bootstrapping using hybrid scheduler is a complex process. Each node sends minimum of 15 beacons to nearby devices and await response. Based on this, the link's PDR is computed, which must not be less than 0.5 for a qualifying stable node. The configuration parameters follow RFC 5673 [26]. The RSSI is set to -97dBM, indicating the ability to translate the weak signal without consuming excess power. The maximum power consumption is limited to 14mA. These configuration parameters are briefly explained in Chapter 3.

The joining process is explained in Subsection 3.1.4.1 in Chapter 3. The only difference here is the dedicated cells are allocated on demand-basis, whereas for all the other unicast data, nodes use pre-computed autonomous cell. The propagation characteristic follow minimal cell configuration (single broadcast cells, situated at 0^{th} slot in slotframe 1, which is only one slot long. To ensure that EBs are not generated excessively, a probability value is assigned, which is 0.1. The broadcast probability for DIOs is 0.33 (is same for most experiments). This means the networks experiences no significant difference in RSSI and PDR despite $2/3^{rd}$ reduction, is as per the assessment of *Vučinić et al.,* [221]: this significantly reduces consumption.Table 12 shows configuration parameters used with most experiment in this chapter, besides the values may change for each experiment, dedicated to test specific scenarios.

Name	**Parameters**	**Name**	**Parameters**
Deployment Area	[2*2] km	PDR	0.5
Communication patter	MP2P	Maximum number of packets sent	15
Node's buffer	[10] packets	Battery capacity	[2821.5] mAH
VRB Table Length	[2] rows	Radio sensitivity	[-97]decibel-milliwatts
Radio Frequency Band	[2.4]GHz	Number of nodes	[50,60,70,80,90,100]
Maximum available channels	16	Topology	Random, Linear
Max retransmission attempt	5	MAX_NUMCELLS	[4,16,32,64,100]
SSR's MAX_NUMCELLS	Not fixed	SlotFrame Length	[33, 101] slots
Housekeeping period	[30]s	Duration per run	[66.7]minutes
RPL's Objective Function	OF0	Number of runs	[100]
DIO's interval	[10]s	Packet generation interval	[0.1, 0.5, 1.0, 2.0, 20]s
DAO's interval	[60]s	Keep Alive (KA) messages	[10]s
Broadcast Beacon probability	0.1	Broadcast probability of DIOs	0.33

Table 12. Configuration parameters for 6TiSCH simulator using connectivity trace.

Table 10 shows for testing network performance, DIOs are dispatched every 10s, while the DAOs are sent every 60s to update the path information at the root. The housekeeping mechanism keeps in check for every 30s and collision in advertisement/shared slots is handled with default back-off mechanism provided in IEEE 802.15.4. Each node implements VRB as described in Chapter 3. The nodes are deployed randomly in the deployment area of 2 square kilometers, with each node showing link PDR greater than or equal to 0.5.

The experiment lasts 66.7 minutes where each slotframe cycles last 1s approximately. The results are an average value, presented with 95% CI. Each experiment follow unique set of parameters to test network performance including packet period, duration per run, number of runs, MAX_NUMCELLS (traffic adaption delay), slotframe size and topology. The remaining configuration parameters are as explained in Chapter 3.

5.5.1. Analysis of Traffic Adaption Delay & Queue Utilization with High Traffic Load

The simulation settings, shown in **Table 13,** highlighted values depicting difference of simulation strategies and traffic conditions. For every experiment, a unique strategy is planned; while this experiment is focused to analyzing the impact of varying traffic adaption delay (MAX_NUMCELLS), introduced by MSF. The results are compared against SSR that does not use a fixed value of the adaption delay.

Name	**Parameters**
Number of nodes	[**50**]
Topology	Random
MAX_NUMCELLS	[4,32,64,100] cells
Slotframe Length	[**33**] slots
Duration per run	[**66.7**]minutes
Number of runs	[100]
Packet generation interval	[**1.0**]s

Table 13. Simulation Parameter for medium-sized network using 33 slots.

This section tests a 50 nodes network using random deployment with in the area of 2*2 km. The slotframe length is reduced by 33 slots, 1/3rd of the maximum slotframe length (101 slots). Each simulation run lasts 66.7 minutes where the experiment is repeated over 100 times.

In terms of packet generation, each node generates 60 packets per minute over a regular interval of time.

This experiment demonstrate the importance of variable traffic adaption threshold where a lower value such as MAX_NUMCELLs= 4, allows traffic adaption fairly sooner and as soon as the total number of 6Top (successful or not successful) surpasses 4, for each node. As this increases, no new cell is given to node for forwarding the traffic that is until it reaches the defined limit. Though, with exceptional increase, the traffic adaption becomes seemingly none and with a lowest threshold, it triggers frequent transaction aiding the nodes to deal with the temporary peak of the traffic **[253]**.

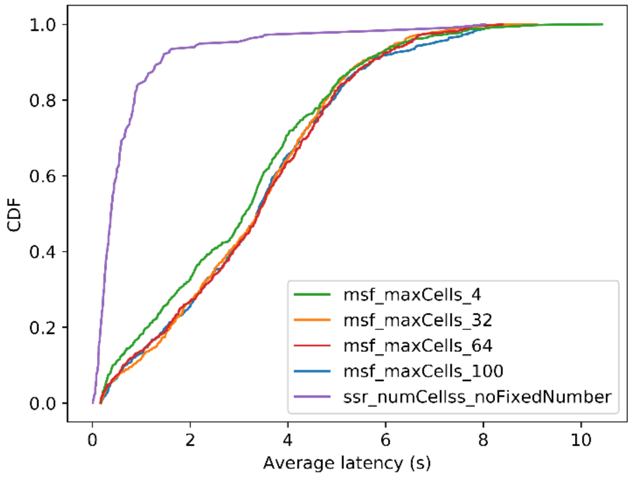

Figure 71.Comparing average latency delay.

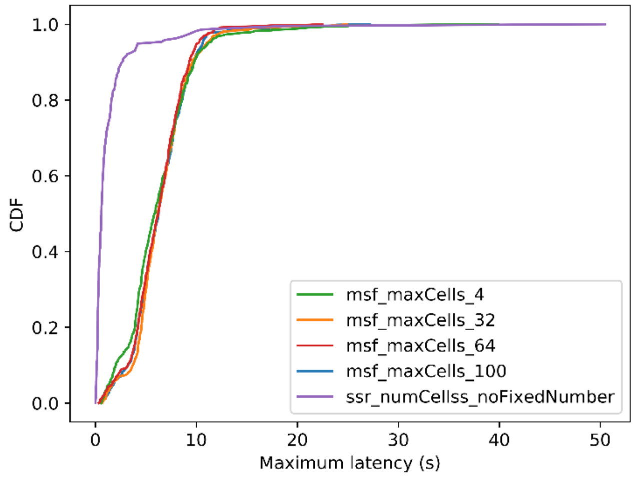

Figure 72.Comparing maximum latency of MSF and SSR.

Figure 71 compares the average latency across different configurations of MSF and SSR using Cumulative Distribution Function (CDF) graph. SSR outperforms all MSF configurations by achieving significantly lower latency, as evident from its steep rise to near-complete distribution within 1 second. In contrast, MSF configurations towards adaption delay exhibit slower improvements with decreasing number of cells. That is, even, at shortest delay (MAX_NUMCELLS= 4), MSF lags behind SSR. Figure 72 shows that SSR triggers lower maximum latency compared to MSF's all configuration. The CDF in both Figure 71 and 72 exhibit average latency by MSF is *3s* at a probability of about 90% and the maximum latency is viable and larger (reaching about *10s*), with very few outliers (some nodes take longer to deliver than others). Clearly, the impact of smaller slotframe and lower threshold does not gain traction for MSF. In contrast, SSR maintains a smooth curve showing both average and average maximum latency delay at a 90% probability, being roughly *2s*, which is a lower value compared to the latencies triggered by MSF.

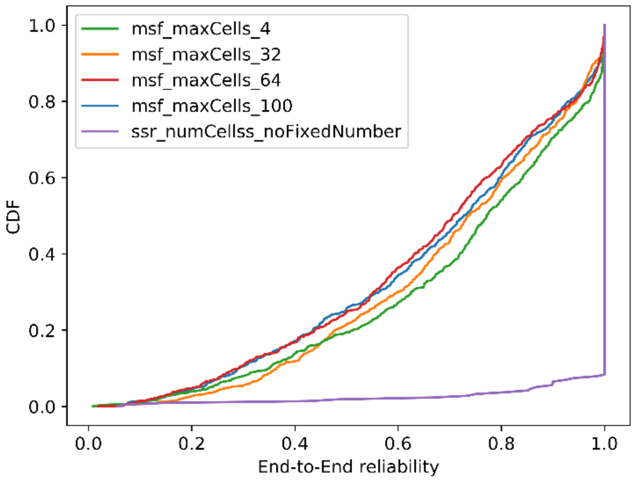

Figure 73.Comparing end to end reliability.

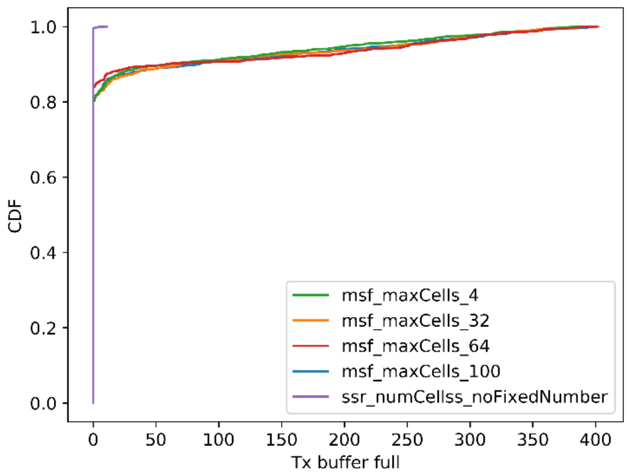

Figure 74.Comparing congestion-induced loss.

Figure 73 shows the impact of variable and fixed adaption delay on reliability using CDF plot. The results show that SSR achieves near-perfect reliability for most nodes with a steep curve, highlighting its superior performance compared to MSF, which shows more gradual improvements as the adaption delay (maxCells) increases. The mean reliability for SSR approaches 1.0, while MSF ranges from 0.80 (maxCells_4) to approximately lower ratio for all other thresholds. The key reason for this difference is congestion: SSR demonstrates significantly reduced congestion losses in Figure 74, with its curve indicating fewer instances of the Tx buffer being full. In contrast, MSF configurations show increasing losses as maxCells decrease, with the mean Tx buffer occupation (volume of packets) being notably lower for SSR compared to MSF (mean for SSR <50 vs. MSF_maxCells_4 >200). Overall, MSF registers significant output loss, up to 20% as is shown in Figure 74.

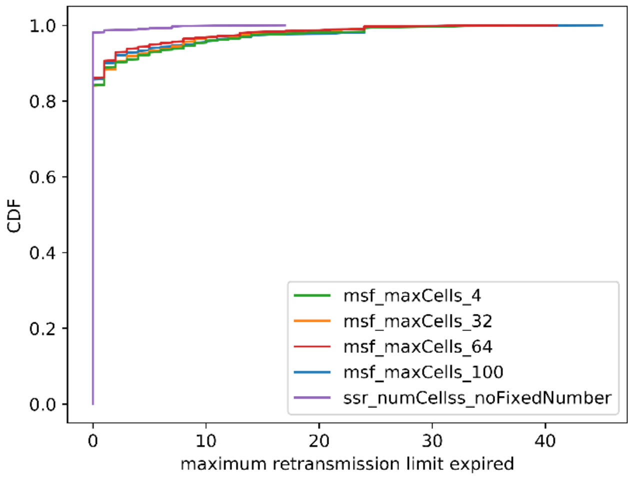

Figure 75.Comparing loss due to exhausted retries.

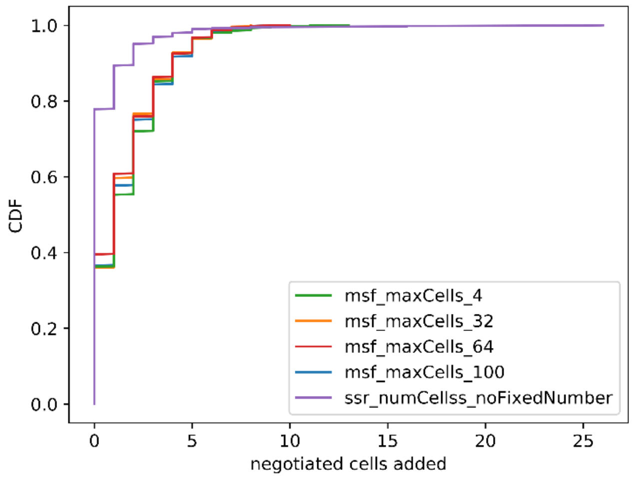

Figure 76.Comparing Tx cell utilization by both SFs.

As far as the impact of retries is concerned, SSR maintains minimal loss due to maximum retransmission limited expired, as indicated by its sharp rise to near-complete CDF (in Figure 75) within fewer retransmissions. In contrast, MSF shows variability, particularly for lower delay (lower maxCells threshold), with mean loss higher for MSF_maxCells_4 compared to MSF_maxCells_100. The standard error for SSR is negligible, emphasizing its efficiency. There are two key reasons for the surge in retries led by MSF: (a) *higher transmission delay* such that if the delay is significant, radio is tuned off after waiting for certain time that is packet is made to be retransmitted. (b) *poor propagation*, which is not exclusive to MSF except the increased hop distance causing distant node to reset the clock (see Figure 79). This gets worsen under random topology.

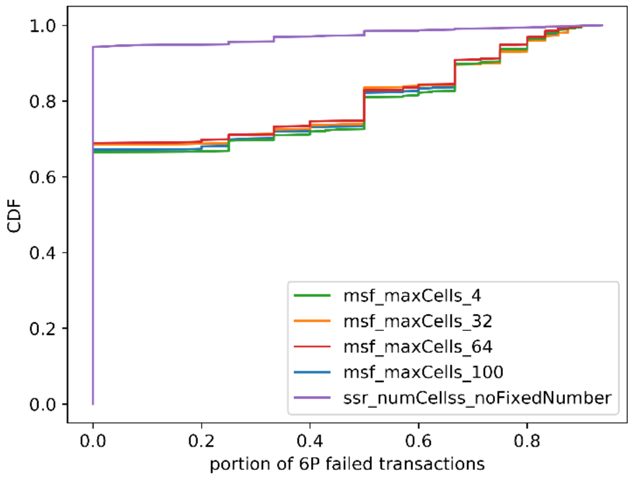

Figure 77.Comparing average portions of failed 6P transactions.

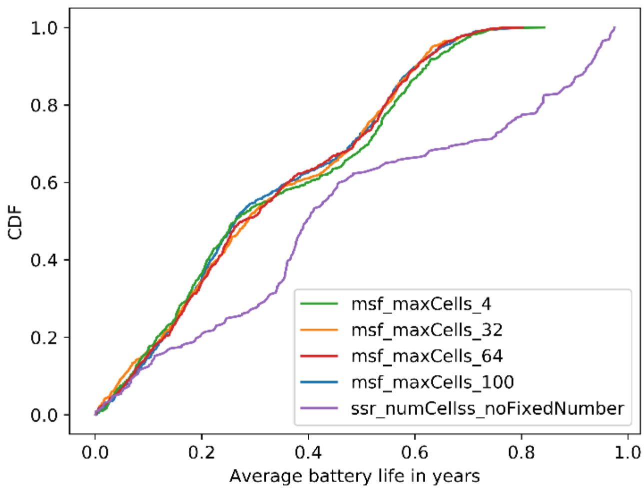

Figure 78.Comparing average battery life, 33 slots, 60ppm.

Apart from that, in smaller slotframe (33 slots), retransmission can impede energy consumption. This is reflected in **Figure 78,** showing difference in the battery life for MSF and SSR. The reason for the variance can vary based on the adaption delay using a multitude of causes: Energy consumption can be affected by the way Tx cell utilization occurs (as shown in Figure 76) along with failed transactions (6P errors shown in Figure 77); TSCH scheduler reports these erroneous transactions besides the reason may varies depending status of the cells (such as cells being used elsewhere in the network or still serving quarantine period due to collision). As a result, MSF triggers poor Tx utilization, use higher volume of cells (shown in **Figure 76),** with significantly higher volume of failed 6P transactions (shown in **Figure 77)** and higher retransmission (as shown in **Figure 75)**. Conversely

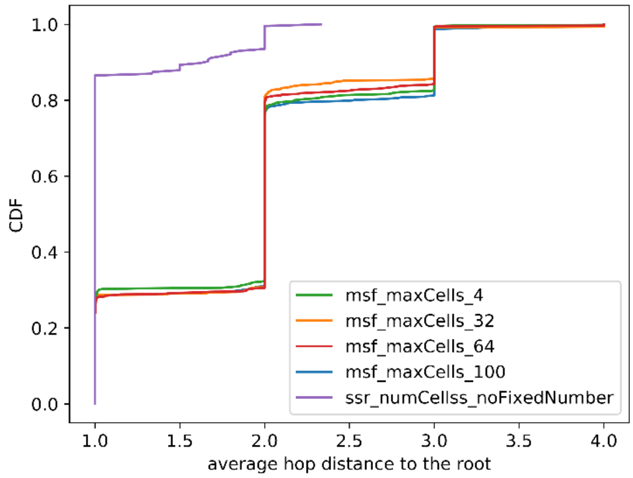

Figure 79.Comparing average hop distance for MSF and SSR.

Figure 79 provides insights into how the random topology translates into the volume of hops over an hour long operation using the given settings. It demonstrates that SSR achieves a more compact and efficient network topology. In remotely operated wireless networks, nodes frequently connect and disconnect, and if the root node goes down or reboots, the entire network hierarchy is lost. Therefore, a lower joining delay is preferred to quickly resume data streaming.

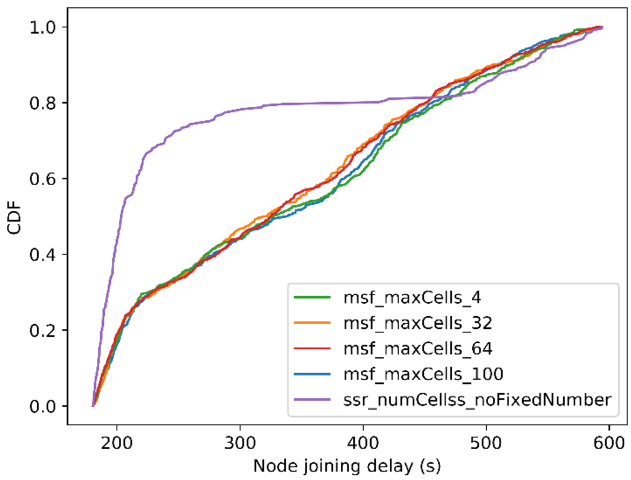

Figure 80.Comparing node joining delay using 33 slots.

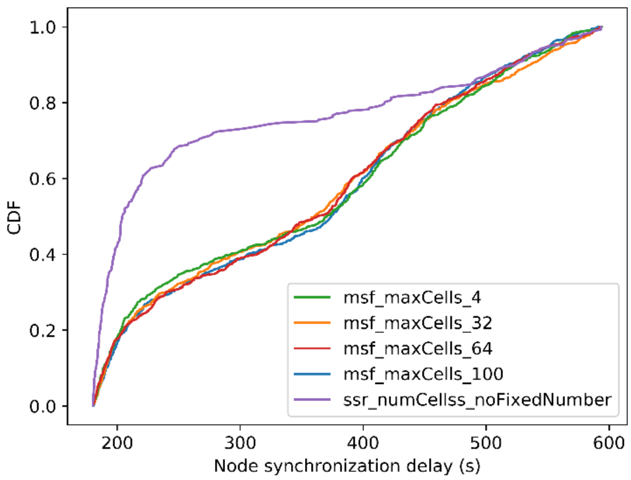

Figure 81.Comparing synchronization delay using 33 slots.

The process for node joining is roughly the same for both MSF and SSR. **Fig. 80** and **81** present average joining and synchronization delays caused by both SF over given network conditions and using varying configurations of MAX_NUMCELLS. In a smaller slotframe size, SSR exhibits a shorter joining and synchronization delay for most nodes and renders a more compact topology. That way, it allows nodes to join network at a lower distance to root. The increased distance **(Fig. 79)** provokes propagation loss where nodes receives EBs at delay. This is te key reason why nodes using MSF takes longer to join and synchronize. Essentially; the delay between joining and synchronization is negligible for both SFs following their individual joining delay assessment.

5.5.2. Scalability Analysis

This section assesses scalability using varying density of nodes per installation as the packet generation interval is set to 0.5 (120ppm). This experiments undertakes increased network size and increased load factor. The CDF are kept side by side to allow comparison. Since each experiment is unique, the modification across configuration parameters is highlighted in bold text in **Table 14**.

Name	**Parameters**
Number of nodes	[**50,60,70,80,90,100**]
Topology	Random
MAXNUMCELLS	[**32]** cells
Slotframe Length	[**101**] slots
Duration per run	[66.7]minutes
Number of runs	[100]
Packet generation interval	[**0.5**]s

Table 14. Configuration parameters for scalability experiment using hybrid scheduling design.

This experiment demonstrate scalability of 6TiSCH network where both MSF and SSR are to be tested with growing traffic load and increasing number of network densities.

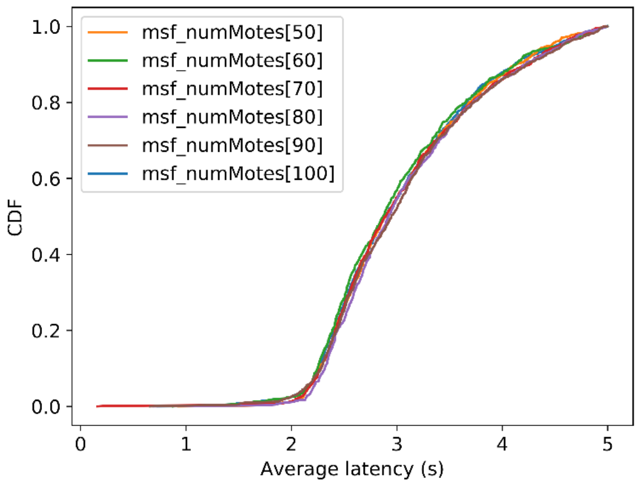

Figure 82. Comparing MSF's latency using 101 slots, 120ppm.

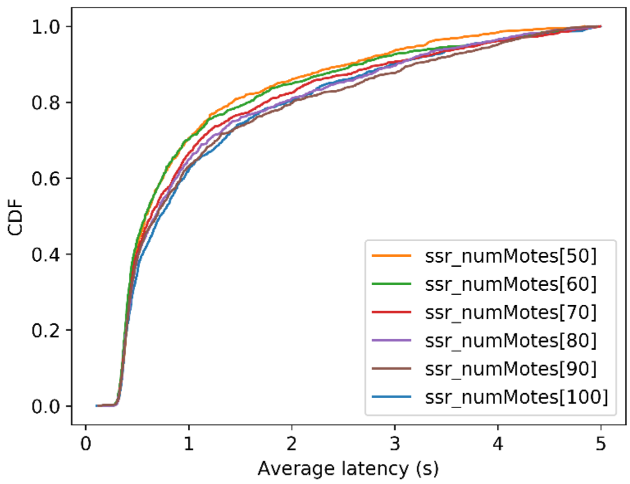

Figure 83. Comparing SSR's latency using 101 slots, 120ppm

The CDF shown in Figure 82 and 83 documents latency performance of SSR and MSF, with maximum adaption delay being 32 cells. Further analysis pertaining latency is provided separately for each graph, making it easier to interpret.

Latency (Figures 82 and 83):

- **MSF:**
  - Latency gradually increases with higher mote counts, reflecting congestion due to limited cell allocations and poor adaptation. The mean latency ranges from approximately 2.2 seconds (50 nodes) to 3.5 seconds (100 nodes).
  - The CDF curves for MSF indicate slower convergence to the maximum, especially for higher node counts, suggesting delays for a significant portion of packets.
  - Standard error increases with node count due to variability in latency.
- **SSR:**
  - SSR achieves consistently lower latency across all node counts. The mean latency ranges from about 0.8 seconds (50 motes) to 1.2 seconds (100 motes), which is significantly lower than MSF.
  - The steep CDF curve for SSR indicates minimal latency variation, and standard errors are consistently small, even for higher node counts.

SSR outperforms MSF, with latency reductions of approximately 60%–70%, and its low standard error highlights its stability. Clearly MSF is not a latency-centric design where it uses fixed threshold-based hysteresis throughout the scheduling allocation. These results are representative of heavier traffic condition to 120ppm, where each node forms a random topology following industrial network requirements.

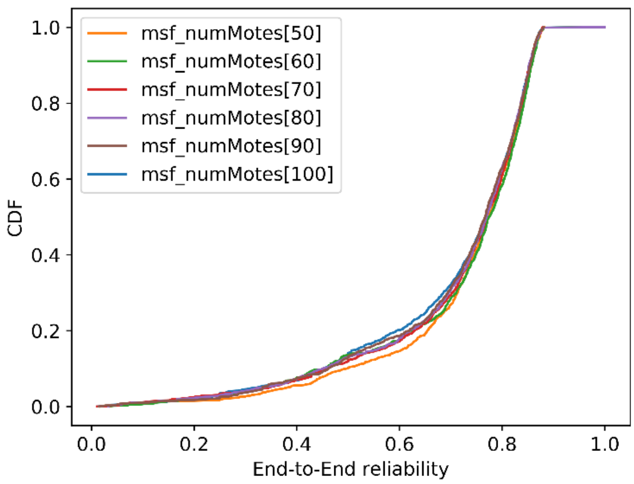

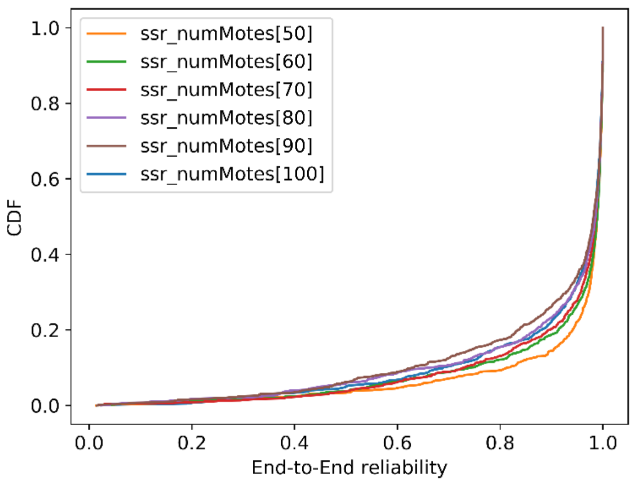

Figure 84. Comparing MSF's reliability using 101 slots, 120ppm. **Figure 85. Comparing SSR's reliability using 101 slots, 120ppm.**

MSF makes poor decisions in terms of adapting traffic on demand, causing poor mismatch with actual traffic condition, and impedes power-savings where nodes are given higher volume of cells recurrently. The key highlight relating reliability performance by both SSR and MSF is provided, as follows:

End-to-End Reliability (Figures 84 and 85):

- **MSF:**
    - Reliability decreases with an increase in network density, with mean reliability ranging from ~90% (50 nodes) to ~75% (100 nodes). The reliability decline is due to poor traffic adaption, leading to packet loss.
    - The CDF curves for MSF reveal that only a fraction of packets achieve high reliability for larger networks, and standard error increases significantly with network density.
- **SSR:**
    - SSR maintains near-perfect reliability (>98%) across all node counts. The CDF curves converge steeply, indicating that almost all packets achieve high reliability, even under dense networks.
    - The standard error for SSR is negligible, showing its robustness in handling network scaling.

Overall SSR demonstrates superior reliability, with an average reliability improvement of 20%–25% compared to MSF, and it sustains performance with minimal errors.

The next CDF plots reveal battery performance by each SF, though, the consumption may not vary by a large proportion for the given amount of traffic load (120 ppm) and random placement. Figures **86** and **87** depict the battery consumption of the network, across various network densities, while providing key insight relating energy efficiency for the given configurations.

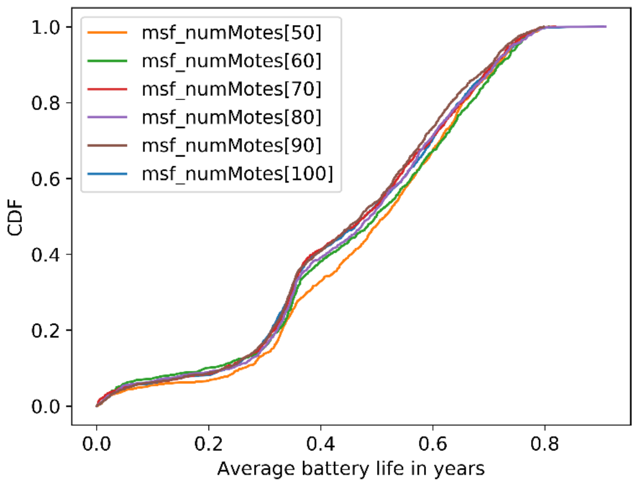

Figure 86. MSF's battery life, using 101 slots, 120ppm.

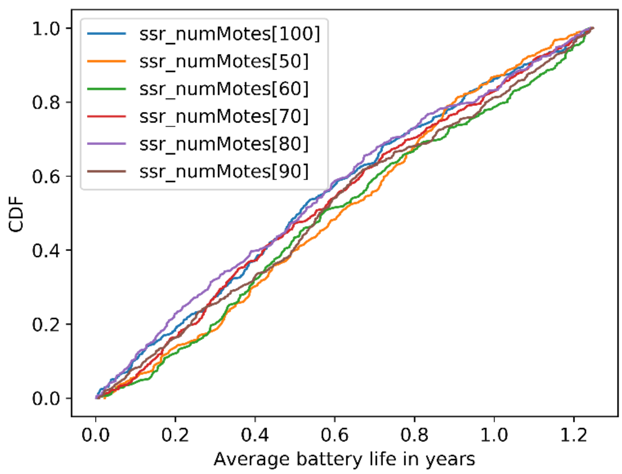

Figure 87 SSR's battery life using 101 slots, 120ppm.

MSF registers shortcoming in terms of inconsistent duty-cycle for some nodes indicated as a distinct change in its CDF in addition to a shorter battery life compared to the SSR.

Battery Life (Figures 86 and 87):

- **MSF:**
  - Battery life decreases as node count increases due to higher retransmissions and inefficient cell usage. Mean battery life ranges from ~1.0 years (50 motes) to ~0.6 years (100 nodes).
  - The CDF curves exhibit slower convergence as the node count increases, indicating increased energy consumption. The standard error also rises due to uneven energy consumption across nodes, influenced by fixed thresholds, causing slight variations (kink) in the shape of the curve as observed across all node counts.
- **SSR:**
  - SSR achieves significantly better battery life, with means ranging from ~1.2 years (nodes) to ~1.0 years (100 nodes). Its efficient scheduling reduces retransmissions and optimizes energy use.
  - The steep CDF curve and negligible standard error for SSR indicate consistent energy performance across all network densities.

Overall Comparison indicates SSR consistently outperforms MSF across all KPIs metrics:

- **Latency:** Reduced by ~60%–70%.
- **Reliability:** Improved by ~20%–25%.
- **Battery Life:** Extended by ~25%–40%.
- **Standard Errors:** SSR exhibits minimal variability in all KPI metrics, emphasizing its efficiency and scalability.

These results proves SSR's superiority over MSF, especially in dense IoT networks, making it a more reliable and energy-efficient SF.

5.5.3. Analysis using Linear Topology

This section focuses on the controlled deployment of a large-scale network using a linear topology. Linear deployment is also popular for reduced interferences from nearby nodes. The aim is to observe the impact of various periodic traffic patterns by evaluating both SFs in terms of stable, sustainable, and scalable performance. For this comparison, boxplots are used where removing the offset and maintaining horizontal alignment will result in overlapping (mix the values), making the graphs less readable. Consequently, the values are offset to improve clarity. Table 15 highlighted the key changes in bold text across the configuration parameters tailored for this experiment.

Name	Parameters
Number of nodes	[**100**]
Topology	**Linear**
MAXNUMCELLS	[32] cells
Slotframe Length	[101] slots
Duration per run	[66.7]minutes
Number of runs	[100]
Packet generation interval	[**0.1,0.5,1.0,2.0**]s

Table 15. Configuration parameters for analysis using Linear topology

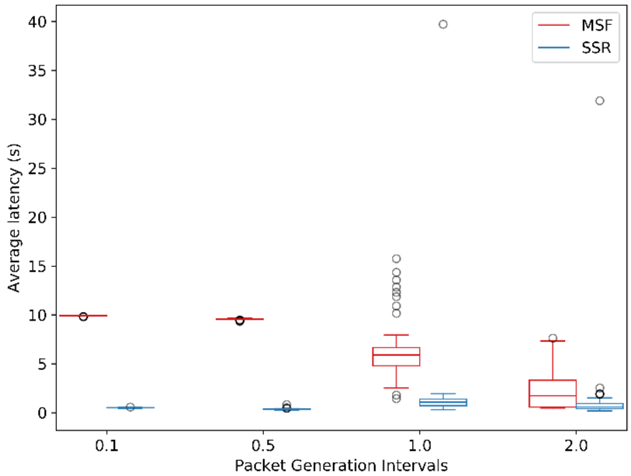

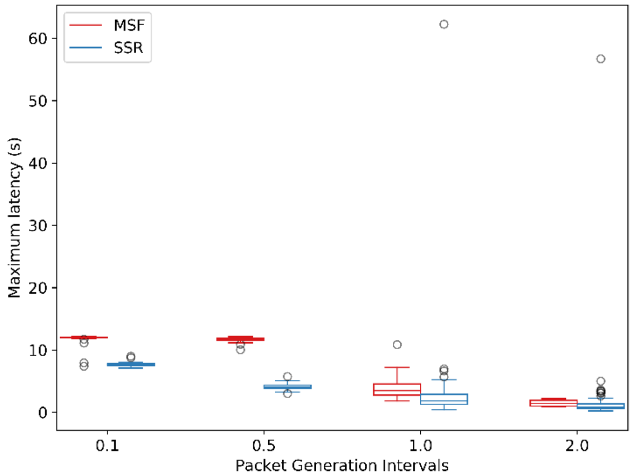

Figure 88. Average latency as a function packet period.

Figure 89.Maximum latency as a function packet period.

Figures 88 and **89** illustrate a near linear proportional increase in latency, with MSF showing a higher delay in both average and maximum latencies across packet period intervals of 0.1, 0.5, 1.0, and 2.0. Notably, the latency for MSF remains above 10s for packet intervals of 0.1 and 0.5, and it does not drop below 3s even for the longest interval. Conversely, for SSR, the average latency is around 1s for most packet generation periods, and the maximum latency decreases linearly from 7.5 to 4.5, 2, and finally *1s* for the different packet generation intervals: MSF consistently registers significantly higher average and maximum delays in controlled linear deployments too. The primary cause is poor traffic adaption and queue handling. This has further impact on packet delivery in a hop by hop manner as some nodes are more occupied than other and MSF simply allows nodes to add more cells.

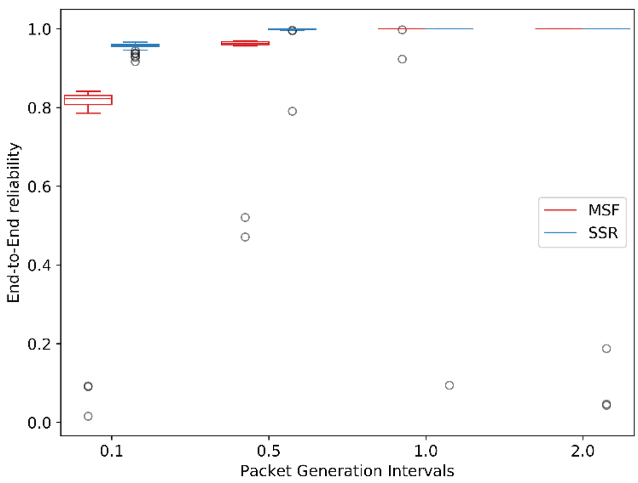

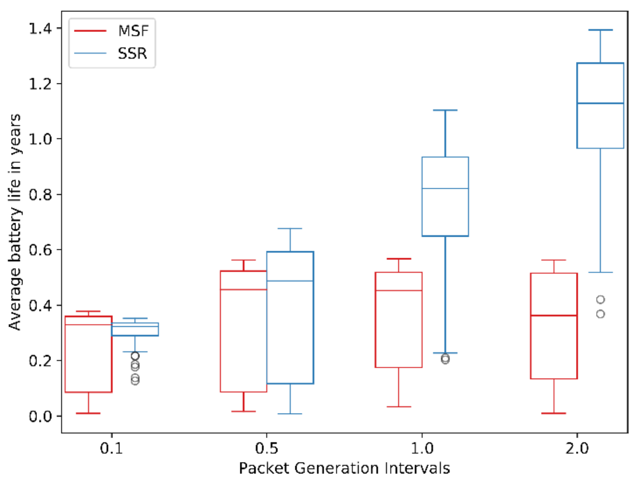

Figure 90.Reliability as a function packet generation interval. **Figure 91.Battery life as a function packet generation intervals.**

Figure 90 illustrates reliability under varying traffic loads using a linear topology. The boxplot indicates that SSR is largely resilient to packet loss. Only under extremely challenging conditions, such as a 0.1 (600 ppm) load, its performance drops slightly to about 96%. Otherwise, reliability remains stable at about 99%. MSF demonstrates equally high reliability for packet periods of 1.0 and 2.0. However, beyond these traffic generation patterns (load), MSF's reliability declines more noticeably to just over 80% for the most challenging setting.

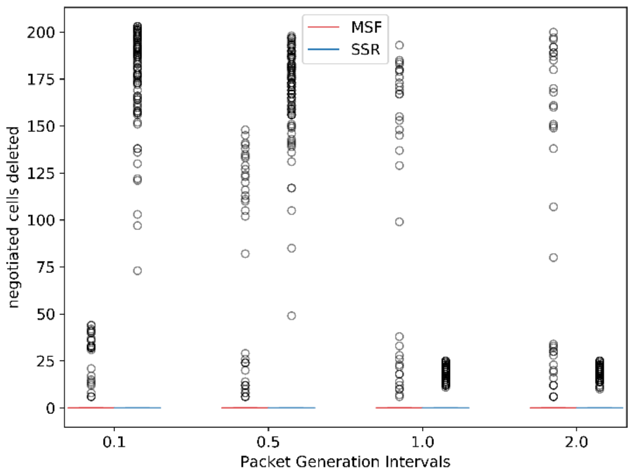

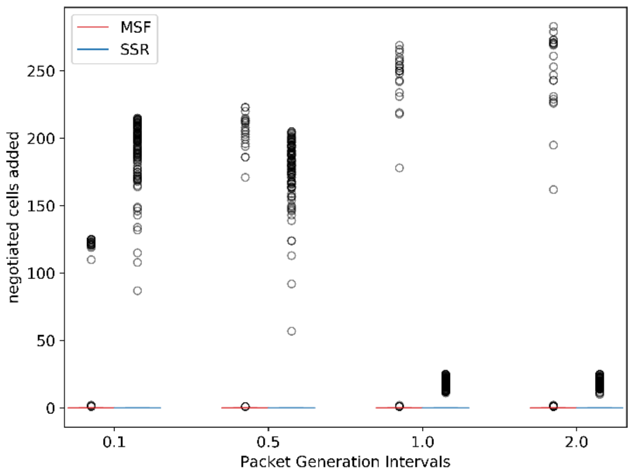

Figure 92.6P DELETE as a function packet period. **Figure 93.6P ADD as a function packet period.**

As far as battery life is concerned, **Figure 91** demonstrates that, with a linear topology, SSR offers a linear proportional increase in network age as traffic load decreases. With a packet period of 2.0s, the battery life of SSR could exceed a year. Under challenging traffic conditions of 60 ppm, the battery lifespan decreases to approximately just over 0.8 years. The lifespan declines to 0.5 years and bottoms out at 0.3 years at 120 ppm and 600 ppm, respectively. Conversely, MSF exhibits a poorer battery life estimate compared to SSR, showing no lifespan improvement with increasing packet generation intervals. Key reasons are higher overheads and fixed traffic adaption rules. This is evident from **Figures 92** and **93**, which illustrates the average volume of cells deleted and added from the negotiated slotframe where cells are not shared. The boxplot reveals a significant number of outliers, attributed to the non-uniform addition and deletion of cells by MSF and SSR due to varying traffic demands across the network. The data shows that the number of 6P cycles for deleting cells exceeds those for adding cells in both SFs. Notably, SSR triggers a minimum number of outliers at packet period interval of 1.0 (60ppm) and 2.0 (30 ppm), which positively impacts battery life efficiency, as depicted in **Figure 93**. However, as traffic load increases to 120ppm (packet period = 0.5) and 600 ppm (packer period=0.1), SSR aggressively adds and deletes cells to maintain higher reliability, however, interestingly, not for all nodes (as they are mostly shown as outliers). Crucially, for the lower packet densities, SSR adds and deletes significantly fewer cells than with the higher packet densities. Conversely, the consumption of cells is lower under the specified loads when using MSF. It's also important to note that MSF registers a decline in battery life by in response to increased traffic loads, as shown in **Figure 91**.

5.6. Summary

This chapter introduced a novel scheduling function (SSR) that implements hybrid scheduling using the TSCH mode of the IEEE 802.15.4 standard. The analysis revealed that MSF experienced a significant goodput loss even when each node generated only 60 packets per minute. This occurred despite using a simple traffic generation model, where the payload could be predicted more accurately compared to random traffic generation models.

SSR (hybrid) demonstrated improved communication efficiency compared to MSF under uniform configurations. These improvements stem from the combined influence of DTS, NDS, QoS, and randomized cell selection. As a result, the proposed solution successfully delivered approximately 99% of the total generated payload, whereas MSF exhibited shortcomings in goodput loss and higher delay. The results from Section 5.5.1 indicate that a fixed adaptation delay does not mitigate MSF's limitations; instead, the key issue lies in ensuring a sufficient number of cells for each node to effectively manage its storage buffer. The challenge of single-path delivery is universal, nodes can form a compact topology with additional reserve cells, enabling closer alignment with the root. However, MSF lacks the necessary cell availability to achieve this, leading to queuing issues and increased delay.

The results in Section 5.5.2 demonstrated that SSR effectively overcomes the limitations of MSF in terms of reliability, latency, and battery life, particularly in large-scale deployments. The experiment in Section 5.5.3 revealed a linear relationship between energy consumption and load sensitivity where SSR exhibited only a minor drop in reliability compared to an approximately 15% decrease by MSF. Additionally, the network benefits more from improved battery life more under a linear alignment where random alignment imposes a greater stress on the network due to fluctuating link stability. This instability can stem from various factors including constrained transmission range, which contributes to link quality degradation.

The comprehensive evaluation concludes that SSR as hybrid scheduling approach significantly enhances network performance, and efficiency, providing scalability and making it a suitable solution for high-traffic, and adaptive data-rate based applications. The limitation includes poor propagation and lack of randomness in traffic generation while evaluating network performance using SSR.

6. DECENTRALIZED, AND BROADCAST-BASED SCALABLE SCHEDULING RESERVATION PROTOCOL

In distributed scheduling, the participating nodes can vary depending on the number of connections (siblings) with the parent node. SSR's performance has been tested for distributed scheduling design where it used 100 dedicated cells and a single broadcast cell for propagation of EBs. While dedicated cells are fairly limited in the slotframe, SSR has performed well in comparison to the other SFs, through the scalability limitation continue to remain despite improved performance. Chapter 4 concluded that SSR under unicast-based distributed scheduling registered packet loss after 70 nodes at 60ppm. Hybrid scheduling showed potential improvement for scaling the performance up to 100 nodes with a more challenging traffic loads (120ppm), however it too showed a sharp decline in network performance over extremely challenging traffic conditions (in Chapter 5) using random deployment. One of the possible causes is the limited participation by nodes located towards the bottom of the routing topology, triggered due to limited proliferation of information.

Decentralized and broadcasted-based distributed scheduler [139] is capable to use more than one broadcast cells, allowing nodes to frequently negotiate for cells under a common ancestry that way many possible alternative routes are discovered. However, this comes at a risk with high energy consumption and shared cells are more prone to collision where communication will fail if no alternate path is available.

6.1. Overview

This section extends SSR's model with consideration to the suitability of decentralized, broadcast-based scheduling operation. A brief review pointing out the feasible adoption of SSR's strategies is necessary to preemptively avoid adverse impact of any of these strategies on the performance. Thus, new developments are planned by taking all possible adversaries into account.

The evaluation of DeSSR was conducted using the 6TiSCH simulator to benchmark its performance against related SFs under both steady and bursty traffic conditions. Furthermore, a scalability test was performed using OTF [20] and LV [21] for comparative analysis. These algorithms are briefly reviewed in Chapter 3. Both OTF and LV are flexible in terms of their implementation with DeBRaS scheduling operation:

OTF was introduced in 2015 as a generic solution for adapting traffic on recurrent basis while providing extra cells using a fixed threshold limit. The author [20] stressed on the setting of OTF's threshold as per the application demand. It is straight-forward solution and once the network has started, the configuration will remain static throughout.

Local Voting (LV) [21] is a load balancing solution, introduced in 2017. Currently, there are two versions of it available. The latter [244] is slightly advanced but shows high dependency on OTF threshold for improving network performance and that way, it violates the original approach considered by LV in 2017. In addition, both versions of LV cause significant end-to-end delay. Another key SF, considered is E-OTF [245]. This proposal extended OTF based on queue monitoring; this is still another threshold-dependent approach, which has not been yet adopted by IETF towards scheduling draft unlike OTF. Further E-OTF is briefly reviewed in Chapter 3. The next section discusses the proposed solution in more detail.

6.2. Proposed solution

The proposal enhances SSR effectively using the DeBRaS-led scheduling. To facilitate improved propagation and faster upstreaming of packets to the root, DeSSR retains a minimum use of *3* broadcast cells, randomly chosen in the network. Current proposal adheres to the following scheduling restrictions:

1. All source nodes send data to the root node using source routing mode of operation.
2. A sensor node can either transmit or receive the packet at a time hence it must follow a half-duplex communication.
3. Parents and children can transmit and receive a packet using the same TSCH cell.
4. A child node from a common ancestor can either transmit or receive packets simultaneously using the same time slot and channel id (cell).

In the following subsection, we propose an enhancement of SSR's core strategies based on the review.

6.2.1. Review of SSR under distributed scheduling model

SSR dynamically allocate cells to each and every node in advance while ignoring monitoring of node's resource. However, it often allocates too many cells to nodes based on the NDS distribution and ignores poor links (set of nodes) on the way to root. Thus, additional screening is necessary to ensure symmetrical bidirectional link allowing nodes to succinctly take shortest path to root. This aspect further reduced wastage of resources.

NDS implementation in Chapter 4 used the fixed interval of 127, regrouping nodes based on the hop-distance. The potential problem with this constant is that when nodes are allowed to use a shared cells rapidly, the current limit of 127 undermines node's participation. SSR's CSS is not suitable for broadcast-based scheduling as the strategy demands *T*x cells to be fairly adjacent to each other in the slotframe. This can effectively trigger a high volume of collided cells, leading to bandwidth outage. Hence, the new proposal must replace CSS with a gap-induced selection mechanism; one option to use is the random selection method, however, this does not guarantee a collision-free operation. As far as the QOS is concerned, SSR-led packet aggregation is specifically advantageous; hence it will be implemented without any modification. Similarly; the cake-slicing method.

6.2.2.DeSSR

DeSSR is a distributed SF, which, on one hand, promotes increased participation between nodes using more than one broadcast cell and enhanced NDS, while eliminating poorly performing nodes to have extra cells on the other hand. It filters the nodes based on PDR- a value between 0.00 to 1.00. The proposed solution does not introduce additional overheads while integrating PDR-based screening on top of the DTS. DeSSR allocates cells when the available cells are not enough for a node to complete the transmission of payload.

Algorithm 1. DeSSR Bandwidth Allocation Algorithm

```
DeSSR ALLOCATION (S, R, T)
        S ← Number of available cells
        R ← Number of requested cells
        rank ← Corresponding RPL rank value of the node
        interval ← [256, 512…..N]                    => 256 by default
        pdr ← Number of available cells
        hop← compute_rank (rank, interval)
        N← number of parents
        Slices← GetSlicer(slotframe length, network depth)
        T← (Slices[hop]>>N ) × pdr                   => DTS threshold
      if R > S and S >=0 then
          if R > 0 and (pdr/1.5) > 0.5 then
                S= R - S + (T+1)/2                    => add cells
           end if
      else if R< (S- T)    then
          S= S- R - (T+1)/2                           => remove cells
      else
          S= 0                                        => do nothing
      end if
```

Figure 94. DeSSR algorithm for bandwidth reservation.

The algorithm for schedule allocation using DeSSR traffic adaption policy is shown in Figure 94. It indicates that only the deserving nodes are given excess cells ensuring the estimated pdr of eligible nodes is greater than 0.5. As far as the role of NDS is concerned, it provides a context to each node where the value of the *interval* is reset from 127 to 256 by default out of many available choices. This means, the higher the NDS interval, the higher the participation.

The algorithm begins with the '*get Slicer'* (cake-slicing) function, which generates a list of values, indexed by node's *hop*. The resultant value is processed using a '*bitwise right-shift'* operator against the number of parents denoted by *N.* Currently, the number of parents that a node can have been limited to 3. But with more wireless links to each node in the topology, this number can be even greater than 3. Here a greater value will get a lower dynamic threshold limit ('*T'*), and a lower number of children will get a high *T* value. The end results are multiplied with '*pdr'* and that is how '*T'* is calculated for overprovisioning in DeSSR. The rest of the algorithm then follows the ADD and DELETE operation; except for an additional PDR-based screening, checking the requested cells (R) are greater then 0 for adding new cells

6.2.3.Performance Evaluation

The network performance of DeSSR is evaluated using the 6TiSCH simulator [262], which is a discreate event-driven simulator. It can be used to deploy and test large-scale networks and can predict network behavior accurately and realistically compared to mathematical models. The simulator uses the algorithm provided by *Pister et al.,* [282] for collision-detection. The energy-consumption is based on a realistic energy model, introduced by Vilajosana et al., [169] for calculating charge consumed during various radio activities. The battery capacity is limited to *2200* milliampere-hour (mAh).

The TSCH slotframe is configured using 101 slots with the maximum duration of 10 milliseconds (ms) each and 16 channels. Hence each slotframe cycle lasts *1010*ms or 1 second approximately. The probability of broadcast beacons is set to 0.33 and the routing beacons including DIOs and DAOs are sent per *1s* and *60s* respectively.

The experiment uses multiple simulation runs and for every run, it generates a new topology. The nodes are positioned randomly, and each one is connected to at least *3* routing parents whose PDR is expected to be about 0.5 or higher. The configuration parameters are as per RFC 5673 [26].

Using the propagation model, the PDR of a node is calculated using the existing estimates of *Received Signal Strength Indicator* (RSSI) provided by [281]. The qualifying RSSI threshold is set to -97 *Decibel Milliwatts* (dBm).

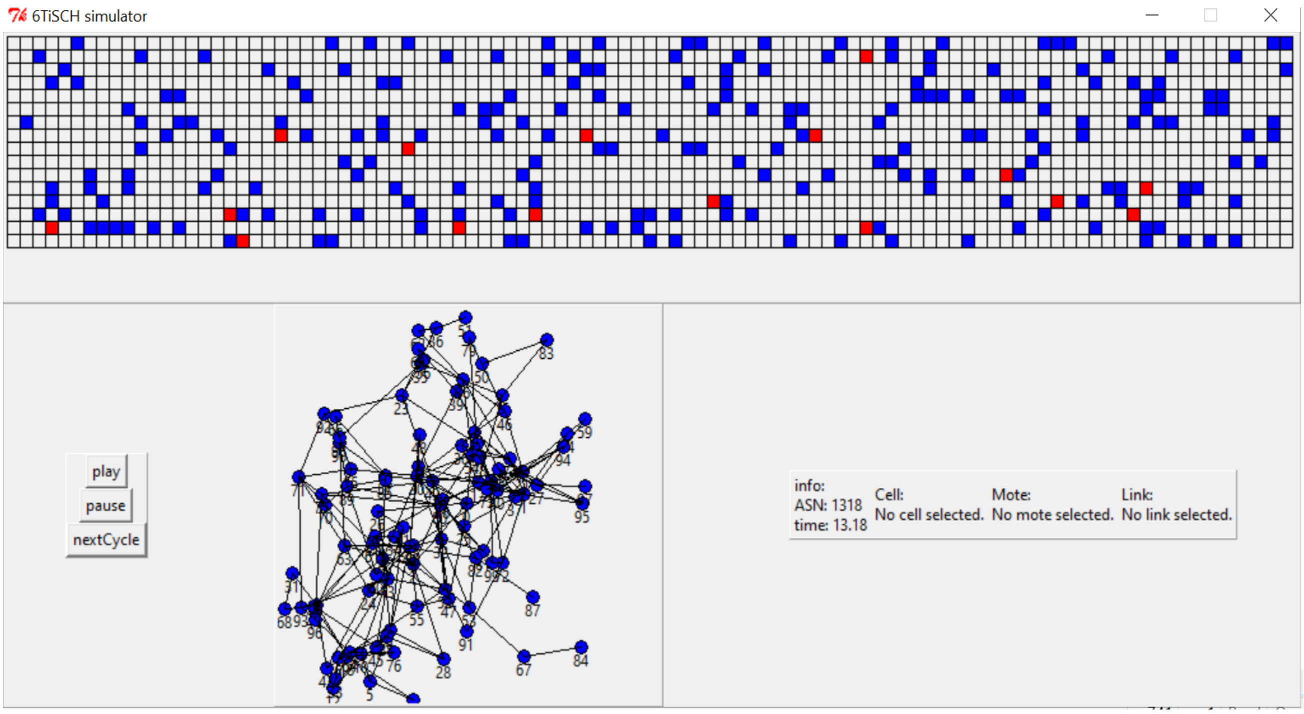

Figure 95. A view of the topology in the 6TiSCH simulator

Figure 95 Figure 95 presents the 6TiSCH simulator utilizing the DeBRaS scheduler. In the topology section (bottom-left), the root node is positioned at the centre, with the remaining nodes forming a multi-hop topology around it. The slotframe length is 101 slots, accommodating up to 16 channels, displayed at the top of the figure. Within the slotframe, cells are categorized as empty (no colour), occupied (blue), or collided (red).

The simulator operates as a standalone tool with a Graphical User Interface (GUI) that allows users to control the simulation, such as pausing or resuming it. By clicking on a specific cell in the slotframe, the GUI provides detailed information, including the node ID (mote), ASN, cell number, link details, and time. The ASN represents the number of slots elapsed since the network's initialization.

This experiment is divided based on the *steady*, and *bursty* traffic-based experiments [244]. In the *steady* traffic scenario, the nodes will experience a continuous flow of packets generated periodically. In the *bursty* traffic scenario, a sample of burst consisting of a stream of packets will be injected given timestamps. In either scenario, packet's destination is the root alone. OTF, and LV are selected for comparison based on the literature review. The remaining set of parameters are given in the corresponding Tables.

6.2.3.1. *Steady Traffic Experiment*

The experiment uses the 6TiSCH simulator, which considers a single IPv6 subnet in which data is gathered continuously at a sample rate of 60ppm. The payload is generated soon after the network is configured. In the 6TiSCH network, nodes takes time to join and synchronize in the network and the sooner a node is assigned rank, the sooner it starts transmitting path information to the root through DAOs. The data packets are transmitted using a multipath scenario depending on the transmission schedule that nodes have reserved with their PP. The configuration parameters for this experiment are given in Table 16.

Parameters	**Value**	**Parameters**	**Value**
Nodes	[100]	Radio Sensitivity	[-97] dBm
Area	Square, [1*1] km	Simulation cycles	[100]
Housekeeping Period	[5]s	Simulation runs	[100]
Packet Generation Interval	[1]s	Confidence Interval	[95] percent
Slot Duration	[10]ms	Number of broadcast cells	[3] cells
Channel Density	[16]	Number of RPL children	[3]
Slotframe Length	[101]	Broadcast probability of DIOs	[0.33]
Buffer Size	[100] packets	DIO period	[1]s
NDS interval	256	DAO Period	[60]s
Keep Alive	[10]ms	Queue Forwarding	FIFO

Table 16. DeSSR's evaluation using steady traffic scenario.

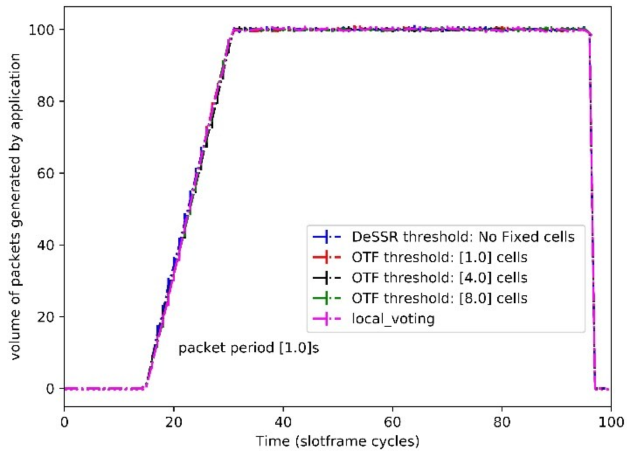

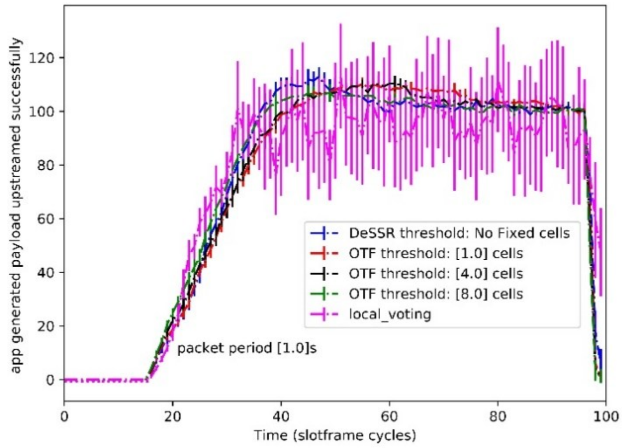

Figure 96. Application-generated packets over time.

Figure 97. Application payload up streamed successfully.

Figure 96 shows a steady packet generation scenario as soon as the *joining* is complete, just slightly ahead of slotframe cycle 20. After this, all SFs maintain a steady payload portion of 100 packets over time. as all nodes have joined the network (post configuration time).

Figure 97 depicts a stream of packets being sent to the root where number of packets are shown on the Y-axis and timestamps in slotframe cycles are given on the X-axis. The presented results in Figure 97 shows the throughput in volume of packets unstreamed by LV, OTF and DeSSR. Here, LV is showing variations as a difference between lower and upper mean values, computed at a 95% confidence interval. The variations are triggered due to scheduling incompetence against changing traffic conditions in dynamic topology. LV distributes the payload equally between nodes and disregards the fact that nodes closer to the root are responsible to send more packets than those at a farther distance from the root. The rest of the SFs show progress with the evidence of DeSSR sending slightly more packets than OTF in the beginning.

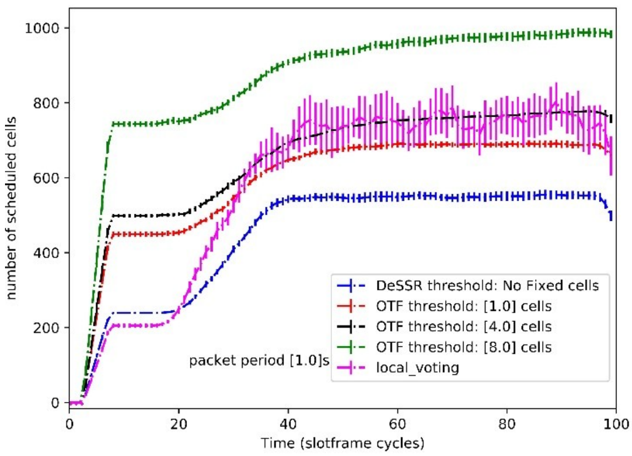

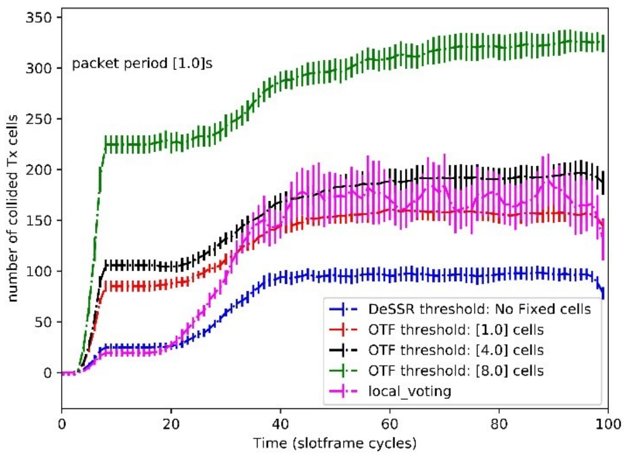

Figure 98. Cell consumption in steady traffic flow over time.

Figure 99. Volume of collided cells over time.

Sensor nodes depend on the slotted medium to dispatch the payload. Figure 98 shows that OTF reserves more cells in advance where a higher threshold limit (8 cells) translates into the highest number of cells being scheduled. LV doesn't use overprovisioning, hence, the volume of scheduled cells by LV is lower than OTF. Albeit, both SFs scheduled significantly higher volumes of cells compared to DeSSR.

In broadcast-based scheduling, collisions can be expected where the key to control is reduced cell consumption. It is evident through **Figure 98** and **Figure 99**. Here, **Figure 98** reflects that high cell consumption causes an increased volume of collided cells and eventually triggers higher charge Consumption. Since DeSSR's consumption was the lowest, hence the collided cells triggered over time are the lowest too.

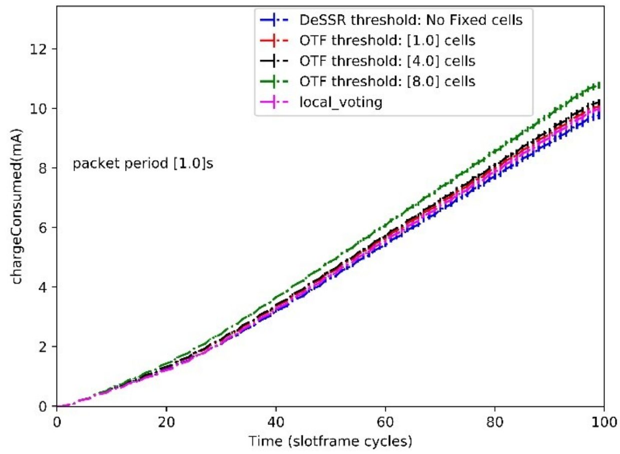

Figure 100. Lowest charge consumption in mA over time.

Figure 100 shows that charge consumption by DeSSR is roughly the same as the others and this is due to the DeBRaS scheduling itself, where the negotiations take place frequently, and beacons are dispatched frequently allowing more and more nodes to participate in negotiations with other nodes.

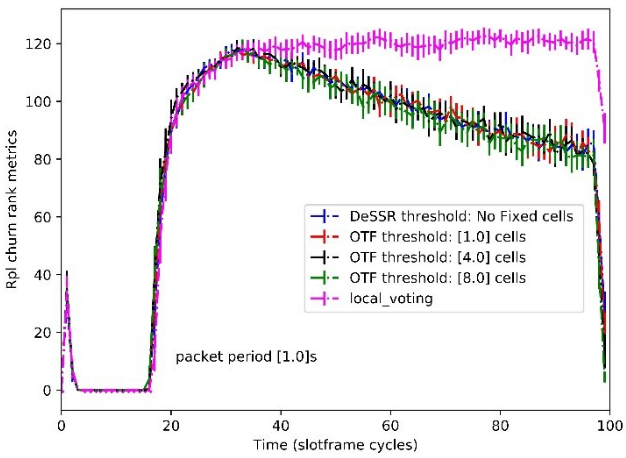

Figure 101. RPL rank-churn over time.

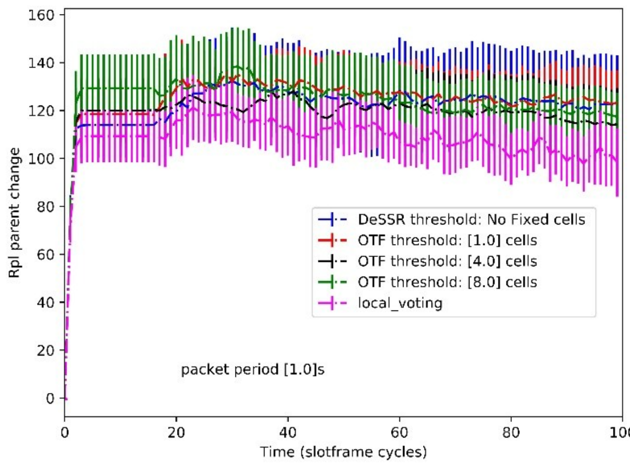

Figure 102. Node-churn over time upper-bound is preferred.

The rank churn depicts a scenario where nodes are frequently changing parents and that way, their rank is frequently adjusted. Due to improved propagation, nodes are frequently assessing the rank by deciphering the propagated EBs. This leads to relocation of schedule as well as rank oscillation. In the dynamic topology, the node's rank increases for two reasons: (1) downgrading link quality, and (2) interference. While the rank fluctuates, it triggers the additional number of 6Top transactions, the nodes are benefited from lower end-to-end delay by selecting a shortest best path to the root. In summary, a lower-bound is preferred for stable topology when there is sufficient connectivity provided and nodes are timely responding to the changes in routing topology.

In **Figure 101**, LV maintains a fairly steady portion *rank-churn* over time, which contrasts *rank-churn* patterns of OTF and DeSSR. The reason of rank oscillation by LV is poor bandwidth allocation, which also leads to many inconsistencies including poor Tx-buffer utilization. Contrary to the *rank-churn*, the *node-churn* is the process that influences network performance positively if an upper-bound is followed. In DeBRaS-led operation, the nodes from an uncommon parent can transmit or receive packets simultaneously. When high *node-churn* is evident, nodes are flexible to progress to the shortest path to root, which cuts down latency, improves utilization of cell, and balances the traffic load. However, if there are not enough cells provided to probe the shortest path, the *node-churn* becomes counterproductive. This is evident in **Figure 102** where a lower-bound *node-churn* is followed by LV while OTF and DeSSR both exhibit a high *node-churn* over time.

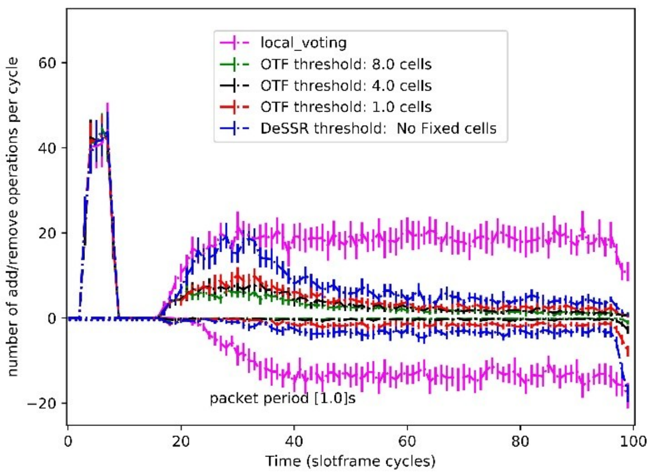

Figure 103.6Top add/remove operations per slotframe cycle.

In general, the SFs add and delete cells to nodes as a result of the changing traffic conditions. **Figure 103** shows a volume of ADD/DELETE transactions per slotframe cycle (time), where ADD transactions are observed above the X-axis and DELETE transactions are observed below the X-axis.

The results show that LV triggers ADD and DELETE transactions most frequently compared to OTF and DeSSR because it lacks overprovisioning. OTF, in order to suppress the recurrent transactions, allocates a fixed number of cells. However, OTF does not match the real-time demand, and that way, it under-or-overestimates the actual demand. This also means, while it underestimates the demand, a slightly more cycles of ADD and DELETE are scheduled.

DeSSR adapts the demand based on the cake-slicing heuristics where nodes closer to the root are allowed to maintain a high throughput.

Figure 103 shows that DeSSR triggers a balanced number of overheads, which is roughly the same as OTF despite the lowest consumption observed by DeSSR. That is necessary to balance the recurrent 6Top overheads for the improved network performance.

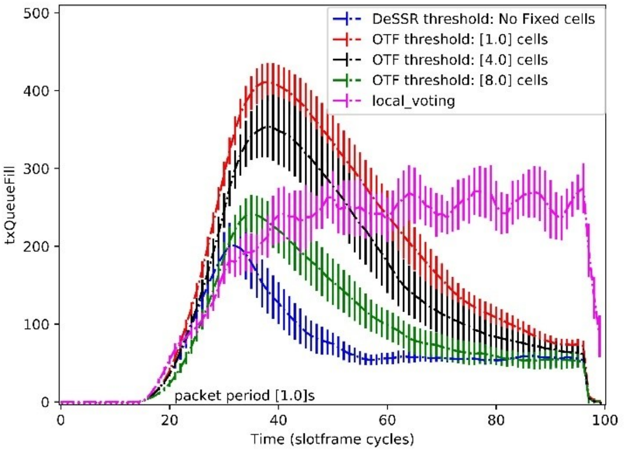

Figure 104. Transmission buffer utilization over time.

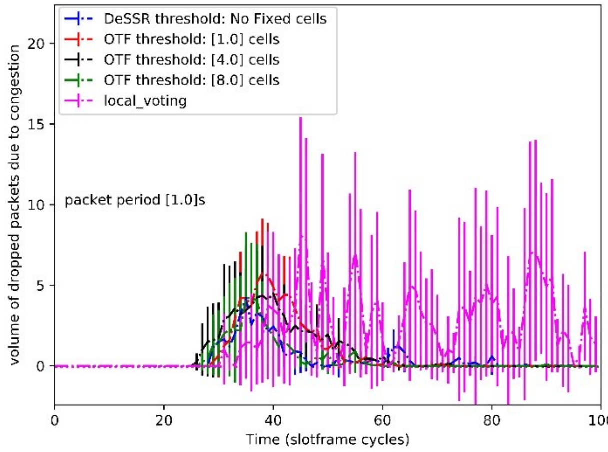

Figure 105. Showing packet loss due to congestion over time.

Figure 104 shows how the Tx-buffer is managed by SFs over time based on the traffic adaption strategies. In this regard, LV maintains a roughly steady portion with a high volume of packets remains in the queue throughout the time. DeSSR and OTF follow a non-linear pattern where DeSSR keeps the lowest volume of packets in the queue to control congestion. **Figure 105** depicts that LV triggers congestion throughout the time and incurs packet loss. DeSSR and OTF trigger congestion for a shorter time where DeSSR registers the lowest estimate of congestion to Tx-buffer ratio.

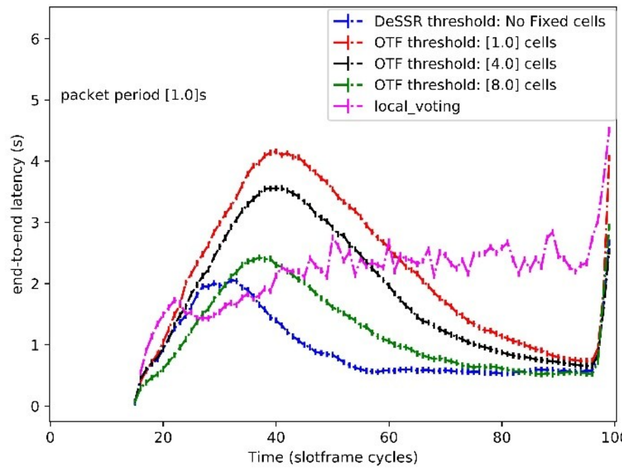

Figure 106. Latency maintains a steady lower-bound.

In **Figure 106**, DeSSR's latency is settling to the lowest over time, while OTF maintains three peaks depending on the multiple threshold limits. It shows that higher threshold causes reduced latency. Unlike OTF, DeSSR settles latency to *1s* over the time, which is optimized to the point that it is free from the trade-off with cell consumption. LV's latency remains largely between *2s* and *3s* and this kind of delay is not ideal for real-time operation given there are other technologies that are only rejected because of the high delay.

6.2.3.2. *Discussion*

The *steady* experiment simulates the industrial deployment using the 6TiSCH standard where the performance of DeSSR was compared with LV and OTF using several key indicators. The results confirmed that DeSSR offers high throughput using the lowest volume of cells compared to other SFs. The charge consumption is roughly the same as others because of decentralized, and broadcast-based scheduling-led operations. Notably, DeSSR showed strong performance over time compared to the LV and OTF, and achieved lowest volume of collided cells, lowest latency, lowest congestion in queue, improved node-churn, and optimized Tx-buffer. However, it triggered a slightly high 6top transactions as these were necessary to adapt rapidly changing network dynamics.

6.2.3.3. *Bursty Traffic Experiment*

The *bursty* traffic experiment draws significance from the real-world industrial scenarios such as leak detection [37]. According to this, nodes experience a sudden gust of traffic. The experiment injects a sample of 25 packets per burst per node in a network of 100 nodes at fixed timestamps of 20 and 60 respectively in slotframe cycles. For analysis, the results are benchmarked with the OTF using multiple thresholds. The queue length for all nodes is 100 packets. The remaining configuration parameters are given in Table 17.

Parameters	**Value**	**Parameters**	**Value**
Nodes	[100]	Radio Sensitivity	[-97] dBm
Area	Square, [1*1] km	Simulation cycles	[100]
Housekeeping Period	[5]s	Simulation runs	[100]
Packet Generation Interval	[1]s	Confidence Interval	[95] percent
Slot Duration	[10]ms	Number of broadcast cells	[3] cells
Channel Density	[16]	Number of RPL children	[3]
Slotframe Length	[101]	Broadcast probability of DIOs	[0.33]
Buffer Size	[100] packets	DIO period	[1]s
NDS interval	[256]	DAO Period	[60]s
Keep Alive	[10]ms	Queue Forwarding	FIFO

Table 17. Simulation parameter bursty traffic experiment

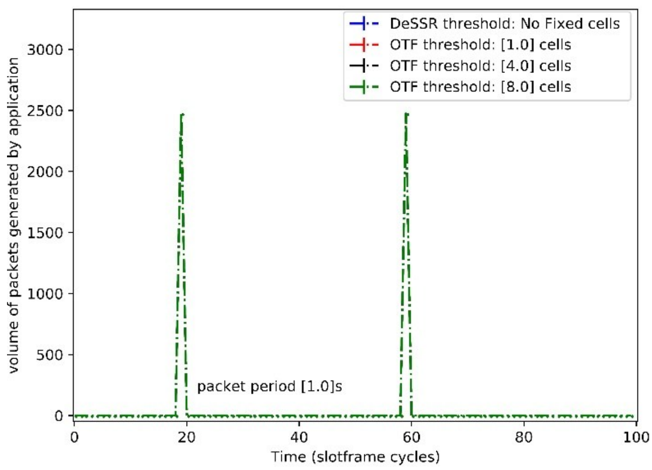

Figure 107.Packets generated during traffic burst over time.

Figure 107 depicts the volume of traffic generated as per the bursty traffic conditions where each node generates roughly the 25 packets over the given time and this process repeats twice per slotframe run. Because a TSCH slotframe repeats itself over time hence for each repetition (run), two traffic bursts are supplied per run. The maximum amount of payload generated by all nodes during each slotframe cycle at the given timestamps, is approximately 2475 packets. Both SFs consistently generate 2475 packets precisely at slotframe cycle 20 and 60 respectively. This estimates is calculated based on the following points:

- Each slotframe contains 100 slots, with each slot lasting 10 milliseconds.
- Thus, one slotframe cycle takes 100 slots * 10 ms = 1000 ms or 1 second.
- For 100 slotframe cycles, the total duration is 100 seconds.

Over this 100-second period, the simulator generated 2475 packets. Dividing the total packets by the time duration, we see that the simulator produced approximately 24.75 packets per second, which aligns closely with the expected value of 25 packets cited at the beginning. This confirms that the simulator's output is consistent with the initial estimation of packet generation.

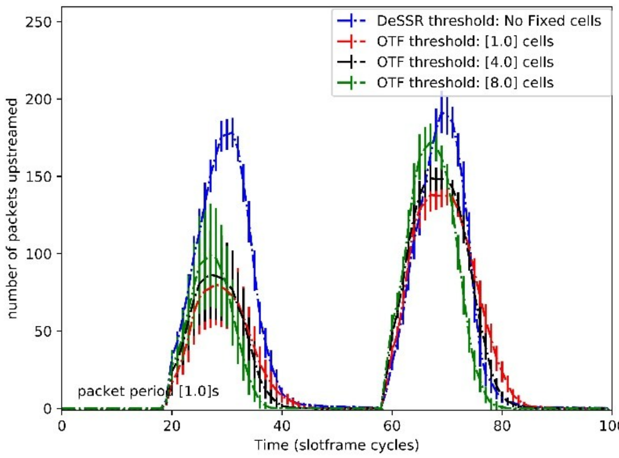

Figure 108.Total number of packets up streamed to root.

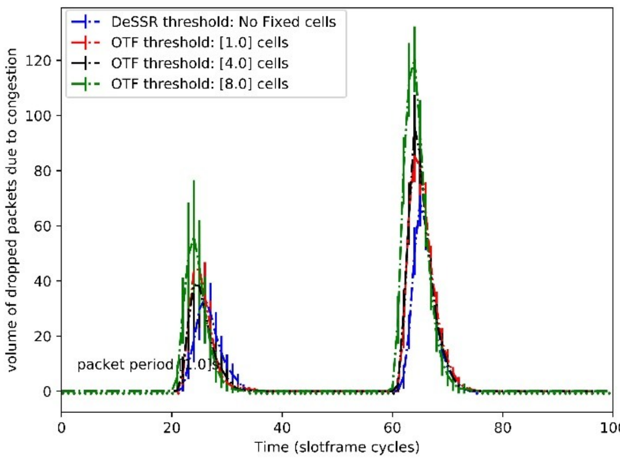

Figure 109. Packet loss due to congestion in the queue.

Figure 108 shows packet transmission capability where OTF drops more packets during the 1st peak compared to 2nd peak. The reason is poor assessment of demand. On the other hand, DeSSR sends more packets than all three variants of OTF throughout time and it is evident in **Figure 108**.

In a sudden gust of heavy traffic, congestion can occur due to fixed queue capacity. **Figure 109** shows that each peak incurs packet loss due to congestion where DeSSR's loss is the lowest considering a toll of 30 packets during 1st peak and 70 packets during the 2nd peak. OTF suffers the worst congestion with the highest volume of cells.

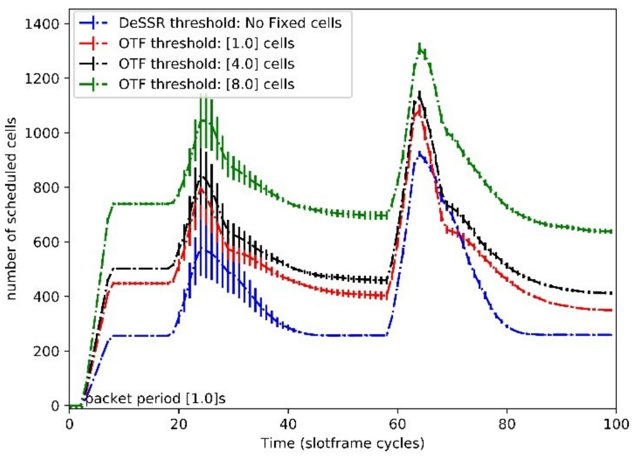

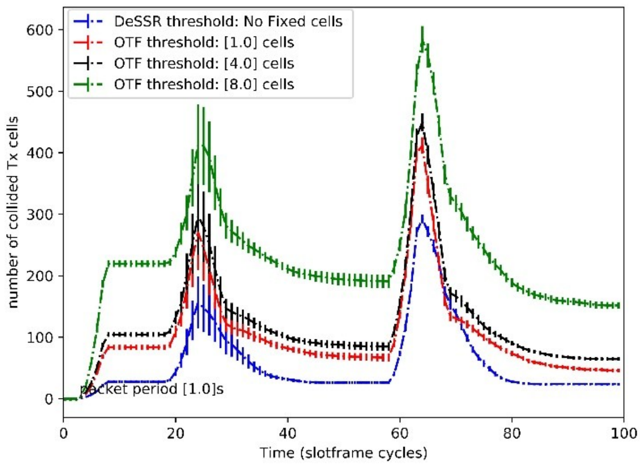

Figure 110.Cell consumption in a bursty traffic scenario. **Figure 111.Collided Tx cells as a function of time, bursty traffic scenario.**

Figure 110 demonstrates the volume of scheduled cells by both SFs over the sudden arrival of a heavy payload. According to this, DeSSR schedules the lowest portion of cells on average and during both events despite there being no packets to send. Conversely, OTF follows a fixed distribution where the higher threshold limit translates into the high consumption of cells and eventually causes an increased collision. The presented results in Figure 110 shows that DeSSR scheduled the lowest volume of cells where it uses scheduled cells efficiently to ensure reliable operation that is free from performance trade-offs.

Figure 111 shows the volume of collided cells triggered by both SFs over time. Here, both SFs randomly select cells from the slotframe, and it is possible that two or more nodes are using the same Tx cells for transmission simultaneously under common parent. So, the collision can be expected. Apart from that, a higher consumption of cells can also influence collision to increase. In Figure 110, DeSSR observes the lowest cell consumption, hence the volume of collided cells triggered by DeSSR is the lowest too as shown in Figure 111, and this is true for both events, and for remaining times when there is no activity (idle times).

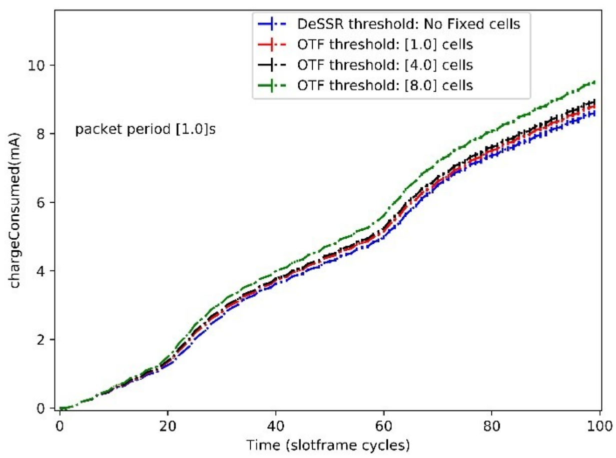

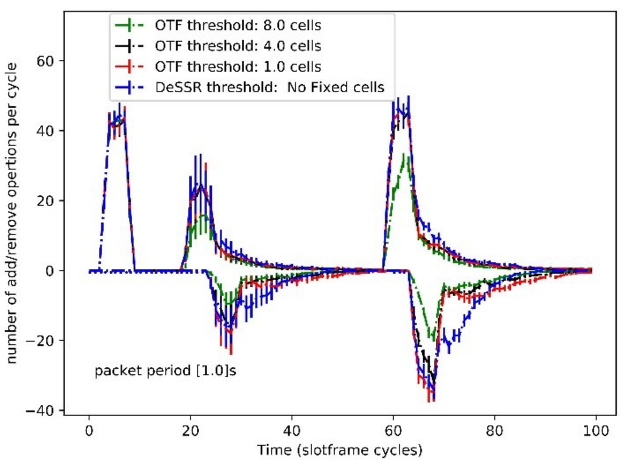

Figure 112.Charge consumption(mA) over time in bursty traffic. **Figure 113. Add/Remove 6Top operation per slotframe cycle.**

Figure 112 shows a charge consumption over time by OTF, and DeSSR. Here, both SFs consumed roughly the same amount of battery charge whereas the DeSSR consumed slightly less charge, however, the margin seems very thin. The key reason is the decentralized, broadcast-based scheduling itself where enhanced beacons take a toll of most charge consumed by both SFs. Charge consumption is further discussed in detail under Subsection 6.2.3.6.1.

Figure 113 shows 6Top ADD/DELETE activities over time where ADD activities are the positive number, shown above the X-axis and DELETE activities are the negative number, shown below the X-axis. In the beginning, the scheduler unanimously adds 40-45 cells to nodes towards bootstrapping. This process is the same for both *steady* and *bursty* traffic scenarios as can be compared with Figure 103. As the first event unfolds at slotframe cycle 20 in Figure 113, both SFs generate marginally the same amounts of overheads except for the OTF with the highest threshold limit. The reason is obvious that each node is given 8 cells already by OTF and when nodes change position, OTF does not have to allocate or deallocate cells more often. On the contrary, DeSSR sends substantially more packets than OTF's high threshold using the lowest volume of cells and when the nodes change their parent frequently in search of closer parent to the root, it releases occupied cells and allocates new ones in an adaptive manner. The key benefit is that released cells are available for other nodes to use and this is why it causes additional ADD/DELETE transactions. The 2nd event at slotframe cycle 60 indicates the toll of 6Top ADD/DELETE transactions is higher than the 1st event. The key reason is that more cells are scheduled at this time by both SFs, as is shown in Figure 110.

6.2.3.4. *Discussion*

In the bursty traffic experiment, DeSSR outperformed OTF considering high throughput, lowest number of packet loss due to congestion, lowest scheduled cells, reduced collisions, lower charge consumption, and a fairly-balanced 6Top cycles. With these key achievements, DeSSR outperforms currently popular decentralized, broadcast-based scheduling functions and it achieved this without monitoring queue occupation. However, further experimentation is ideal to test scalability of DeSSR knowing that its packet transmission capability is higher than the most SFs.

6.2.3.5. *Scalability Analysis*

This experiment tests the scalability of DeSSR, and it is divided into three parts. In the first part, we test the reliability in medium-sized networks against extreme traffic load. In the 2nd part, the network size is increased to 100 nodes. Finally, in the 3rd part, we increased the buffer size. We have followed the steady pattern depending on the *packet period intervals*. The results are compared with multiple variants of the OTF. The configuration parameters are given in Table 18.

Parameters	**Value**	**Parameters**	**Value**
Nodes	**[50, 100]**	Radio Sensitivity	[-97] dBm
Area	Square, **[2*2]** km	Simulation cycles	[100]
Housekeeping Period	[5]s	Simulation runs	[100]
Packet Generation Interval	**[1.0,0.5, 0.1]**s	Confidence Interval	[95] percent
Slot Duration	[10]ms	Number of broadcast cells	[3] cells
Channel Density	[16]	Number of RPL children	[3]

Slotframe Length	[101]	Broadcast probability of DIOs	[0.33]
Buffer Size	**[10, 100]** packets	DIO period	[1]s
Keep Alive	[10]ms	DAO Period	[60]s
NDS interval	256	Queue Forwarding	FIFO

Table 18. Simulation parameters to test scalability limits of DeSSR.

• Scalability Analysis of Medium-sized Network

In this experiment, a total of 50 nodes are deployed randomly where queue length (Tx buffer size) for each node is reduced to 10 packets [244]. The experiment produces a number of subplots reflecting the impact of varying traffic load over time where buffer size is explicitly mentioned.

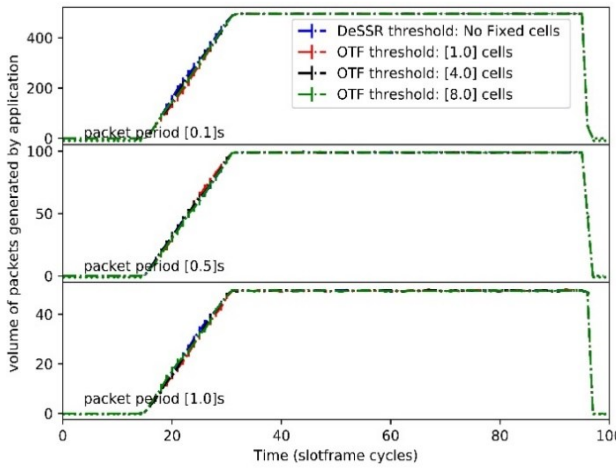

Figure 114.Payload generation over time.

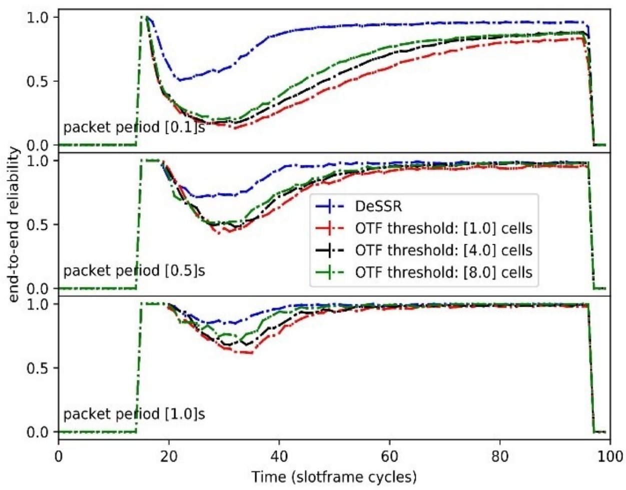

Figure 115. Reliability for medium-range deployment.

Figure 114 is divided into three subplots, each reflecting different traffic load scenarios. The subplots demonstrate a steady distribution of traffic over time:

- In the first subplot, **50 packets** are generated per slotframe cycle (packet period = 1s).
- In the second subplot, **100 packets** are generated per slotframe cycle (packet period = 0.5s).
- In the third subplot, **500 packets** are generated per slotframe cycle (packet period = 0.1s).

These estimates align with the total number of packets generated as per the given traffic rates, corresponding to low, moderate, and extremely high traffic loads, respectively.

Figure 115 reveals that the reliability of both OTF and DeSSR decreases as traffic load increases. A period of packet loss is observed between slotframe cycles 20 and 40, with DeSSR showing **less pronounced packet loss** compared to OTF. Specifically:

- **Low traffic load (packet period = 1s)**: DeSSR performs slightly better than OTF with minimal packet loss during packet loss period that is between slotframe cycles 20 and 40.
- **Moderate traffic load (packet period = 0.5s)**: DeSSR performs better than OTF with minimal packet loss between 20- 25%.

- **High traffic load (packet period = 0.1s)**: DeSSR handles the extremely challenging traffic more efficiently than OTF, delivering a higher volume of traffic while maintaining worse-case reliability up to 50% during the packet loss period. Conversely, OTF struggles with a high consumption-to-collisions ratio, resulting in worse-case packet loss up to 75% approximately or higher. Here, DeSSR drops packets, primarily due to **constrained buffer size**, rather than consumption or collisions.

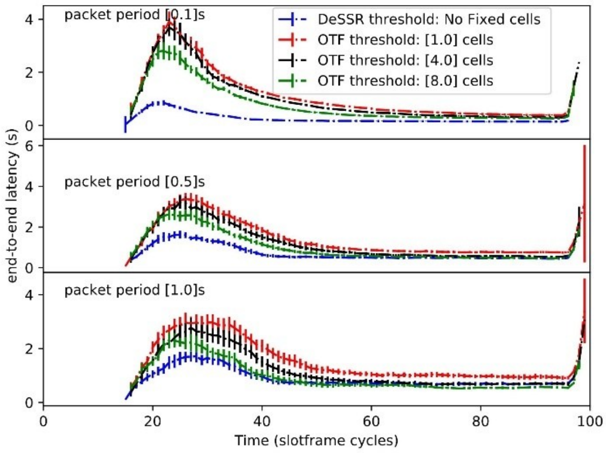

Figure 116. Latency for medium-range deployment.

In **Figure 116**, latency over time is shown for both OTF and DeSSR, with notable changes at slotframe cycles 20 and 40. At these points, DeSSR registers the lowest delay of 2 seconds, though it is important to note that not all packets are delivered at this time. After these cycles, latency stabilizes around 1 second for both DeSSR and OTF, which indicates that most packets are successfully upstreamed by this point. This behaviour reflects DeSSR's ability to streamline the delivery of packets more efficiently than OTF, even under changing traffic conditions.

The 3rd subplot of Figure 116 compares the latency trajectories of OTF and DeSSR. The following observations are taken into account where the key points include: (1) gap between trajectories. That is at slotframe cycles 20 and 40, there is a notable gap between the latency of OTF and DeSSR. DeSSR shows lower delay than OTF. (2) lowest delay with concerns. Although DeSSR achieves the lowest delay, the concern arises from the fact that too many cells were allocated to the nodes against the volume of packets delivered successfully as can be seen in Figure 115 . As a result, the nodes were able to advance quickly to the shortest path to the root, but this does not correspond to the upstreamed payload by the nodes using DeSSR.

- ## Scalability Analysis of Large-Scale Network

The experiment is used for testing scalability and robustness of DeSSR using 100 nodes. This time, the network is twice as dense and queue length is 10 packets for all nodes.

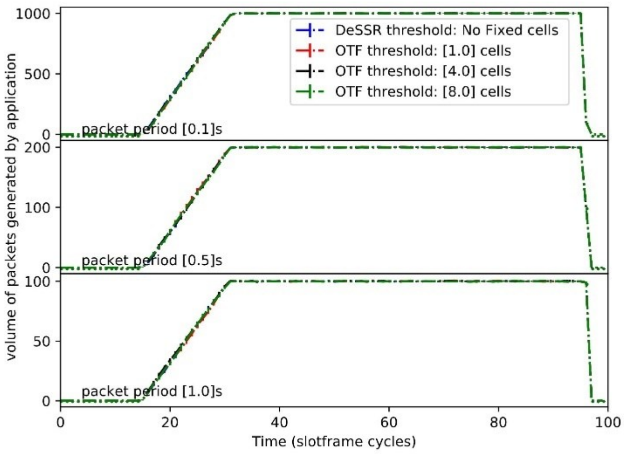

Figure 117. Payload generation over time in large networks.

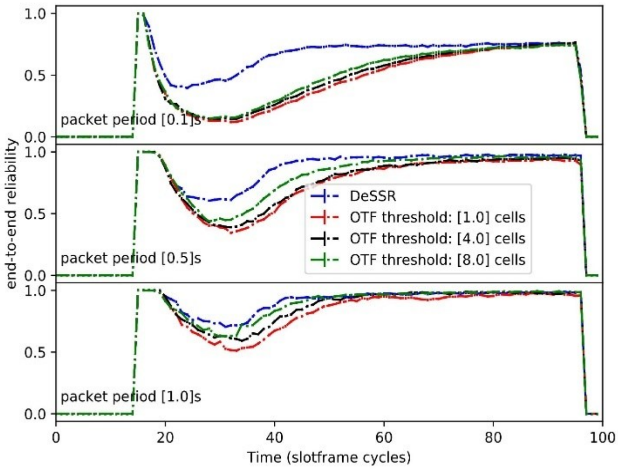

Figure 118 End-to-End reliability as a function of time.

Figure 117 illustrates the application-generated payload over time for three different traffic rates: 100 packets per second (slotframe cycle) (packet period = 1s), 200 packets per second (packet period = 0.5s), and 1000 packets per second (packet period = 0.1s). The subplots in Figure 118 track reliability (Y-axis) over time (X-axis), showing how the network handles varying traffic loads. Following key points are observed from Figure 118:

1. **Packet Drops (Slotframe Cycles 20-60):** Both DeSSR and OTF experience packet drops between slotframe cycles 20 and 60. This is due to network congestion as traffic increases and nodes struggle to handle the volume of packets generated periodically.

2. **DeSSR vs OTF (Recovery and Efficiency)**: While both SFs show a sharp decline in reliability due congestion. DeSSR outperforms OTF by sending more packets successfully during this period and it is more efficient in recovering from packet loss compared to OTF, showing quicker stabilization after the congestion phase has passed.

3. **Increased Load Impact**: As the packet generation rate increases, both SFs face a proportional decline in reliability. However, the leading gap between DeSSR and OTF demonstrates that DeSSR is better at handling high traffic loads and can maintain a higher rate of successful packet delivery and OTF struggles more with increased traffic, leading to greater packet loss and slower recovery.

In summary, DeSSR's superior reliability under heavy traffic conditions, combined with its ability to recover more efficiently from packet loss, highlights its advantage over OTF in handling congested networks. Despite some declines, DeSSR consistently shows better performance in delivering more packets, making it resilient solution under varying load scenarios.

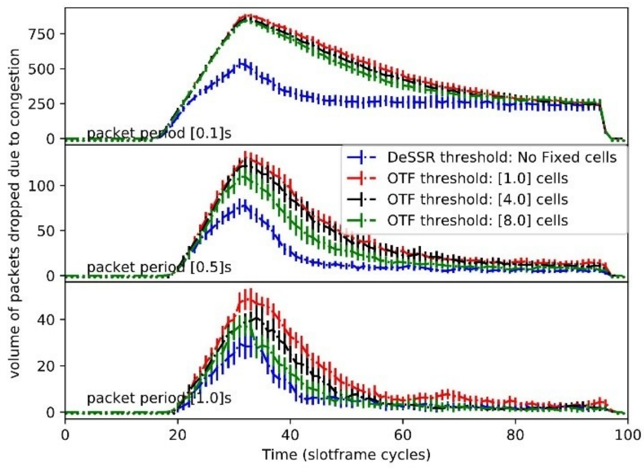

Figure 119. Packet loss due to congestion in the buffer.

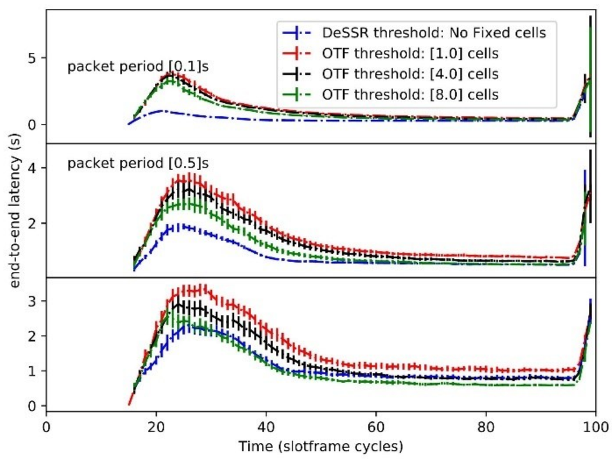

Figure 120. Latency as a function of time, 100 nodes.

Figure 119 examines the backlog of packets lost due to congestion, confirming that congestion is the primary factor behind the packet loss observed in Figure 118. This reinforces the idea that both DeSSR and OTF face performance issues during periods of high traffic, but congestion management plays a crucial role in determining how well each scheduling function handles the traffic load. The key points observed from Figure 119 include:

1. **Congestion as the root cause**: The packet loss depicted in Figure 118 directly correlates with congestion in the network, confirming that traffic overload leads to packets being dropped when nodes are unable to forward or buffer incoming packets.
2. **DeSSR's Performance:** While both SFs experience packet loss due to congestion, DeSSR shows better control over queue handling, minimizing the effects of congestion compared to OTF.

Figure 120 shows latency over time and the results are more or less the same as shown in **Figure 116**. Hence, it will not be accurate to predict the actual behavior.

- **Scalability Analysis using Large-scale Networks with Increased Buffer**

This experiment increases the queue length to 100 packets and uses a *packet period* of 0.5s. The presented results show the impact of congestion in the queue, end-to-end reliability, and latency. With previous approaches including OTF, congestion caused poor performance with OTF's performance significantly degrading during the temporary peak of traffic between slotframe timestamp 20 and 60. The results presented are averaged at a 95% confidence interval using 100 slotframe runs. This drop in performance is indicated by an increase in dropped packets leading to a reliability drop to about 75% and a latency of between 6 and 8s for OTF. DeSSR performs significantly better with reliability staying above 90% over time and latency not exceeding 4s. The simulation parameters are presented in Table 19.

Parameters	**Value**	**Parameters**	**Value**
Nodes	**[100]**	Radio Sensitivity	[-97] dBm
Area	Square, **[2*2]** km	Simulation cycles	[100]
Housekeeping Period	[5]s	Simulation runs	[100]

Packet Generation Interval	**[0.5]**s	Confidence Interval	[95] percent
Slot Duration	[10]ms	Number of broadcast cells	[3] cells
Channel Density	[16]	Number of RPL children	[3]
Slotframe Length	[101]	Broadcast probability of DIOs	[0.33]
Buffer Size	**[100]** packets	DIO period	[1]s
Keep Alive	[10]ms	DAO Period	[60]s
NDS interval	256	Queue Forwarding	FIFO

Table 19. simulation parameters for scalability analysis using extended buffer

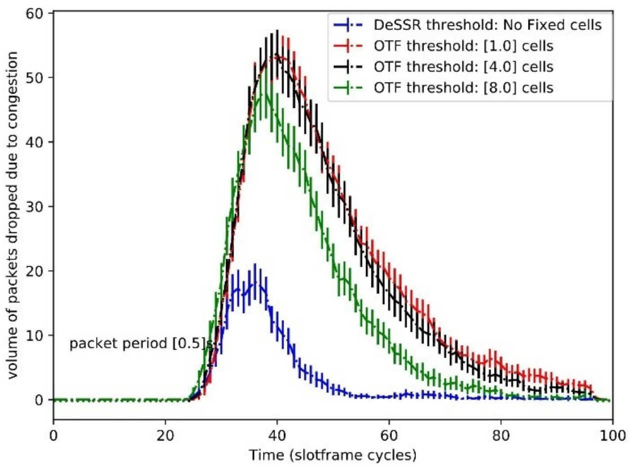

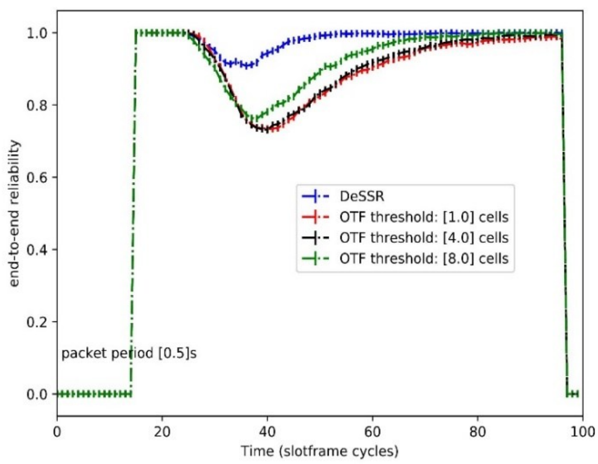

Figure 121. Congestion in the extended buffer over time. **Figure 122. Reliability over time and extended size of buffer.**

Figure 121 shows that at an early stage (slotframe cycle 20 and 40), congestion cannot be ruled out despite an increase in buffer size. Here, both SFs drop packets due to congestion, except DeSSR's loss is 75% less than OTF and it observes quick recovery over time.

Figure 122 shows that the extension to buffer size is rewarding for both SFs. However, both SFs drop packets in the beginning due to congestion, which negatively impacts the end-to-end reliability as is shown in **Figure 122**. Here, DeSSR observes the lowest decline in reliability and provides stability to the network fairly quickly compared to the OTF.

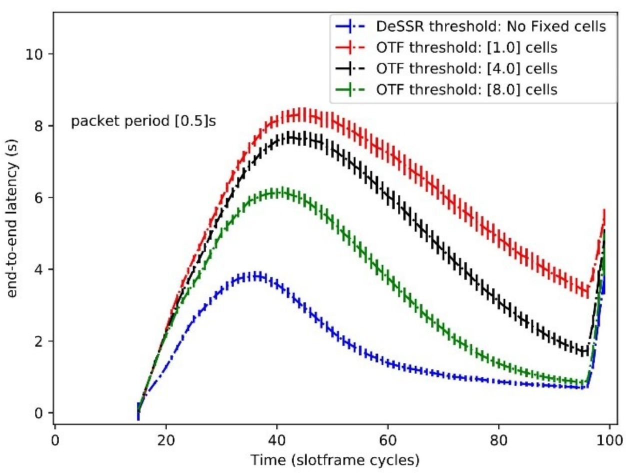

Figure 123.Latency over using extended buffer scenarios.

Figure 123 shows end-to-end latency over time. Here, OTF registers a maximum delay depending on the threshold limits. That is, the higher the threshold limit, the lower the delay. That is because nodes have enough cells to probe the shortest path to the root. Results show that OTF's trajectories take longer to reach optimal latency of 1s while the DeSSR achieves the target in a fairly shorter time, and yet observes the lowest delay comparatively.

6.2.3.6. Analysis

This section discusses the performance of DeSSR in terms of side-effects considering charge-consumption, complexity, and scalability.

6.2.3.6.1. Discussion on charge consumption

In 6TiSCH network, charge consumption is impacted by a number of aspects including the cost of network formation, dynamics of SF, and management of costs incurred due to propagation and control overheads

Network bootstrap is an expensive period in low-power and lossy networks, involving frequent EBs carrying broadcast and unicast traffic. In a fully configured DoDAG topology, nodes periodically generate EBs ensuring nodes are synchronized [262]. Hence, an optimal broadcast strategy is useful to reduce energy consumption. *Vucinic et al.,* [221] studied various broadcast strategies to minimize the delay in network formation by setting an optimal point to control portions of EBs without ignoring the convergence delay and collision. Therefore, all broadcast messages are carried in a form of *slotted aloha* [214]. The author also proposed an optimal threshold (0.1 and 0.33 for EB and DIO), which is representative of the lowest network formation time in the network of 45 nodes considering reduction in the volume of EBs [262]. *Municio et al.,* [262] showed the delay in network formation increases in a steady-linear fashion as the network size increases using the same hysteresis. DeSSR uses the same value as described as optimal in [221] and demonstrates a shorter bootstrap period using more than one broadcast cell from the TSCH slotframe. The remaining portion of the slotframe is left unused for the SFs to implement.

In 6TiSCH network, nodes compute their radio duty-cycle per slot depending on how long it takes to finish the scheduled task. A variation in charge-consumption is likely as different SFs take different approaches adapting and managing the traffic in the network. *Daneel et al.,* [236] highlighted the role of SF carries to prevent recurrent wastage of charge, triggered by poor overprovisioning and static allocation of cells, i.e., a mismatch between the actual traffic and predicted traffic. No defined mechanism so far has been proven optimal. Hence, charge consumption is dependent on the priorities of different SFs (refer to Chapter 3 for review of SFs).

In a dynamic topology, nodes change parents frequently. This has a considerable impact on the underlying TSCH links [239]. That is, each parent-changing node must relocate its resources from one parent to another parent. Hence charge consumption varies from the point of how and to what extent the movement of non-root nodes is controlled. For this reason, many recently introduced SFs do not allow leaf nodes to have a Tx cell. However, this negatively affects the optimal path formation in RPL routing. Thus, constraining parent-change is not only a greedy setup but also has repercussions on overall scalability of the network. Our proposal inherits some of the key drawbacks of using multiple broadcast cells for advertisement [239]. However, it permits non-leaf nodes to have access to Tx cells. To analyze the impact of broadcast cells on charge consumption, a separate experiment is conducted using the same configuration parameters as used in Table 17, except the range of broadcast is set to be 1- 8 cells.

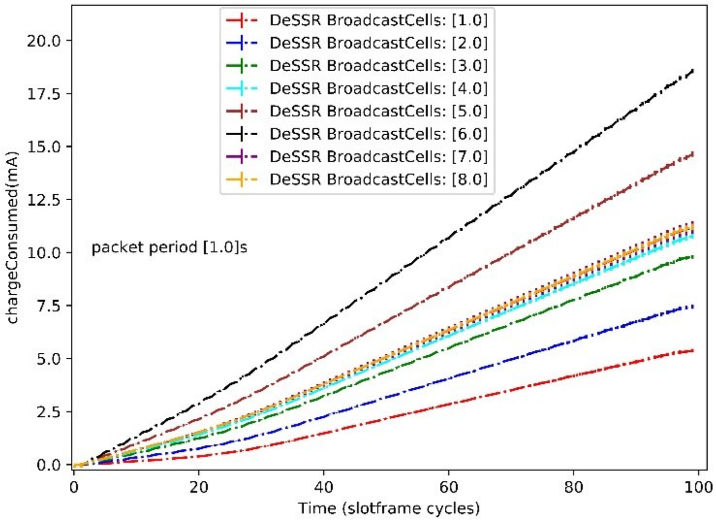

Figure 124.Charge consumed by the varying broadcast cells.

Figure 124 illustrates the cost of managing scheduling dynamics indicating that the lowest number of broadcast cells consume the lowest amount of charge. However, this is not true with the highest portion comprising 7 – 8 cells with the presented results showing a moderate charge-consumption that increases over time and is about the same level as with 3- 4 cells. The highest amount of charge is consumed with 6 and 5 broadcast cells. *Municio et al.,* [239] argues the key reason for this behaviour being the increased waiting time for contention-access in large-scale networks. Hence, the charge-consumption decreases in larger networks. DeSSR retains the same number of broadcast cells as used by other algorithms.

6.2.3.6.2. Discussion on complexity

The complexity of DeSSR is analyzed in terms of control overheads (6Top transactions). This is further illustrated in **Figure 103** where key SFs are shown to have added and deleted negotiated cells over time. The exchange is facilitated using 6Top unicast transactions, which take a longer time to execute and are resource intensive. Hence, the fewer number of cells are used the better. DeSSR manages complexity of control overheads by allowing extra cells to be reserved for the nodes closer to the sink and ensuring a strong PDR. However, this is not an absolute allocation. For nodes which change parent, the resources attached are only diverted to the new parent depending on the criteria provided by DeSSR. Hence the requirement is managed dynamically. This is evident in the analysis presented in Section 6.2.3.1, and Section 6.2.3.3.

The complexity of EBs overshadows the complexity due to control overheads. This is shown under **Figure 100** where no significant variations are present in charge consumption by DeSSR, LV and OTF, with DeSSR observing the lowest cell consumption, lowest collision, and roughly same complexity level as OTF. This suggests the complexity of DeSSR in terms of propagation is comparable to the other SFs. DeSSR does not add new overheads, instead, it allows a high availability of collision-free cells without causing trade-offs with latency and reliability. It achieves improved scalability allowing hundreds of nodes to use spare cells under a single DoDAG tree. The flow of RPL control messages is unaffected by DeSSR.

6.2.3.6.3. Discussion on scalability

We studied performance degradation factors in large-scale industrial networks using multiple simulation-based experiments, and benchmarked results of DeSSR against other SFs in **Section 6.2.3.4**.

The selection of SFs was made as per the literature review presented in **chapter 3** and **Section 6.1**. A number of recently published SFs such ALICE, and MSF, do not qualify for this comparison due to poor propagation, and limited throughput [226]. The significance of the contribution by DeSSR is presented using the following points:

- Improved availability of Tx cells at both steady and bursty traffic conditions. **(Figure 98 and Figure 110** in **Section 6.2.3**).
- Improved throughput despite using the lowest portion of cells. (**Figure 109, and 115**).
- Reduced collision among Tx cells so that extra cells can be allocated to nodes experiencing a temporary peak. (**Figure 99 and Figure 100**).
- The complexity of DeSSR in terms of 6Top overheads is comparable with OTF and is significantly lower than LV. (**Figure 103**).
- There are no trade-offs involved with latency and charge consumption. (**Figure 97, Figure 104 and Figure 106).**

Further experiments are carried out to test scalability using several hundred nodes. E-OTF's performance, as per the literature review, has been unknown for larger networks. Hence, DeSSR and E-OTF are included in the experiment to test performance considering the scalability being the prominent concern. The E-OTF is configured with no extra cells and the rest of the configuration parameters are the same as shown in **Table 18** except the network density is increased to several hundred nodes, and packet generation interval is se to 1s.

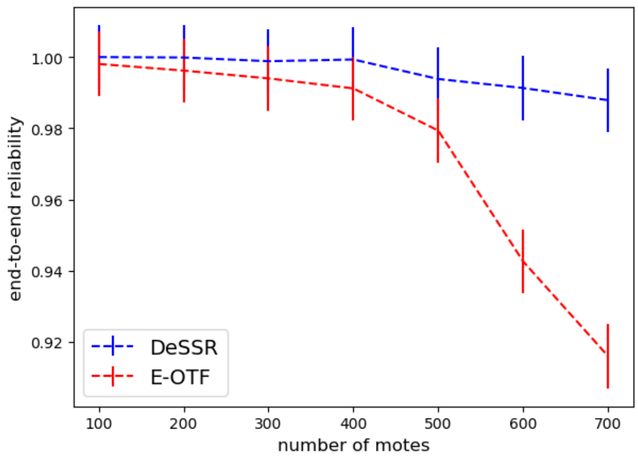

Figure 125. Scalability of DeSSR over several hundred nodes using 60 packets per minutes.

Figure 125 highlights reliability loss corresponding to network sizes; DeSSR achieves approximately 99% reliability corresponding to the 700 nodes (95% confidence interval) where as the performance of E-OTF beyond 400 nodes experiences a significant decline. Consequently, DeSSR is a strong candidate for managing large-scale networks which does not trigger communication loss due to scaling.

6.3. Summary

Chapter 6 introduced DeSSR with the aim of improving the scalability of IEEE 802.15.4 networks, particularly under the TSCH-MAC mode in a decentralized and broadcast-based operation. The key contributions of DeSSR stem from PDR-based DTS and a flexible NDS assessment, allowing fast forwarding (adaption) of unexpected heavy traffic where the proposal can also detect asymmetric links on the way to destination.

The performance of DeSSR was rigorously tested under various scenarios:

- Section 6.2.3.1 and Section 6.2.3.3 describe experiments conducted in a 100-node network with a packet generation period of 1 second, simulating both steady and bursty traffic conditions. In the steady traffic experiment, DeSSR outperformed both LV and OTF, achieving the best results across key metrics like reliability, latency, and charge consumption. In the bursty traffic experiment, the performance of DeSSR was superior to that of multiple versions of OTF thresholds demonstrating its ability to handle sudden traffic spikes more efficiently.
- Scalability has been a major focus of this chapter, with DeSSR being tested against varying buffer sizes and traffic rates. The results from both medium-scale and large-scale network experiments confirmed the advantage in terms of assessing traffic and its efficiency across different network sizes and conditions.
- One of the most important findings was in the scalability test, where DeSSR achieved 99% reliability in a network with up to 700 nodes, each generating 60 packets per minute (ppm). In contrast, E-OTF showed a sharp decline in performance after reaching 400 nodes, losing up to 10% of the total payload generated by the time as it reached 700 nodes.

The results conclusively demonstrate that DeSSR significantly outperforms OTF, LV, and E-OTF, particularly in larger networks, making it a highly scalable and efficient solution for industrial IoT applications that require robust performance in dense, high-traffic environments. The primary limitation of this approach is its relatively higher battery consumption, though it remains lower than that of the existing DeBRaS-led SF. Additionally, it has been tested with a periodic traffic generation where scheduling is more straightforward compared to the random traffic generation patterns that introduce an uncertainty in node traffic. This aspect is noted for future work.

7. CONCLUSION

This Chapter summarises the core findings and contributions of this thesis, and discusses limitations of the approach and future work items.

7.1. Thesis Summary

This thesis contributes to the body of knowledge by addressing the scalability limitations of 6TiSCH networks which have traditionally been restricted to 30-50 nodes per subnet. Wireless networks are prone environmental interference and RF-challenges, causing signal quality loss as a result of scaling (given the increased demand by industrial networks worldwide). This significantly impacts the goodput. Chapter 1 has provided a brief summary focused on the signal loss caused by EIs and multipath propagation.

IoT networks designed for wide area coverage (under low power, and low data-rate mission) prefers asynchronous communication model and these are constrained by Tx power usage (duty-cycle), and spectrum sharing. LPWANs use unlicensed RF bands where they offer a trade-off between the coverage and load sensitivity. In addition, latency is not a priority for them. Therefore, industrial IoT networks can not use these solutions where data gathering takes place rather frequently. Section 2.4 in Chapter 2 evaluated the key LPWA technologies on the pretext of design gaols of the industrial networks.

In terms of Cellular IoT, these are standards solutions which are benefited from high bandwidth availability by using paid frequencies, hence adding more devices does not affect load scalability or network performance. The downside of these networks is that these are purely subscriber-based technologies that means a user will have to pay for the service (the cost does not exceeds \$2-\$5 per month), though the subscription cost is lower than the monthly cost per equipment using the mobile service providers like 3G, Orange, Vodafone, etc. 5G wireless communication technologies is becoming increasingly popular. However, this is not primarily designed to integrate well with resource-constrained devices but rather focused on high data rate, a long-range mobile ad-hoc wireless solution. The industrial networks require agility whereby using standard mobile networks or CIoT networks, the user cannot claim independence from tariffs (that are inclusive of data rate, reception, etc).

6TiSCH standard is tailored for industrial usage where scalability is an open challenge. The scaling is important for 6TiSCH to expand coverage. The other ways to do that is by deploying increased number of subnets with each subnet having limited number of nodes (30-50 nodes). The latter is more complex and incurs cost for setting a new subnet. This thesis contributes to enhancing scalability using a single subnet with only 1 subnet. The thesis identified scheduling issues within the TSCH model of IEEE 802.15.4. The proposed solution introduces a novel finding which demonstrates that an IPv6 subnet within a range of 1-2 km is effectively managed with hundreds of nodes without sacrificing QoS. This capability is highly sought for industrial automation worldwide.

Chapter 1 begins with an overview of the background, aims, and objectives of the study, along with the structure of the thesis. The key contributions of the proposed research are also outlined in this chapter.

Chapter 2 reviewed, and evaluated IoT communication technologies which confirms that across many popular IoT technologies IEEE 802.15.4-6TiSCH is the most suitable solution for industrial networks with potential for further expansion.

Chapter 3 briefly reviewed the architecture reference model of 6TiSCH while focusing on routing, scheduling, and physical layer functionalities.

- Section 3.1 provides a detailed review of 6TiSCH architecture.
- Section 3.2 offered an extensive literature review, incorporating nearly all relevant surveys. Subsections 3.2.1 to 3.2.3 reviewed the scheduling solutions for 6TiSCH networks and Subsection 3.2.4 identified the causes behind poor scheduling performance through evaluation of SFs using key KPIs. These are illustrated in Table 7. The insights gained laid the groundwork for developing new strategies to address the inconsistencies observed across the existing scheduling designs.
- Section 3.3 evaluated the testing tools based on hardware compatibility, complexity, coding platforms, scalability, full-stack implementation, TSCH implementation, traffic flow, and MSF implementation. The analysis concluded that simulation does not perfectly reflect the physical environment and corresponding challenges such as interference, connectivity, mobility and so on. Apart from that testing larger network with expensive hardware devices on real-time basis is not cost-effective either. The 6TiSCH simulator is an ideal simulation tool for testing large-scale networks which is specifically designed for testing TSCH-based scheduling functions. Here, a majority of existing contributions including those adopted simulation methodology have been using the 6TiSCH simulator.
- Section 3.4 reproduced results from OTF to initiate experimentation and gain practical insights into problem analysis. OTF is a widely cited SF in TSCH-based scheduling research. The reproduced results align with the original graphs in the article, enabling further experiments using the same version of the 6TiSCH simulator.
- Finally, Section 3.5 summarized key topics covered through Chapter 3.

Chapter 4 designed, and developed Scalable Scheduling Reservation protocol (SSR) incorporating the cake-slicing technique, and four key strategies: NDS, DTS, CSS, and QOS. Together, these represent a model where each component (strategy) is thoroughly described using examples and algorithms demonstrating potential to improve the scheduling performance of 6TiSCH networks. The cake-slicing technique is tested with various patterns orchestrating key pattern illustrated by Figure 41.

The proposed solution (SSR), was thoroughly evaluated for industrial small factory network. The configuration settings reflected parameter values adequately using appropriate references and coherent description of each parameter. These parameters are independent of testing tools. The evaluation is carried out by focusing on different traffic conditions (fixed periodic traffic) and network sizes:

- Subsection 4.6.1 tested SSR's resilience under varying traffic conditions. It showed zero packet loss in the given settings, demonstrating the robustness of SSR in managing traffic effectively.
- Subsection 4.6.2 analyzed the impact of SSR’s strategies, enabled and disabled. KPIs such as latency, charge consumption, collision, and reliability were included. An additional experiment examined the influence of the PAS with increased volume of nodes in the network (100 to 160 nodes) highlighting the crucial role of PAS in enhancing performance in larger networks.
- Subsection 4.6.3 compared SSR’s performance against other popular SFs, including SF0, ESF0, LV, ReSF, and MSF. KPIs like latency, reliability, collision, and battery life were used to benchmark performance. The results demonstrated that SSR performed well without trade-offs, unlike the other SFs, which showed compromises in different areas of performance.
- Subsection 4.6.4 evaluated SSR’s performance over an extended period of 200 slotframe cycles (equivalent to 200 seconds of network time) with an increased traffic rate of 60 ppm. The results proved SSR’s clear advantage over OTF across various configurations. SSR offered significant improvements (in lowering consumption, reducing collision, reducing latency, and optimizing 6Top overheads) highlighting SSR's efficiency in longer network operations.
- Subsection 4.6.5 focused on densely populated networks, while testing SSR in networks with increasing higher densities, initially starting from 40 nodes and expanding up to 100 nodes. Consequently, SSR consistently outperformed OTF in terms of cell consumption, collision rates, latency, battery life, and reliability. However, beyond 70 nodes, SSR's performance began to gradually decline; though at a significantly lower rate than OTF.

In conclusion, the results demonstrated SSR’s effectiveness in terms of addressing many key scheduling inconsistencies (particularly in terms of scalability, energy efficiency, and reliability). However, despite low consumption of TSCH cells and being energy-focused, unicast solution, SSR suffers a gradual decline in packet upstreaming rate as the number of nodes increases from 70 to 100 during heavy traffic conditions (60 ppm) and other SFs performs fare worse under the similar condition. The registered loss of packets beyond 70 nodes is due to the constrained buffer size and poor propagation (fewer paths available in the network).

Chapter 5 proposed the implementation of SSR under hybrid scheduling model, focusing on enhancing network scalability under various challenging conditions. The hybrid scheduling is witnessing a surge due to it’s ability to separate the control packets from the data packet and providing increased goodput. This proposal addressed several critical issues; while improving the scalability of the 6TiSCH network:

- **Variable adaption delay:** Managing the traffic adaption window responsible for adding or deleting a cell on the recurrent basis over a certain period (time in slotframe) particularly when data packets are using a dedicated slotframe.

- **Challenging traffic conditions**: The ability to manage scheduling resources against the dense networks using periodic traffic generation model (with increased traffic rate) effectively than its counterpart.
- **Topological alignment:** It provided key insights, crucial for understanding the behaviour following controlled and random deployment scenarios where the network topology follows the same propagation model.

For benchmarking, SSR was compared to its counterpart called MSF, the current internet draft for 6TiSCH scheduling (RFC 9033). The evaluation focused on essential performance metrics such as latency, battery life, and reliability under different traffic conditions. The results demonstrated that SSR implemented within the hybrid design outperformed MSF and other distributed scheduling-led SSR in terms of scalability. However, SSR did experience goodput loss under an extremely challenging traffic condition. The primary causes identified behind the packet loss are as follow:

- **Complex scheduling design:** The hybrid scheduling intricate more following the less challenging traffic conditions. The hybrid scheduler had to maintain individual slotframes with different cell types making it difficult reduce excess consumption by preventing nodes to access the active slots less frequently. This is particularly led by the change events in the routing topology, causing trickle timer to resume frequent beaconing (these beacons are comprised of constrained payload (number of bytes) compared to the size of data packet). Unlike the distributed SFs, the period of inactivity is more predictable where change events are immediately assessed; hence it is easier to manage EDC of a node by providing extra cells that can be used for any type of packet. In contrast, the hybrid scheduler must keep some cells active at all the time, causing battery consumption to be less predictable. This complexity was introduced to both MSF and SSR whereby the differences in energy consumption by network sizes and densities were less significant in some cases, leading to challenges in parameterization for less load-sensitive networks.
- **Poor propagation using a single broadcast cell:** Relaying EBs and DIOs on a single broadcast cell for network-wide communication was a major drawback. This impacted network stability, particularly for distant nodes positioned outside the parent hierarchy, had struggled to participate in scheduling negotiations. While adding more broadcast cells could mitigate this issue, it would also complicate the scheduling design and require further adjustments to the slotframes.

Chapter 6 proposed an enhancement to SSR to address the scalability limitations identified in Chapters 4 and 5. After reviewing SSR's performance and its shortcomings, the decentralized and broadcast-based scheduling operation was chosen. This led to the introduction of DeSSR which incorporated additional measures to optimize resource allocation, provide a faster adaption of unexpected traffic, and support to symmetric links.

DeSSR was evaluated through simulations and compared with key SFs, which had previously been regarded as the popular solutions. The evaluation utilized the 6TiSCH simulator whereby various scenarios were tested and analyzed under *steady* and *bursty* traffic conditions through subsections 6.2.3.1 and 6.2.3.3. The traffic conditions introduced in subsection 6.2.3.1 and 6.2.3.3 in Chapter 6 were representative of numerous scenarios tested with heavy-traffic conditions.

The analysis of DeSSR in Chapter 6 provided substantial insights into its capabilities and performance. However, the initial simulations were insufficient to fully evaluate network scalability. To address this, an additional experiment was conducted in subsection 6.2.3.5 using medium-sized and large-scale networks where multiple variables were grouped and tested to observe goodput loss over time.

The results of these *scalability tests* revealed that DeSSR has maintained a high goodput ratio, proving its effectiveness over other SFs in handling high traffic loads and larger network scales (particularly within the range of 50-100 nodes): this improvement in scalability was independent of its impact on latency and energy consumption, which positioned DeSSR as a novel solution in deployment environments for an instance, factory automation in large industrial plant [40], component assembly using a robotic arm considering critical material handling [41], logistics and transportation for efficient supply chain management [34], automating irrigation systems and moisture detection in real-time [27] [38], etc.

The study concludes that SSR is a robust solution for medium-sized network, deployable without a significant expenditure. For example, home automation [22] [23], small factory automation [24], smart Parking [25], industrial plant automation in remote area [26], research and scientific applications such as IoT-based volcano surveillance [28], food processing industry [29], IoT prison break monitoring and altering systems for remotely located centers [30], IoT-based ward medical monitoring systems for remotely located care homes [32], etc.

Finally, there are some limitations of the current study, acknowledging areas where further improvements could be possible particularly in handling open issues. The chapter is closed with recommendations for future work and potential open issues suggesting some potential avenues for refining the DeSSR model, exploring additional enhancements in hybrid scheduling functions, and conducting real-world implementations with some randomness applied in traffic generation to further validate the scalability performance improvements demonstrated in the simulations.

7.2. Meeting the aims and objectives of this thesis

The aims and objectives were defined to address the critical need for enhancing the scalability of 6TiSCH networks within a single-sink IPv6 subnet. The study focused on improving scheduling performance through an analytical distribution model. A novel "cake-slicing" technique was developed to achieve traffic awareness without monitoring node's buffer and delivering improved QoS at a competitive scale. The objectives addressed in this study are summarized as follows:

The thesis reviews popular IoT communication technologies and standards, followed by the evaluation of related technologies in context of Industrial-grade operation.

Chapter 2 provided a comprehensive review of various IoT communication technologies and standards in the context of Industrial IoT networks, framing the problem at hand. The technologies and standards were grouped into three categories: LPWA, CIoT (Cellular IoT), and LP-WPAN. Tables 2, 3, and 4 illustrated basic characteristics of each technology and Table 5 evaluated them in relation to the challenges being addressed in the thesis. The analysis evaluated key technologies based on their design objectives: low-power adaptability for improved deployment cycles, resilience to wireless interference and multipath propagation, latency, and scalability.

The analysis found that:

- LPWA technologies suffer from high latency, frequent connection loss, interoperability issues, and most importantly goodput loss. Industrial network necessitate connection stability for a period of time amid the sensor nodes are interacting with their corresponding next hop (BS or a gateway router). As a result, LPWA technologies are not suitable for industrial automation.
- Among CIoT standards, LTE-M is the only network offering lower latency and mobility. However, it is a subscription-based solution that provides low-power, long-range connectivity with an enhanced data rate. Its adoption in the industrial domain is often impractical due to signal attenuation caused by path fading. This is particularly evident in urban indoor environments. In rural areas, LTE-M's outreach is limited or provided via roaming (using the existing mobile carriers present in that area). This can occur an additional cost in accessing some of its new services that are only provided by LTE-M.
- LP-WPAN are the private network setup with or without the internet connectivity. These solutions suffer from constrained coverage, confined to a few hundred meters. Apart from the poor range, the technical specifications of physical layer across LP-WPANs are consistent (frame size, carrier frequency, hardware capacity, etc.) except for Wi-Fi 802.11ah. The devices implementing 802.11ah are IP-operable and can provide a direct connection to the internet hosting various APIs such as DALI, MATTER, etc. As an indoor technology, this variant of Wi-Fi offers profoundly greater range than all LP-WPANs, but suffers from multipath propagation, causing poor reliability. 6TiSCH and WirelessHART implements channel-hopping to combat multipath challenges and are more efficient in terms of reliability, a key requirement of industrial networks. WirelessHART lack scalability and IP-compatibility. Chapter 2 led to the conclusion that the 6TiSCH standard stands out as the most suitable solution for industrial automation offering improved protection from EI and multipath-fading using frequency diversity mechanism and it is lightweight standard compared WirelessHART or Wi-Fi 802.15ah. IETF 6TiSCH presents a promising path forward with the potential to upscale its communication performance beyond 30-50 devices per subnet.

The thesis briefly navigates through the core components of the 6TiSCH Architecture and reviews scheduling functions where it assesses the suitability of MSF being a scalable solution based on the traffic adaption, energy saving, latency, and reliability.

Chapter 3 provided a detailed description of the architecture reference model of 6TiSCH where it focused on Ipv6 layer, 6Top, and Physical layer capabilities. This chapter laid the groundwork for understanding how the 6TiSCH protocol stack operates. In terms of scheduling, the 6Top layer provided a brief review of MSF where it assessed the suitability of MSF to be a scalable solution following traffic adaptation, energy efficiency, latency, and scalability. The insights from this chapter are fed directly into the development of the core approach in later chapters.

The thesis reviews existing 6TiSCH scheduling approaches and provides justification over selection of evaluation methodology

Section 3.2 provided a comprehensive review of scheduling algorithms categorized into centralized, distributed, and hybrid scheduling approaches. A more in-depth exploration was conducted examining SFs based on unicast and broadcast-based approaches. The evaluation of existing SFs is led by Table 7 where the key limitations of each SF were presented in terms of reliability, latency, energy efficiency, and scalability. The conclusion of this evaluation was that each SF exhibits limitations primarily due to design constraints where scalability fails to align with adequate QoS considerations of 6TiSCH industrial network. Further, existing SFs inaccurately predict traffic conditions and occurs a compromise with consumption of link-layer resources. This shortfall underscores the necessity for more advanced scheduling approaches that can effectively address these inconsistencies and improve overall communication performance with improved scalability.

Section 3.3 decides the evaluation methodology where a clear justification for selecting simulation-based methodology is provided considering several factors and scope of this research. The analysis concluded that the 6TiSCH simulator is widely used for evaluating the performance of an IPv6 WSN, especially for testing a large number of nodes per subnet. In addition to its wide usage, the cost-effectiveness of the 6TiSCH simulator was a key factor in its selection. This decision was supported by the technical specifications presented in Table 8.

Section 3.4 reproduced simulation results from a key paper using 6TiSCH simulator demonstrating consistency across most reproduced graphs. This process not only validated the methodology but also highlighted key challenges impeding the scalability of 6TiSCH networks, reinforcing the need for improved scheduling mechanisms to enhance network performance in larger-scale deployments.

This thesis will design an analytical technique called cake-slicing to facilitate efficient scheduling operation in 6TiSCH network. This technique is further exploited to optimize synergies between key scheduling metrics (network depth, traffic adaptation, cell selection, and queue optimization).

Chapter 4 proposed a model where the cake-slicing technique is the core approach used by remaining component of the model. This chapter provided algorithms with supporting examples in terms of addressing the scheduling metrics holistically. The cumulative strength of all four strategies and cake-slicing technique (components) was expected to improve scheduling performance and achieve improved scalability. After that, the performance evaluation is carried out using the 6TiSCH simulator. The configuration parameters and their values are justified under Section 4.6 based on RFC 5673.

This thesis will evaluate the performance of the proposed solution (SSR) using distributed scheduling, benchmark results against key related SFs, and outlines the key limitations in terms of scalability.

The designed model was tested in the context of unicast-based distributed scheduling. The first experiment outlined in Section 4.6.1 evaluated SSR's resilience to traffic variability. According to the results, it successfully handled varying traffic loads.

In Section 4.6.2, the analysis conveyed the impact of SSR's key strategies across the key metrics such as latency, reliability, and energy-efficiency.

Section 4.6.3 highlighted SSR's strong performance compared to most SFs, showing that SSR achieved improved communication performance without any trade-offs between latency, energy consumption, and reliability. In contrast, other SFs exhibited trade-offs, particularly in balancing energy consumption and latency.

In the final experiment, Section 4.6.4 tested SSR under challenging traffic loads of 60 ppm. The results were compared to OTF using multiple thresholds. The findings showcase a significant advantage over fixed threshold-based overprovisioning as implemented by OTF using all three variants. This suggested that fixed allocation provides no particular advantage in managing scheduling resources. However, as the network size increased beyond 70 nodes SSR showed a slight decline in reliability; though it remained more stable than the sharp performance decline exhibited by OTF.

The key takeaway from this experiment is that distributed scheduling using dedicated cells is expensive where an SF struggles with heavy queue occupation due to single broadcast reference. The packet loss (beyond 70 nodes under challenging traffic conditions) cannot be directed toward shortage of cells; in fact, SSR scheduled fewer cells than OTF and still performed better in most scenarios. To improve network performance of distributed scheduling, it is crucial to enhance negotiations within the network topology, which is constrained by the poor proliferation of information. This gap in broadcast efficiency undermines the broader utilization of scheduling resources across the network.

To address scalability limitation posed by distributed scheduling using dedicated cells, the thesis proposes implementation of SSR in hybrid scheduling model. This thesis evaluates the performance of the SSR and benchmarked results using MSF.

In Chapter 5, SSR is carefully examined to ensure that each strategy enhances network performance whilst implemented within the hybrid scheduling model. This chapter particularly focuses on enhancement of NDS and DTS whereas the CSS is intentionally excluded since it aligns slots closer together; hence the risk of collisions is higher in the shared slots. Typically, a higher volume of collided cells would be negatively impacting the Tx buffer by forcing retransmissions.

The evaluation is presented in Section 5.5 where Section 5.5.1 evaluates the impact of fixed traffic adaptation delay in MSF compared to a dynamic traffic adaptation delay in SSR. The experiment measured Tx queue utilization under challenging traffic conditions (60 ppm) for over a 66.7-minute test. The results showed improvement in performance by using SSR; while remained stable using only 1/3rd (33 slots) of the total capacity of the slotframe.

In the random topology, SSR showed significant improvements in latency, reliability, and queue utilization compared to MSF. However, the battery life did not shift significantly, attributed to complex hybrid design where autonomous cells positioned centrally in the network remain always active, consuming equal amount of energy during the period of inactivity.

Additionally, SSR achieved the lowest cell consumption, fewest 6P failures, and minimal retries, but the node joining and synchronization delay remained a challenge; according to this, sensor nodes tend to form an extended hop distance to the root using a fixed adaption delay (MSF), which is more pronounced with a single broadcast reference (for propagation). Consequently, MSF led to a higher transmission delay and affected synchronization accuracy as the resulting routing topology formed an extended hop distance to the root.

In Section 5.5.2, the experiments conducted used the full capacity of the slotframe (101 slots) and a higher traffic load of 120 ppm testing scalability of the network. The performance was evaluated using various network sizes ranging from 50-100 nodes. The CDFs at 90% probability revealed that SSR delivered significant improvements over MSF in terms of latency, reliability, and battery life. One notable observation was that the battery life across different networks under SSR did not show significant variance despite varying network conditions. In contrast, networks utilizing distributed scheduling alone demonstrated a linear trend in battery consumption where battery life shifted more predictably (to a lower bound) with network expansion (Figure 56 (C)).

Section 5.5.3 extended the performance testing of SSR to 100 node network under the increasingly challenging traffic conditions using a linear topology. The packets were generated in the network using periodic generation model using a fixed packet period threshold. The boxplots revealed key insights showing the the effect of topology on network scalability and overall scheduling performance:

- Under linear topology, the energy consumption showed a more linear association for all scenarios (network densities and varying packet generation intervals). This demonstrated that topological alignment plays a crucial role in the scalability and performance of the 6TiSCH network. The performance of SSR in this linear topology offered several advantages over MSF, particularly in challenging conditions. However, it was noted that MSF can still achieve high battery life when the traffic load remains manageable, such as at 30 ppm.

- SSR incurs goodput loss with a 100-node network; while SSR significantly enhances scalability and outperforms MSF under various conditions under extreme traffic load, the limitations imposed by the single broadcast cell had a notable impact on network performance, especially under higher extreme traffic loads where the inefficiency in broadcasting through the distant nodes triggered recurrent change-events, accompanied by higher beaconing cost (trickle timer reset), and subdue the efficiency gained by distributed scheduling (poor participation by nodes for exchanging cells).
- This results are based on the periodic packet generation model where traffic condition per node are fixed (more predictable). Notably, with random packet generation, the impact on performance is unknown so this is envisaged as a limitation of the hybrid SSR.

To further improve scalability, the thesis proposes an enhancement of SSR using additional sets of measures and implementing the final solution in decentralized, broadcast-based scheduling operation. This thesis evaluates the performance of the DeSSR using steady traffic, bursty traffic experimentation where key algorithms (LV and OTF) were included for analysis.

DeSSR is an enhanced version of SSR, which introduced a PDR-based screening to improve node performance and avoid worse-performing nodes without generating any additional overhead. This screening mechanism was layered on top of the DTS proposed by distributed SSR, aiming to improve overall network performance by carefully selecting reliable nodes for allocating extra cells. In addition to the PDR-based screening; NDS was also enhanced in DeSSR. This enhancement in NDS led to reorganising the nodes based on the new threshold. DeSSR combined both the DTS and the enhanced NDS into a single, unified algorithm. Apart from these additions, CSS was set to random and the QOS remained unchanged. The cake-slicing technique was retained as a core logic towards resource distribution.

This thesis evaluates the performance of the DeSSR using steady traffic, bursty traffic experimentation where state-of-art algorithms (LV and OTF) were included for analysis.

Section 6 thoroughly evaluated DeSSR using steady traffic, and a bursty traffic experiment. The results showed that DeSSR performance over time, with 100 nodes, offered latency around 1s, maintained lowest consumption compared to LV and multiple variants of OTF, triggered a balanced volume of overheads, and improved Tx-buffer utilization significantly. Under an bursty traffic trend, DeSSR is an advantage to improve scalability and resilience. The results showed that DeSSR consistently outperformed OTF considering the volume of packets upstreamed over time at both events of burst using the lowest volume of cells and triggered lower collisions.

The thesis now evaluates the scalability limit of DeSSR under exceptionally challenging traffic load in a dense and large-scale deployment, and concludes the study undertaken.

In Section 6, the reliability of DeSSR was evaluated under exceptionally high traffic conditions in both medium-ranged and large-scale networks. The key findings highlighted DeSSR superiority compared to OTF, LV, and E-OTF, particularly in terms of reliability under varying traffic loads. Despite the outstanding performance, DeSSR encountered some limitations, especially under exceptionally high traffic loads whereby goodput loss were observed. The primary cause of this was attributed to congestion in the network which stemmed from the limited size of the Tx buffer available for packet storage. However, the evaluation also demonstrated that DeSSR is capable to upstream a large amount of data (200-600 packets) efficiently and rapidly within networks of up to 100 nodes. Despite the constrained buffer size, DeSSR offered superior goodput compared to other SFs, showcasing its ability to handle high traffic conditions effectively.

The results further confirmed scalability strength of DeSSR in larger networks with the potential to support several hundred nodes per installation (subnet) under common conditions. In summary, DeSSR proved to be a reliable and high-performing solution, especially in dense and traffic and time-intensive networks; though congestion remains a challenge under extreme traffic loads due to the buffer limitations. These results are confined to a fixed traffic generation model implemented by 6TiSCH simulator.

7.3. Limitations

This section highlights limitations of the proposed work undertaken and outlines possible future work.

7.3.1. Dependency on RPL routing

The proposed approach uses NDS to assess node's whereabouts in the topology, which is inherently dependent on RPL's rank metrics hysteresis. RPL is a proactive routing protocol, which calculates link-quality based on the PDR or RSSI metrics. These are reviewed in Chapter 3. A critical evaluation of different OFs is provided in *Ghaleb et al.*, [171]. The thesis outlines number of limitations where one of the key limitations is dependency is on RPL.

7.3.2. Collision control

Controlling collision in a densely populated 6TiSCH Network requires building a collision-free schedule in the slotframe, which is currently an open challenge [195]. Channel-hopping is certainly an advantage as it reduces impact of EIs and multipath-fading, but when multiple nodes are attempting to transmit packets using the same cell due to poor propagation, collision is difficult to be avoided. In this context, the IEEE 802.15.4 standard provides a default back-off mechanism dealing with collision in broadcast, and shared schedule. Here, a singleton broadcast slotframe may not be sufficient for the entire network. In the slotframe of soft cells, cells are added and deleted by nodes to adapt traffic conditions. The housekeeping mechanism is provided to deal with a cell or the entire bundle of cells (in the cellist of node) that are not performing well. For deterministic performance, collision avoidance is beneficial. SSR using unicast-based distributed scheduling implements the channel-change scheme defined in ESF0 in Chapter 4 only and this was more suitable for a unicast-based distributed scheduling network. This thesis does not propose channel-change algorithm separately.

7.3.3. Cake-slicing and change of hypothesis

The scope of *cake-slicing* technique is however broader where it resolves disputes between multiple entities making reservations to limited resources. The new behaviors in the distribution are not admissible without a change of hypothesis. For example: the current hypothesis states that some nodes are busier than others depending on the distance to the root. Hence, the cake-slicing produces data sets accordingly. Apart from that, cake-slicing is not ideal for smaller data sets especially in the context of scheduling therefore the work of cake-slicing is forbidden to channel-change in TSCH-led scheduling operation (16 channels at most in 2.4GHz RF module of IEEE 802.15.4 standard).

7.4. Future work and open issues

This section outlines potential future work focused on enhancing the scalability of 6TiSCH networks.

7.4.1. Further optimization of bandwidth

Decentralized, broadcast-based scheduling drains battery current rapidly by default. It uses multiple connections and for each node, allowing packets to be upstreamed using different-2 routes. This process incurs a significant amount of control overheads. The challenge is to improve energy-savings through optimization of beaconing in the network. With improved propagation, nodes seek to get closer to the root using RPL preferred parenting and with more nodes assigned closer to the root having improved link quality (high PDR), DeSSR will provide these nodes with extra cells, which leads to wastage as these nodes may not be equally employed in relaying payload to root.

7.4.2. Parameterization for improving energy efficiency

Currently, parameterization is an open issue and there is more work needed to enhance energy saving in 6TiSCH networks, for an instance DeSSR employs 3 broadcast cells, while other implementations of SSR used only 1 cell. The difference in charge consumption between SSR and DeSSR is significant. Subsection 6.2.3.6.1 showed that with broadcast cells ranging from 1 to 8, consumption is highest with 6 cells and second highest with 5 cells. It also shows that the difference in charge consumed (mA) between using 3 cells and 8 cells is not significant. In fact, with 3 cells, the consumption is slightly lower. Anything fewer than 3 cells shows a linear increase in charge consumption; for example, 1 cell offers the lowest estimate, while 2 cells result in a linear growth in consumption. Parameterization could offer relief here besides most deployments of 6TiSCH is assumed to occur without a prior site-testing.

7.4.3. 6LoWPAN fragment recovery

Proposed solution was evaluated using a simulation tool where SSR's implementation across both unicast and broadcast-based distributed scheduling used FIFO towards packet assembly: the receiving node will have to wait until entire set of fragment are recovered. The future work may utilize VRB technique that allows faster delivery, but it suffers from poor fragment recovery, leading to the entire packet being dropped when a particular fragment is not received (only the first fragment carries routing header). Albeit, fragment recovery is currently open challenges, one can explore ways to accommodate VRB towards minimal queuing delay across both unicast-based scheduling; in broadcast-based scheduling, recovery of a missing fragment may not be influential because there is more than 1 broadcast cell is being used by default, allowing streaming via multiple routes.

7.4.4. Randomness in traffic generation

The thesis adopted simulation as a key evaluation methodology for testing larger networks. The standard 6TiSCH simulator uses a periodic traffic generation model, where a fixed amount of traffic is distributed at predefined times in the slotframe through propagated beacons. This approach simplifies scheduling compared to more advanced traffic models that introduce randomness over time. Exploring new traffic generation models, such as '*Poisson'* or '*Pareto',* is desirable for assessing their impact on scheduling performance, particularly in terms of collision rates. Notably, collision-mitigation remains an open issue in 6TiSCH networks.

7.4.5. Test-bed implementation

Proposed solution was evaluated using 6TiSCH simulator which is a simulation tool. When gathering the data from such evaluation, the node position is as per the connectivity module defined by the simulation tool and interferences are managed differently by each version of the 6TiSCH simulator. The performance of SSR and DeSSR can be further evaluated using real-time testbed.

References

[1] Cisco, "Cisco Annual Internet Report (2018–2023) White Paper," CISCO, 2020.

[2] Ericsson, "IoT connections outlook," ericsson.com, 2023.

[3] T. Watteyne, M. R. Palattella and L. A. Grieco, "Using IEEE802.15.4e Time-Slotted Channel Hopping((TSCH) in the Internet of Things (IoT): ProblemStatement," *Internet Engineering Task Force, IETF,* 2015.

[4] Connectivity standards alliance, "zigbee The Full Stack Solution for All Smart Devices," 2024. [Online]. Available: https://csa-iot.org/all-solutions/zigbee/. [Accessed 6 2024].

[5] Wikipedia, "Bluetooth Low Energy," 1 2 2021. [Online]. Available: https://en.wikipedia.org/wiki/Bluetooth_Low_Energy.

[6] A. N. Kim, F. Hekland, S. Petersen and P. Doyle, "When HART goes wireless: Understanding and implementing the WirelessHART standard," in *2008 IEEE International Conference on Emerging Technologies and Factory Automation*, Hamburg, germany, 2008.

[7] The International Society of Automation, "ISA 100.11A Wireless Systems for Industrial Automation: Process Control and Related Applications," ISA, 4 May 2011. [Online]. Available: https://standards.globalspec.com/std/1413497/ISA%20100.11A. [Accessed 10 07 2019].

[8] 802.11ah, "IEEE 802.11ah," 1 22 2021. [Online]. Available: https://en.wikipedia.org/wiki/IEEE_802.11ah.

[9] N. Kushalnagar, G. Montenegro and C. Schumacher, "IPv6 over LowPower Wireless Personal Area Networks (6LoWPANs): Overview, Assumptions, Problem Statement, Goals," RFC 4919, 2007.

[10] P. Thubert and J. Hui, " Compression Format for IPv6 Datagrams Over IEEE 802.15.4-Based Networks," RFC 6282, 2011.

[11] T. Watteyne, S. Lanzisera, A. Mehta and K. J. Pister, "Mitigating Multipath Fading through Channel Hopping in Wireless Sensor Networks," in *2010 IEEE International Conference on Communications*, Cape Town, SA, 2010.

[12] T. Winter, P. Thubert, A. Brandt, J. Hui, R. kelsey, P. Levis, K. Pister, R. Struik, J. Vasseur and R. Alexander, "RPL: IPv6 Routing Protocol for Low-Power and Lossy Networks," IETF RFC 6550, 2012.

[13] Wikipedia, "Time-division multiple access," 6 2024. [Online]. Available: https://en.wikipedia.org/wiki/Time-division_multiple_access.

[14] Q. Wang, X. Vilajosana and T. Watteyne, "6TiSCH Operation Sublayer (6top)," 4 06 2014.

[15] P. Thubert, "draft-thubert-6tisch-architecture," *IETF Draft,* 2019.

[16] C. Perkins, E. Belding-royer and S. das, "Ad Hoc on demand distance vector (AODV)routing," IETF RFC 3561, 2003.

[17] D. Johnson, Y. Hu and D. Maltz, "The Dynamic source routing protocol (DSR) for mobile ad hoc networks for ipv4," IETF RFC 4728, 2007.

[18] R. T. Hermeto, G. Antoine and T. Fabrice, "Scheduling for IEEE802.15.4-TSCH and slow channel hopping MAC in low power industrial wireless networks: A survey," *Computer Communication,* vol. 114, pp. 84-105, 2017.

[19] P. T. Duy, T. Dinh and Y. Kim, "Distributed cell selection for schedulling function in 6TiSCH networks," *Compter Standard & Interfaces,* vol. 53, pp. 80-88, 2017.

[20] T. Watteyne, m. r. palattela, Q. Wang, K. Muraoka, n. Accettura, D. Dujovne, a. l. Grieco and t. Engel, "On-the-fly bandwidth reservation for 6TiSCH wireless industrial network," *IEEE sensor journal,* pp. 1-11, 2016.

[21] K. Kralevska, D. Vergados, Y. Jiang and M. Angelos, "A Load balancing algorithm for resource allocation in IEEE 802.15.4e Networks," in *IEEE International Conference on Pervasive Computing and Communications Workshops (PerCom Workshops)*, Athens, Greece, 2018.

[22] E. Borgia, "The Internet of Things vision: Key features, applications and open issues," *Computer Communications,* vol. 54, pp. 1-31, 2014.

[23] V.-M. Sempere-Payá and J. Silvestre-Blanes, "Evaluation of TSCH scheduling implementations for real WSN applications," in *Conference: 2016 IEEE 21st International Conference on Emerging Technologies and Factory Automation (ETFA)*, 2016.

[24] G. Patti, G. Alderisi and L. L. Bello, "Introducing multi-level communication in the IEEE 802.15.4e protocol: The MultiChannel-LLDN," in *Proceedings of the 2014 IEEE Emerging Technology and Factory Automation (ETFA)*, Barcelona, Spain, 2014.

[25] A. Fahim, M. Hasan and M. A. Chowdhary, "Smart parking systems: comprehensive review based on various aspects," *Heliyon,* vol. 7, no. 5, 2021.

[26] K. Pister, T. Phinney, p. Thubert and S. Dwars, "Industrial Routing Requirements in Low-Power and Lossy Networks," *IETF:RFC 5673,* pp. 1-25, 2009.

[27] K. Brun-Laguna, A. L. Diedrichs, D. Dujovne, R. Leone and X. Vilajosana, "(Not so) Intuitive Results from a Smart Agriculture Low-Power Wireless Mesh Deployment," in *ACM International Conference on Mobile Computing and Networking (MobiCom), Workshop on Challenged Networks (CHANTS)*, NY, USA, 2016.

[28] P. Patel and A. K. Pandey, "IoT based Volcano Multipara meter Surveillance Method," in *2023 3rd International Conference on Advance Computing and Innovative Technologies in Engineering (ICACITE)*, Greater Noida, India, 2023.

[29] H. Dadhaneeya, P. K. Nema and V. K. Arora, "Internet of Things in food processing and its potential in Industry 4.0 era: A review," *Trends in Food Science & Technology,* vol. 139, p. 104109, 2023.

[30] U. C. Joyce, B. R. Luckyn and S. Orike, "Improved Internet of Things Based Prison Break Monitoring and Alarming System: A Case Study of Degema Prisons," *ICONIC RESEARCH AND ENGINEERING JOURNALS ,* vol. 6, no. 5, 2022.

[31] V. Tanasiev , G. C. Patru, D. Rosner, G. Sava, H. Necula and A. Badea, "Enhancing environmental and energy monitoring of residential buildings through IoT," *Automation in Construction,* vol. 126, 2021.

[32] Q. Li, "Design of Ward Medical Monitoring System Based on Internet of Things," in *ISAIMS '23: Proceedings of the 2023 4th International Symposium on Artificial Intelligence for Medicine Science*, 2024.

[33] Intellias, "IoT in Hotels: Solutions That are Transforming the Industry," 30 10 2024. [Online]. Available: https://intellias.com/internet-of-things-iot-hospitality-industry/. [Accessed 1 11 2024].

[34] A. Rajeb, S. Simske, k. Rajeb, H. Treiblmaier and S. Zailani, "Internet of Things research in supply chain management and logistics: A bibliometric analysis," *Internet of things,* vol. 12, 2020.

[35] S. Rahman, M. Pipattanasomporn and M. Kuzlu, "Review of communication technologies for smart homes/building applications," in *2015 IEEE Innovative Smart Grid Technologies - Asia (ISGT ASIA)*, 2015.

[36] Z. Ahmad, M. Pasha, A. Ahmad, A. Muhammad, S. Masud and M. Schappacher, "Performance evaluation of IEEE 802.15.4-compliant smart water meters for automating large-scale waterways," in *2017 9th IEEE International Conference on Intelligent Data Acquisition and Advanced Computing Systems: Technology and Applications (IDAACS)*, Bucharest, Romania, 2017.

[37] T. G. Kessel, M. Ramachandran, L. Klein, D. Nair, N. HInds and H. Hamann, "Methane Leak Detection and Localization Using Wireless Sensor Networks for Remote Oil and Gas Operations," in *2018 IEEE SENSORS*, New Delhi, India, 2018.

[38] Steven Schriber, "Sensor Technology:Smart Agriculture Sensors: Helping Small Farmers and Positively Impacting Global Issues, Too," Mouser Electronics, 3 1 2023. [Online]. Available: https://www.mouser.co.uk/applications/smart-agriculture-sensors/?_gl=1*oue39m*_ga*dW5kZWZpbmVk*_ga_15W4STQT4T*dW5kZWZpbmVk*_ga_1KQLCYKRX3*dW5kZWZpbmVk. [Accessed 12 9 2024].

[39] E. S. Nadimi, H. T. Søgaard, T. Bak and F. W. Oudshoorn, "ZigBee-based wireless sensor networks for monitoring animal presence and pasture time in a strip of new grass," *Computers and Electronics in Agriculture,* vol. 61, no. 2, pp. 79-87, 2008.

[40] N. Accettura, E. Vogli, M. R. Palattella, L. A. Grieco, G. Boggia and M. Dohler, "Decentralised Traffic Aware Schedulling in 6TiSCH network: design and experimental evaluation," *IEEE internet of things journal,* vol. 2, no. 6, pp. 455-470, 2015.

[41] T. Ainsworth, J. Brake, P. Gonzalez, D. Toma and A. F. Browne, "A Comprehensive Survey of Industry 4.0, IIoT and Areas of Implementation," in *SoutheastCon 2021*, Atlanta, GA, USA, 2021.

[42] Siemens, "HVAC Optimization," Siemens, 12 1 2024. [Online]. Available: https://www.siemens.com/global/en/products/buildings/energy-sustainability/hvac-optimization.html?gclid=Cj0KCQiAouG5BhDBARIsAOc08RTyOVTH3Ezn6A8G80pDC4jLUOJ5SQGPW8LfKD2biIUydPZ4nQWmThsaAq2sEALw_wcB&acz=1&gad_source=1. [Accessed 1 11 2024].

[43] A. Paventham, D. Darshini, H. Krishna, N. Pahuja, F. K. Mohammad and A. Jain, "Experimental evaluation of IETF 6TiSCH in the context of Smart Grid," in *https://ieeexplore.ieee.org/xpl/conhome/7383415/proceeding*, Milan, Italy, 2015.

[44] M. Saravanan, A. Das and V. Iyer, "Smart water grid management using LPWAN IoT technology," in *2017 Global Internet of Things Summit (GIoTS)*, Geneva, Switzerland, 2017.

[45] M. I. Nashiruddin and A. A. F. Purnama, "NB-IoT Network Planning for Advanced Metering Infrastructure in Surabaya, Sidoarjo, and Gresik," in *2020 8th International Conference on Information and Communication Technology (ICoICT)*, Yogyakarta, Indonesia,, 2020.

[46] S. K. Wilson, S. Wilson and E. Biglieri, Academic Press Library in Mobile and Wireless Communications:Transmission Techniques for Digital Communications, Academic Press, 2016.

[47] L. Atzori, A. Iera and G. Morabito, "The Internet of Things: A survey," *Computer Networks,* vol. 54, no. 15, pp. 2787-2805, 2010.

[48] J. C. Cano, V. Berrios, B. Garcia and C. K. Toh, "Evolution of IoT: An Industry Perspective," *IEEE Internet of Things Magazine,* vol. 1, no. 2, pp. 2576-3180, 2018.

[49] Intel, "Internet of Things(IoT) Home:Explore the Essential Elements of IoT," 2 8 2024. [Online]. Available: https://www.intel.com/content/www/us/en/internet-of-things/overview.html.

[50] B. Buurman, J. KAMRUZZAMAN, G. Karmakar and S. Islam, "Low-Power Wide-Area Networks: Design Goals,Architecture, Suitability to Use Cases and Research Challenges," *IEEE Access,* pp. 17179- 17220, 2020.

[51] J. Lin, W. Yu, N. Zhang, X. Yang, H. Zhang and W. Zhao, "A Survey on Internet of Things: Architecture, Enabling Technologies, Security and Privacy, and Applications," *IEEE INTERNET OF THINGS JOURNAL,* vol. 4, no. 5, pp. 1125-1143, 2017.

[52] J. Granjal, E. Monteiro and J. S. Silva, "Security for the Internet of Things: A Survey of Existing Protocols and Open Research Issues," *IEEE COMMUNICATION SURVEYS & TUTORIALS,* vol. 17, no. 3, pp. 1294-1312, 2015.

[53] A. Al-Fuqaha, M. Guizani, M. Mohammadi, M. Aledhari and M. Ayyash, "Internet of Things: a Survey on enabling technologies, Protocols, and Applications," *IEEE COMMUNICATION SURVEYS & TUTORIALS,* vol. 17, no. 4, pp. 2347-2377, 2015.

[54] U. Raza, P. Kulkarni and M. Sooriyabandara, "Low Power Wide Area Networks: An Overview," in *in IEEE Communications Surveys & Tutorials*, 2017.

[55] ARM, "Unlimited Opportunities for an Intelligent IoT," 1 03 2024. [Online]. Available: https://www.arm.com/markets/iot.

[56] Atmel, "Atmel," 1 7 2024. [Online]. Available: https://en.wikipedia.org/wiki/Atmel.

[57] Silab, "Matter: A Unified Approach to IoT Device Development," 2 7 2024. [Online]. Available: https://www.silabs.com/wireless/matter?source=Media&detail=Google-PPC&cid=med-gos-mat-041923&s_kwcid=AL!16736!3!582185200773!b!!g!!matter%20chip&gad_source=1&gclid=Cj0KCQjwzva1BhD3ARIsADQuPnUQ0RmRYlkEKkD46hmb5Tpl2_ZbP1tNm0WfBCijjHoMGx8GCmWn8pkaAnm_EALw_wc.

[58] Texas Instruments, "Texas Instruments," 11 2 2024. [Online]. Available: https://en.wikipedia.org/wiki/Texas_Instruments#:~:text=Texas%20Instruments%20Incorporated%20(TI)%20is,worldwide%20based%20on%20sales%20volume..

[59] Nvidia, "Reinvent Manufacturing—From Design to Delivery," 1 3 2024. [Online]. Available: https://www.nvidia.com/en-gb/industries/manufacturing/.

[60] Samsung, "Control your home with ease," 3 2 2024. [Online]. Available: https://www.samsung.com/levant/smartthings/.

[61] S. R. Kota and N. S. Swami, "An Empirical Study on System Level Aspects of Internet of Things (IoT)," *IEEE Access,* vol. 8, pp. 188082-188134, 2020.

[62] I. Andrea, . C. Chrysostomou and G. Hadjichristofi, "Internet of Things: Security vulnerabilities and challenges," in *2015 IEEE Symposium on Computers and Communication (ISCC)*, Larnaca, Cyprus, 2015.

[63] G. Glissa and A. Meddeb, "6LowPSec: An end-to-end security protocol for 6LoWPAN," *Ad Hoc Networks,* vol. 82, pp. 100-112, 2019.

[64] W. Ayoub, A. W. Samhat and F. Nouvel , "Internet of Mobile Things: Overview of LoRaWAN, DASH7, and NB-IoT in LPWANs Standards and Supported Mobility," *IEEE Communications Surveys & Tutorials ,* vol. 21, no. 2, pp. 1561-1581, 2018.

[65] P. Sethi and S. R. Sarangi, "Internet of Things: Architectures, Protocols, and Applications," *Hindawi Journal of Electrical and Computer Engineering,* vol. 2017, no. https://doi.org/10.1155/2017/9324035, pp. 1-25, 2017.

[66] R. Gorrepotu, N. Korivi, k. Chandu and S. Deb, "Sub-1GHz miniature wireless sensor node for IoT applications," *Internet of Things,* vol. 1, no. 2, pp. 27-39, 2018.

[67] Starlink, "Starlink:regular access to space," 1 11 2024. [Online]. Available: https://www.starlink.com/gb/technology. [Accessed 3 11 2024].

[68] M. Vaezi, A. Azari, R. S. Khosravirad, m. Shirvanimoghaddam, M. M. Azari, D. Chasaki and P. Popovski, "Cellular, Wide-Area, and Non-Terrestrial IoT: A Survey on 5G Advances and the Road Toward 6G," *IEEE COMMUNICATIONS SURVEYS & TUTORIALS,* vol. 24, no. 2, pp. 1117-1173, 2023.

[69] Lora-alliance, "LoRaWAN® transforms businesses by connecting wireless IoT sensors simply and affordably," 1 8 2024. [Online]. Available: https://lora-alliance.org/.

[70] A. Zourmand, A. L. Kun Hing, C. Wai Hung and M. AbdulRehman, "Internet of Things (IoT) using LoRa technology," *2019 IEEE International Conference on Automatic Control and Intelligent Systems (I2CACIS)*, Selangor, Malaysia, 2019, pp. 324-330, doi: 10.1109/I2CACIS.2019.8825008.

[71] G. Peruzzi and A. Pozzeborn, "A Review of Energy Harvesting Techniques for Low Power Wide Area Networks (LPWANs)," *Energies,* vol. 13, no. 13, p. 3433, 2020.

[72] R. Falanji, M. Heusse and A. Duda, "Range and Capacity of LoRa 2.4 GHz," in *EAI Mobiquitous 2022*, 2022.

[73] K. Mekki, E. Bajic, F. Chaxel and F. Meyer, "A comparative study of lpwan technologies for large-scale iot deployment," *ICT Express,* vol. 5, pp. 1-7, 2019.

[74] B. N. Silva, M. Khan and K. Han, "Towards sustainable smart cities: A review of trends, architectures, components, and open challenges in smart cities," *Sustainable Cities and Society,* vol. 38, pp. 697-713, 2018.

[75] Brandon Lewis, "Building Automation for the Hybrid Work Era," Mouser Electronics, 3 6 2024. [Online]. Available: https://eu.mouser.com/applications/building-automation-hybrid-work-era/. [Accessed 2 10 2024].

[76] Sigfox, "SigFoX OG Technology:What is Sigfox 0G Technology," 2 7 2022. [Online]. Available: https://www.sigfox.com/technology.

[77] A. Lavric, A. I. Petrariu and V. Popa, "Long Range SigFox Communication Protocol Scalability Analysis Under Large-Scale, High-Density Conditions," in *IEEE Access*, vol. 7, pp. 35816-35825, 2019, doi: 10.1109/ACCESS.2019.2903157.

[78] Mouser Electronics, "Industrial Automation," Mouser Electronics, 122 1 2024. [Online]. Available: https://eu.mouser.com/c/industrial-automation/. [Accessed 21 4 2024].

[79] Dash7 Alliance: , "An Open Specification for Industrial IoT :sub-Ghz Low power communication," 1 1 2024. [Online]. Available: https://www.dash7-alliance.org/.

[80] W. Ayoub, A. E. Samhat, F. Nouvel, M. Mroue and J.-C. Prévotet, "Internet of Mobile Things: Overview of LoRaWAN, DASH7, and NB-IoT in LPWANs Standards and Supported Mobility," *IEEE communication surveys & Tutorials,* vol. 21, no. 2, pp. 1561-1581, 2018.

[81] K. Mekki, E. Bajic, F. Chaxel and . F. Meyer, "Overview of cellular LPWAN technologies for IoT deployment: Sigfox, LoRaWAN, and NB-IoT," in *2nd International Workshop on Mobile and Pervasive Internet of Things*, Athens, 2018.

[82] Wikipedia, "DASH7," 29 7 2024. [Online]. Available: https://en.wikipedia.org/wiki/DASH7.

[83] M. Grabia, T. Markowski, J. Mruczkiewicz and K. Plec, "Design of a DASH7 low power wireless sensor network for Industry 4.0 applications," in *2017 IEEE International Conference on RFID Technology & Application (RFID-TA)*, Warsaw, Poland, 2017.

[84] RPMA, "INGENU:It's simply Genious Technology:Unprecedented Coverage.," INGENU, 1 8 2024. [Online]. Available: https://www.ingenu.com/technology/rpma/. [Accessed 1 11 2024].

[85] INGENU, "TECHNOLOGY," 1 7 2024. [Online]. Available: https://www.ingenu.com/technology/?doing_wp_cron=1719950162.2675149440765380859375.

[86] N. S. CHILAMKURTHY, O. J. PANDEY, A. GHOSH, L. R. CENKERAMADDI and H. N. DAI, "Low-Power Wide-Area Networks: A Broad Ovwerview of Its Different Aspects," 2022.

[87] M. T. a. G. Abbas, K. Johan, A. Johan and Stefan and Rajiullah, Mohammad and Brunstrom, Anna, "Energy-Saving Solutions for Cellular Internet of Things–A Survey," *IEEE Access,* vol. 10, pp. 62073-62096, 2022.

[88] Weightless, ", May 2016, [online] Available:," 12 february 2021. [Online]. Available: http://www.weightless.org/..

[89] GSMA, "Extended Coverage – GSM – Internet of Things (EC-GSM-IoT)," 2 7 2022. [Online]. Available: https://www.gsma.com/solutions-and-impact/technologies/internet-of-things/extended-coverage-gsm-internet-of-things-ec-gsm-iot/.

[90] A. Lavric and V. Popa, "LoRa™ wide-area networks from an Internet of Things perspective"," in *2017 9th International Conference on Electronics, Computers and Artificial Intelligence (ECAI)*, 2017.

[91] Y. Lalle, M. Fourati, L. C. Fourati and J. P. Barraca, "Routing Strategies for LoRaWAN Multi-Hop Networks: A Survey and an SDN-Based Solution for Smart Water Grid," in *IEEE Access*, vol. 9, pp. 168624-168647, 2021, doi: 10.1109/ACCESS.2021.3135080.

[92] Dentisa Prodanova, "Listen Before Talk – The Key to Good LoRaWAN® Communication," 10 9 2022. [Online]. Available: https://news.rakwireless.com/listen-before-talk-the-key-to-good-lorawan-r-communication/.

[93] J. M. Marais, A. M. Abu-Mahfouz and . G. P. Hancke, "A Survey on the Viability of Confirmed Traffic in a LoRaWAN," *IEEE Access,* vol. 8, pp. 9296-9311, 2020.

[94] C. L. Athanasiadis, T. A. Papadopoulo and G. C. Kryonidis, "A Review of Smart Meter Data Analytics for Distribution Network Applications," in *2023 IEEE Belgrade PowerTech*, Belgrade, Serbia, 2023.

[95] M. A. Mamun; Mehmet Rasit Yuce and M. R. Yuce, "Sensors and Systems for Wearable Environmental Monitoring Toward IoT-Enabled Applications: A Review," *IEEE Sensors Journal,* vol. 19, no. 18, pp. 7771 - 7788, 2019.

[96] V. Selvakumar, S. Sivanandan, V. Saillaja and A. Subbarayudu, "Smart Asset Management: Tracking and Optimizing Assets with IoT Sensors," in *2023 2nd International Conference on Edge Computing and Applications (ICECAA)*, Namakkal, India, 2023.

[97] H. R. Walker, "Ultra narrow band modulation," in *2004 IEEE/Sarnoff Symposium on Advances in Wired and Wireless Communication*, princeton, NJ, USA, 2004.

[98] P. Thubert, X. Vilajosana, D. Cavalcanti, C. Schmitt and J. Farkas, "Reliable and Available Wireless Technologies," 10 july 2023. [Online]. Available: https://datatracker.ietf.org/doc/html/draft-ietf-raw-technologies-08#name-80211ax-high-efficiency-he.

[99] W. Ayoub, F. Nouvel, A. S. Samhat, J.-c. Prevotet and M. Mroue, "Overview and Measurement of Mobility in DASH7," in *2018 25th International Conference on Telecommunications (ICT)*, Malo, France, 2018.

[100] A. Khalifeh, K. Aldahdouh and K. A. Darab, "A Survey of 5G Emerging Wireless Technologies Featuring LoRaWAN, Sigfox, NB-IoT and LTE-M," in *2019 International Conference on Wireless Communications Signal Processing and Networking (WiSPNET)*, Chennai, India, 2019.

[101] LTE-M, "LTE-M," 25 7 2024. [Online]. Available: https://en.wikipedia.org/wiki/LTE-M.

[102] G. A. Medina-Acosta, L. Zhang, J. Chen, K. Uesaka, Y. Wang and O. Lundqvist, "3GPP Release-17 Physical Layer Enhancements for LTE-M and NB-IoT," *IEEE Communications Standards Magazine ,* vol. 6, no. 4, pp. 80-86, 2022.

[103] N. Mangalvedhe, R. Ratasuk and Ghosh, "NB-IoT deployment study for low power wide area cellular IoT," in *2016 IEEE 27th Annual International Symposium on Personal, Indoor, and Mobile Radio Communications (PIMRC*, 2016.

[104] M. Kanj, V. Savaux and M. Le Guen, "A Tutorial on NB-IoT Physical Layer Design," in *IEEE Communications Surveys & Tutorials*, vol. 22, no. 4, pp. 2408-2446, Fourthquarter 2020, doi: 10.1109/COMST.2020.3022751.

[105] L. Nuaymi, WiMAX: Technology for Broadband Wireless Access, John Wiley & Sons, 2007.

[106] D. Pareit, B. Lannoo, I. Moerman and P. Demeester, "The History of WiMAX: A Complete Survey of the Evolution in Certification and Standardization for IEEE 802.16 and WiMAX," *IEEE Communication Surveys and Tutorials,* vol. 14, no. 4, pp. 1183-1211, 2012.

[107] V. Vomhoff, S. Raffeck, S. Gebert, S. Geissler and T. Hossfeld, "NB-IoT vs. LTE-M: Measurement Study of the Energy Consumption of LPWAN Technologies," in *2023 IEEE International Conference on Communications Workshops (ICC Workshops)*, Rome, Italy, 2023.

[108] Sony-semicon, "Smart Meters," Sony, 12 1 2024. [Online]. Available: https://altair.sony-semicon.com/iot-applications/smart-metering/. [Accessed 12 2 2024].

[109] R. Ratasuk, N. Mangalvedhe, Y. Zhang, M. Robert and J. -P. Koskinen, "Overview of narrowband IoT in LTE Rel-13," *2016 IEEE Conference on Standards for Communications and Networking (CSCN)*, Berlin, Germany, 2016, pp. 1-7, doi: 10.1109/CSCN.2016.7785170.

[110] M. Forcolin, E. Fracasso and F. Tu, "EURIDICE — IoT applied to logistics using the Intelligent Cargo concept," in *2011 17th International Conference on Concurrent Enterprising*, Aachen, Germany, 2011.

[111] E. DEUSSOM, D. S. Petmegni, E. Tonye and B. A. R. Fouba, "External Interferences Detection by Examples in LTE Networks for 4G and 5G Networks Efficient Deployments," in *Network and Communication Technologies*, 2024.

[112] lansitec, "NB-IoT Container Tracker," lansitec.com, 2 9 2024. [Online]. Available: https://www.lansitec.com/products/nb-iot-container-tracker/. [Accessed 4 2 2024].

[113] A. D. Zayas, F. J. R. Tocado and P. Rodriguez, "Evolution and Testing of NB-IoT Solutions," *Appl. Sci,* pp. 10-21, 2020.

[114] E. M. Migabo, K. D. Djouani and A. M. Kurien, "The Narrowband Internet of Things (NB-IoT) Resources Management Performance State of Art, Challenges, and Opportunities," in *IEEE Access*, vol. 8, pp. 97658-97675, 2020, doi: 10.1109/ACCESS.2020.2995938.

[115] J. L. R. Sarmiento, "Interfeence Management in NB-IoT for Heterogeneous Wireless Network," PhD thesis, 2019.

[116] S. Ugwuanyi, J. Hansawangkit and J. Irvin, "NB-IoT Testbed for Industrial Internet of Things," in *2020 International Symposium on Networks, Computers and Communications (ISNCC)*, Montreal, QC, Canada,, 2020.

[117] S. Ugwuanyi, J. Hansawangkit and j. Irvine, "NB-IoT Testbed for Industrial Internet of Things," in *2020 International Symposium on Networks, Computers and Communications (ISNCC)*, Montreal, QC, Canada, 2020.

[118] M. Lukic, S. Sobot, I. Mezei, D. Vukob and D. Danilovic, "In-depth Real-World Evaluation of NB-IoT Module Energy Consumption," in *2020 IEEE International Conference on Smart Internet of Things (SmartIoT)*, Beijing, China, 2020.

[119] Zensys, "Zensys informatica E technologia," 1 8 2022. [Online]. Available: https://www.zensys.com.br/en/gisa/..

[120] T. Kim and P. Linh, "A Study of the Z-Wave Protocol: Implementing Your Own Smart Home Gateway," in *2018 3rd International Conference on Computer and Communication Systems (ICCCS),*, nagoya, Japan, 2018.

[121] Bluetooth Low Energy, "Bluetooth Low Energy," 2024. [Online]. Available: https://en.wikipedia.org/wiki/Bluetooth_Low_Energy. [Accessed 5 8 2022].

[122] V. A. Karbolin and V. Nosov, "Performance Analysis of Ultra Wide Band Communication System in Terms of Data Rate Dependency and Sampling Rate Dependency of an Indoor Wireless Channel Impulse Response," in *2018 XIV International Scientific-Technical Conference on Actual Problems of Electronics Instrument Engineering (APEIE)*, Novosibirsk, Russia, 2018.

[123] Ultra-wideband, "Ultra-wideband," 2024. [Online]. Available: https://en.wikipedia.org/wiki/Ultra-wideband. [Accessed 31 7 2024].

[124] S. D. Padiya and V. S. Gulhane, "IoT and BLE Beacons: Demand, Challenges, Requirements, and Research Opportunities- Planning-Strategy," in *2020 IEEE 9th International Conference on Communication Systems and Network Technologies (CSNT)*, Gwalior, India, 2020.

[125] k. E. Jeon, J. She, P. Soonsawad and P. Chet, "BLE Beacons for Internet of Things Applications: Survey, Challenges, and Opportunities," *IEEE Internet of Things Journal,* vol. 5, no. 2, pp. 811-828, 2018.

[126] R. S. Sherke, P. C. Kamble and K. R. Lakshmappa , "A compact ultra wide band antenna using slots for Internet of Things applications," in *2017 Fourteenth International Conference on Wireless and Optical Communications Networks (WOCN)*, Mumbai, India, 2017.

[127] S. Soni, M. Shrivastava and A. Agwekar, "A Detail Concept and Survey on Ultra Wide Band (UWB) Antennas," *2nd International Conference on Data, Engineering and Applications (IDEA)*, Bhopal, India, 2020, pp. 1-7, doi: 10.1109/IDEA49133.2020.9170657.

[128] V. Niemelä, J. Haapola, M. Hämäläinen and J. Iinat, "An Ultra Wideband Survey: Global Regulations and Impulse Radio Research Based on Standards," in *IEEE Communications Surveys & Tutorials,*, 2017.

[129] S. Dhar and A. Dasgupta, "NFC technology: Current and future trends in India," in *2014 International Conference on Contemporary Computing and Informatics (IC3I)*, 2014.

[130] H. Guo and A. A. Ofori,, "The Internet of Things in Extreme Environments Using Low-Power Long-Range Near Field Communication," *The Internet of Things in Extreme Environments Using Low-Power Long-Range Near Field Communication,* vol. 4, no. 1, pp. 34-38, 2021.

[131] D. M. Prieto, T. Chang, X. Vilajosana and T. Watteye, "Distributed PID-based Scheduling for 6TiSCH Networks," *IEEE Communications Letters,* vol. 20, no. 5, pp. 1006-1010, 2016.

[132] A. Bansal, R. Khanna and S. Sharma, "UHF-RFID Tag Design for Improved Traceability Solution for workers' safety at Risky Job sites," in *2021 IEEE International Conference on RFID Technology and Applications (RFID-TA)*, 2021.

[133] K. Suresh, V. Jeoti, S. Soeung, M. Drieberg, M. Go and M. J. Aslam, "A Comparative Survey on Silicon Based and Surface Acoustic Wave (SAW)-Based RFID Tags," vol. 8, pp. 91624-91647, 2020.

[134] X. Cheng, J. Lu and W. Cheng,, "A Survey on RFID Applications in Vehicle Networks," in *2015 International Conference on Identification, Information, and Knowledge in the Internet of Things (IIKI)* , 2015.

[135] T. V. Morozova and V. V. Gurov, "Research in RFID vulnerability," 2017 IEEE Conference of Russian Young Researchers in Electrical and Electronic Engineering (EIConRus)," 2017.

[136] B. Makwana, N. Barodawala, Y. Punjabi and C. Bhatt, "Home Automationa using IoT," NY, USA, 2018.

[137] Dali-alliance, "The international IEC 62386 standard," 2024. [Online]. Available: https://www.dali-alliance.org/dali/standards.html. [Accessed 1 8 2024].

[138] KNX, "What is KNX," 2024. [Online]. Available: https://www.knx.org/knx-en/for-professionals/benefits/knx-internet-of-things/. [Accessed 2 7 2024].

[139] Matter, "Matter Protocol," 2024. [Online]. Available: https://www.nordicsemi.com/Products/Technologies/Matter?utm_term=matter%20protocol&utm_campaign=M_ALL_GE_US&utm_source=adwords&utm_medium=ppc&hsa_tgt=kwd-1543757786149&hsa_grp=139493655062&hsa_src=g&hsa_net=adwords&hsa_mt=b&hsa_ver=3&hsa_ad=680036204541&h. [Accessed 4 2 2024].

[140] Threadgroup, "White Papers: Thread Network Fundamentals," 1 7 2024. [Online]. Available: https://www.threadgroup.org/support#Whitepapers.

[141] J. Hui and R. Kelsey, "RFC7731: Multicast Protocol for Low-Power and Lossy Networks (MPL)," 2 2016. [Online]. Available: https://www.rfc-editor.org/rfc/rfc7731.txt. [Accessed 12 08 2019].

[142] G. Tang, Y. Han, J. Wang and Q. Zhao, "Smart Meter Data Analytics for Distribution Network," *2018 37th Chinese Control Conference (CCC)*, Wuhan, China, 2018, pp. 8882-8887, doi: 10.23919/ChiCC.2018.8483503.

[143] N. Ahmed, D. Debashis and F. A. Barbhui, "MAC Protocols for IEEE 802.11ah-Based Internet of Things: A Survey," *IEEE Internet of things Journal,* pp. 916-938, 2021.

[144] L. Tian, J. Famaey and S. Latré, "Evaluation of the IEEE 802.11ah Restricted Access Window mechanism for dense IoT networks," in *2016 IEEE 17th International Symposium on A World of Wireless, Mobile and Multimedia Networks (WoWMoM)*, Coimbra, Portugal, 2016.

[145] P. Z. Sotenga, K. Djouani and A. M. Kurien, "Evaluation of 802.11ah TIM and RAW Scheduling Protocol for IoT," in *IEEE AFRICON*, Accra, Ghana, 2019.

[146] A. Z. Yonis, H. A. Dweig and A. K. Tareed, "Comprehensive analysis of IEEE 802.11ah for Wireless Communication Networks," in *2021 IEEE Integrated STEM Education Conference (ISEC)*, NJ, USA, 2021.

[147] B. Ramos, S. Savazzi, J. M. Winter, V. Ojeda, M. Chalen, E. D. Rosario and M. A. varez, "A Perfomance Comparison of WirelessHART and ZigBee in Oil Refinery," in *2018 IEEE-APS Topical Conference on Antennas and Propagation in Wireless Communications (APWC)*, 2018.

[148] A. Edward, "New Standards Initiatives on Ultrawideband [Standards]," *IEEE Vehicular Technology Magazine,* vol. 16, no. 3, pp. 162-162, 2021.

[149] K. Pister and D. Doherty, "TSMP: Time synchronised mesh protocol," in *In procceeding of IASTED Distributed Sensor Networks*, 2008.

[150] E. Kim, D. Kaspar and J. Vasseur, "Design and Application Spaces for IPv6 over Low-Power Wireless Personal Area Networks (6LoWPANs)," RFC 6568, 2012.

[151] ZigBee, "ZigBee," 31 7 2024. [Online]. Available: https://en.wikipedia.org/wiki/Zigbee. [Accessed 2 8 2024].

[152] P. Baronti, P. Pillai, V. Chook, S. Chessa, A. Gotta and Y. Hu, "Wireless sensor networks: A survey on the state of the art and the 802.15.4 and ZigBee standards," *Computer Communications,* vol. 30, no. 7, pp. 1655-1695, 2007.

[153] F. Kuhn, R. Wattenhofer and A. Zollinger, "Worst-Case Optimal and Average-Case Efficient Geometric Ad Hoc Routing," in *4th International conference of Mobile Computing and Networks*, 2003.

[154] NFC.ORG, "NFC: About Near Field Communication," NFC, 2017. [Online]. Available: http://nearfieldcommunication.org/about-nfc.html. [Accessed 10 09 2019].

[155] RFID, "Radio-frequency identification," Wikipedia, 1 09 2019. [Online]. Available: https://en.wikipedia.org/wiki/Radio-frequency_identification. [Accessed 10 09 2019].

[156] P. Thubert and J. Hui, "Compression Format for IPv6 Datagrams Over IEEE 802.15.4-Based Networks," *IETF draft, RFC 6282,* p. 1111111, 2011.

[157] C. Bormann, T. Watteyne and P. Thubert, "RFC 8930 On Forwarding 6LoWPAN Frangments over a Multi-hop IPv6 Network," *IETF,* 2020.

[158] D. Dujovne, T. Watteyene, X. Vilajosana and P. Thubert, "6TiSCH: deterministic IP-ena-bled industrial internet (of things)," *IEEE Comm. Mag,* vol. 52, no. 12, pp. 36-41, 2014.

[159] M. A. Adegboye, W.-K. Fung and A. Karnik, "Recent advances in pipeline monitoring and oil leakage detection technologies: principles and approaches," *Sensors,* vol. 19, no. 11, p. 2548, 2019.

[160] Y. Zhang, h. Huang, Q. Huang and Y. Han, "6TiSCH IIoT network: A review," *Computer Networks,* vol. 254, no. https://doi.org/10.1016/j.comnet.2024.110759, p. 110759, 2024.

[161] F. Gu, J. Niu, L. Jiang, X. Liu and M. Atiquzzaman, "Survey of the low power wide area network technologies," *Journal of Network and Computer Applications,* vol. 149, pp. 1-13, 2020.

[162] R. S. Sinha, Y. Wei and S. H. Hwang, "A survey on lpwa technology: lora and nb-iot," *ICT express,* vol. 3, pp. 14-21, 2017.

[163] N. Ahmed, H. Rahman and I. M. Hussain, "A comparison of 802.11ah and 802.15.4 for IoT," in *ICT Express*, 2016.

[164] F. Rincon, T. Watteyene and Y. Tanaka, "On the Impact of WiFi on 2.4 GHz Industrial IoT Networks," in *2018 IEEE International Conference on Industrial Internet (ICII)*, 2018.

[165] F. C. D. Oliveira, J. J. Rodrigues, R. A. Rabelo and S. Mumtaz, "Performance Delay Comparison in Random Access Procedure for NB-IoT, LoRa, and SigFox IoT Protocols," in *2019 IEEE 1st Sustainable Cities Latin America Conference (SCLA)*, Arequipa, Peru, 2019.

[166] S. -M. Oh and J. Shin, "An efficient small data transmission scheme in the 3GPP NB-IoT system," *IEEE Communication Letters,* vol. 21, no. 3, pp. 660-663, 2017.

[167] K. Mikhaylov and T. Haenninen, "Analysis of capacity and scalability of the LoRa low power wide area network technology," in *European Wireless 2016; 22th European Wireless Conference*, Oulu, Finland, 2016.

[168] Transformainsights, "Low Power Wide Area (LPWA) connectivity," 2024. [Online]. Available: https://transformainsights.com/low-power-wide-area-networks. [Accessed 12 6 2024].

[169] X. Vilajosana, Q. Wang, F. Chraim, T. Watteyne, T. Chang and K. J. Pister, "A realistic Energy Consumption Model for TSCH Networks," *IEEE Sensors,* vol. 14, no. 2, pp. 482-489, 2014.

[170] N. Jovalekic, V. Drndarevic, I. Darby, M. Zennaro, E. Pietrosemoli and F. Ricciato, "LoRa Transceiver With Improved Characteristics," *IEEE Wireless Communications Letters,* pp. 1058 - 1061, 2018.

[171] B. Ghaleb, A. Al-Dubai, E. Ekonomou, A. Alsarham, Y. Nasser, L. Mackenzie and A. Boukerche, "A survery of limitation and enhancement of the IPV6 routing protocol for low-power and lossy networks: A focus on core operations," *IEEE communication survey and tutorials,* vol. 21, no. 2, pp. 1607 - 1635, 2018.

[172] A. Khalifeh, K. Aldahdouh and S. Alouneh, "Optimizing the Energy Consumption Level in LoRaWan Networks," in *2020 21st International Arab Conference on Information Technology (ACIT)*, Giza, Egypt, 2020.

[173] Ted's corner, "The Economics of Receiver Sensitivity and Spectral Efficiency," 2016. [Online]. Available: https://www.ingenu.com/2016/07/the-economics-of-receiver-sensitivity-and-spectral-efficiency/?doing_wp_cron=1723915015.5345740318298339843750. [Accessed 3 1 2024].

[174] W. Yang, M. Wang, J. Zhang, J. Zou, M. Hua and T. Xia, "Narrowband Wireless Access for Low-Power Massive Internet of Things: A Bandwidth Perspective," *IEEE Wireless Communications,* vol. 24, no. 3, pp. 138-145, 2018.

[175] N. Abramson, "The Aloha System — Another alternative for computer communications," in *Proceedings of the November 17–19 1970 Fall Joint Computer Conference AFIPS70 (Fall)*, 1970.

[176] OFDMA, "What is OFDMA?," 2024. [Online]. Available: https://www.cisco.com/c/en/us/products/wireless/what-is-ofdma.html#~q-a. [Accessed 2 5 2024].

[177] I. Aqeel, E. Iorkyase, H. Zangoti, C. Tachtatzis, R. Atkinson and I. Andonovic, "LoRaWAN-implemented node localisation based on received signal strength indicator," *IET wireless sensor systems,* pp. 1-16, 2022.

[178] FHSS, "Frequency-hopping spread spectrum," 2024. [Online]. Available: https://en.wikipedia.org/wiki/Frequency-hopping_spread_spectrum. [Accessed 5 8 2024].

[179] PSK, "Phase-shift keying," 2024. [Online]. Available: https://en.wikipedia.org/wiki/Phase-shift_keying. [Accessed 31 7 2024].

[180] Sigfox.com, "Sigfox build/Radio Configurations," 2024. [Online]. Available: https://build.sigfox.com/sigfox-radio-configurations-rc. [Accessed 21 9 2024].

[181] H. Lieske, G. Kilian, M. Breiling, S. Rauh, J. Robert and A. Heuberger, "Decoding Performance in Low-Power Wide Area Networks With Packet Collisions," *IEEE Transactions on Wireless Communications,* vol. 15, no. 12, pp. 8195 - 8208, 2016.

[182] A. Zanella, N. Bui, A. Castellani, L. vangelista and M. Zorzi, "Internet of Things for Smart Cities," *IEEE Internet of Things Journal,* vol. 1, no. 1, pp. 22-32, 2014.

[183] F. Beltran, S. K. ray and J. A. Gutiérrez, "Understanding the Current Operation and Future Roles of Wireless Networks: Co-Existence, Competition and Co-Operation in the Unlicensed Spectrum Bands," *IEEE Journal on Selected Areas in Communications ,* vol. 34, no. 11, pp. 2829 - 2837, 2016.

[184] R. Sakauchi, H. yabe, S. ishkawa, Y. Nomoto , S. Segawa and M. S. tanaka, "Study of Communication Reliability Improvement using Multi-channel Communication for LoRa," in *2021 IEEE 11th International Conference on Consumer Electronics (ICCE-Berlin)*, Berlin, germany, 2021.

[185] S. Yamazaki and Y. Nakajima, "A Sigfox Energy Consumption Model via Field Trial: Case of Smart Agriculture," *IEEE Access,* vol. 11, pp. 145320 -145330, 2023.

[186] E. Shih, S.-H. Cho, N. Ickes, R. Min, A. Sinha, A. Wang and A. Chandrakasan, "Physical layer driven protocol and algorithm design for energy-efficient wireless sensor networks," in *MobiCom '01: Proceedings of the 7th annual international conference on Mobile computing and networking*, 2001.

[187] G. Christiansen, "Data whietening and random TX model- Design note dn509," 2010. [Online]. Available: https://www.ti.com.cn/cn/lit/an/swra322/swra322.pdf.

[188] A. Ikpehai, b. Adebisi, K. Rabie, K. Anoh, R. Ande and M. Hammoudeh, "Low-Power Wide Area Network Technologies for Internet-of-Things: A Comparative Review," *IEEE Internet of Things Journal,* vol. 6, no. 2, pp. 2225 - 2240, 2019.

[189] Ericsson, "Extending coverage of IoT devices in distant locations: challenges," 2024. [Online]. Available: https://www.ericsson.com/en/cases/2019/extending-coverage-of-iot-devices-in-remote-locations. [Accessed 21 7 2024].

[190] M. P. Đurišić, Z. Tafa and G. Dim, "A survey of military applications of wireless sensor networks," Bar, Montenegro, 2012.

[191] C. W. Park, D. Hwang and T. J. Lee, "Enhancement of IEEE 802.11ah MAC for M2M Communications," *IEEE Communications Letters,* vol. 18, no. 7, pp. 1151-1154, 2014.

[192] N. Ahmed, D. De, F. A. Barbhuiya and M. I. Hussain, "MAC Protocols for IEEE 802.11ah-Based Internet of Things: A Survey," *IEEE Internet of Things Journal,* vol. 9, no. 2, pp. 916-938, 2022.

[193] A. Z. Yonis, H. A. Dweig and A. T. Tareed, "Comprehensive analysis of IEEE 802.11ah for Wireless Communication Networks," in *2021 IEEE Integrated STEM Education Conference (ISEC),*, 2021.

[194] M. Vucinic, M. P. Djurisic and T. Watteyne, "SODA: 6TiSCH Open Data Action," in *2018 IEEE Workshop on Benchmarking Cyber-Physical Networks and Systems (CPSBench)*, Porto, Portugal, 2018.

[195] R. M. Senouci, B. Djamaa and A. Tabouche, "Traffic-Aware Reliable Scheduling in TSCH Networks for Industry 4.0: A Systematic Mapping Review," *IEEE COMMUNICATIONS SURVEYS & TUTORIALS,* vol. 25, no. 4, pp. 2834-2859, 2023.

[196] MQTT, "MQTT: The Standard for IoT Messaging," 1 2 2024. [Online]. Available: https://mqtt.org/.

[197] C. Bormann, A. P. Castellani and Z. Shelby, "CoAP: An Application Protocol for Billions of Tiny Internet Nodes," in *IEEE Internet Computing*, vol. 16, no. 2, pp. 62-67, March-April 2012, doi: 10.1109/MIC.2012.29.

[198] HTTP, "HTTP," Wikipedia, 11 11 2024. [Online]. Available: https://en.wikipedia.org/wiki/HTTP#cite_note-4. [Accessed 14 11 2024].

[199] Ericsson, "OSCORE: A look at the new IoT security protocol," 7 11 2019. [Online]. Available: https://www.ericsson.com/en/blog/2019/11/oscore-iot-security-protocol.

[200] Wikipedia, "Data Distirbution Service," 8 6 2024. [Online]. Available: https://en.wikipedia.org/wiki/Data_Distribution_Service.

[201] Wikipedia, "Advanced Messaging Queuing Protocol," 24 5 2024. [Online]. Available: https://en.wikipedia.org/wiki/Advanced_Message_Queuing_Protocol.

[202] Wikipedia, "XMPP," 5 8 2024. [Online]. Available: https://en.wikipedia.org/wiki/XMPP.

[203] G. Selander, J. Mattsson, F. Palombini and L. Sei, "Object Security for Constrained RESTful Environments (OSCORE)," *IETF RFC 8613,* 2019.

[204] P. Thubert, E. Nordmark, S. Chakrabarti and C. E. Perkins, "Registration Extensions for IPv6 over Low-Power Wireless Personal Area Networks (6LoPWAN) Neighbor Discovery," *RFC 8505,* 11 2018.

[205] P. Thubert, "ROLL: Internet Draft," IETF ROLL, 11 06 2012. [Online]. Available: https://tools.ietf.org/html/draft-thubert-roll-asymlink-02. [Accessed 1 10 2019].

[206] B. Pavkovic, F. Theoleyre and A. Duda, "Multipath opportunistic RPL routing over IEEE 802.15.4," in *Proceedings of the 14th ACM international conference on Modeling, analysis and simulation of wireless and mobile systems MSWiM '11*, NY, USA, 2011.

[207] C. Thompson, I. Wadhaj, I. Romdhani and A. Al-dubai, "Performance of evaluation of RPL metrics in environments with strained transmission ranges," in *13th ACS/IEEE International Conference on Computer Systems and Applications (AICCSA 2016),* , At Agadir, Morocco, 2016.

[208] J. V. Sobral, J. Rodrigues, R. A. Rabelo, J. Al-Muhtadi and V. Korotaev, "Routing Protocols for Low Power and Lossy Networks in Internet of Things Applications," *Sensors,* vol. 19, no. 2144, pp. 2-40, 2019.

[209] B. Ghaleb, A. Al-Dubai, E. Ekonomou, A. Alsarham, Y. Nasser, L. Mackenzie and A. Boukerche, "A survey of limitation and enhancement of the IPV6 routing protocol for low-power and lossy networks: A focus on core operations," *IEEE Communication Survey and Tutorials (Early Access),* pp. 1-31, 2018.

[210] O. Lova, F. Theoleyre, T. Watteyne and T. Neol, "The love-hate relationship between IEEE 802.15.4 and RPL," *IEEE Communications Magazine ,* vol. 55, no. 1, pp. 188-194, 2017.

[211] P. Levis, T. Clausen, J. Hui, O. Gnawali and J. Ko, "The trickle algorithm: IETF RFC 6206," *IETF draft,* pp. 1-11, 2011.

[212] O. Iova, G. P. Picco, T. Istomin and C. Kiraly, "RPL: the routing standard for the internet of things... Or Is IT?," *IEEE communication Magzine,* vol. 54, no. 12, pp. 16-22, 2016.

[213] Z. Shelby and C. Bormann, 6LoWPAN: The Wireless Embedded Internet, Wily publishing, 2010.

[214] X. Vilajosana, T. Watteyne, T. Chang,, M. Vučinić, S. Duquennoy and P. Thubert, "IETF 6TiSCH: A Tutorial. Communications Surveys and Tutorials," *IEEE Communications Society,* vol. 22, no. 1, 2020.

[215] M. Almistarihi, M. Al-shuruman and A. Qusaimat, "Tree based dynamic address autoconfiguration in mobile ad hoc network," *computer networks,* vol. 55, no. 8, pp. 1894-1908, 2011.

[216] S. E. Deering and A. Conta, "Generic Packet Tunneling in IPv6 Specification," *IETF RFC 2473,* 12 1998.

[217] É. Vyncke , "IPv6 over Networks of Resource-constrained Nodes WG (6lo)," IETF, 18 3 2024. [Online]. Available: https://datatracker.ietf.org/doc/charter-ietf-6lo/. [Accessed 10 8 2024].

[218] P. Thubert, "A Routing Protocol for Low-Power and Lossy Networks (RPL) Destination-Oriented Directed Acyclic Graph (DODAG) Configuration Option for the 6LoWPAN Routing Header," IETF, 4 2021. [Online]. Available: https://datatracker.ietf.org/doc/html/rfc9035. [Accessed 10 8 2024].

[219] Q. Wang, X. Vilajosana and T. Watteyne, "6TiSCH Operation Sublayer (6top) Protocol (6P)," *IETF RFC 8480,* 2018.

[220] PSK, "Pre-shared key," 2019. [Online]. Available: https://en.wikipedia.org/wiki/Pre-shared_key. [Accessed 24 7 2024].

[221] M. Vučinić, T. Watteyne and X. Vilajosana, "Broadcasting strategies in 6TiSCH networks," *Internet Technology letter,* 2017.

[222] D. Hauweele, R.-A. Koutsiamanis and B. Qu, "Thorough Performance Evaluation & Analysis of the 6TiSCH Minimal Scheduling Function (MSF)," *Springer Link,* vol. 94, pp. 3-25, 2022.

[223] T. Watteyne, X. Vilajosana, B. Kerkez,, F. Chraim, K. Weekly, Q. Wang and S. Gla, "OpenWSN: a standards-based low-power wireless development environment," *Transactions on Emerging Telecommunications Technologies,* vol. 23, no. 5, pp. 480-493, 2012.

[224] M. Mohamadi and R. M. Senouci , "Scheduling Algorithms for IEEE 802.15.4 TSCH Networks: A Survey," in *A. (eds) Advances in Computing Systems and Applications*, 2018.

[225] S. Kharb and A. Singhrova, "A survey on network formation and scheduling algorithms for time slotted channel hopping in industrial networks," *Journal of Network and Computer Applications,* vol. 126, no. 15, pp. 59-97, 2019.

[226] F. Righetti, C. Vallati and G. Anastas, "Performance Evaluation of Adaptive Autonomous Scheduling Functions for 6TiSCH Networks," *IEEE Access,* vol. 9, pp. 127576-127594, 2021.

[227] A. Elsts, S. Kim, H.-S. Kim and C. Kim, "An Empirical Survey of Autonomous Scheduling Methods for TSCH," *IEEE Access,* vol. 8, pp. 67147 - 67165, 2020.

[228] S. Duaquennoy, B. A. Nahas, T. Watteyne and O. Landsiedel, "Orchestra: Robust Mesh Networks Through Autonomously Scheduled TSCH," in *ACM Conference on Embedded Networked Sensor Systems (Sensys)*, Seoul, South Korea, 2015.

[229] A. R. Urke, Ø. Kure and K. Øvsthus, "A Survey of 802.15.4 TSCH Schedulers for a Standardized Industrial Internet of Things," *Sensors,* vol. 22, no. 1, 2022.

[230] M. R. Palattela, N. Accettura, M. Dohler, L. A. Grieco and G. Boggia, "Traffic aware scheduling algorithm for reliable low power multii-hop IEEE 802.15.4e Networks," in *IEEE 23rd International Symposium on Personal, Indoor and Mobile Radio Communications - (PIMRC)*, Sydney, NSW, Australia, 2012.

[231] K. Choi and S. H. Chung, "Enhanced time-slotted channel hopping with quick setup time for industrial internet of things," *international journal of distributed sensor network,* vol. 6, p. 13, 2017.

[232] Á. A. Farías and D. Dujovne, "A queue-based scheduling algorithm for PCE-enabled Industrial Internet of Things networks," in *2015 Sixth Argentine Conference on Embedded Systems (CASE)*, 2015.

[233] T. Huyun, F. Theoleyre and W. -j. Hwang, "On the street opportunistic anycast scheduling for wireless low power lossy networks," *Computer communications,* vol. 104, pp. 55-66, 2017.

[234] D. Dujovne, L. A. Grieco, M. R. Palattela and N. Accettura, "6TiSCH 6Top schedulling function Zero," *IETF-6TiSCH Draft,* pp. 1-9, 2016.

[235] T. Chang, T. Watteyne, Q. Wang and X. Vilajosana, " LLSF: low latency scheduling function for 6TiSCH networks," in *Proceedings of International Conference on Distributed Computing in Sensor Systems (DCOSS)*, 2016.

[236] G. Daneel, B. Spinnewyn, S. Latre and J. famaey, "ReSF: recurrent Low-Latency scheduling in IEEE 802.15.4e TSCH networks," *Ad-Hoc networks,* vol. 69, pp. 80-88, 2018.

[237] R. Soua, E. Livolant and P. Minet, "A Distributed Joint Channel and Slot Assignment for Convergecast in Wireless Sensor Networks," in *2014 6th International Conference on New Technologies, Mobility and Security (NTMS)*, 2014.

[238] H. Wang, W. Yang, Y. Cao and Z. Zhang , "EDSF: Efficient Distributed Scheduling Function for IETF 6TiSCH-based Industrial Wireless Networks," *Springer LInk,* vol. 27, pp. 2244-2253, 2022.

[239] E. Municio and S. Latre, "Decentralized broadcast-based scheduling for dense multihop TSCH networks,," in *MobiArch '16 Proceedings of the Workshop on Mobility in the Evolving Internet Architecture*, NY, USA, 2016.

[240] N. Accettura, M. R. palettela, G. Boggia, M. Dohler and L. A. Grieco, "Decentralized traffic aware scheduling for multi-hop low power lossy networks in the Internet of Things," in *WoWMoM*, 2013.

[241] A. Aijaz and U. Raza, “DeAMON: a decentralized adaptive multi-hop scheduling protocol for 6Tisch wireless networks,” *IEEE Sensors Journal ,* vol. 17, no. 20, pp. 1-10, 2017.

[242] R. Soua, P. Minet and E. Livolant, "DiSCA: a distributed scheduling for convergecast in multichannel wireless sensor networks," in *Proceedings of 2015 International Symposium on Integrated Network Management*, 2015.

[243] I. Hosni and F. Theoleyre, "Self-healing distributed scheduling for end-to-end delay optimization in multihop wireless networks with 6TiSCH," *Computer communications,* vol. 11o, pp. 103-119, 2017.

[244] D. J. Vergados a, K. Kralevska, Y. Jiang and A. Michalas, "Local voting: A new distributed bandwidth reservation algorithm for 6TiSCH networks," *Computer Networks,* vol. 180, 2020.

[245] F. Righetti, C. Vallati, G. Anastasia and S. K. Das, "Analysis and improvement of the on-the-fly bandwidth reservation algorithm for 6tisch," in *2018 IEEE 19th International Symposium on "A World of Wireless, Mobile and Multimedia Networks" (WoWMoM)*, 2018.

[246] H. Wang and A. O. Fapojuwo, "Design and Performance Evaluation of a Hysteresis-Free On-the-Fly Scheduling Function for 6TiSCH," *IEEE Internet of Things Journal,* vol. 8, no. 13, pp. 10499 - 10508, 2021.

[247] A. Morell, X. Vilajosana, T. Watteyne and J. L. Vicario, "Label-Switching over IEEE 802.15.4e Networks," *Telecommunication,* vol. 24, no. 5, pp. 458-476, 2013.

[248] D. Papadimitriou, "Generalized Multi-Protocol Label Switching (GMPLS) Signaling Extensions for G.709 Optical Transport Networks Control," IETF: RFC 4328, 1 2006. [Online]. Available: https://www.rfc-editor.org/rfc/rfc4328.html#:~:text=RFC%204328%3A%20Generalized%20Multi%2DProtocol,709%20Optical%20Transport%20Networks%20Control. [Accessed 12 1 2024].

[249] RSVP-TE, "RSVP-TE," Wikipedia, 1 2023. [Online]. Available: https://en.wikipedia.org/wiki/RSVP-TE. [Accessed 3 1 2024].

[250] T. Chang, X. Vilajosana, M. Vucinic, S. Duquennoy and D. Dujovne, "6TiSCH Minimal Scheduling Function (MSF)," 2 July 2019. [Online]. Available: https://tools.ietf.org/html/draft-ietf-6tisch-msf-04. [Accessed 5 August 2019].

[251] A. Paventhan, D. Dashini, H. Krishna, N. Pahuja , M. Khan and A. Jain, "Experimental evaluation of IETF 6TiSCH in the context of Smart Grid," in *2015 IEEE 2nd World Forum on Internet of Things (WF-IoT),*, 2015.

[252] Y. H. Pratama and S. Chung, "RL-SF: Reinforcement Learning based Scheduling Function for Distributed TSCH Networks," in *2022 IEEE 12th International Conference on Electronics Information and Emergency Communication (ICEIEC)*, Beijing, China, 2022.

[253] T. Chang, M. Vucinic, X. Vilajosana, D. Dujovne and T. Watteyne, "6TiSCH minimal scheduling function: Performance evaluation," *Internet Technology letters,* vol. 3, no. 4, 2020.

[254] T. Hamza and G. Kaddoum, "Enhanced Minimal Scheduling Function for IEEE 802.15.4e TSCH Networks," in *2019 IEEE Wireless Communications and Networking Conference (WCNC)*, Marrakesh, Morocco, 2019.

[255] K. N. A. Tapadar, M. Khatua and V. Tamarapalli, "IMSF: Improved Minimal Scheduling Function for Link Scheduling in 6TiSCH Networks," in *ICDCN '22: Proceedings of the 23rd International Conference on Distributed Computing and Networking*, 2022.

[256] Y. Tanaka, P. Minet, M. Vucinic, X. Vilajosana and T. Watteyene, "YSF: A 6TiSCH scheduling function minimizing latency of data gathering in IIoT," *IEEE Internet of Things,* vol. 9, no. 11, pp. 8607-8615, 2022.

[257] S. Kim, H. -S. Kim and C. Kim, "Autonomous Link-based TSCH Cell Scheduling," in *2019 18th ACM/IEEE International Conference on Information Processing in Sensor Networks (IPSN)*, Montreal, cananda, 2019.

[258] S. Jeong, J. Paek, H. -S. Kim and S. Bahk, "TESLA: Traffic-aware elastic slotframe adjustment in TSCH networks,," *IEEE Access,* vol. 7, pp. 130468-130483, 2019.

[259] Y. Tanaka, P. Minet, T. Watteyne and F. Teraoka, "Accelerating 6TiSCH Network Formation," in *2021 17th International Conference on Distributed Computing in Sensor Systems (DCOSS)*, 2021.

[260] T. Watteyene, J. Doherty, J. Simon and K. Pister, "Technical overview of SmartMesh IP," in *Seventh International Conference on Innovative Mobile and Internet Services in Ubiquitous Computing*, 2013.

[261] D. Dujovne, L. A. Grieco, M. R. Palattela and N. Accettura, "6TiSCH 6Top schedulling function Zero," *IETF-6TiSCH Draft,* pp. 1-9, 2016.

[262] E. Municio, G. Daneels, M. Vucinic, S. Latre, J. Famaey, Y. Tanaka, K. Brun, k. Muraoka, X. Vilajosana and T. Watteyne, "Simulating 6TiSCH network," *Telecommunication journal,* pp. 1-17, 2018.

[263] Y. Tanaka, K. Brun-Laguna and T. Watteyne, "Demo: Simulating a 6TiSCH Network using Connectivity Traces from Testbeds," in *IEEE INFOCOM 2019 - IEEE Conference on Computer Communications Workshops (INFOCOM WKSHPS)*, Paris, france, 2019.

[264] Contiki-NG, "Contiki-NG, the OS for Next Generation IoT Devices," 2018. [Online]. Available: https://www.contiki-ng.org/. [Accessed 12 2 2021].

[265] P. Levis, S. Madden, J. Polastre, R. Szewczyk, E. Brewer and D. Culler, "TinyOS: An Operating System for Sensor Networks.," *Springer,* pp. 115-148, 2005.

[266] NS simulator , "ns (simulator)," Wikipedia, 13 09 2024. [Online]. Available: https://en.wikipedia.org/wiki/Ns_(simulator). [Accessed 2 1 2024].

[267] E. Baccelli, O. Hahm, M. Gunes, M. Wählisch and T. C. Schmidt, "RIOT OS: Towards an OS for the Internet of Things," in *2013 IEEE Conference on Computer Communications Workshops (INFOCOM WKSHPS)*, Turin, Italy, 2013.

[268] P. Levis, N. Lee, M. Welsh and D. Culler, "TOSSIM: accurate and scalable simulation of entire TinyOS applications," in *SenSys '03: Proceedings of the 1st international conference on Embedded networked sensor systems*, 2003.

[269] M. R. Palattella, X. Vilajosana, T. Chang, R. Ortega and T. Watteyne, "Lessons Learned from the 6TiSCH Plugtests," in *Interoperability Internet of Things Summit*, 2015.

[270] T. Chang, P. Tuset-Peiro and X. Vilajosana, "OpenWSN & OpenMote: Demo'ing a Complete Ecosystem for the Industrial Internet of Things," in *2016 13th Annual IEEE International Conference on Sensing, Communication, and Networking (SECON)*, London, UK, 2016.

[271] B. Martinez, X. Vilajosana, H. I. Kim, Z. ZHou, P. Tuset-piero, A. Xhafa, D. Poissonnier and X. Lu, "I3Mote: An Open Development Platform for the Intelligent Industrial Internet," *MDPI sensors,* vol. 17, no. 5, 2017.

[272] ANALOG DEVICES, "LTP5902-IPM:SmartMesh IP Wireless 802.15.4e PCBA Module with Antenna Connector," Analog Devices, 1 12 2023. [Online]. Available: https://www.analog.com/en/products/ltp5902-ipm.html#part-details. [Accessed 12 2 2024].

[273] Fit IoT-LAB, "IoT-LAB M3," IoT Lab, 1 12 2022. [Online]. Available: https://iot-lab.github.io/docs/boards/iot-lab-m3/. [Accessed 1 12 2024].

[274] IoTeam, "We are IOTEAM," IOTEAM, 2 1 2024. [Online]. Available: https://ioteam.mystrikingly.com/. [Accessed 1 11 2024].

[275] Nordic Semiconductor, "nRF51822:Bluetooth Low Energy and 2.4 GHz SoC," Nordic Semiconductor, 3 1 2024. [Online]. Available: https://www.nordicsemi.com/Products/nRF51822. [Accessed 1 11 2024].

[276] P. Boccadoro, G. Piro, D. Striccoli and L. A. Grieco, "Experimental Comparison of Industrial Internet of Things Protocol Stacks in Time Slotted Channel Hopping Scenarios," in *2018 IEEE International Conference on Communications (ICC)*, Kansas City, MO, USA, 2018.

[277] Zolertia, "Re-Mote," zolertia , 2 1 2018. [Online]. Available: https://zolertia.io/. [Accessed 1 12 2023].

[278] M. Silva, D. Cerdeira, S. Pinto and T. Gomes, "Operating Systems for Internet of Things Low-End Devices: Analysis and Benchmarking," *IEEE INTERNET OF THINGS JOURNAL,* vol. 6, no. 6, pp. 10375-10383, 2019.

[279] T. Claeys, F. X. Molina, M. Vucinic, T. Watteyne and E. Baccelli, "RIOT and OpenWSN 6TiSCH: Happy Together.," in *PEMWN 2020 - 9th IFIP/IEEE International Conference on Performance Evaluation and Modeling in Wired and Wireless Networks,*, Berlin, Germany, 2020.

[280] X. Vilajosan, P. Tuset, T. Watteyne and K. Pister, "OpenMote: OpenSource Prototyping Platform for the Industrial IoT)," in *7th International Conference AdHocHets 2015*, 2015.

[281] H.-P. Le, M. John and K. Pister., "Energy-Aware Routing in Wireless Sensor Networks with Adaptive Energy-Slope Control," University of California, Berkeley, 2009.

[282] K. S. Pister, X. Vilajosan, N. Accettura, T. Watteyne and k. Muraoka, "Simple Distributed Scheduling With Collision Detection in TSCH Networks," *IEEE Sensors Journal,* vol. 16, no. 15, pp. 5848-5849, 2016.

[283] B. Andrew, "Strategy Analytics Discusses IoT Use Cases and Deployments at MWC 2019," Strategy Analytics, 07 03 2019. [Online]. Available: https://www.strategyanalytics.com/strategy-analytics/blogs/enterprise/iot/iot/2019/03/07/strategy-analytics-discusses-iot-use-cases-and-deployments-at-mwc-2019. [Accessed 10 10 2019].

[284] I. Robles, V. d. P. Stok, A. Retana, M. Richardson, R. Cragie and T. A. Pugnolet, "Routing Over Low power and Lossy networks (roll)," 22 03 2019. [Online]. Available: http://datatracker.ietf.org/wg/roll/charter/. [Accessed 5 09 2019].

[285] M. Vucinic, J. Simon, K. Pister and M. Richardson, "6TiSCH Working Group: Minimal Security Framework for 6TiSCH," 20 11 2018. [Online]. Available: https://tools.ietf.org/html/draft-ietf-6tisch-minimal-security-09. [Accessed 10 07 2019].

[286] Q. M. Qadir, T. A. Rashid, N. K. Al-salihi, B. ISMEAL, A. A. Kist and Z. Zhang, "Low Power Wide Area Networks: A Survey of Enabling Technologies, Applications and Interoperability Needs," *IEEE Access,* vol. 6, pp. 2169-3536, 2018.

[287] S. Li, L. D. Xu and S. Zhao, "The internet of things: a survey," *S.Inf Syst Front (2015),* vol. 17, no. 2, pp. 243-259, 2014.

[288] Continuity 1, "Ten reasons to use IoT platform-based services," Continuity 1, 15 July 2015. [Online]. Available: https://www.continuity1.com/ten-reasons-to-use-iot-platform-based-services/. [Accessed 10 08 2019].

[289] H. Fotouhi, D. Moriera and M. Alves, "MRPL: boosting mobility in the internet of things," *Ad Hoc Networks,* vol. 26, pp. 17-35, 2015.

[290] AL-karaki and J. N. kamal, "Routing techniques in wireless sensor networks: a survey," *IEEE Wireless Communications,* vol. 11, no. 6, pp. 6-28, 2004.

[291] K. Akkaya and M. Younis, "A survey on routing protocols for wireless sensor networks," *Ad Hoc Networks,* vol. 3, no. 3, pp. 325-349, 2005.

[292] G. Anastasi, M. Conti, M. Francesco and A. Passarella , "Energy Conservation In Wireless Sensor Networks: A survey," *Ad-Hoc network,* vol. 7, pp. 537-568, 2009.

[293] O. O. Ogundile and A. S. Alfa, "A Survey on an Energy-Efficient and Energy-Balanced routing protocl for wireless sensor networks," *Sensors,* vol. 17, pp. 1084-1135, 2017.

[294] P. Rawat, K. D. Singh, H. Chaouchi and M. J. Bonnin, "Wireless sensor networks: a survey in recent development and potential synergies," *The journal of Supercomputing,* vol. 68, no. 1, pp. 1-48, 2014.

[295] Y. Xu, J. Heidemann and D. Estrin, "Geography-informed energy conservation for ad hoc routing," in *Proceedings of the 7th Annual ACM/IEEE International Conference on Mobile Computing and Networking*, Rome, Italy, 2001.

[296] H. Aznaoui, s. RAGHAY and l. Aziz, "Location-Based Routing Protocols GAF and its enhanced versions in Wireless Sensor Network a Survey," *international journal of computer science and information security,* vol. 14, no. 6, pp. 497-507, 2016.

[297] J. Heidemann, D. Estrin and Y. Xu, "Geography informed energy conservation for Ad Hoc routing," in *Proceedings of the 7th annual international conference on Mobile computing and networking*, Rome, Italy, 2001.

[298] Y. Yu, D. Estrin and R. Govindan, "Geographical and Energy-Aware Routing: A Recursive Data Dissemination Protocol for Wireless Sensor Networks," UCLA Computer Science Department Technical Report, 2001.

[299] J. Grover, Shikha and m. sharma, "Location based protocols in Wireless Sensor Network — A review," in *Fifth International Conference on Computing, Communications and Networking Technologies (ICCCNT)*, Hefei, China, 2014.

[300] C. Intanagonwiwat, R. Govindan and D. Estrin, "Directed Diffusion: A Scalable and Robust Communication Paradigm for Sensor Networks," in *Proceedings of the 6th Annual ACM International Conference on Mobile Computing and Networking*, Boston, 2000.

[301] B. Karp and T. H. Kung, "GPSR: Greedy Perimeter Stateless Routing for wireless networks," in *The 6th Annual International Conference on Mobile Computing and Networking (MobiCom 2000)*, 2000.

[302] Q. Nadeem, M. B. Rasheed, N. Javaid, Z. A. Khan, Y. Maqsood and A. Din, "M-GEAR: Gateway-Based Energy-Aware Multi-hop Routing Protocol for WSNs," in *2013 Eighth International Conference on Broadband and Wireless Computing, Communication and Applications*, Compiegne, France, 2013.

[303] S. Li, H. Gao and D. Wu, "An energy-balanced routing protocol with greedy forwarding for WSNs in cropland," in *2016 IEEE International Conference on Electronic Information and Communication Technology (ICEICT)*, Harbin, China, 2016.

[304] L. Xiangxiang and L. Zhang, "Research on GEAR with Network Coding," in *2018 IEEE 3rd International Conference on Communication and Information Systems (ICCIS)*, singapore, 2018.

[305] K. Sohrabi and J. Pottie, "Protocols for Self-Organization of a Wireless Sensor Network," *IEEE journal of communication,* vol. 7, no. 5, pp. 16-27, 2000.

[306] I. Stojmenovic and X. Lin, "Loop-free Location Based Routing in Wireless Networks," in *International conference in Parallel and Distributed Computing and Systems*, 1999.

[307] H. Qin and Y. Cui, "A Novel Rumer Routing for Wireless Sensor Network," in *2010 Fourth International Conference on Genetic and Evolutionary Computing*, Shenzhen, China, 2010.

[308] L. Hong and J. Yang, "An Energy-Balance Multipath Routing Based on Rumor Routing for Wireless Sensor Networks," in *2009 Fifth International Conference on Natural Computation*, Tianjin, China, 2009.

[309] H.-H. Liu, J.-j. Su and C.-f. Chou, "On Energy-Efficient Straight-Line Routing Protocol for Wireless Sensor Networks," *IEEE System Journal,* vol. 11, no. 4, pp. 2374-2382, 2017.

[310] M. Radi, B. Dezfouli, k. a. Bakar and m. Lee, "Multipath routing in Wireless sensor networks: survey and research chellenges," *Sensors,* vol. 12, pp. 650-685, 2012.

[311] D. Braginsky and D. Estrin, "Rumer Routing Algorithm for Sensor Networks," in *Proceedings of first ACM International Workshop on Wireless Sensor Network and Applications, WSNA 2002*, atlanta, GA, 2002.

[312] W. heinzelmann, j. kulik and h. balakrishnan, "Adaptive protocol for information dessimination in wireless sensor networks," in *5th Annual ACM/IEEE international conference for mobile computing and networking (MobiComm)*, seattle, 1999.

[313] W. B. Heinzelman, "Application specific protocol architectures for wireless networks," MIT Cambridge, MA, USA, 2000.

[314] J. Kulik, w. heinzelman and h. Balakrishnana, "Negotiation-Based Protocols for Disseminating Information in Wireless Sensor Networks," *wireless network,* vol. 8, pp. 169-185, 2002.

[315] D. Bhattacharyya, T.-h. Kim and P. Subhajit, "A Comparative Study of Wireless Sensor Networks and Their Routing Protocols," *Sensors,* vol. 10, no. 12, pp. 10506-10523, 2010.

[316] D. Estrin, R. Govindan, J. Heidemann and S. Kumar, "Next Century Challenges: Scalable Coordination in Sensor Networks," in *Proceedings of the 5th annual ACM/IEEE international conference on Mobile computing and networking*, seattle, Washington, USA, 1999.

[317] M. Chu, H. Haussecker and F. zhao, "scalable information driven sensor networks querying and routing for heterogenous sensor networks," *internation journal of high performance computing applications,* vol. 16, no. 3, pp. 293-313, 2002.

[318] R. C. Shah and J. M. Rabaey, "Energy aware routing for low energy ad hoc sensor networks," in *2002 IEEE Wireless Communications and Networking Conference Record. WCNC 2002 (Cat. No.02TH8609)*, OL, Florda, USA, 2002.

[319] D. Ganeshan, R. Govindan, S. shenker and D. Estrin, "Highly resilient, energy efficient multipath routing in wireless sensor networks," *ACM SIGMOBILE Mobile Computing and Communications Review ,* vol. 5, no. 4, pp. 11-25, 2002.

[320] A. Ahtiainen, "Summary of Rumer Routing in Wireless Sensor Networks," Helsinki University of Technology, Finland, 2015.

[321] H. Luo, F. Ye, J. Cheng, S. Lu and L. Zhang, "TTDD: Two-Tier data dissemination in large scale wireless network," *Springer Journal on Wireless Networks,* vol. 11, pp. 161-175, 2005.

[322] X. Liu, "Atypical Hierachical routing protocols for Wireless Sensor Networks: A review," *IEEE Sensor Journal,* vol. 15, no. 10, pp. 5372-5383, 2015.

[323] S.-N. Kim and K.-j. Han, "A power efficient routing protocol based on balanced tree in wireless sensor networks," in *First International Conference on Distributed Frameworks for Multimedia Applications*, Besancon, France, 2005.

[324] E. Skafidas, W. Qiu and P. Hao, "Enhanced tree routing for wireless sensor networks," *Ad-Hoc Journal,* vol. 7, no. 3, pp. 638-650, 2009.

[325] L. Buttyan and P. Schaffer, "PANEL: Position-based Aggregator Node Election in Wireless Sensor Networks," in *IEEE International Conference on Mobile Adhoc and Sensor Systems*, Pisa , Italy, 2007.

[326] J. H. Shin, J. Kim, K. Park and D. park, "Railroad:Virtual infrastructrue for data desimination in wireless sensor networks," in *2nd ACM International Workshop on Performance Evaluation of Wireless Ad Hoc, Sensor, and Ubiquitous Networks*, 2005.

[327] E. B. Hamida and G. Chelius, "A line based data-dessimination protocol for wireless sensor networks with mobile sink," in *2008 IEEE International Conference on Communications*, Beiing, China, 2008.

[328] J. Garcia-Luna-Aceves and E. Madruga, "A multicast routing protocol for ad-hoc networks," in *IEEE INFOCOM '99. Conference on Computer Communications. Proceedings. Eighteenth Annual Joint Conference of the IEEE Computer and Communications Societies. The Future is Now (Cat. No.99CH36320)*, NY, USA, 1999.

[329] M. A. Mojamed, "A One Hop Overlay System for Mobile Ad HoC Networks: MANET routing protocols," University of Stirling, Stirling, 2016.

[330] A. Neumann, C. Aichele, M. Lindner and S. Wunderlich, "Better Approach To Mobile Ad Hoc networking (BATMAN)," IETF Draft, 2008.

[331] T. Clausen and P. Jacquet, "Optimised Link state routing protocol (OLSR)," IETF, 2003.

[332] V. Rodoplu and T. H. Meng, "Minimum Energy Mobile wireless networks," *IEEE JSAC,* vol. 17, no. 8, pp. 1333-1344, 1999.

[333] L. Li and Y. J. halpern, "Minimum-Energy Mobile Wireless networks revisited," *IEEE ICC,* vol. 1, pp. 278-283, 2001.

[334] H. Singh, M. Agrawal, N. Gour and N. Hemrajani, "A review on routing protocols in wireless sensor networks," *International journal of engineering research and technology(IJERT),* vol. 3, no. 1, pp. 1512--1521, 2014.

[335] M. Zorzi and R. R. Rao, ""Geographic random forwarding (GeRaF) for ad hoc and sensor networks: Mutlihop performance," *IEEE Transactions on mobile Computing,* vol. 2, no. 4, pp. 337-348, 2003.

[336] J. A. Sanchez, P. M. Ruiz and P. M. Martin, "Beacon-less geographic routing made practical: challenges, design guidelines, and protocols," *IEEE Communications Magazine,* vol. 47, no. 8, pp. 85-91, 2009.

[337] J. A. Stankovic, T. He, c. Lu and t. abdelzaher, "SPEED: a stateless protocol for real time commuicationin in sensor networks," in *23rd International Conference on Distributed Computing Systems, 2003. Proceedings.*, Rhode Island, 2003.

[338] S. Bocchino, M. Petracca, p. pagano, m. ghibaudi and f. lertora, "SPEED routing protocol in 6LoWPAN networks," in *ETFA2011*, Toulose, France, 2011.

[339] B. Chen, K. jamieson, H. Balakrishnana and R. Moris, "Span: An Energy-Efficient Coordination Algorithm for Topology Maintenance in Ad Hoc Wireless Networks," *Springer,* vol. 8, no. 5, pp. 481-494, 2002.

[340] M. Chu, H. Haussecker and H. Zhao, "scalable information driven sensor querying rand routing for Ad Hoc heterogeneous networks," *internationa journal of high performance computing and applications,* vol. 16, no. 3, 2002.

[341] C. Schuregers and M. B. Srivastava, "Energy efficient routing in wireless sensor networks," in *2001 MILCOM Proceedings Communications for Network-Centric Operations: Creating the Information Force (Cat. No.01CH37277)*, McLean, VA, USA, USA, 2001.

[342] J. Hao, Z. Yao and B. Zhang, "A gradient-based multi-path routing protocol for low duty-cycled wireless sensor networks," *IEEE ICC 2012- Ad Hoc sensor network symposium,* pp. 233-248, 2012.

[343] Y. Yao and J. Gehrke, "The COUGAR approach to in-network query proccessing in sensor networks," *ACM SIGMOD Record,* vol. 31, no. 3, pp. 9-18, 2002.

[344] N. Sadagopan, B. Krishnamachari and Hel, "The Acquire Mechanism for Efficient Querying in Sensor Networks," in *Proceedings of the First IEEE International Workshop on Sensor Network Protocols and Applications, 2003*, Anchorage, AK, USA, USA, 2003.

[345] M. Ding, X. Cheng and G. Xue, "Aggregation tree construction in sensor Networks," in *2003 IEEE 58th Vehicular Technology Conference. VTC 2003-Fall (IEEE Cat. No.03CH37484)*, Oralando, FL, USA, 2003.

[346] K.-H. Chen, J. M. Huang and C.-C. Hsiao, "CHIRON: an energy efficient chain-based hierarchical routing protocol in wireless sensor networks," in *Wireless Telecommunications Symposium, 2009*, Taichung, Taiwan, 2009.

[347] K. Arasu and R. Ganeshan, "Effective implementation of Energy Aware Routing for Wireless Sensor Network," in *International Conference on Processing of Materials, Minerals and Energy (July 29th – 30th) 2016, Ongole, Andhra Pradesh, India*, Chennai, 2016.

[348] C. Perkins, S. Ratliff and J. Dowdell, "Dynamic MANET On-demand routing protocol(DYMO)," IETF, 2005.

[349] Q. Fang, F. Zhao and L. Guibas, "Lightwieghted sensing and communication protocols for Target enumuration and aggregation," in *Proceedings of the 4th ACM international symposium on Mobile ad hoc networking & computing*, Annapolis, Maryland, USA , 2003.

[350] J. N. Al-Karaki, R. UI-mustafa and A. E. kamal, "Data aggregation in wilreless sensor networks- exact and appropriate algorithms," in *2004 Workshop on High Performance Switching and Routing, 2004. HPSR*, Pheonix, AZ,USA, 2004.

[351] J. N. AL-KARAKI (a) and A. E. Kamal, "On the Correlated data gathering problem in wireless sensor networks," in *Proceedings. ISCC 2004. Ninth International Symposium on Computers And Communications (IEEE Cat. No.04TH8769)*, Alexandria, Egypt, 2004.

[352] S. M. Jung, Y. J. Han and T. M. Chung, "The concentric clustering scheme fro efficient energy consumption in the PEGASIS," in *The 9th International Conference on Advanced Communication Technology*, Gangwon-Do, Korea, 2007.

[353] N. Gautam, W. I. Lee and J. Y. Pyun, "Track-Sector Clustering for Energy Efficient Routing in Wireless Sensor Networks," in *2009 Ninth IEEE International Conference on Computer and Information Technology*, Xiamen, China, 2009.

[354] J. Liang, J. wang and J. chen, "A delay constrained and maximum lifetime data gathering algorithm for wireless sensor networks," in *2009 Fifth International Conference on Mobile Ad-hoc and Sensor Networks*, Fujian, China, 2009.

[355] X. Bao, S. zhang, D. Xue and Z. Qie, "an energy -balanced chain cluster routing protocol for wireless sensor networks," in *2010 Second International Conference on Networks Security, Wireless Communications and Trusted Computing*, Wuhan, Hubei, China, 2010.

[356] H. O. Tan and I. Korpeoglu, "Power efficient data gathering and aggregation in wireless sensor networks," *ACM SIGMOD Record ,* vol. 32, no. 4, 2003.

[357] A. Jiang and L. Zheng, "An Effective Hybrid Routing Algorithm in WSN: Ant colony Optimization in combination with Hop Count Minimization," *Sensors,* vol. 18, no. 4, pp. 1020-1037, 29 March 2018.

[358] S. W. Damein, b. o. yenke, a. forster and p. dayang, "Optimized Clustering Algorithms for Large Wireless Sensor Networks: A Review," *Sensors,* vol. 19, no. 2, pp. 2-27, 2019.

[359] V. Loscri, G. Morabito and S. Marano, "A two-levels hierarchy for low-energy adaptive clustering hierachy (TL-LEACH)," in *IEEE 62nd Semiannu, vehicle technology conference*, Dallas, TX, 2005.

[360] L. B. Oliveira, A. Farreira , M. A. Vilaca, H. c. Wong, m. Bern, r. Dahab and A. A. Loureiro, "SecLEACH—On the security of clustered sensor networks," *Signal processing ,* vol. 87, no. 12, pp. 2882-2895, 2007.

[361] S. Lindsey and C. S. Raghvesndra, "PEGASIS: Power-efficient gathering in sensor information systems," in *Proceedings, IEEE Aerospace Conference*, Big Sky, MT, USA, USA, 2002.

[362] W. Heinzelman, A. chandrakasan and h. balakrishnan, "Enenrgy efficient communication protocols for wirless sensor networks," in *Proceedings of the 33rd Annual Hawaii International Conference on System Sciences*, Hawaii, USA, 2000.

[363] A. Manjeshwar and D. P. Agrawal, "TEEN: a protocol for energy efficiency in wireless sensor networks," in *Proceedings of the 15th International Parallel & Distributed Processing Symposium (IPDPS-01)*, san franscisco, CA,, 2001.

[364] A. Manjeshwar and D. P. Agrawal, "APTEEN: a hybrid protocol for efficient routing and comprehensive information retrieval in wireless," in *Proceedings 16th International Parallel and Distributed Processing Symposium*, Florida, 2001.

[365] F. Xiangning and S. Yulin, "Improovement on LEACH Protocol of wireless sensor network," in *International conference of sensor technology and Application*, Valencia, Spain, 2007.

[366] M. B. Yassein, A. Al-zou, Y. Khamayesh and W. Mardini, "Improovement on LEACH protocol of wireless sensor networks," *International journal of Digital content technologies and aplications,* vol. 3, no. 2, pp. 132-136, 2009.

[367] G. Ran, H. Zhang and S. Gong, "Improoving on LEACH protocolof wireless sensor networks using Fuzzy logic," *journal of information and computer science ,* vol. 7, no. 3, pp. 767-775, 2010.

[368] H. M. Abdulsalam and L. K. Kamel, "W-LEACH: Wieghted low energy adaptive clustering hierarchy aggregation algorithm for data streams in wireless sensor networks," in *international conference of data mining workshops*, Sydney, 2010.

[369] J. Hong, J. Kook, S. Lee, D. Kwon and S. Yi, "T-LEACH: the method of threshold -based cluster head replacement for wireless sensor networks," *Information system Frontiers,* vol. 11, no. 5, pp. 513-521, 2009.

[370] E. Fasolo, M. Rossi, J. Widmer and M. Zorzi, "“In-network aggregation techniques for wireless sensor networks: A survey," *IEEE wireless communication,* vol. 14, no. 2, pp. 70-87, 2007.

[371] M. O. Farooq and D. Pesch, "Reduced Overhead Roting in Short-Range Low Power and Lossy Wireless Networks," *Sensors,* vol. 19, pp. 1-19, 2019.

[372] A. Ali, A. G. Shah, M. O. Farooq and O. Ghani, "Technologies and challenges in developing Machine-to-Machine applications: A survey," *Journal of Network and Computer Applications,* vol. 83, pp. 124-139, 2017.

[373] www.elstermetering.com, "en/network-architecture," 27 6 2017. [Online]. Available: https://www.elstermetering.com/en/network-architecture.

[374] L. Alexandru and V. Popa, "Internet of Things and LoRaTM Low-Power WideArea Networks: A Survey," in *2017 International Symposium on Signals, Circuits and Systems (ISSCS)*, Lasi, Romania, 2017.

[375] K. E. Jeon, J. She, P. Soonsawad and P. C. Ng, "BLE Beacons for Internet of Things Applications: Survey, Challenges, and Opportunities," in *IEEE Internet of Things Journal*, vol. 5, no. 2, pp. 811-828, April 2018, doi: 10.1109/JIOT.2017.2788449.

[376] ZigBee Allaince;, "ZigBee Specification," 2006.

[377] ZigBee Alliance;, "ZigBee PRO Specification," ZigBee Alliance, 2007.

[378] C. M. G. Algora, V. A. Reguera and K. Steenhaut, "Experimental evaluation of IEEE 802.15.4 TSCH on 6TiSCH network," CONVENCIÓN INTERNACIONAL 2017 UNIVERSIDAD CENTRAL "MARTA ABREU" DE LAS VILLAS., Brussel, 2017.

[379] V. Kumar and S. Tiwari, "Routing in IPv6 over Low-Power Wireless Personal Area Networks (6LoWPAN): A Survey," *Journal of Computer Networks and Communications,* vol. 2012, pp. 1-10, 2012.

[380] R. H. Babu and U. Dey, "Routing Protocols In IPv6 enabled LoWPAN," *International Journal of Scientific and Research Publications,* vol. 4, no. 2, pp. 1-6, 2014.

[381] N. Saputro, K. Akkaya and S. Uludag, "A survey of routing protocols for smart grid communications," *Computer Networks,* vol. 56, pp. 2742-2771, 2012.

[382] A. Oliviera and T. Vazao, "Low-power and lossy networks under mobility: A survey," *Computer Networks,* vol. 107, no. 2, pp. 339-352, 2016.

[383] H.-S. Kim , J. Ko , D. E. Culler and J. Paek, "Challenging the IPv6 Routing Protocol for Low-Power and Lossy Networks (RPL): A Survey," *IEEE Communications Surveys & Tutorials,* vol. 19, no. 4, pp. 2502-2525, 2017.

[384] O. Gaddour, A. Koubaa, R. Rangarajan, O. Chiekhrouhou, E. Tovar and M. Abid, "Co-RPL: RPL routing for mobile low power wireless sensor networks using corona mechanism," in *Industrial Embedded Systems (SIES), 2014 9th IEEE International Symposium on (2014*, 2014.

[385] T. Clausen, J. Yi and U. Herberg, "Performance Evaluation of LOADng Routing Protocol in IoT P2P and MP2P Applications," *Computer Networks,* vol. 126, pp. 125-140, 2017.

[386] j. Yi and T. Clausen, "Collection Tree Extension of Reactive Routing Protocol for Low-Power and Lossy Networks," *International Journal of Distributed Networks,* vol. 2014, pp. 1-12, 2014.

[387] G. Oikonomou, L. Phillips and T. Tryfonas, "IPv6 Multicast Forwarding in RPL-Based Wireless Sensor Networks," *Wireless Personal Communications,* vol. 73, no. 6, pp. 1089-1116, 2013.

[388] A. Fadeel and E. K. Sayed, "Enhanced stateless multicast RPL forwarding for IPv6-based low-Power and lossy networks," in *the 2015 Workshop on IoT challenges in Mobile and Industrial Systems*, Florence , Italy, 2015.

[389] G. G. Lorente, B. Lemmens, M. Carlier, A. Barken and K. Steenhaut, "BMRF: Bidirectional Multicast RPL Forwarding," *Ad Hoc Networks,* vol. 54, pp. 69-84, 2017.

[390] J. Ko, J. Jeong, J. Park, A. J. June, O. Gnawali and J. Paek, "DualMOP-RPL: supporing multiple mode of downward routing in a single RPL network," *ACM transaction on sensor network,* vol. 11, no. 2, pp. 1-39, 2015.

[391] C. KIRALY, T. ISTOMIN, O. IOVA and G. P. PICCO, "D-RPL:overcoming memory limitation in RPL point to multipoint routing," in *local comupter networks (LCN)*, florida, 2015.

[392] M. Zhao, I. W.-H. Ho and p. h. j. Chong, "An Energy-Efficient Region-Based RPL Routing Protocol for Low-Power and Lossy Networks," *IEEE Internet of Things Journal,* vol. 3, no. 6, pp. 1319-1333, 2016.

[393] M. Goyal , E. Barccelli, M. Phillipp, A. Brandt and J. Martocci, "RFC 6997: Reactive Discovery of Point-to-Point Routes in Low-Power and Lossy Networks," IETF, 2013.

[394] S. Taghizadeh, H. Bobarshad and H. Elbiaze, "CLRPL: Context-Aware and Load Balancing RPL for IoT Networks under Heavy and Highly Dynamic load," *IEEE Access,* vol. 6, pp. 23277 - 23291, 09 04 2018.

[395] S. Anamalamudi, M. Zhang, C. Perkins, S. Anand and B. Lui, "Asymmetric AODV-P2P-RPL in Low-Power and Lossy Networks (LLNs)," 8 09 2019. [Online]. Available: https://tools.ietf.org/html/draft-ietf-roll-aodv-rpl-06. [Accessed 17 09 2019].

[396] H. Liu, B. Zhang, H. Mouftah, X. Shen and J. Ma, "Opputunitstic Routing in Wireless Ad Hoc and Sensor Networks: Present and Futrue Directions," *IEEE Communication Magzine ,* vol. 47, no. 12, pp. 103-109, 2009.

[397] N. Chakchouk, "A Survey on Opputunistic Routing in Wireless Communication Networks," *IEEE COMMUNICATION SURVEYS & TUTORIALS,* vol. 17, no. 4, pp. 2214-2242, 2015.

[398] S. Duquennoy, O. Landsiedel and T. Voigt, "Let the Tree Bloom:scalable opputunistic routing with ORPL," in *Proceedings of the 11th ACM Conference on Embedded Networked Sensor Systems*, Rome, Italy, 2013.

[399] S. Biswas and R. Morris, "ExOR: Opportunistic Multi-hop Routing for Wireless Networks," in *Proceedings of the ACM SIGCOMM 2005 Conference on Applications, Technologies, Architectures, and Protocols for Computer Communications*, Pennsylvania, USA, 2005.

[400] S. Chachulski, M. Jennings, S. Katti and D. Katabi, "Trading Structure for Randomness in Wireless Opputunistic Routing," *ACM SIGCOMM Computer Communication Review,* vol. 37, no. 4, pp. 169-180, 2007.

[401] Z. Zhao and T. Braun, "Real-World Evaluation of sensor context-aware Adaptive duty-cycled Opputunitstic Routing," in *39th annual IEEE conference on Local computer networks*, 2014.

[402] O. Landsiedel, E. Ghadimi, S. Duquennoy and M. Johansson, "Low Power Low Delay: opputunitisic routing meet duty cycling," in *ACM/IEEE 11th International Conference on Information Processing in Sensor Networks (IPSN)*, Beijing, China, 2012.

[403] S. J. Douglas , D. A. De Couto and B. R. John , "A High-Throughput Path Metric for Multi-Hop Wireless Routing," in *Proceedings of the 9th annual international conference on Mobile computing and networking*, San Diego, CA, USA, 2003.

[404] T. Liu, A. kamthe, L. Jiang and A. Cerpa, "Performance Evaluation of Link Quality Estimation Metrics for Static Multihop Wireless Sensor Networks," in *2009 6th Annual IEEE Communications Society Conference on Sensor, Mesh and Ad Hoc Communications and Networks*, Rome, Italy, 2009.

[405] F. Cuomo, E. Cipollone and A. Abbagnale, "performance analysis of IEEE 802.15.4 wireless sensor networks: an insight into topology formation process," *elsevier computer network,* vol. 53, no. 18, pp. 3057-3075, 2009.

[406] K.-S. Hong and C. Lynn, "Dag-based multipath routing for mobile sensor networks," in *ICTC 2011*, Seoul, South Korea, 2011.

[407] O. Ofonso and T. Vazao, "Low-power and lossy networks under mobility: A survey," *Computer Networks,* vol. 107, pp. 339-352, 2016.

[408] W. Gan, Z. shi, C. Zhang, L. Sun and D. ionescu, "MERPL:a more memory efficient storing mode in RPL," in *19th IEEE International Conference on Networks (ICON)*, SINGAPORE, 2013.

[409] E. Ancillotti, R. Bruno and M. Conti, "On the Interplay between RPL and Address Autoconfiguration protocols in LLNs," in *2013 9th International Wireless Communications and Mobile Computing Conference (IWCMC)*, Sardinia, Italy, 2013.

[410] S. Chakrabarti, "IPv6 LoWPAN Neighbor Discovery and Addressing Choices," 01 March 2010. [Online]. Available: https://tools.ietf.org/id/draft-chakrabarti-6lowpan-ipv6-nd-simple-00.html#anchor4. [Accessed 13 June 2019].

[411] E. talipov, H. shin, S. han and H. cha, "A lightweight statefull address autoconfiguration for 6lowpan," *Wirelss Networks,* vol. 17, no. 1, pp. 183-197, 2011.

[412] Draft-ietf-6tisch-minimal-02, "Minimal 6TiSCH Configuration," 4 july 2014. [Online]. Available: https://datatracker.ietf.org/doc/draft-ietf-6tisch-minimal/02/?include_text=1. [Accessed 2019].

[413] A. Tinka, T. Watteye, K. S. Pister and A. M. Bayen, "A decentralised schedulling algorithm for time synchronised channel hopping," *Mobile communication,* vol. 11, no. 1, pp. 1-16, 2011.

[414] I. WG, Director, *IETF.* [Film]. Bangkok: Meetecho, 2018.

[415] S. Rekik, N. Baccour, M. Jmaiel and K. Drira, "A performance analysis of Orchestra scheduling for time-slotted channel hopping networks," *Internet Technology Letters,* vol. 1, no. 3, 2017.

[416] P. Bahl, R. Chandra and J. Dunagan, "SSCH: slotted seeded channel hopping for capacity improvement in IEEE802.11 ad-hoc wireless networks," in *internation conference on mobile computing and networking (ACM)*, 2004.

[417] I. Rhee, J. Warrier, J. Min and L. Xu, "DRAND: distributed randomised TDMA schedulling for wireless adHoc Networks,," in *Mobile ad hoc netwokting and computing*, 2006.

[418] R. H. Hwang, C. C. Wang and W. B. Wang, "A distributed schedulling algorithms for IEEE 802.15.4e wireless sensor networks," *computing standards interfaces,* vol. 52, pp. 63-70, 2017.

[419] K. H. Phung, B. Lemmens, M. Goossens, A. Nowe, L. Tran and K. Streenhaut, "schedule based multi-channel communication in wireless sensor networks: a complete design and performance evaluation," *Ad Hoc Nerwoking,* vol. 16, pp. 19-24, 2015.

[420] E. Municio, G. Daneels, M. Vucinic, S. Latre, J. Famaey, Y. Tanaka, K. Brun, k. Muraoka, X. Vilajosana and T. Watteyne, "Simulating 6TiSCH network," *telecommunication journal,* pp. 1-17, 2018.

[421] C. H. Barriquello, G. W. Denardin and A. Campos, "A geographic routing approach for IPv6 in large-scale low-power and lossy networks," *Computers and Electrical Engineering,* vol. 45, pp. 182-191, 2015.

[422] O. Gaddour and A. Koubaa, "RPL in a nutshell: A survey," *Computer Networks,* vol. 56, no. 14, pp. 3163-3178, 2012.

[423] M. Barcelo, A. Correa, X. Vilajosana, J. L. Vicario and A. Morell, "Novel Routing Approach for the TSCH Mode of IEEE 802.15.14e in Wireless Sensor Networks with Mobile Nodes," in *2014 IEEE 80th Vehicular Technology Conference (VTC2014-Fall)*, Vancouver, BC, Canada, 2014.

[424] L. D. P. Pugliese, D. Zorabas, F. Guerriero and C. Douligeris, "Optimal routing approaches for IEEE 802.15.4 TSCH networks," *Transactions on Emerging Telecommunications Technologies,* vol. 30, no. 3, November 2018.

[425] A. I. PETRARIU and A. LAVRIC, "SigFox Wireless Communication Enhancement for Internet of Things: A study," *2021 12th International Symposium on Advanced Topics in Electrical Engineering (ATEE)*, Bucharest, Romania, 2021, pp. 1-4, doi: 10.1109/ATEE52255.2021.9425213.

[426] S. Dawaliby, A. Bradai and Y. Pousset, "In depth performance evaluation of LTE-M for M2M communications," in *Wireless and Mobile Computing Networking and Communications (WiMob) 2016 IEEE 12th International Conference on*, 2016.

[428] M. R. palattella, T. Watteyne, Q. Wang, K. Muraoka, N. Accettura, D. Dujovne, A. L. Grieco and T. Engel, "On-the-fly bandwidth reservation for 6TiSCH wireless industrial network," *IEEE sensor journal,* vol. 16, no. 2, pp. 550 - 560, 2016.

[429] R. Soua, P. Minet and E. Livolant, "Wave: a distributed scheduling algorithm for convergecast in IEEE 802.15.4e TSCH networks," *Emerging telecommunication technologies,* vol. 27, no. 4, 2016.

[430] X. Wang, Y. Yang, Y. Yao and H. Cheng, "An address configuration protocol for 6LoWPAN wireless sensornetworks based on PDAD," *Computer Standards and Interface,* vol. 36, pp. 918-927, 2014.